Ad Majorem Dei Gloriam

An Investigation into the Mechanism of Bioleaching of a Predominantly-Chalcopyrite Concentrate with Mesophiles

by

Ashraf Jaffer
BSc Eng. (Chemical)
University of Cape Town

Dissertation submitted as fulfilment of the requirements for the degree of Master of Science in Engineering (Chemical)

University of Cape Town

August 2002

Acknowledgements

I would like to express my deepest gratitude to the following people and organisations for their efforts in seeing this project to its completion:

My Supervisor, Prof. G.S. Hansford, for his leadership and guidance.
Dr A.W. Breed for his contribution and constructive criticism
Dr S. Moosa for her advice and words of wisdom.
The Council of Mineral Technology for its financial support.
Dr A. Pinches from MINTEK for his valuable insight.
My colleagues and friends from the Minerals Bioprocessing Research Group.
Bill Randall and his staff at the Electronic Workshop.
Sue Jobson from the Bioprocess Research Group.
All other Chemical Engineering staff members who contributed to the outcome of this study.
The staff at UCT's SEM unit.
My wife, Dilshud Sonday for her tireless patience, unwavering support and encouragement.
My family and friends for their support

Abstract

Bioleaching is an established technology for the treatment of refractory gold ores and concentrates. The bioleaching of sulphide minerals is a complex process in which bacterial and chemical oxidation processes occur simultaneously. Recent studies has provided convincing evidence that the bioleaching of pyrite occurs via a two-step mechanism (Boon, 1996). A similar multiple sub-process mechanism has been proposed for the bioleaching of chalcopyrite. A primary ferric-ion and proton attack on the mineral produces ferrous-ions and some form of polysulphide intermediary compound. The oxidation of sulphur compounds can occur chemically under certain conditions. The bacterial role is to oxidise the ferrous-ion back to ferric-ion and the sulphur/sulphur compounds to sulphuric acid (Sand *et al.*, 1999).

This work assesses the available literature on the chemical ferric leaching and the bioleaching of chalcopyrite to prescribe the state-of-the-art. The reworking of published literature data showed that the rate of ferrous-ion production during the chemical ferric leaching of a predominantly chalcopyrite concentrate is a function of the solution redox potential or ferric/ferrous-ion ratio. It has also been shown that the chemical rate passes through a maximum in the region of 430mV (SCE). The build-up of product layers during the leaching of chalcopyrite result in diffusional barriers which limit the rate of leaching. The exact nature of this layer is unresolved.

Another objective was to test the applicability of the experimental and theoretical methodology developed by Boon (1996) in studying the mechanism of bioleaching of a chalcopyrite concentrate with mesophiles. The methodology has already successfully been used to study the mechanism and kinetics of pyrite bioleaching. Staged additions of two different chalcopyrite concentrates were performed, whereby the mineral was added every 2 hours to a batch bioleach at 35 °C. During the course of the experiments, the redox potential, oxygen and carbon dioxide utilisation rates were monitored continuously. Decreasing redox potentials and increasing specific oxygen utilisation rates with each mineral addition were observed. The trends for both concentrates were in agreement with that presented by Boon (1996) for pyrite bioleaching. The results are consistent with the multiple sub-process mechanism. It indicates that the chemical ferric leaching of the mineral to produce ferrous-ion, and bacterial ferrous-ion oxidation to produce ferric-ion are separate sub-processes. The results also show that staged mineral additions to a batch bioleach can be successfully used to study the mechanism and kinetics of chalcopyrite bioleaching. The results further showed that the rates of ferrous-ion production from the chemical leaching of a chalcopyrite concentrate and the rate of ferrous-ion consumption from bacterial oxidation can be independently

determined, and expressed as functions of the ferric/ferrous-ion ratio. The kinetics of these two sub-processes can then be used to predict the steady state behavior during the batch bioleaching of the mineral.

The fate of the sulphur moiety was not considered, and future work should address this issue.

Table of Contents

Chapter 4: Materials and Methods

Chapter 5: Chemical Ferric leaching of chalcopyrite concentrates

Chapter 6: Results of the staged addition of chalcopyrite concentrates to a batch bioleach

LIST OF FIGURES

LIST OF TABLES

Chapter 1: Introduction

1.1 Background

Bioleaching has since become an accepted technology for the leaching of copper ores in heaps and the pretreatment of refractory arsenical gold-bearing ores and concentrates (Breed *et al.*, 1999(a)). The success the stirred tank bioleaching applications in the area of base-metal extraction is attributed to its environmental and economic advantages over conventional pretreatment techniques like pressure oxidation and roasting, especially since the latter is associated with high capital and operating costs as well as the release of hazardous fumes (van Aswegen, 1993). The projected low capital and operating cost of bioleaching plants make it an attractive alternative especially in view of depressing metal prices (Brierley *et al.*, 1999).

The environmental advantages include a stable liquid effluent in the case of bioleaching as opposed to a gaseous one in the case of smelting. Other advantages cited by mine operators include the process robustness, ease of operation because of the relatively conditions of temperature and pressure, shorter equipment construction periods and less stringent safety considerations as compared to the aforementioned processes. However, commercial applications of bioleaching is still a developing technology and this allows for improvements and expansions of the use of this process (Rawlings, 1997).

1.2 Commercial Copper bioleaching

The most commonly practiced ore bioleaching process is copper sulphide *in-situ* or dump leaching processes that are responsible for 15% of the world's primary copper production (Rossi, 1990). Chalcopyrite, covellite, chalcocite and bornite are the principle copper sulphides from which copper is extracted, with chalcopyrite being the most common and abundant source of copper from mineral copper sulphides. In addition the low solubility of chalcopyrite in water and the high activation energy for the oxidation of chalcopyrite is an indication of the mineral's recalcitrant behavior to leaching at low temperatures (Rossi, 1990).

Table 1-1 shows the recent commercial applications of copper bioheap leaching plants. In addition stirred tank bioleaching plants in South Africa; Brazil and Ghana have been commissioned to treat gold flotation concentrates. Bioleaching is also showing potential for the extraction of other metals like cobalt and nickel from sulphide minerals (Miller *et al.*, 1999).

Table 1-1: Commercial applications of copper-ore bioheap leaching (Rawlings, 1997; Brierley, 1997)

Plant	Tonnage	Ore type	Process
Lo Aguirre, Chile	3500 mt/d	Chalcocite	SX/EW
Cerro Colorado, Chile	1600 mt/d	Chalcocite	SX/EW
Quebrada Blanca, Chile	17300 mt/d	Chalcocite	SX/EW
Ivanzar, Chile	1500mt/d	Chalcocite	SX/EW
Girilambone, Australia	2000mt/d	Chalcocite	SX/EW
Newmont, USA	10000mt/d	sulphidic	NEWMONT Bioheap

1.3 Thermophilic vs Mesophilic bioleaching

Most commercial bioleaching plants in operation until 1999 use sulphidic refractory gold-bearing concentrates as feedstocks and operate at temperatures between 35 and 42 °C. To date no successful commercial scale stirred tank bioleaching plant has been in operation to treat a chalcopyrite concentrate feedstock. This is because the kinetics of bioleaching of chalcopyrite with mesophiles such as *Acidithiobacillus ferrooxidans* and *Leptospirillum ferrooxidans* at temperature ranges employed in current commercial stirred tank bioleaching operations is slow in comparison to that observed with the use of thermophiles at higher temperatures (Brierley *et al.*, 1979; Murr, 1980; Le Roux *et al.*, 1987; Schnell, 1997). The faster kinetics of copper solubilisation in dump-leaching has been associated with the action of thermophilic organisms rather than mesophilic organisms (Murr and Berry, 1979). The slow kinetics of chalcopyrite leaching at low temperatures questions the economic viability of using mesophiles to bioleach chalcopyrite. Enhanced kinetics of chalcopyrite bioleaching at mesophilic temperatures have been reported in the presence of silver (Blancarte-Zurita *et al.*, 1987, Palencia *et al.*, 1987; Blazquez *et al.*, 1999; Sato *et al.*, 2000). It still remains unclear whether the silver catalysed process is economically feasible at commercial scale.

However, pilot scale testing of Mt Lyell chalcopyrite by the Mintek-Bactech consortium at 50 °C using moderately thermophilic bacteria and 70 °C using extreme thermophiles, as well as the successful batch and continuous tests performed by Billiton Process Research at 68 and 78 °C using thermophilic cultures, has shown promise by achieving in excess of 94% extraction of copper (Miller *et al.*, 1999; Pinches, 1997; Rhodes *et al.*, 1998; van Staden, 1998; Dew *et al.*, 1999). Other heap leaching processes developed to treat chalcopyrite concentrates include the GEOCOAT™ Process developed by Geobiotics, Inc. which uses thermophilic

archae at 70 °C and feed agglomeration or coating onto coarser ore in order to achieve an overall 86% extraction of copper (Johansson *et al.*, 1999).

Brierley *et al.*, (1999) identified the following important parameters for successful chalcopyrite bioleaching.

- Redox potential in the 350-450mV (SHE) range.
- High temperatures in the 55-80 °C range.
- Fine particle size ranges in the 6-12 um range.
- Low pH in the 1.1-2 range to minimize precipitate formation.
- A minimisation of acid production.

This increasing interest in the potential use of thermophilic bacteria and thermophilic archae for commercial scale bioleaching of chalcopyrite concentrates has been as a result of the higher extraction rates observed with the use of this organism. Possibilities include the higher temperature of operation and the lower range of redox potential operation. However, reservations in the use of thermophiles for chalcopyrite bioleaching are centred around the relative lack of knowledge or understanding of these organisms in comparison to mesophiles like *Acidithiobacillus ferrooxidans* and *Leptospirillum ferrooxidans* which are well researched, as well as the thermophiles potential susceptibility to shear damage as high solids concentrations (Brierley *et al.*, 1999). The use of mesophiles for chalcopyrite bioleaching therefore remains an option, even though chalcopyrite is recalcitrant to bioleaching at those temperature ranges.

Because of the slow kinetics of leaching at mesophilic conditions, the improved control of essential operating parameters such as pH, temperature, aeration rate and redox potential are imperative for the optimisation of the process in order to improve copper extraction rates. This creates a need for mechanistically based kinetic models to describe the performance of bioleaching processes. Therefore an understanding of the bioleaching mechanism of chalcopyrite with mesophiles is important to develop mechanistically based kinetic models to design and control the performance of mesophilic chalcopyrite bioleach systems to achieve optimum rates of extraction.

1.4 Two step mechanism for bioleaching

The bioleaching of sulphide minerals is a complex process in which bacterial and chemical oxidation processes occur simultaneously. Recent work has provided convincing evidence that the bioleaching of pyrite occurs via a two-step mechanism (Boon, 1996). This mechanism involves a chemical ferric-ion oxidation on pyrite in a bioleaching medium to produce ferrous-ion as equation (1.1).

$$FeS_2 + 14Fe^{3+} + 8H_2O \mapsto 15Fe^{2+} + 2SO_4^{2-} + 16H^+ \qquad (1.1)$$

The ferrous-ion produced by this reaction is subsequently bacterially oxidised to ferric-ion as in equation (1.2).

$$4Fe^{2+} + O_2 + 4H^+ \mapsto 4Fe^{3+} + 2H_2O \qquad (1.2)$$

The existence of the two-step mechanism for pyrite bioleaching has been supported by evidence of the dominance of *Leptospirillum ferrooxidans* and *Acidithiobacillus caldus* in continuous bioleaching operations for pyrite/arsenopyrite concentrates (Rawlings *et al.*, 1999(a))). This is because the mineral sulphide sulphur moeity is oxidised directly to sulphate during the bioleaching of pyrite and as in Equation (1.1).

This project investigates the mechanism of bioleaching of chalcopyrite with mesophilic bacteria by employing the experimental and theoretical methodology developed by Boon (1996).

1.5 The multiple sub-process mechanism

A similar mechanism has been proposed for the case of bioleaching of chalcopyrite. Schippers *et al.*, (1999) have proposed a reaction scheme which constitutes a primary chemical ferric attack to produce ferrous iron and some form of polysulphide intermediary compound. The oxidation of sulphur compounds to elemental sulfur can also occur chemically under certain conditions.

The primary attack can be accompanied with or without a proton attack on the mineral surface. The role of *Acidithiobacillus ferrooxidans* and *Leptospirillum ferrooxidans* is to re-

oxidise the ferrous iron back to ferric form thus maintaining a high redox potential. The bacterial role is extended in that the sulphur oxidising capacity of *Acidithiobacillus ferrooxidans, Acidithiobacillus thiooxidans* and possibly *Acidithiobacillus caldus* is thought to be instrumental in the oxidation of sulphur and/or sulphur compounds to sulphuric acid thereby re-supplying the protons for the primary attack on the mineral.

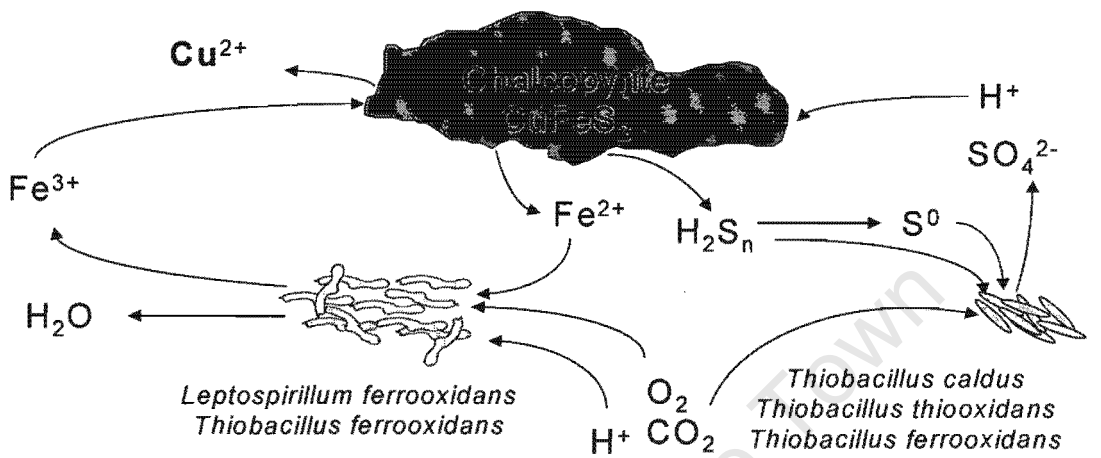

Fig 1.1: Diagrammatic representation of the bioleaching of chalcopyrite with mesophiles via the multiple-sub-process meachanism (Sand *et al.*, 1999).

A representation of the mechanism is shown in Figure 1.1. The bacteria shown are unattached for reasons of clarity. This means that the overall process can be reduced into a number of independent sub-processes. The bioleaching of chalcopyrite should take place via the Reactions (1.3)-(1.7) according to Shippers *et al.* (1999). Equation's (1.3) and (1.5) are based on that proposed by Shippers *et al.* (1999) for the metal sulphides (MS) Chalcopyrite, Galena and Sphalerite. Because the nature of the polysulphide compound has not been confirmed, Equations (1.3) and (1.5) does not represent the equations in its balanced form.

Ferric-ion and proton attack (where $n \geq 2$):

$$MS + Fe^{3+} + H^{+} \rightarrow M^{2+} + Fe^{2+} + \tfrac{1}{2}H_2S_n \qquad (1.3)$$

Ferric iron leaching without proton attack, shown for the case of chalcopyrite:

$$CuFeS_2 + 4Fe^{3+} \mapsto Cu^{2+} + 5Fe^{2+} + 2S^0 \qquad (1.4)$$

Polysulphide oxidation :

oxidise the ferrous iron back to ferric form thus maintaining a high redox potential. The bacterial role is extended in that the sulphur oxidising capacity of *Acidithiobacillus ferrooxidans, Acidithiobacillus thiooxidans* and possibly *Acidithiobacillus caldus* is thought to be instrumental in the oxidation of sulphur and/or sulphur compounds to sulphuric acid thereby re-supplying the protons for the primary attack on the mineral.

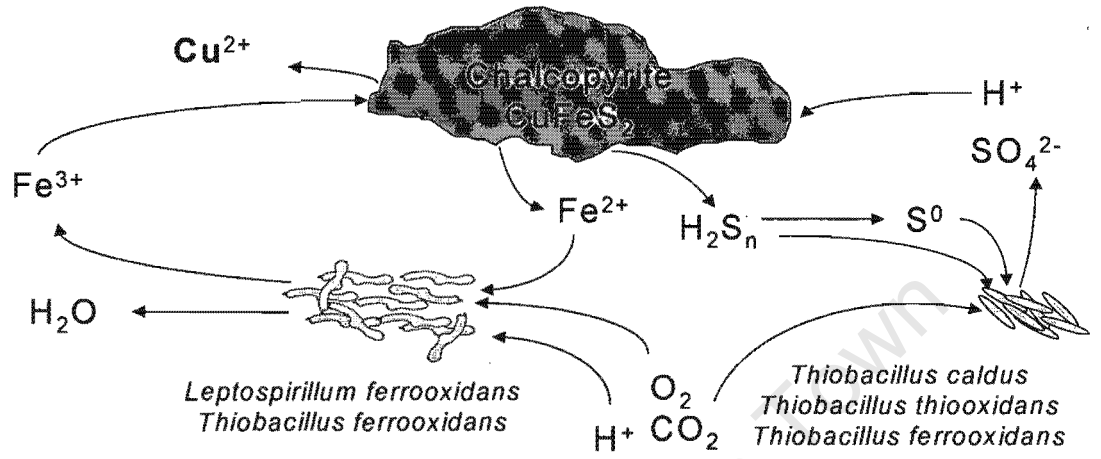

Fig 1.1: Diagrammatic representation of the bioleaching of chalcopyrite with mesophiles via the multiple-sub-process meachanism (Sand *et al.*, 1999).

A representation of the mechanism is shown in Figure 1.1. The bacteria shown are unattached for reasons of clarity. This means that the overall process can be reduced into a number of independent sub-processes. The bioleaching of chalcopyrite should take place via the Reactions (1.3)-(1.7) according to Shippers *et al.* (1999). Equation's (1.3) and (1.5) are based on that proposed by Shippers *et al.* (1999) for the metal sulphides (MS) Chalcopyrite, Galena and Sphalerite. Because the nature of the polysulphide compound has not been confirmed, Equations (1.3) and (1.5) does not represent the equations in its balanced form.

Ferric-ion and proton attack (where $n \geq 2$):

$$MS + Fe^{3+} + H^{+} \rightarrow M^{2+} + Fe^{2+} + \tfrac{1}{2}H_2S_n \qquad (1.3)$$

Ferric iron leaching without proton attack, shown for the case of chalcopyrite:

$$CuFeS_2 + 4Fe^{3+} \mapsto Cu^{2+} + 5Fe^{2+} + 2S^0 \qquad (1.4)$$

Polysulphide oxidation (where $n \geq 2$):

$$\tfrac{1}{2}H_2S_n + Fe^{3+} \mapsto \tfrac{1}{8}S_8^0 + Fe^{2+} + H^+ \quad (1.5)$$

Biological ferrous oxidation :

$$4Fe^{2+} + O_2 + 4H^+ \mapsto 4Fe^{3+} + 2H_2O \quad (1.6)$$

Biological sulphur oxidation :

$$\tfrac{1}{8}S_8^0 + \tfrac{3}{2}O_2 + H_2O \mapsto SO_4^{2-} + 2H^+ \quad (1.7)$$

1.6 Implications of the mechanism

The existence of this mechanism implies that the overall mechanism can be reduced to a number of critical sub-processes, the kinetics of which can be independently studied and modelled. The results can then be used to predict the performance of batch or continuous reactors.

This independence of bacterial and chemical steps has already lead to the development and of an economically feasible commercial process for chalcopyrite bioleaching at moderate temperatures by the Mintek/Bactech consortium. This so called "indirect leaching" process employs an aerated bacterial ferrous-ion oxidation reactor (BFIG) to control and sustain the leaching solution within an optimal range of redox potentials required for successful chemical leaching of the copper sulphide feed. Actual copper extraction from the mineral concentrate is then achieved by a separate high temperature chemical ferric-leaching process. The advantage of this configuration is that it allows for the independent optimisation of chemical leaching and bacterial ferrous-ion oxidation processes (Van Staden, 1998)

1.7 The chemical ferric leaching of chalcopyrite

The mechanism has indicated that the chemical ferric oxidation of chalcopyrite is crucial constituent of the overall bioleaching mechanism. The kinetics of this step would have a significant effect on the kinetics of bioleaching. Previous kinetic models for pyrite and arsenopyrite have been empirical (Boon, 1996) and electrochemical (May *et al.*, 1997; Ruitenberg *et al.*, 1999) expressing the rate of chemical reaction as a function of the redox potential or ferric/ferous-iron ratio and assuming that electron transport from the surface to

the surrounding is rate controlling, and that the driving force for this electron transfer is the difference between the solution redox potential and the mineral rest potential. Both these models have shown an increase in the rate of leaching of the mineral with increasing ferric/ferrous-ion ratio.

Many studies has been conducted on the ferric-sulphate leaching of chalcopyrite, but until recently very few studies (Kametani and Aoki, 1985; Hansford *et al.*, 1999; Hiroyoshi *et al.*, 2000) have looked at the effect of redox potential or ferric/ferrous-ion ratio on the rate of leaching. This created a need to establish from the available literature whether the observed dependency on redox potential or ferric/ferous-iron ratio seen by other mineral sulphides also applies to chalcopyrite.

Another question surrounded the actual stochiometry of the chemical ferric-ion leaching of the chalcopyrite concentrate used in the study. This furthered the need to study the ferric-ion oxidation of the chalcopyrite-concentrate at conditions similar to those prescribed in bioleaching.

1.8 Bacterial ferrous-ion oxidation

The multiple sub-process mechanism shows that bacterial ferrous-ion oxidation is another important step in the bioleaching of chalcopyrite. To date a number of kinetic models have been proposed and reviewed to describe the kinetics of bacterial ferrous-ion oxidation (Nemati *et al.*, 1998). Recent work has shown that a Michaelis Menten/Monod based model which expresses the rate of substrate utilization as traditional enzyme kinetics has successfully described the bacterial oxidation kinetics in both exclusively ferrous-ion oxidation systems as well as pyrite and arsenopyrite bioleaching systems (Boon, 1996, Breed *et al.*, 1999(a)). This model, written in terms of the specific ferrous-ion or oxygen utilization rate is expressed in terms of the ferric/ferrous-iorn ratio, the parameters of which has been derived for both *Acidithiobacillus ferrooxidans* and *Leptospirillum ferrooxidans* at temperatures between 30-40 °C and pH 1.2-1.8. A study of the mechanism of bioleaching of chalcpyrite would also involve testing the applicability of this model in describing the bacterial ferrous-ion oxidation during chalcopyrite bioleaching.

1.9 Objectives

The introduction has illustrated the motivation for studying the mechanism and kinetics of the bioleaching of chalcopyrite with mesophiles. The broad objective of the project is to establish

the state-of-the-art in the bioleaching of chalcopyrite with mesophiles by assessing the available literature and furthermore to test the applicability of the multi-sub-process mechanism in describing the bioleaching of chalcopyrite by using the experimental and theroretical methodolgy devised by Boon, (1996). The specific key objectives have been formulated as follows:

1. To assess the available literature on the bioleaching of chalcopyrite with mesophiles and the chemical leaching of chalcopyrite with ferric-ion in order to prescribe the current state-of-the-art in the subject matter.

2. To test the applicability of the experimental and theoretical methodology developed by Boon, (1996) in studying the mechanism and kinetics of bioleaching of chalcopyrite.

3. To test the applicability of the Michaelis-Menten based bacterial oxidation kinetic model in describing the kinetics of bacterial ferrous-ion oxidation during the bioleaching of chalcopyrite with mesophiles.

4. To determine the effect of the solution redox potential or ferric/ferrous-ion on the rate of ferric leaching leaching of chalcopyrite from a literature persepective.

5. To determine if the kinetics for the chemical leaching of a predominantly chalcopyrite concentrate and the kinetics of bacterial ferrous-ion oxidation can be used to predict the performance for the batch bioleaching of the same concentrate.

The build-up of product layers around the mineral under certain conditions is thought to cause diffusional resistance and passivation in the case of chalcopyrite bioleaching (Murr, 1980, Rossi, 1990). Certain questions pertaining to the passivation of chalcopyrite remains unanswered.

1. What is the nature of the passivating layer in a mesophilic bioleaching system?
2. What effect do *Acidithiobacillus ferro-oxidans* , *Leptospirillum ferro-oxidans and Acidithiobacillus thio-oxidans* have on passivation or conversely what effect does the mineral passivation have on the activity of these bacteria?
3. Does elemental sulphur formation play a role in passivation during bioleaching?
4. What is the dominant bacterial strain at mesophilic conditions during chalcopyrite bioleaching and what factors are involved in its selection?

1.10 Thesis Layout

This thesis is divided into eight chapters.

Chapter One outlines the background and motivation for studying the mechanism and kinetics of the bioleaching of chalcopyrite, as well as the specific objectives of the current project.

Chapter Two is a review of the literature relevant to the mechanism of mesophilic bioleaching of chalcopyrite as well as the stochiometry and kinetics of chemical ferric leaching of chalcopyrite. Chapter two includes the results of reworking published literature data to establish the effect of redox potential of the kinetics of ferric-ion leaching of chalcopyrite.

Chapter Three presents the theoretical methodology devised by Boon(1996) for pyrite bioleaching, which is relevant to studying the mechanism of bioleaching of a chalcopyrite concentrate and highlights certain limitations in applying this methodology.

Chapter Four outlines the experimental methods and materials employed to study both the bioleaching and the stochiometry of chemical ferric-ion leaching of a chalcopyrite concentrate.

Chapter Five is a presentation of the results and discussion of the investigation into the stochiometry of the chemical ferric-ion leaching of the chalcopyrite concentrate.

Chapter Six reports the results of the employing the theoretical and experimental methodology of Boon (1996) for studying the bioleaching of a chalcopyrite concentrate during the staged addition of mineral to a batch culture.

Chapter Seven is an attempt to predict the steady state the behavior of the bioleaching of the chalcopyrite concentrate during the batch experiments presented in chapter six, by bringing together the independently determined kinetics of bacterial ferrous-ion oxidation and chemical ferric-ion leaching.

Chapter Eight are the conclusions and recommendations for further research on the subject.

Chapter 2: Literature Review

2.1 Introduction

It has been proposed that the bioleaching of chalcopyrite occurs via a multiple sub-process mechanism involving the chemical of the mineral to produce ferrous-ion, copper and sulphur/sulphur compounds; the bacterial oxidation of ferrous-ion to regenerate ferric iron and the bacterial oxidation of sulphur to generate sulphuric acid (Sand *et al.*, 1999). General aspects concerning the bioleaching of sulphide minerals has been extensively reviewed by other workers (Rossi, 1990; Rawlings, 1997). Those features reported in literature which directly concern the mechanism and kinetics of the bioleaching of chalcopyrite or predominantly chalcopyrite concentrates with mesophiles are discussed in this chapter. It must also be pointed out that this review is specific to the mesophilic bioleaching of chalcopyrite.

It is assumed that the chemical ferric-ion leaching of chalcopyrite, the bacterial ferrous-ion oxidation and bacterial sulphur oxidation processes make up the mechanism. The scope of this review is three fold, i.e.,

1. To assess those studies which are exclusively concerned with mesophilic bioleaching of chalcopyrite
2. It reviews the kinetics and stochiometry of ferric-ion leaching of chalcopyrite.
3. It determines the effect of the redox potential on the rate of chalcopyrite chemical leaching.

Previous studies have already reviewed the kinetics of bacterial ferrous-ion oxidation by mesophiles (Nemati *et al.*, 1998; Boon, 1996; Breed, 2000) and this aspect will not be extensively dealt with in this chapter.

2.2 The ferric leaching of chalcopyrite

2.2.1 Stochiometry

Most workers agree that the dissolution of chalcopyrite in acidic ferric media produces elemental sulphur. This can be represented according to Equation (2.2.1) (Dutrizac, 1978; Munoz *et al.*, 1979; Dutrizac, 1981; Hirato *et al.*; 1987; Dutrizac, 1989)

$$CuFeS_2 + 4Fe^{3+} \mapsto Cu^{2+} + 5Fe^{2+} + 2S^0 \qquad (2.2.1)$$

However, recent work has shown that in addition to the products from Equation (2.2.1) minor amounts of sulphate is formed according to Equation (2.2.2) (Dutrizac, 1982; Dutrizac, 1989).

$$CuFeS_2 + 16Fe^{3+} + 8H_2O \mapsto Cu^{2+} + 17Fe^{2+} + 16H^+ + 2SO_4^{-2} \qquad (2.2.2)$$

Equation (2.2.1) predicts a dissolved ferrous-ion to copper ratio of 5, while Equation (2.2.2) predicts 17. It has been shown that 94% of the sulphide moeity reports to elemental sulphur while 6% to sulphate at 95 °C in 70 hr of leaching. In addition, a ferrous-ion to copper ratio of 5 was established (Dutrizac, 1989). This implies that the dominant leaching reaction at 95 °C is Equation (2.2.1). It still remains unclear if this is the case at 30-40 °C. The dominance of either Equation (2.2.1) or (2.2.2) during the leaching reaction would imply a varying stochiometry and hence a changing ferrous-ion to copper ratio during the course of the reaction. Most workers have presented the leaching kinetics as concentrations of copper solubilised *vs* time or the percentage of copper extracted *vs* time. To date there has been very few published studies which present the amount of ferrous-ion and copper solubilised during the chemical ferric leaching of chalcopyrite in acidic sulphate media at mesophilic temperatures since most of the literature work has been conducted at higher temperature ranges (60-90 °C).

2.2.2 Factors affecting the kinetics of ferric leaching of chalcopyrite

The leaching kinetics in most previous work is typically presented as the concentration of copper solubilised *vs* time and is shown to display a parabolic curve (Beckstead *et al.*, 1976; Jones and Peters, 1976; Munoz *et al*, 1979; Dutrizac, 1981; Kametani and Aoki, 1985; Hirato *et al*, 1987, Hiroyoshi *et al*, 1997; Hiroyoshi *et al*, 1999; Lu *et al*, 2000). The rate has been found to be strongly dependent on the following factors provided that the acidity is low enough to prevent iron hydrolysis :

i. temperature
ii. active particle suface area
iii. type of lixiviant
iv. the ratio of initial ferric/ferrous-ion concentrations

Other parameters such as the pH are believed to have a minimal effect on the rate of leaching, depending on the ferric-ion medium used (Dutrizac, 1978; Munoz *et al*, 1979, Dutrizac, 1981; Hirato *et al*, 1987). The effect of each of the above mentioned factors will be discussed

inturn. It seems well established that the kinetics of leaching is independent of stirring speeds above those which are necessary to maintain a homogenous solution of oxidant media and particle suspensions (Beckstead *et al.*, 1976; Dutrizac, 1978). This implies that the rate of chalcopyrite ferric-ion leaching is not controlled by mass transfer across the liquid boundary.

To date a number of studies have been conducted to elucidate the effect of temperature, mineral surface area and type of lixiviant, either ferric sulphate or ferric chloride, on the reaction kinetics.

2.2.2.1 Effect of temperature

It has been established that the rate of leaching increases with increasing temperature irrespective of the lixiviant used. This has been established by most workers in the case of both ferric sulphate and chloride media in the ranges 30-50 °C (Braithworth *et al.*,1976), 50-100 °C (Dutrizac, 1978), 60-90 °C (Munoz et al., 1979), 55-95°C in chloride media only (Dutrizac, 1982) and 50-80 °C (Hirato *et al.*, 1987). A marked increase in the leaching kinetics above 120 °C has been attributed to the melting of the sulphur product coating on the surface of the mineral. The change in kinetics has been associated with a shift in mechanism from diffusion to reaction control after the melting of the sulphur product and has been supported by a significant difference in calculated activation energies before and after 120 °C (Braithworth *et al.*,1976).

The assessment of accurate activation energies from literature data for the ferric leaching of chalcopyrite in sulphate media has been problematic due to the difficulty in obtaining pure chalcopyrite samples and the methodology employed in calculation (Dutrizac, 1981). The activation energies for the ferric leaching of chalcopyrite in sulphate media are calculated from the rates which are known to be non-linear. This means that the rates are either defined by their initial or final slopes, and the subsequent calculated activation energies would be therefore be strongly dependent on the above decision. Despite the above mentioned factors most workers have established activation energies in the range of 75-85 kJ/mol for the ferric leaching of chalcopyrite in sulphate media (Munoz *et al.*, 1979; Dutrizac, 1981; Hirato *et al.*,1987)

2.2.2.2 Effect of mineral particle surface area

It is widely believed that the rate of leaching can be improved by fine grinding of the mineral to increase the available surface area for attack by the oxidant species. A higher leaching rate has been reported for smaller mineral particle size fractions as opposed to larger ones in the size ranges from 0.5-12 μm (Beckstead *et al.*, 1976); 4-47μm (Munoz *et al.*, 1979); and 10-37 μm (Dutrizac, 1981). Earlier work indicates that the leaching rate is independent of particle size below 100 mesh in chloride media (Jones and Peters, 1976). In contradiction, it has also been shown that the rate of leaching increases with decreasing mean particle size in both chloride and sulphate media, with the rates being higher in the chloride media (Dutrizac, 1981). An increase in leaching rate with a decrease in particle was also shown in for the oxiditive leaching of Mt Isa Mines chalcopyrite in a mixed sulphate-chloride media (Lu *et al.*, 2000). It is widely thought that the initial rate of leaching of chalcopyrite in ferric sulphate media is proportional to the initial available surface area of the mineral irrespective of the particle size or lixiviant used(Beckstead *et al.*, 1976; Munoz *et al*, 1979; Dutrizac, 1981).

2.2.2.3 Effect of Lixiviant

All bioleaching systems involve ferric sulphate media since chloride ions, even in minute quantities is known to have inhibitory effects on the activity of most mesophilic bacteria (Lawson *et al.*, 1995). However, the purely chemical ferric-ion leaching of chalcopyrite has been investigated in both ferric sulphate and ferric chloride solutions. Although, the focus of the current work concerns ferric sulphate leaching, the response of chalcopyrite dissolution in the alternative ferric chloride lixiviant is considered because it has been shown that leaching behavior is dramatically different in this media. Also, interest in the ferric-sulphate leaching remains high because downstream electrowining technology to recover copper from leach solutions is most suited for sulphate media as opposed to chloride media (Dutrizac, 1989). The determination of stochiometric information on the ferric leaching reaction is made possible by comparing the proposed kinetics and reaction products in both these media. Most studies compare the kinetics of chemical ferric-ion leaching of chalcopyrite in exclusively ferric sulphate-sulphuric acid or ferric chloride-hydrochloric acid media. An enhanced leaching rate in the exclusively chloride system has been noted by a number of workers (Brown and Sullivan, 1934; Jones and Peters, 1976; Dutrizac, 1978; Dutrizac, 1981; Palmer *et al.*, 1981; Dutrizac, 1982; Hirato *et al.*, 1987; Lu *et al.*, 2000). A recent study has shown 97% extraction of copper in 9 hrs of leaching at 95 °C in a predominantly ferric sulphate media containing significant quantities of chloride-ions (Lu *et al.*, 2000). The author's speculated

that the presence of chloride-ions promotes the formation of a porous sulphur product as opposed to a compact sulphur product on the surface of the mineral, which prevents diffusional rate limitation in the latter case.

Table 2-1 shows a comparison of the observed kinetics and product formation for ferric sulphate and ferric chloride leaching of chalcopyrite. The kinetics of leaching in chloride media is 5 to 20 times faster than that in the sulphate media (Brown and Sullivan, 1934; Jones and Peters, 1976; Dutrizac, 1978; Dutrizac, 1981; Dutrizac, 1982; Hirato *et al.*, 1987). From Table 2-1 it can be seen that in contrast to the parabolic kinetics seen in the ferric sulphate-sulphuric acid media, linear kinetics are reported in the ferric chloride-hydrochloric acid system up to about 90% copper dissolution (Jones and Peters, 1976; Dutrizac, 1978; Dutrizac, 1981; Hirato *et al*, 1987; Lu *et al.*, 2000).

The reaction in the chloride media is described in Equation (2.2.1). This stochiometry predicts a ferrous-ion to copper ratio of 5 and a ferrous-ion to sulphur ratio of 2.5. This is confirmed for ferric chloride leaching by establishing that 96-98% of the sulphide reports to sulphur in the temperature range 50-95 °C in acidic media, although the sulphur/sulphate yield from the sulphide mineral during the leaching chalcopyrite in ferric-sulphate media was not presented (Dutrizac, 1978; Dutrizac, 1982). Earlier workers had reported minimal sulphate formation in ferric-chloride systems (Jones and Peters, 1976) but significant sulphate formations amounting to 18% (Jones and Peters, 1976) after 17 days of leaching a relatively pure chalcopyrite at 90 °C in sulpate media. In contrast, later work established 2.5% (Tiwari *et al.*, 1980) sulphate formation for leaching a 80% pure chalcopyrite at 93 °C and 6% (Dutrizac, 1989) sulphate formation for leaching a 98% pure chalcopyrite over 70 hrs at 90 °C in ferric sulphate media.

Table 2-1: A comparison of the kinetics and products for the ferric-ion leaching of chalcopyrite in varous lixiviants established by previous workers.

Lixiviant	$FeCl_3$-HCl	$Fe_2(SO_4)_3$-H_2SO_4
Kinetics	Linear and fast	Parabolic and slow
Sulphate formation (%)	2%	15-25%
Sulphur formation (%)	98%	75%
$Fe^{2+}/Cu^{2}+$	5	Varying
Activation energy ($KJmol^{-1}$)	20-60	60-80

It has been suggested that the ratio of ferrous-ion to copper is 5 (Dutrizac, 1978) during ferric chloride leaching. The 98% yields of sulphur and the ferrous-ion to copper ratio of 5 is strongly dependent on the purity of the chalcopyrite sample leached since it is impossible to separate sulphate contributions from the leaching of mineral impurities such as pyrite. The molar ratios of ferrous-ion to copper and ferrous-ion to sulphur increase from 5-13 and 2.5 to 5 respectively, with a decrease in chalcopyrite purity (Dutrizac, 1982). The ferrous-ion to copper ratio would be strongly dependent on the presence of rapidly leaching sulphide minerals which would reduce ferric-ion to ferrous-ion and also produce sulphate but not solubilise copper.

2.2.2.4 Effect of initial ferric-ion concentration.

The effect of the initial ferric-ion concentration on the rate of chemical ferric-ion leaching of chalcopyrite in ferric-sulphate media has been contradictory in literature. Table 2-2 indicates a summary of the more recent literature findings on the effect of the initial ferric-ion concentration on the rate of chalcopyrite leaching.

Most earlier studies have presented a rate dependency of rate $\propto [Fe^{+3}]^{1.5-}$ and have concluded that the rate is dependent of the ferric-ion concentration in sulphate media up to a certain limiting dilute concentration value at 0.01M (Dutrizac, *et al*, 1969; Baur *et al*, 1972; Wadsworth, 1972; Dutrizac and MacDonald, 1974; Beckstead *et al.*, 1976; Jones and Peters, 1976).

The dependency of the rate of leaching on the ferric-ion concentration is different in ferric-chloride and ferric-sulphate media. Later studies all report a lower power rate dependency on ferric-ion concentration for the oxidative leaching of chalcopyrite in ferric sulphate. However, many authors disagree with regards to the range of ferric-ion concentrations overwhich this dependency applies, as well as the quantitative nature of the dependency. It could be argued that an increase in reaction rate with increasing ferric-ion concentration would only be expected if reactant transport were the rate limiting step. Since the rate becomes diffusion limiting, it is no longer dependent on the initial ferric-ion concentration. Other workers showed via activation energy plots that the rate was completely independent of the initial ferric-ion concentration although the range of initial concentrations studied were larger than the critical concentration of 0.01M (Munoz *et al*, 1979).

Table 2-2 : Literature findings on the dependency of the rate of ferric leaching of $CuFeS_2$ on the $[Fe^{+3}]$ in chloride and sulphate media

Author	Range	Ferric chloride	Ferric sulphate
Sullivan, 1934	0.25-5%	-	Rate independent of $[Fe^{+3}]$
Beckstead *et al.*, 1976	0.5-2 M		Rate independent of $[Fe^{+3}]$
Jones and Peters, 1976	0.03-1M for sulphate media 0.1-1M for chloride media	rate $\propto [Fe^{+3}]^{0.3}$ for $[Fe^{+3}] < 1$ M Rate inhibition for $[Fe^{+3}] > 1$ M	Rate increase up to 0.01 M Rate inhibition beyond 0.01M
Dutrizac, 1978	0.001-0.2 M	rate $\propto [Fe^{+3}]^{0.8}$ for $[Fe^{+3}] < 0.01$ M rate independent of $[Fe^{+3}]$ for $[Fe^{+3}] >$ 0.01 M	-
Munoz *et al.*, 1979	0.06-0.5 M	-	rate independent of $[Fe^{+3}]$
Dutrizac, 1981	0.01-2 M	rate $\propto [Fe^{+3}]^{0.34}$	rate $\propto [Fe^{+3}]^{0.12}$
Hirato *et al.*, 1986	0.01-1M	rate $\propto [Fe^{+3}]^{0.5}$	-
Hiskey, 1993		rate $\propto [Fe^{+3}]^{0.5}$	Rate independent of $[Fe^{+3}]$
Hirato *et al.*, 1987	0.001-1M		rate $\propto [Fe^{+3}]$ up to 0.1M

In contrast, it was later shown that the rate is dependent on the initial ferric-ion concentration in ferric sulphate media between 0.01-2M (Dutrizac, 1981). The dependency of rate on the ferric-ion concentration in sulphate media has been confirmed by recent work which presented a first order rate dependence at very small ferric-ion concentrations (0.001-0.1 M), but differed in the critical limiting ferric-ion concentration value beyond which the rate independence is observed (Hirato *et al.* 1987). This declining effect of the ferric-ion concentration on the rate of chalcopyrite leaching with increasing ferric-sulphate concentration will be discussed later. It must be noted that all of the previous work on ferric-ion rate dependency was conducted at temperatures higher than 50 °C.

There is also little quantitative agreement on the rate dependency on the ferric-ion concentration in a chloride media, although the effect of the initial ferric-ion concentration is much more clearly seen in the case of chloride media as compared to sulphate media. This is partly due to the linear kinetics seen in the former case as opposed to the parabolic kinetics

seen in the latter case. Table 2-2 summarizes the literature findings in ferric chloride media. Most workers agree that the linear rate of ferric-ion leaching in chloride media clearly increases with increasing initial ferric-ion concentrations (Jones and Peters, 1976; Dutrizac, 1978; Dutrizac, 1981; Hirato *et al.*, 1986) All the workers present these findings at temperatures higher than 70 °C. The contradiction arises in the power dependence of the rate on the initial concentration of ferric-ion. Earlier work showed a 0.3 power dependence up to $[FeCl_3] = 1$ M presented at 90 °C (Jones and Peters, 1976; Ammou-Chokrum, 1979) This has been confirmed at 95 °C and 65 °C for natural chalcopyrite (Dutrizac, 1981). This finding is in contradiction to earlier work which found a 0.8 order dependence (Dutrizac, 1978) for synthetic chalcopyrite at 85°C. Later work has reported a 0.5 power dependence for natural chalcopyrire at 70 °C (Hirato *et al.*, 1986; Hiskey, 1993), which is close to the 0.3 dependence observed by previous workers. It could be argued that the rate dependency of ferric-chloride leaching of chalcopyrite is strongly dependent on the source of chalcopyrite and hence its purity. It appears that the power dependency of the rate on the initial ferric-chloride concentration is highest (0.8-1) for pure chalcopyrite and decreases to around 0.3-0.5 with an increase in mineral impurity. The rate of leaching of chalcopyrite has also shown to be directly dependent on the concentration of chloride-ions up to 0.5M in a ferric-sulphate media (Lu *et al.*, 2000).

2.2.2.5 The speciation of ferric-ion complexes in acidic ferric-sulphate

The speciation of ferric-ion complexes is of importance since there is evidence that the rate of chalcopyrite leaching is dependent on the free ferric-ion concentration (Dutrizac, *et al*, 1969; Baur *et al*, 1972; Wadsworth, 1972; Dutrizac and MacDonald, 1974; Beckstead *et al.*, 1976; Jones and Peters, 1976, Dutrizac, 1981, Hirato *et al.*,1987). The stable ferric-ion complexes in the aqueous ferric-sulphate-sulphuric acid, $Fe_2(SO_4)_3$-H_2SO_4, solutions are free ferric-ion, Fe^{3+} , ferric-sulphato, $FeSO_4^+$, and ferric-bisulphato, $FeHSO_4^{2+}$, complexes (Sapieszko *et al.*, 1977). The distribution of free ferric-ion in relation to ferric-sulphato and ferric-bisulphato complexes would determine the actual concentration of free ferric-ion, which forms the primary oxidising agent during the chalcopyrite leaching process. Literature has shown that the leaching rate of chalcopyrite shows an approximate first order dependency on the ferric-ion concentration up to a certain limiting dilute concentration value. It is generally accepted that this dependency refers to the free ferric-ion concentration only since it is thought to be the only leaching agent in solution.

Recent work indicates that this limiting concentration is 0.1M ferric-sulphate (Hirato *et al.*,1987) while earlier work showed it to be 2M (Dutrizac, 1981). Beyond this concentration, the leaching rate is shown to be independent of the ferric-sulphate concentration. This decreasing effect of the ferric-sulphate concentration of the leach rate could be explained by examining the speciation of ferric-sulphate in aqueous sulphuric acid solutions (Hirato *et al.*, 1987). The formation of the $FeSO_4^+$ and $FeHSO_4^{2+}$ complexes together with the aqueous dissociation of sulphuric acid are shown in Equations (2.2.3), (2.2.4) and (2.2.5) and (2.2.6) respectively;

$$Fe^{3+} + SO_4^{2-} \mapsto FeSO_4^+ \qquad (2.2.3)$$

$$Fe^{3+} + HSO_4^- \mapsto FeHSO_4^{2-} \qquad (2.2.4)$$

$$H_2SO_4 \mapsto 2H^+ + SO_4^{2-} \qquad (2.2.5)$$

$$H_2SO_4 \mapsto H^+ + HSO_4^- \qquad (2.2.6)$$

Furthermore, the material balances for the total iron,[Fe], total sulphur, [S], and total hydrogen,[H], concentrations are shown in Equations (2.2.7), (2.2.8) and (2.2.9) respectively;

$$[Fe] = [Fe^{3+}] + [FeSO_4^+] + [FeHSO_4^{2+}] \qquad (2.2.7)$$

$$[S] = [FeSO_4^+] + [FeHSO_4^{2+}] + [SO_4^{2-}] + [HSO_4^-] \qquad (2.2.8)$$

$$[H] = [H^+] + [FeHSO_4^{2+}] + [HSO_4^-] \qquad (2.2.9)$$

The extent of formation of $FeSO_4^+$, $FeHSO_4^{2+}$ and HSO_4^- is dependent on the equilibrium constant. The speciation varies with temperature since the equilibrium constants are functions of temperature. The variation in the equilibrium constants of $FeSO_4^+$, $FeHSO_4^{2+}$ and HSO_4^- with temperature is shown in Equations (2.2.10), (2.2.11) and (2.2.12) (Dry, 1984) respectively.

$$K_{FeSO_4^+} = \exp\left[\ 900.421 + \frac{39111}{T} + 136.6\ln(T)\right] \qquad (2.2.10)$$

$$K_{FeHSO_4^{2+}} = \exp[\ 33.3 - \frac{7630}{T}] \qquad (2.2.11)$$

$$K_{HSO_4^-} = \exp[14.031 - \frac{2835}{T}] \qquad (2.2.12)$$

The variation of the equilibrium constants for the formation of $FeSO_4^+$, $FeHSO_4^{2+}$ and HSO_4^- with temperature is shown in Figure 2.1.

From Figure 2.2.1 it is clear that the temperature has a greater effect on the speciation of the stable ferric-ion complexes than HSO_4^-.

Hirato *et al.*,(1987) used the material balances in (2.5), (2.6) and (2.7) and the equilibrium constants, 1020 and 4 at 353 K for the formation of $FeSO_4^+$ and $FeHSO_4^{2+}$ (Sapieszko *et al.*, 1977) respectively, together with the dissociation constant for the formation of HSO_4^-, enables the prediction of the $[Fe^{3+}]$, $[FeSO_4^+]$ and $[FeHSO_4^2]$ as a function of $[Fe_2(SO_4)_3]$, knowing the solution pH (and therefore the $[H^+]$ and $[HSO_4^-]$).

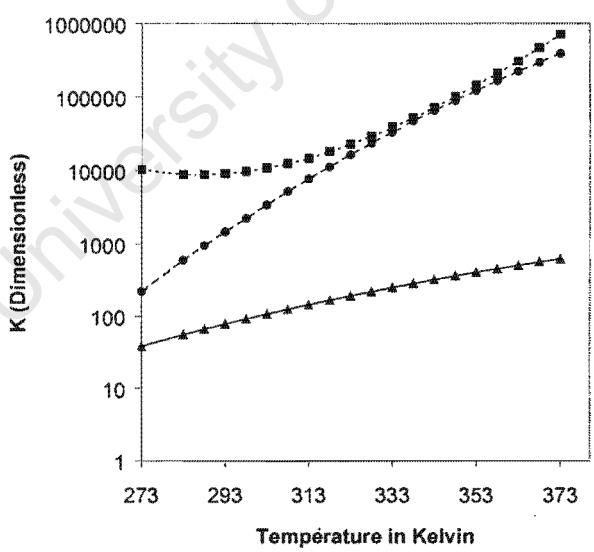

Figure 2.2.1: The variation of equilibrium constants with temperature for the formation of [■]$FeSO_4^+$, [●]$FeHSO_4^{2+}$ and [▲] HSO_4^- (Dry, 1984)

This calculation shows that the $[Fe^{3+}]$ and $[FeHSO_4^2]$ increases with an increase in $[Fe_2(SO_4)_3]$ only up to 0.1M, but declines at higher concentrations of $[Fe_2(SO_4)_3]$. The $[FeSO_4^+]$ increases linearly even at $[Fe_2(SO_4)_3]$ larger than 0.1M. For this reason the $[Fe^{3+}]$

and [$FeHSO_4^{2}$] is thought to play a vital role in the leaching of chalcopyrite with $Fe_2(SO_4)_3$ since they are more easily reduced to ferrous-ion complexes than [$FeSO_4^{+}$]. The declining dependence of the rate of chalcopyrite leaching with increasing ferric-sulphate concentration is thought to be due to speciation of the ferric-sulphate complexes in the presence of sulphuric acid (Hirato *et al.*, 1987).

2.2.2.6 The effect of the ferric/ferrous-ion ratio

Earlier work has shown a reduction in the rate of leaching rate of chalcopyrite in the presence of high ferrous-ion concentrations (Dutrizac and McDonald, 1969; Jones and Peters, 1976; Linge, 1976;) while others showed that the kinetics were independent of the ferrous-ion concentration in solution (Beckstead *et al.*, 1976, Munoz *et al.*, 1979) in ferric-sulphate media.

Recent work has shown that the rate of chalcopyrite oxidation is enhanced by the presence of ferrous-ions (Hiroyoshi *et al.*, 1997; Hiroyoshi *et al.*, 1999; Hiroyoshi *et al.*, 2000). This suggests that the rate of chalcopyrite leaching is strongly dependent on the redox potential of solution instead of the absolute ferric and ferrous-ion concentrations. This postulation has been confirmed by the reworking of earlier work which measured the rate of chalcopyrite leaching at constant redox potentials via the controlled addition of permanganate. The rate is shown to increase with increasing redox potential until a maximum is reached at 450mV (SCE). The rate then decreases with a further increase in the redox potential $KMnO_4$ (Kametani and Aoki, 1985). The methadology employed in reworking this literature data is seen in section 2.4 of this chapter.

Figure 2.2.2 expresses the variation in the initial rate of ferrous-ion production from chalcopyrite oxidation as functions of the initial ferric/ferrous-ion ratios for reworked literature data (Dutrizac, 1981; Hirato *et al.*, 1987). In both cases the literature rates were originally expressed as rates of chalcopyrite oxidised. Both authors concluded a decrease in leaching rate with increasing ferrous-ion concentration but did not express the rate of leaching as a function of the ferric to ferrous-ion ratio. In Figure 2.2.2 the rate data presented by Dutrizac, 1981 was reconverted and expressed as specific surface area rates ie moles Cu^{2+} formed per available surface area of chalcopyrite per unit time. This rate was then stochiometrically converted via Equation 2.2.1 to the rate of ferrous-ion produced per available surface area of chalcopyrite. In both cases the authors determined the rate of copper dissolution from the ferric-sulphate leaching of chalcopyrite during the initial linear phase of reaction. The rates are therefore indicative of the reaction control phase of the reaction.

The effect of temperature in clear in Figure 2.2.2 since the area specific rates presented by Hirato *et al*, (1987) at 70 °C are an order of magnitude smaller than those presented by Dutrizac, (1981) at 90 °C. It is apparent from Figure 2.2.2 that the rate of leaching of chalcopyrite increases with an increase in the initial ferric/ferrous-ion ratio up to ferric/ferrous-ion ratio's of 1 or conversely decreases with a decrease in the ferric/ferrous-ion ratio up to 0.2. The rate appears to be unchanged by any further decrease in the initial ferric/ferrous-ion ratio beyond 0.2. This result is in contradiction of the earlier work which concluded minimal rate dependency on the ferrous-ion concentration (Beckstead *et al.*, 1976, Munoz *et al.*,1979).

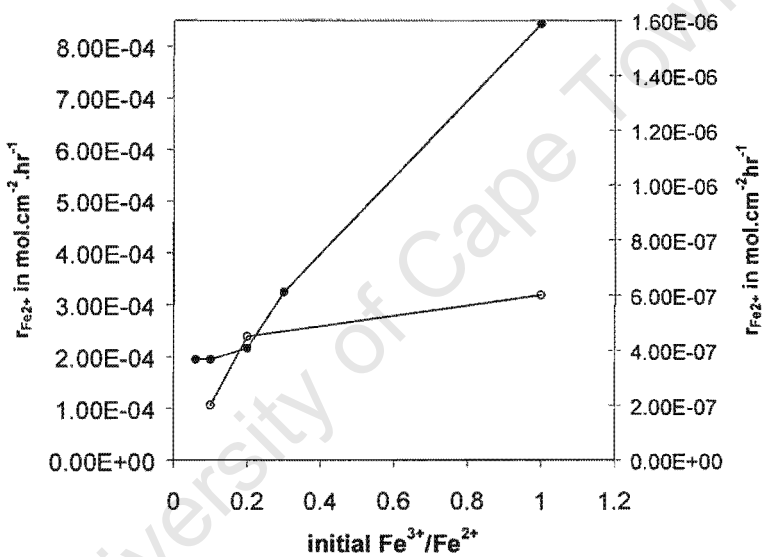

Figure 2.2.2: The rate of ferrous production (mol $Fe^{2+}cm^{-2}hr^{-1}$) calculated using the stochiometry of equation 1.1 from the rate of chalcopyrite oxidation as a function of the initial ferric/ferrous-ion ratio as shown by [•] Dutrizac, 1981 at 90 °C on the left axis and [o] Hirato *et al.*, 1987 at 70 °C on the right axis for the ferric-ion leaching of chalcopyrite

Figure 2.2.3 expresses the calculated rates of ferrous-ion production per cm^2 of chalcopyrite for the chemical ferric leaching of chalcopyrite of the data reworked from published literature (Kametani and Aoki, 1985). The ferric/ferrous-ion ratio was calculated from the measured redox potential by using theoretical values for E^0 and RT/zF at 90 °C via the Nernst equation. The rates presented as a function of the ferric/ferrous-ion ratio in Figure 2.2.2 and 2.2.3 are indicative of the increasing region shown before 450mV (SCE). Both figures express the rates in similar units. The rates seen in Figure 2.2.3 (Kametani and Aoki, 1985) at temperatures of 70 °C are in the same order of magnitude to those of figure 2.2 (Hirato *et al.*, 1987) at the same temperature. However, the rates in Figure 2.2.3 (Kametani and Aoki, 1985) at 90 °C are two orders of magnitude smaller than those in 2.2.2 (Dutrizac, 1981)

despite the common basis and temperature. This difference in rates can possibly be attributed to the difference in mineral sample composition. The work conducted by Dutrizac, (1981) was performed on pure chalcopyrite, while that used by Kametani and Aoki, (1985) was only 75 % pure chalcopyrite.

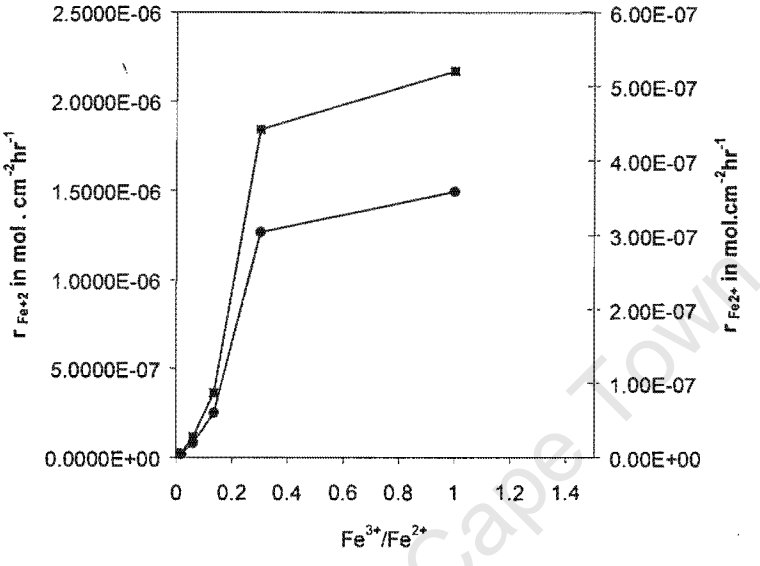

Figure 2.2.3: The of ferrous-ion production expressed per area of chalcopyrite (mol Fe^{2+} cm^{-2} $CuFeS_2$ hr^{-1}) from the chemical ferric-sulphate leaching of chalcopyrite as a function of the ferric/ferrous-ion ratio from the reworking of literature data (Kametani and Aoki, 1985) at [■] 90 °C on the left axis and [●]70 °C on the right axis.

2.2.2.7 Passivation of chalcopyrite during chemical leaching

The kinetic of chemical leaching of chalcopyrite has been shown to retard due to passivation by the build-up of product layers which result in diffusional limitations (Jones and Peters, 1976; Dutrizac 1978; Munoz *et al.* 1979; Hirato *et al.* 1987; Dutrizac,1989). This film then has the following possible effects :

1. It slows the rate of transfer of attacking oxidant species or ion from the bulk electrolyte to the chalcopyrite reaction surface .

2. It slows the rate of transfer of electrons and product ions and species from the reacting surface to the bulk electrolyte.

3. It slows the speed of electron transfer to the oxidants in the bulk electrolyte.

4. It allows the transfer of ions from the electrolyte to the surface or visa versa but is electronically insulating

5. It follows on to entirely coat the surface and prevent the attacking oxidant ion from contacting the active $CuFeS_2$ surface.

The nature of the passivating layer during the ferric leaching of $CuFeS_2$ has not been conclusively established. Table 2-3 presents a review of the nature of this layer speculated by previous workers.

Table 2-3: The nature of the passivating layer and its effect on ion , electron and species transport during the ferric leaching of chalcopyrite presented by previous workers

Author	Nature of layer	Effect on transport
Jones and Peters, 1976; Dutrizac 1978; Munoz *et al.* 1979; Hirato *et al.* 1986; Dutrizac,1989, Klauber *et al.*, 2000	Porous Sulphur ,	1 or 2 or 3 or 5
Braithwaite *et al.* 1976; Dutrizac, 1978	Iron precipitates like Hermatite or Jarosite and Sulphur	1 or 2 or 3 or 5
McMillan *et al.*, 1982	Solid Electrolyte Interphase made up of polysulphides	4
Tiwari *et al.* 1980; Parker *et al.* 1981	A semiconducting iron deficient polysulphide layer like Covellite(CuS) or Chalcocite(Cu_2S) or Bornite(Cu_5FeS_4)	1 or 2 or 3
Warren *et al.* 1982; Biegler and Horne, 1985; Holliday and Richmond, 1990; Hiskey, 1993; Hackl *et al.*, 1995, Gomez *et al.*, 1996	Two iron deficient polysulphide layers of differing nature like CuS and Cu_2S	1 or 2 or 3

Ammou Chokroum *et al.*, 1979	Iron difficient polysulphides like CuS and Cu_2S layers and Sulphur	1 or 2 or 3 or 5

In all of these studies the nature of these films have been established via detailed surface analysis of the leached or electrolysed $CuFeS_2$ either by SEM photomicrographs coupled with X-ray Diffraction Analysis , X-ray Photoelectron Spectroscopy or Auger Electron Spectroscopy. Earlier work (Ammou-Chokroum, 1979; Dutrizac, 1982, Dutrizac, 1989; Hirato *et al.* 1987) as well as a recent study (Kluaber et al., 2000) has evidently proven that the sulphur morphology had a strong effect on the nature of the passivating layer. In contrast, electrochemical studies have discounted the idea that sulphur alone passivates the rate and have proposed the build-up of electronically insulating polysulphide layers (Tiwari *et al.* 1980; Parker *et al.* 1981; McMillan *et al.*, 1982; Warren *et al.* 1982; Biegler and Horne, 1985; Holliday and Richmond, 1990; Hiskey, 1993; Hackl *et al.*, 1995, Gomez *et al.*, 1996)

It appears that sulphur formation and coating of the surface is not solely responsible for passivation but does in itself contribute to the some form of diffusional rate limitation during the ferric leaching of chalcopyrite. A more likely explanation would be a dual contribution of copper polysulphides and sulphur , each playing a dominant role in various stages of the passivating mechanism. The thickness of this layer has not been conclusively established. Literature has also been vague as to whether the sulphide layer passivates the entire surface or only sections of it.

2.3 Bioleaching of chalcopyrite

The purpose of this section is to critically analyse the literature presented on the bioleaching of chalcopyrite in order to establish an initial understanding of the mechanism, kinetics and products associated with the process and to propose a state-of-the-art. The first section of this review introduces the mesophilic organisms relevant to chalcopyrite bioleaching. The effect of operating parameters such as mineral particle size, pH, temperature and ferric or ferrous-ion concentrations or redox potentials on the kinetics of bioleaching will be highlighted. In addition, suggested reasons for the slow rate of copper extraction during the process will be alluded to in more extensive detail when dealing with the chemical leaching of chalcopyrite by ferric-ion. The literature analysis on the subject has been complicated by the fact that most previous work is confined to kinetics studies to test the bioleachability of copper-sulphide concentrates containing chalcopyrite. These studies, although useful in obtaining information on the observed kinetics, provides very little in termes of mechanistic information. The information from literature on chalcopyrite bioleaching has been systematically classified according to the following catergories each dealing with the type of information which can be analysed.

1. Mechanistic studies on pure chalcopyrite
2. Kinetic studies of copper sulphides containing large proportions of chalcopyrite
3. Kinetic studies on the effects of various physical parameters, ie, pH, particle size, temperature and solids concentration, Ferric and ferrous-ion concentrations.
4. Kinetic studies on the effects of natural galvanic interactions which enhance chalcopyrite bioleaching
5. Electrochemical studies on the bioleaching of chalcopyrite
6. Kinetic studies on the effects of added chemical agents like silver-chloride which enhance chalcopyrite bioleaching.

2.3.1 Mesophilic Bacteria

Mesophilic bioleaching of chalcopyrite is performed by the catalytic action of aerobic, acidophilic, obligately autotrophic bacteria. Acidophilic refers to the group of bacteria which are only capable of growing under pH values of 4. In addition, the term mesophiles is further classification involving the temperature range of 25-40 °C which is deemed optimal for bacterial growth. Table 2-4 lists the mesophilic bacteria most commonly found in sulphide mineral bioleaching systems,.along with their respective substrates.

Most of the research has been performed on *Acidithiobacillus ferrooxidans* since this was the organism thought to be responsible for mineral sulphide bioleaching. Recent work has shown that *Leptospirillum ferrooxidans* is the most commonly found organism in mesophilic bioleaching systems involving pyrite and arsenopyrite. (Rawlings *et al.* 1999(a); Boon, 1996, Breed, 2000). It is believed that the range of operating redox potentials plays an important role in the selection of a dominating bacterial species during the bioleaching of sulphide minerals.

Acidithiobacillus ferrooxidans gains energy for metabolic growth from electrons donated via the oxidation of ferrous-ion, sulphur or reduced sulphur compounds, while *Leptospirillum ferrooxidans* is only able to do so via the oxidation of ferrous-ion alone. *Acidithiobacillus thiooxidans* is only able to oxidise sulphur or sulphur compounds. The electron transport chain involved in the mechanism of growth of *Acidithiobacillus ferrooxidans* by ferrous-ion oxidation has been reviewed by Ingledew (1982). It becomes difficult to differentiate between the iron and sulphur oxidising *Acidithiobacillus ferrooxidans* strains since it is suggested that this organism are able to switch between iron and sulphur oxidising abilities (Corbett *et al.*, 1987; Suzuki, 1990; Breed, 2000)

Table 2-4: General Characteristics and substrates utilized by the most commonly encountered autotrophic mesophilic bioleaching organisms (Rawlings, 1997; Breed, 2000).

Mesophilic micro-organism	Shape and size in length	Substrate utilized
Acidithiobacillus ferroxidans	Rod-shaped at 0.9-2 μm	Ferrous-ion, Sulphur, Reduced Sulphur compounds, sulphide minerals
Acidithiobacillus thiooxidans	Rod-shaped at 0.9-2 μm	Sulphur, Reduced sulphur compounds
Leptospirillum ferrooxidans	Spiral shaped at 0.5-3 μm	Ferrous-ion

Recent work has also suggested that *Acidithiobacillus ferrooxidans* grows anaerobically by reducing ferric-ion to ferrous-ion in the presence of sulphur compounds (Pronk *et al.*, 1992).

2.3.2 Mechanism and stochiometry

Earlier work has presented the overall reaction for the bioleaching of chalcopyrite with *Acidithiobacillus ferrooxidans* according to Reaction (2.3.1) (Sakaguchi, *et al.* 1976; Berry *et al.*, 1978; Bosecker *et al.* 1979)

$$4CuFeS_2 + 17O_2 + 2H_2SO_4 \mapsto 4CuSO_4 + 2Fe_2(SO_4)_3 + 2H_2O \qquad (2.3.1)$$

These workers assumed that bacterial oxidation of the metal sulphides was as a result of an enzymatic attack which resulted in the sulphur moiety being oxidised directly to sulphate without any intermediate. This hypothesis has lead to the assumption that bacterial attachment to the chalcopyrite surface is pertinent to its dissolution during bioleaching, which resulted in a number of studies on the role of bacterial attachment in the bioleaching process. These studies will be discussed later.

In contrast, other workers who employed the same batch, shake flask experimental technique did not include the contribution from acid leaching and formulated Reaction (2.3.2) as the overall bioleaching reaction with *Acidithiobacillus ferrooxidans* and only presented the formation of ferrous and copper sulphate (Shrihari *et al.*, 1991). These workers also acknowledged the contribution of chemical leaching (Reaction (2.2.1)) along with Reaction (2.3.1) during the bioleaching mechanism (Torma, 1987; Kingma *et al.*, 1980; Bhattacharya *et al.*, 1990; Rossi, 1990; Balaz *et al.*, 1991, Shrihari *et al.*, 1991; Jordan *et al.*, 1993).

$$CuFeS_2 + 4O_2 \mapsto CuSO_4 + FeSO_4 \qquad (2.3.2)$$

Recent work presented both Reaction (2.3.1) as the overall reaction but maintained that the action of bacteria was not enzymatic but involved the oxidation of ferrous-ion and sulphur substrates formed during chemical oxidation of the mineral. These workers showed that Reaction (2.3.1) might hold for the overall stochiometry but was inturn made up of Reactions (2.3.2)-(2.3.5) which consist of the chemical leaching of chalcopyrite, bacterial ferrous-ion oxidation and bacterial sulphur oxidation respectively (Boon *et al.*, 1993). This two-step mechanism consisting of chemical leaching and bacterial ferrous-ion oxidation has been confirmed for the case of pyrite bioleaching with *Acidithiobacillus ferrooxidans* and *Leptospirillum ferrooxidans* (Boon, 1996).

$$CuFeS_2 + 2Fe_2(SO_4)_3 \mapsto CuSO_4 + 5FeSO_4 + S \qquad (2.3.2)$$

$$2FeSO_4 + 0.5O_2 + H_2SO_4 \mapsto Fe_2(SO_4) + H_2O \quad (2.3.4)$$

$$2S + 2H_2O + 3O_2 \mapsto 2H_2SO_4 \quad (2.3.5)$$

This two step mechanism is extended to the multiple sub-process mechanism for sulphide minerals and the polysulphide mechanism for chalcopyrite bioleaching in particular by Sand *et al.*, (1999). This mechanism is presented in Chapter One who confirmed that chalcopyrite is dissolved by the action of chemical species like ferric-ion or protons only. This was done by the analysis of the degradation products occurring during the bioleaching reaction and the analysis of the extracellular polymeric substances (EPS layer) which envelopes the cell and allows attachment to the mineral surface. An analysis of the pH, redox potential and ion concentration in this layer showed that it was the reaction compartment where ferrous-ion released from chemical mineral oxidation was oxidised to ferric-ion. Two mechanisms for the degradation of sulphide minerals in the presence of bacteria were proposed depending on the intermediate compounds seen during the bioleaching reaction and the semi-conducting properties, electronic structure and crystal lattice of the sulphide mineral. Since chalcopyrite is amenable to an acid attack it follows the polysulphide mechanism (Sand *et al.*, 1999).

Table 2-5 lists the conditions and observed products for most of the earlier studies on chalcopyrite bioleaching with *Acidithiobacillus ferrooxidans*. In most cases batch, shake flask experiments were conducted with chalcopyrite containing copper sulphides by measuring dissolved species like copper and ferrous-ion during bioleaching at temperature ranges from 30-35 °C and pH's between 1-6.

All the studies presented in Table 2-5 observed the formation of copper sulphate and ferric sulphate. A literature analysis of the products from the bioleaching of chalcopyrite has been hampered by presence of other mineral impurities other than chalcopyrite in most of the concentrates previously studied. There has been no consistency on the formation of sulphuric acid during the bioleaching of chalcopyrite. Most workers controlled the pH but others observed an initial increase followed by a decrease in pH during the course of bioleaching (Sakaguchi *et al.*, 1976; Bosecker *et al.*, 1979; Khinvasara *et al.*, 1987; Toro *et al.*, 1989). This suggests initial acid consumption followed by acid formation during the bioleaching reaction. In contrast later work (Bevilaqua-Mascarin *et al.*, 1999) observed an increase in the

Table 2-5: Literature studies on the batch bioleaching of chalcopyrite concentrates by *Acidithiobacillus ferrooxidans*

Author	Conditions pH, Temp, % solids, particle size, leach time	Concentrate	Products	Rate of Copper extraction ($mgl^{-1}hr^{-1}$)
Sakaguchi *et al.*, 1976	PH uncontrolled decreasing from 3.2-1.4 T= 25-45 °C 1-25 % solids 37 um 400 hrs	Pred. $CuFeS_2$	Copper	215 at pH=2.3, T =35 °C, 22% solids
Berry *et al.*, 1978	PH controlled at 2.1 T= 28 °C -6um 1344 hrs	$CuFeS_2/FeS_2$	Copper Ferric-ion Ferrous-ion Sulphuric acid	-
Bosecker *et al.*, 1979	PH uncontrolled decreasing from 3.5-2 35 °C 37 um 720 hrs	Pred. $CuFeS_2$	Copper Sulphuric acid	40
Kingma *et al.*, 1980	PH controlled at 2.2 T= 27 °C 500 hrs	$CuFeS_2/PbS$	Copper Cell protein	20.6
Khinvasara *et al.*, 1987	PH uncontrolled decreasing from 6-2 T=25 °C 106 um 40% 1140 hrs	Pred $CuFeS_2$	Copper	-
Briceno *et al.*,	PH controlled at	Pred $CuFeS_2$	Copper	10 at 5% solids

1988	2 T=30 °C 150-400 mesh 5, 10% 670			16 at 10%
Toro *et al.*, 1989	PH uncontrolled decreasing from 3-1.5 T = 30 °C -38 um 5, 10, 20 % 408 hrs	Pred. $CuFeS_2$	Copper Ferric-ion Sulphate	10 at 5 % solids 20 at 10% solids 30 at 20 % solids
Almendras *et al.*,1989	PH controlled at 1.6 T=30 °C -325 mesh 0.5% , 500 hrs	$CuFeS_2$	Copper Bacterial cells Ferrous-ion Ferric-ion Sulphur	24
Balaz *et al.*, 1991	PH controlled at 2 T = 30 °C -100um 20% 600 hrs	Chemically leached $CuFeS_2$	Copper	-
Shrihari *et al.*, 1991	PH controlled at 2 T= 30 °C 63-74; 150-335; 1000-1400 um 20% 1800 hrs	$CuFeS_2$	Copper Ferrous-ion Ferric-ion	5 for 63-74 um 23 for 150-335 um 66 for 1000-1400 um
Jordan *et al.*, 1993	PH control at 1.2 T= 30 °C 5% 900hrs	$CuFeS_2$/ZnS	Copper Ferrous-ion Sulphur Sulphate	66

Bevilaqua-Mascarin *et al.*, 1999	Uncontrolled pH Increasing 2-3.5 T= 30 °C -200 um 2.5 % 1140 hrs	$CuFeS_2$	Copper Ferrous-ion Ferric-ion	11.8 at initial Fe^{3+}/Fe^{2+} of 100 54.3 at initial Fe^{3+}/Fe^{2+} of 0.016
Hiroyoshi *et al.*, 1999	PH control at 1.8 T= 30 °C 1 % 168 hrs	$CuFeS_2/ZnS$	Copper Ferrous-ion Total-iron	50.4 mgl^{-1} Cu without additional Fe^{2+} 252 mgl^{-1} Cu with 0.04 $moll^{-1}$ Fe^{2+}
Third *et al.*, 2000	PH control at 1.5 T= 37 °C 45 um 4 % 350 hrs	$CuFeS_2/FeS_2$	Copper Ferrous-ion	63 at 10% innoculum 18.3 at 50% innoculum

pH during prolonged bioleaching. This suggests only acid consumption during the bioleaching of chalcopyrite. It could be argued that the observed pH trend is dependent on the purity of the chalcopyrite concentrates and the contribution of acid formation from the bioleaching of other mineral sulphides, as well as the relative concentration of the sulphur oxidising bacteria in the system.

Two studies (Almendras *et al.*, 1987; Jordan *et al.*, 1993) were able to measure sulphur from the mineral residue after mesophilic bioleaching, suggesting that not all the sulphur formed during chemical leaching is oxidised to sulphate.

2.3.3 Effect of parameters on the kinetics of bioleaching of chalcopyrite

All the authors listed in Table 2-5 have established the kinetics of chalcopyrite bioleaching by measuring amount of copper solubalised during a batch run. The shape of the dissolved metal species vs time curve is parabolic in all cases. A rapid initial linear rate is observed which decreases. This shape is similar to the kinetic curves observed for the case of chemical ferric-ion leaching as will be shown in the next section. Listed in Table 2-5 are the rates of copper

dissolution either presented by the workers themselves or estimated from the e slope of dissolved copper vs time curves when presented in the studies. These rates differ significantly depending on the conditions of the solids loading, temperature, mineral particle size, leach time and ferric or ferrous-ion concentrations.

2.3.3.1 Effect of solids loading

Earlier workers observed a linear increase in the rate with solids loading up to 20 % (Sakaguchi *et al.*, 1976; Toro *et al.*, 1989). Other workers confirmed this effect by changing the solids concentration from 5 to 10 % which corresponded to an increase in rate from 10 to 16 $mgl^{-1}hr^{-1}$ (Briceno *et al.*, 1988). The rate of bioleaching is directly proportional to the solids concentration prescribed, if sufficient oxygen and carbon dioxide is supplied to prevent any growth limitations. This is consistent with more recent findings on the effect of solids concentration on the biooxidation of gold-bearing sulphides (Bailey, 1993).

2.3.3.2 Effect of temperature

Earlier work reported an that the rate of mesophilic bioleaching is maximum at 35 °C, and then decreases with a further increase in temperature up to 45 °C. The same study reported an activation energy of 50.2 $KJ.mol^{-1}$ (Sakaguchi.*et al.*, 1976). Reasons for the apparent decrease in rate with an increase in temperature beyond 35 °C is not presented. It must be noted from this result that the observed optimum is also the optimum temperature for the rate of ferrous-ion oxidation by *Acidithiobacillus ferroxidans* (Boon, 1996). It could be argued that a higher temperature of operation (45 °C) resulted in the thermal degradation of the bacteria, since this temperature value is well beyond the limit for the existence of *Acidithiobacillus ferrooxidans*, and the subsequent shifting of the mechanism from a bacterial leach to a chemical leach. It is difficult to quantify a temperature effect by comparing the rates for the various studies in table 2-5, even though some studies were performed at different temperatures. These studies do not exhibit any common particle size or solids loading.

2.3.3.3 Effect of pH

The effect of pH on the bioleaching of chalcopyrite is not well studied. Earlier work reported an optimum pH of 2.3 at 35 °C (Sakaguchi *et al.*, 1979). Subsequent studies have only

reported pH trends (Boesecker *et al.*, 1979; Khinvasara *et al.*, 1987; Toro *et al.*, 1989; Bevilaqua-Mascarin *et al.*, 1999).

2.3.3.4 Effect of leachable surface area

Earlier work reported an increase in the rate of bioleaching with decreasing particle size (Ehrlich *et al.*, 1967) and specifically a exponential increase in the rate of column bioleaching of chalcopyrite with *Acidithiobacillus ferrooxidans* with decreasing particle size for a coarse size range of +4760 – 45000 um (Bruynesteyn *et al.*, 1974). The authors concluded that the rate of bioleaching was not directly proportional to the available surface area because it is influenced by the solids loading and the depth of penetration of the bacterially contained liquor into the column.

Other authors used the shrinking core model to relate the decreasing rate of chalcopyrite bioleaching with the decreasing particle diameter. The authors simulated the decrease in chalcopyrite concentration during bioleaching and found it compare relatively accurately with that observed during experimentation. However it still remains unclear as to the methods employed in estimating the decrease in chalcopyrite concentration during the experiment (Bhattacharya *et al.*, 1990).

The improvement of the bioleaching rate by virtue of an increased available surface area due to a lower particle size has been confirmed in recent studies for particle size ranges between 0.3-177 um (Blancarte-Zurita *et al.*, 1986; Espejo *et al.*, 1987; Balaz *et al.*, 1996). In contrast to the conventional reasoning a recent study has reported the opposite effect (Shrihari *et al.*, 1991). These authors observed an increased rate of leaching with an increase particle size (see table 2-5) inspite of the larger surface area offered by the smaller particles and attributed this phenomenon to the greater attachment efficiency of the bacteria on larger particles.

2.3.3.5 Effect of ferric and ferrous-ion concentrations.

Earlier workers concluded that the rate of chalcopyrite bioleaching would be directly proportional to the bacterial concentration (Sakaguchi *et al.*, 1976). However, according to the multiple sub-process mechanism, the rate of copper extraction is essentially the rate of ferric-leaching of chalcopyrite since ferric-ion is thought to be the primary oxidising agent during bioleaching. The bacteria only act as the generators of the primary oxidant. This implies that the rate of chalcopyrite bioleaching would be directly dependent on the concentration of ferric-ion in solution since it is the primary oxidant species.

In contrast, recent work has shown that increases in the concentration of ferric sulphate does not necessarily result in a corresponding increase in the either the rate of chemical leaching (Munoz *et al.*, 1979, Dutrizac, 1981; Hirato *et al.*, 1987; Hiroyoshi *et al.*, 1997; Hiroyoshi *et al.*, 2000) or bioleaching of the mineral (Almendras *et al.*, 1987; Hiroyoshi *et al.*, 1999; Third *et al.*, 2000).

Table 2-5 also shows the final calculated rate of copper dissolution from the bioleaching of chalcopyrite with *Acidithiobacillus ferrooxidans* increased by 4 times when the initial ferric/ferrous-ion ratio was lowered by a factor of 10 000. (Bevilaqua-Mascarin *et al.*, 1999). (The rates of copper dissolution in each case was calculated from the slope of the copper vs time curves). Hiroyoshi *et al.*, 1999 established a five fold increase in the final amount of copper extracted by comparing chalcopyrite batch bioleaching runs with *Acidithiobacillus ferrooxidans*, in the presence and absence of an initial amount of 0.04 $mol.l^{-1}$ ferrous-ion. Although the initial ferric-ion concentration is not reported in this study, it could be argued that the initial ferric/ferrous-ion ratio was much lower in the presence the additional ferrous-ion.

The effect of an increasing rate of bioleaching with increasing cell concentration for chalcopyrite bioleaching with *Acidithiobacillus ferrooxidans* has also been reported by workers who found that the final concentration of extracted copper from a batch run increased by a factor of 2 when the cell number used in the experiments was increased 10 fold (Hiroyoshi *et al.*, 1997). In contrast to this result, Table 2-5 shows that the rate of bioleaching of chalcopyrite was also found to be three times smaller when using five times as much bacteria (Third *et al.*, 2000).

Recent workers have reported that the rate of chalcopyrite bioleaching is enhanced at high ferrous-ion concentrations and suppressed at high ferric-ion concentrations (Hiroyoshi *et al.*, 1999; Bevilaqua-Mascarin *et al.*, 1999; Hiroyoshi *et al.*, 2000). This means that the rate is faster at low ferric/ferrous-ion ratios. These results are consistent with that observed for the case of chemical leaching of chalcopyrite (Kametani and Aoki, 1985, Dutrizac, 1981, Hiroyoshi *et al.* 2000) as was discussed in the previous section and that which is obtained by establishing the rate of ferric leaching as a function of the ferric/ferrous-ion ratio by the reworking of published literature, shown in section 2.4 of this chapter.

2.3.4 Galvanic interaction between sulphide minerals during bioleaching

Galvanic interactions are of interest in this work because the concentrates used in the experiment contains proportions of pyrite and chalcopyrite.

The selective dissolution of chalcopyrite over pyrite been reported by a number of workers during the chemical leaching and bioleaching of concentrates containing both minerals (Ahonen *et al.*, 1986; Berry *et al.*, 1978; Mehta *et al.*, 1982; Mehta *et al.*, 1983, Natarajan, 1988; Jyothi *et al.*, 1989, Natarajan, 1992). This is due to the formation of galvanic couples between mineral species, whereby the mineral with the lower rest potential acts as an anode, while the mineral with the higher rest potential becomes cathodically protected (Natarajan, 1988). The various factors affecting galvanic interactions are the relative electrochemical activity of the mineral (which depends on its rest potential), the relative surface area between the minerals in contact, the presence of redox species in the solution (Jyothi *et al.*, 1989). The measured rest potential values in a bioleach system for commonly found sulphide minerals in order of increasing electrochemical activity is shown in Table 2-6

Table 2-6: Galvanic series for commonly found sulphide minerals in systems containing bacteria (Jyothi *et al.*, 1989)

Sulphide Mineral	Rest potential (mV vs SHE)
Pyrite	450
Chalcopyrite	310
Sphalerite	-50

The values in Table 2-6 indicate that sphalerite would be preferentially leached over chalcopyrite, and chalcopyrite over pyrite in concentrates containing the above three mineral sulphides. This has been confirmed by earlier studies during the bioleaching of a chalcopyrite/pyrite/sphalerite concentrate with *Acidithiobacillus ferroxidans* (Berry *et al.*, 1978, Mehta *et al.*, 1982) and a pyrite/chalcopyrite concentrate (Jyothi *et al.*, 1989).

2.4 Literature predictions on the effect of ferric/ferrous-ion ratio on the chemical rate of chalcopyrite leaching.

The rate of ferric leaching of pyrite and arsenopyrite has been shown by others (May *et al.*, 1997; Ruitenberg *et al.*, 1997) to be a function of the redox potential or ferric/ferrous-ion ratio. The chemical leaching of chalcopyrite by ferric iron is an electrochemical process. The aim of this section is to predict the rate of ferric leaching of chalcopyrite as a function of redox potential or ferric/ferrous-ion ratio by reworking published literature data.

Kametani and Aoki (1985) conducted a study on the effect of redox potential on the oxidation rate of a Kosaka Mine chalcopyrite concentrate in a sulphuric acid solution. The chalcopyrite concentrate was oxidised in I000 mmol.l^{-1} H_2SO_4 at 90 °C and at a number of different redox potentials across the range from 300mV to 650mV (SCE). The problem encountered in many leaching studies of this nature is the dynamic redox behaviour during the electrochemical oxidation. This was overcome by maintaining a constant redox potential in the suspension by the controlled addition of permanganate solution.

Two sets of experiments were carried out. In the first set containing 20 gms of concentrate was oxidised at constant redox potentials. The second set involved the addition of another 20gms of concentrate after complete oxidation of the first set. The data for the first set of experiments has been reanalysed and reported in the form of the rate of ferrous production, r_{Fe2+}, as a function of redox potential, E, in an attempt to determine its effect on the rate of chalcopyrite leaching.

The concentrate used by Kametani and Aoki (1985) consisted primarily of 75% chalcopyrite and 17% pyrite. It also contained small amounts of sphalerite (3%) and galena (2%).

2.4.1 Results reported by Kametani and Aoki(1985)

2.4.1.1 Experimental Methods

The concentrate is oxidised via two processes depending on whether elemental sulphur or sulphate is produced.

$$CuFeS_2 \mapsto CuS + Fe^{2+} + S^{\circ} + 2e^{-} \quad (2.4.1)$$

$$CuS \mapsto Cu^{2+} + S^{\circ} + 2e^{-} \quad (2.4.2)$$

$$CuFeS_2 \mapsto Cu^{2+} + Fe^{2+} + 2S^{\circ} + 4e^{-} \quad (2.4.3)$$

$$CuFeS_2 + 8H_2O \mapsto Cu^{2+} + Fe^{2+} + 2HSO_4^{-} + 14H^{+} + 16e^{-} \quad (2.4.4)$$

$$FeS_2 + 8H_2O \mapsto Fe^{2+} + 2HSO_4^{-} + 14H^{+} + 14e^{-} \quad (2.4.5)$$

During the experiments performed by Kametani and Aoki (1985), the ferrous-ion produced as indicated in Equations 2.4.1-2.4.5 above was instantaneously re-oxidised to ferric-ion by the controlled addition of permanganate. This enabled a constant redox potential ie a constant

ferric/ferous-iron ratio being maintained in the leaching solution. The redox potential is related to the ferric/ferrous-ion ratio by the Nernst equation. The oxidation of ferrous-ion by permanganate proceed via reaction 2.4.6.

$$KMnO_4 + 8H^+ + 5Fe^{2+} \rightarrow K^+ + Mn^{2+} + 5Fe^{3+} + 4H_2O \quad (2.4.6)$$

From Equation 2.3.6 it is clear that the amount of permanganate required to maintain a certain ferric/ferrous-iorn ratio can therefore be stochiometrically related to the amount of ferrous-ion produced at a certain redox potential via Equation 7.

$$[Fe^{2+}] = 5[KMnO_4] \quad (2.4.7)$$

Equation 2.4.7 provides a convenient means of generating $-r_{Fe2+}$ data at a constant redox potential. The rate of ferrous production $-r_{Fe2+}$ can be in turn be related to the rate of chalcopyrite oxidation via Equation 2.3.1, 2.3.2 or 2.3.5.

2.4.1.2 Results

The results obtained by Kametani and Aoki(1985), shown in Figures 2.4(a)-(c), were

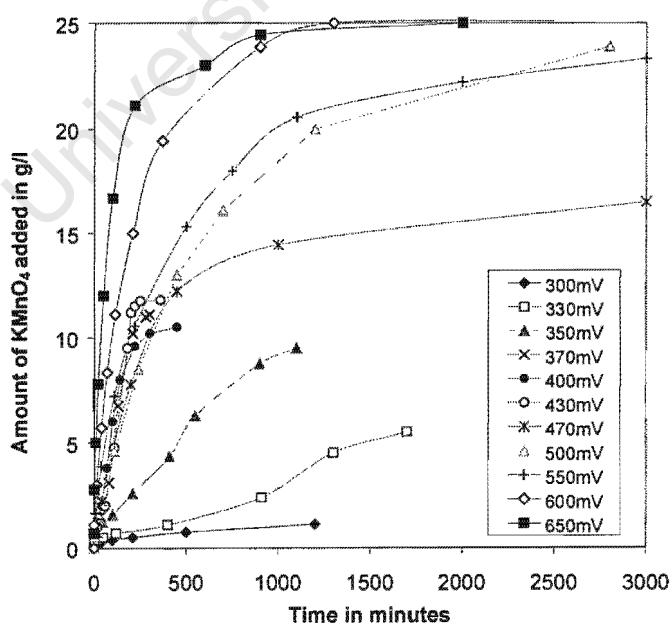

Figure 2.4a: [$KMnO_4$]added vs log(time) for the oxidation of Fe^{2+} to Fe^{3+} at 90 °C for redox potentials from 300mV to 650mV (Kametani and Aoki (1985))

presented in the form of the amount of $KMnO_4$ added vs log(time) at 90 °C (figure 2.4(a)) and at constant redox potentials. Kametani and Aoki(1985) presented the effect of temperature (Figure 2.4(b)) at 400mV between 50 °C and 90 °C.

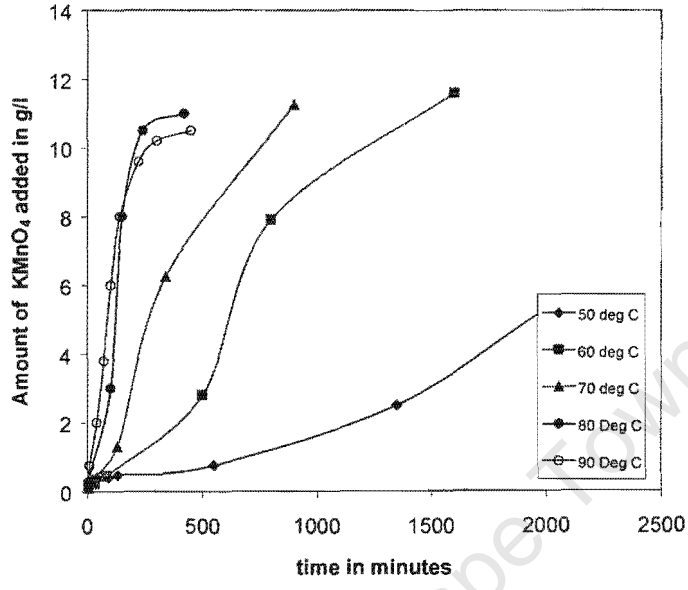

Figure 2.4(b): The effect of temperature on the reaction curves. [$KMnO_4$] added vs time for the oxidation of Fe^{2+} to Fe^{3+} at 400mV for temperatures from 50 to 90 °C.(Kametani and Aoki (1985)

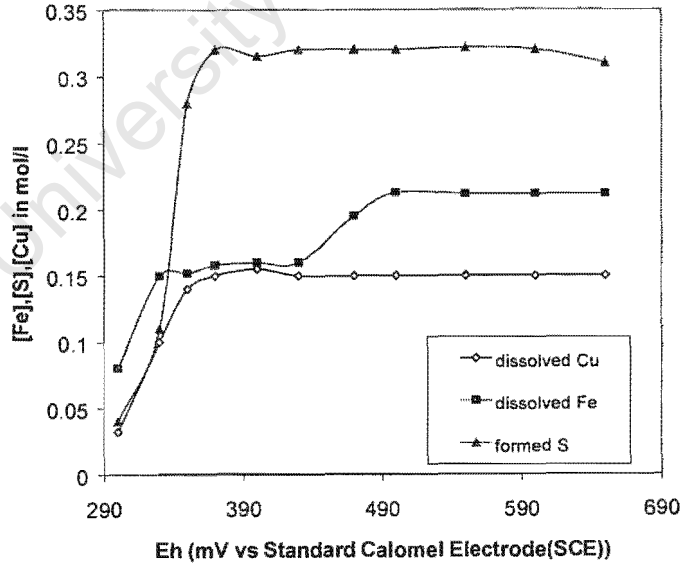

Figure 2.4(c) : Variation in the amount of S°, dissolved Fe and dissolved cu as a function of redox potential (Kametani and Aoki (1985).

The leach residue was analysed by X-ray diffraction after each experiment to determine the elemental sulphur and undissolved iron and Cu (Figure 2.4(c)). The authors speculated that

Cu precipitation from solution to form CuS at 300mV and 330mV resulted in the incomplete oxidation at these potentials.

2.4.2 Methodology of reworking the data

The data presented by Kametani and Aoki in Figures 2.4.1(a) and (b) was used to calculate the rate of ferrous iron production, $r_{Fe^{2+}}$,at each of the redox potentials as follows :

I. The time scale data to was converted from log scale to normal time scale data
II. The value of permanganate added in g/l was converted to moles of ferrous iron produced using the stochiometry of reaction 6.
III. The moles of ferrous iron was plotted vs time.
IV. The rate of ferrous iron production, $r_{Fe^{+2}}$, was calculated by determining the slope of the plot of ferrous-ion concentration vs time the reaction control regime.

The above procedure provides a means of establishing an $r_{Fe^{2+}}$ vs redox potential curve at a temperature of 90 °C. However this temperature is above the temperatures at which mesophilic or thermophilic bioleaching operations takes place. In order to establish $r_{Fe^{2+}}$ as a function of redox potential at lower temperatures it was necessary to assume a relationship between the rate of leaching and the temperature at which the reaction occurs. It was assumed that the rate law for the leaching of chalcopyrite is dependent on the redox potential as in Equation 2.4.7:

$$r_{CuFeS_2} = k\left[\frac{[Fe^{+3}]}{[Fe^{+2}]}\right]^m \qquad (2.4.7)$$

For most chemical reactions the relationship between the rate constant, k, and the temperature is governed by the Arrhenius equation (2.4.8) ; viz ,

$$k = k_0 e^{\frac{E_a}{RT}} \qquad (2.4.8)$$

In the Arrhenius equation the activation energy ,E_a, and the frequency factor,k_0, are specific to the reaction. For a particular reaction, the true activation energy would be calculated under conditions of reaction control only; any smaller value would be associated with the reaction being diffusion limited.

The ferric/ferrous-ion ratio is related to the redox potential via the Nernst equation (2.4.10):

$$E = E_0 + \frac{RT}{zF} \ln \frac{[Fe^{+3}]}{[Fe^{+2}]} \qquad (2.4.10)$$

Therefore, as the ferric/ferrous-ion ratio is constant at a particular redox potential, the rate of ferrous iron production at any temperature can therefore be calculated using the scaling ratio, viz , Equation (2.4.11)

$$\frac{r_{Fe^{+2},T_1}^{E_h^1}}{r_{Fe^{+2},T_2}^{E_h^1}} = \frac{e^{\frac{E_a}{RT_1}}}{e^{\frac{E_a}{RT_2}}} \qquad (2.4.11)$$

2.4.3 Results from reworked data

2.4.3.1 Kinetics

Figure 2.4(d) and 2.4(e) indicates calculated ferrous iron concentrations in solutions as a function of time during the leaching of the concentrate. From Figure 2.4 it is clear that at potentials greater than 350mV two distinct regions are evident. The initial region ($t < 1000$ sec) is characteristic of the leaching being under reaction control whereas at $t > 2000$ sec the rate is diffusion limiting. This distinction between reaction and diffusion control is most evident at redox potentials above 350mV and is responsible for retardation of the rate in the curves obtained at redox potentials of 400mV and 470mV at 90 °C.

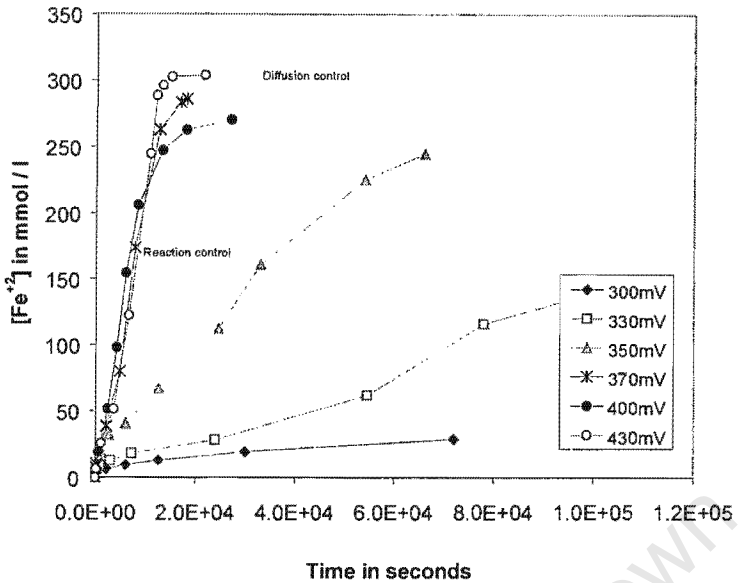

Fig 2.4(d) : Concentration of ferrous iron produced during the oxidation of chalcopyrite concentrate vs t calculated from the equation 7 at 90 °C from 300mV to 430mV (Kametani and Aoki (1985))

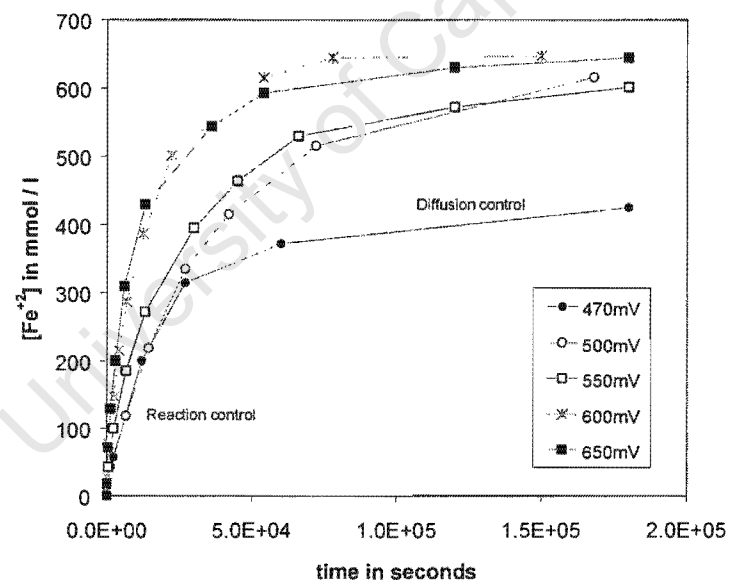

Fig 2.4(e) : Concentration of ferrous iron produced during the oxidation of chalcopyrite concentrate vs t calculated from the equation 7 at 90 °C from 300mV to 430mV (Kametani and Aoki (1985))

For the purposes of this investigation the region of interest is the reaction control regime in which the concentration of ferrous iron produced exhibits a linear dependence on time. The calculated rates of ferrous production (r_{Fe2+}) for the reaction control regime over the redox range 300mV to 650mV are displayed in Appendix I.

2.4.3.2 Chemical oxidation rate.

Figure 2.4(f) indicates the rate of ferrous production calculated from the procedure outlined in section as a function of redox potential at 90 °C. It is apparent that the oxidation rate increases with redox potential between 300mV and 430mV. A maximum rate at 430mV is followed by a decline in oxidation rate till 450mV is reached. It must be pointed out that no experimental data was available at 450mV and could therefore not be manipulated to establish the minimum oxidation rate. It is therefore possible given the scope in variation of the data between 430mV and 470mV that a minimum oxidation rate is present between these limits. If this were the case then the curve would exhibit a much lower minimum than is displayed in Figure 2.4(f). The oxidation is further complicated by the presence of pyrite in the concentrate. The region between 470mV and 650mV is characterised by a pronounced increase in the rate. This region must be analyzed in conjunction with Figure 2.4(c). The amount of dissolved copper and iron in solution were equal until a critical potential of 430mV was reached. Beyond this potential the amount of iron increased.

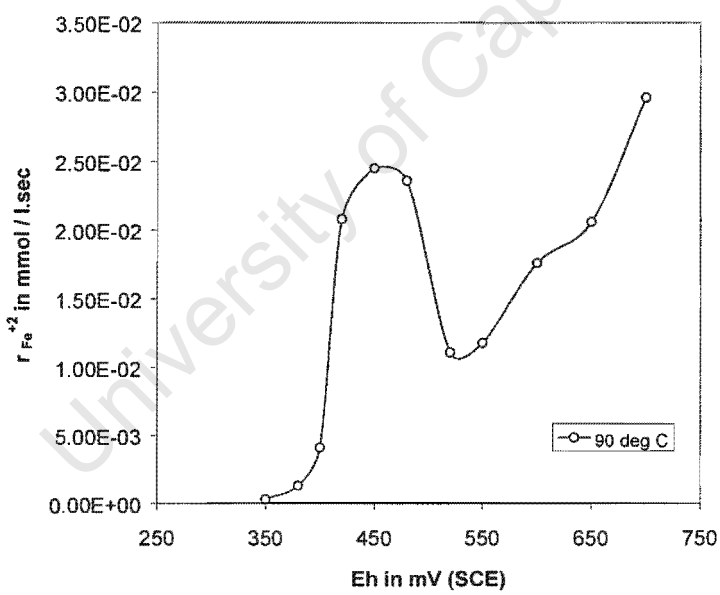

Fig 2.4(f) : Rate of ferrous iron production ,r_{Fe2+}, during the leaching of chalcopyrite concentrate as a function of Redox potential from 30 to 50 °C between 300mV to 650mV reworked from Kametani and Aoki, (1985)

until it reached a maximum at 500mV and remained constant till 650mV. The copper remained at a fixed value when 370mV was reached for all subsequent potentials. The elemental sulphur curve is similar to the dissolved Cu curve. It also follows from Figure 2.4(C) that chalcopyrite is oxidised to elemental sulphur irrespective of the potential. The authors conceded that pyrite oxidation took place at potentials exceeding 450mV. This deduction ties in with the observed increase in dissolved Fe at potentials greater than 450mV.

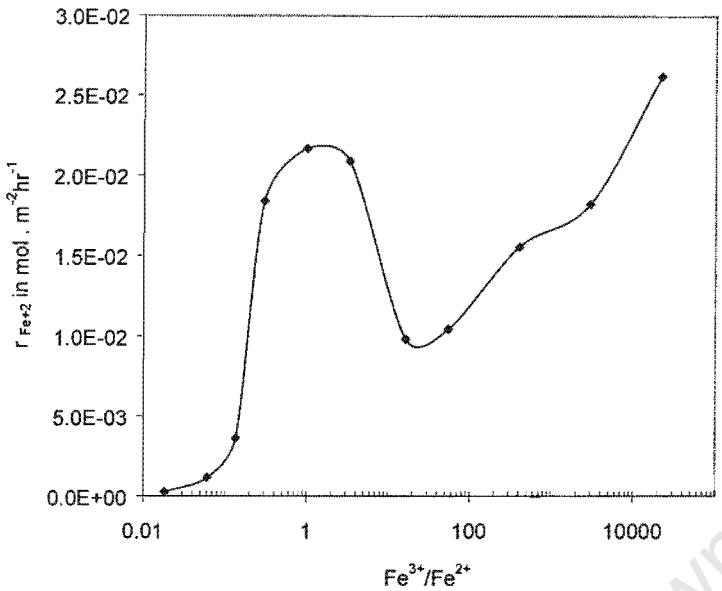

Fig 2.4(g) : Rate of ferrous iron production ,r_{Fe2+}, during the leaching of chalcopyrite concentrate as a function of Redox potential from 30 to 50 °C between 300mV to 650mV reworked from Kametani and Aoki, (1985)

The increase in the rate of ferrous-production at potentials beyond 450mV could be attributed to both the oxidation of pyrite and chalcopyrite. The rates below 450mV is therefore representative of pure chalcopyrite and can be associated with its behavior as a function of redox potential. Any deductions about the rate behaviour beyond 450mV can only be speculative. The behaviour for pure chalcopyrite beyond 450mV would most likely display a passivated rate at those potentials and this would be depicted as a less pronounced increase in the rate beyond 450mV.

Figure 2.4(g) shows the rate of ferrous production expressed per available surface area of chalcopyrite mineral as a function of the ferric/ferrous-ion ratio. The ferric/ferrous-ion ratios were calculated from the redox potentials via the Nernst equation by applying theoretical values for parameters E_o and RT/zF. Figure 2.4(g) shows the initial increase in rate up to ratio's of 1. This suggests that the rate is faster when there is more ferrous-ion in the system than ferric-ion. This result is consistent with other workers who suggested that ferrous-ions promote the rate of leaching (Hiroyoshi *et al.*, 1997; Hiroyoshi *et al.*, 1999, Hiroyoshi *et al.*, 2000; Third *et al.*, 2000)

2.4.3.3 The effect of passivation

The effect of passivation when the rate becomes diffusion limiting has not been considered in this analysis.

2.4.3.4 The effect of temperature

Figure 2.4(h) indicates the effect of temperature on the reaction curves calculated from the stochiometry of reaction 2.4.6. Figure 2.4(i) indicates the Arrhenius plot for the activation energy determination. Figure 2.4(j) indicates the effect of temperature on the rate of ferrous production established via the procedure outlined in Section 2.4.2. It appears that temperature has some effect on the r_{Fe+2} vs E_h curve. The estimated activation energy was for the reaction control regime was 93kJ/mol. The authors (Kametani and Aoki, 1985) obtained an apparent activation energy of 47 kJ/mol which encompassed both reaction control and diffusion control regimes. The regression analysis to obtain the rates for the reaction control regime are indicated in Appendix I. The temperature scaling technique is dependent on the form of the rate law, which has been shown in Section 2.4.2. If the rate of ferrous iron production is only a function of redox potential then at a particular redox the ferric to ferrous iron ratio term and the frequency constant could be lumped together as one constant. This would effectively mean that these terms would fall away when scaling up or down to a higher or lower temperature.

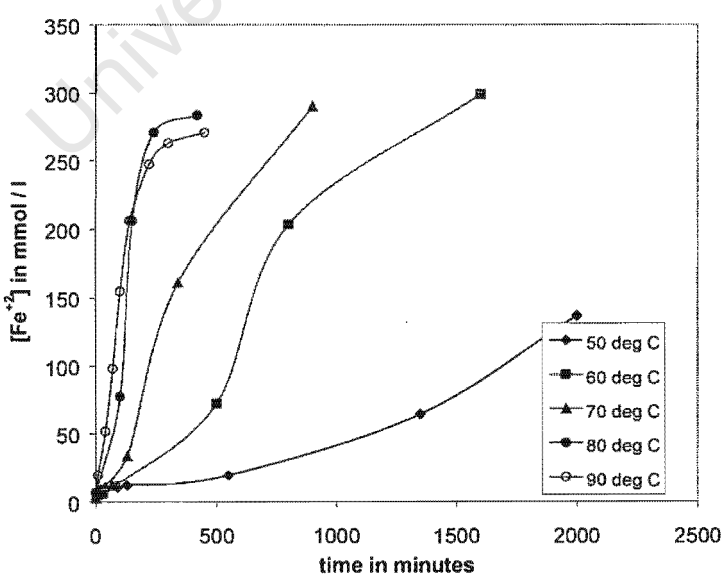

Fig 2.4(h) : The effect of temperature on the reaction curves. Concentration of ferrous iron produced vs t for the oxidation of chalcoyrite concentrate at 400mV for temperatures from 50 to 90 °C.(Kametani and Aoki (1985)

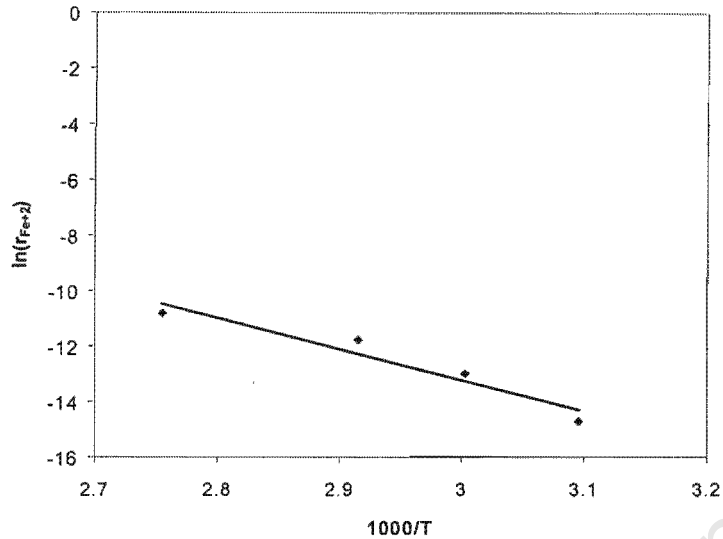

Fig 2.4(i) : The effect of temperature on the reaction curves. Arrhenius plot of $\ln(r_{Fe+2})$ vs 1000/T for rates of ferrous iron production at 400mV from the oxidation of chalcoyrite concentrate at temperatures from 50 to 90 °C. Regression analysis indicates a slope of 11.203, intercept of 23.37 for R^2 of 0.92.

This means that r_{Fe2+} at a redox potential and lower temperature could be calculated by knowing r_{Fe2+} at the same redox potential and a higher temperature given the activation energy for the surface reaction. Diffusional constraints are not considered in this approach. The rates beyond 450mV are indicative of both pyrite and chalcopyrite oxidation.

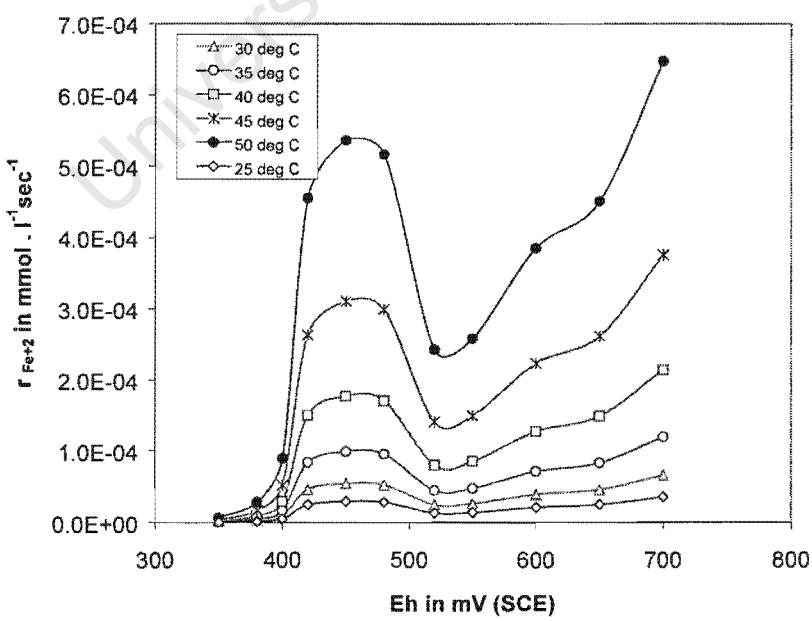

Fig 2.4(j) : Rate of ferrous iron production ,r_{Fe2+}, during the leachingof chalcopyrite concentrate as a function of Redox potential from 30 to 50 °C between 300mV to 650mV

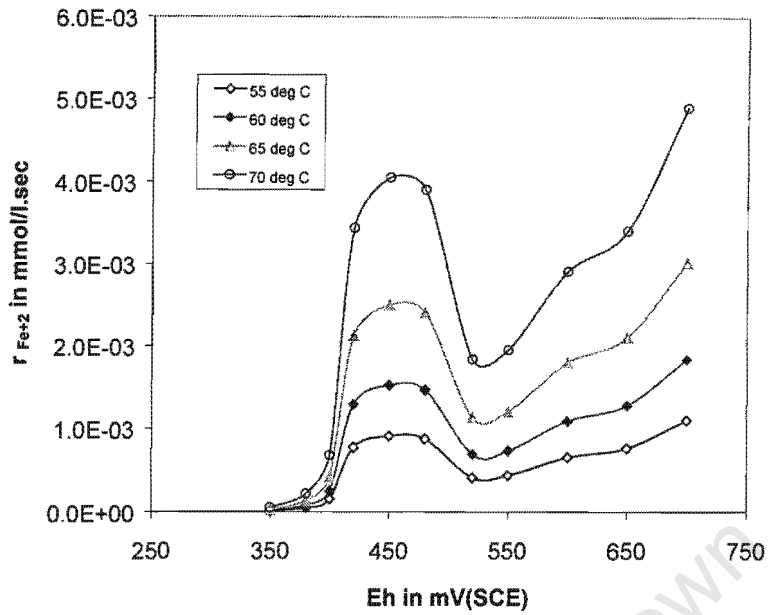

Fig 2.4(k) : Rate of ferrous iron production during the oxidation of chalcopyrite concentrate as a function of Redox potential from 55 to 70 °C between 300mV to 650mV

2.4.4 Proposed Model for the leaching of chalcopyrite at low redox potentials

Recent work has proposed a model for the leaching of chalcopyrite which describes its chemical behavior within range of ferric/ferrous-ion ratios or redox potentials where the rate is maximum (Hiroyoshi *et al.*, 2000). This model consists of two steps, viz,

Step 1: The reduction of chalcopyrite by ferrous-ion in the presence of cupric ion to form chalcocite (Equation 2.4.12), ie,

$$CuFeS_2 + 3Cu^{2+} + 3Fe^{2+} \mapsto 2Cu_2S + 4Fe^{3+} \qquad (2.4.12)$$

Step 2: The oxidation of chalcocite to by oxygen (Equation 2.4.13) and ferric iron (2.4.14), ie,

$$2xCu_2S + 8xH^+ + 2xO_2 \mapsto 4xCu^{2+} + 2xS + 2H_2O \qquad (2.4.13)$$

$$2(1-x)Cu_2S + 8(1-x)Fe^{3+} \mapsto 4(1-x)Cu^{2+} + 8(1-x)Fe^{2+} + 2(1-x)S \qquad (2.4.14)$$

where x is the ratio of Cu_2S oxidised in (2.4.13) to that formed in (2.4.12).

This model suggests that at high ferrous-ion concentrations (low redox potential), chalcopyrite leached via the formation of an intermediate copper sulphide phase, which is not stable but is more readily oxidised to cupric-iron and sulphur by dissolved oxygen or ferric-ion. The author also showed that the formation of this intermediate was thermodynamically possible when the solution redox potential was lower than the critical potential (E_c) for the reduction of cupric ion by ferrous-ion (Equation 2.4.15) and above the oxidation potential for Cu_2S (E_{ox}) (equation 2.4.16).

$$E_C = E_C^0 + \frac{RT}{4F}\ln\frac{(a_{Cu^{2+}})^3}{(a_{Fe^{2+}})} \qquad (2.4.15)$$

$$E_{OX} = E_{OX}^0 + \frac{RT}{4F}\ln(a_{Cu^{2+}}) \qquad (2.4.16)$$

2.4.5 Conclusions

1. The outcome of the reanalysis of published literature data indicates that the initial rate of ferrous production during the chemical ferric oxidation of chalcopyrite as a function of redox potential. The initial rate is the rate under reaction control.

2. The chemical oxidation of chalcopyrite presents a mixed reaction / diffusion control model. The rate is initially reaction control. Diffusional limitations slow down the rate even it is maintained at a constant redox potential. The distinction between reaction control and diffusion control is more evident at redox potentials above 350mV (SCE).

3. The critical redox potential, at which the rate is a maximum, is in the region of 430mV (SCE) which theoretically corresponds to a ferric/ferrous-ion ratio of 1. The rate of chemical leaching of chalcopyrite decreases beyond with any increase beyond this redox potential value.

4. The effect of redox potential on the oxidation rate of chalcopyrite beyond 450mV has not been exclusively established due to the presence of pyrite in the concentrate.

5. The activation energy of reaction under surface reaction control is 93KJ.mol^{-1}. This is compared with 47 kJ.mol^{-1}, calculated by Kametani and Aoki (1985) for both the reaction and diffusion control regimes. The rate of chalcopyrite oxidation exhibits a linear dependence on temperature over the range 25 °C to 90 °C when under reaction control.

Chapter 3: Theoretical Methodology

3 Theoretical Methadology

The bioleaching of chalcopyrite is thought to occur via a multiple sub-process mechanism involving the chemical leaching of the mineral to produce ferrous-ion and sulphur/sulphur compounds and the bacterial oxidation of these products by iron and sulphur oxidisers to regenerate ferric-ion and sulphuric acid respectively (Sand *et al.*,1999). This means that the *kinetics* of bioleaching of chalcopyrite involves a complex interaction of substrate utilisation and bacterial growth rates especially since the bioleaching involves a dual bacterial substrate (ferrous-ion and sulphur). Furthermore, bioleaching involves the use of aerobic micro-organisms which assimilate carbon for bacterial growth, and therefore requires the supply of both oxygen and carbon dioxide. Any attempt to study the mechanism or kinetics of chalcopyrite bioleaching would therefore need to apply a theoretical understanding of the interaction between the substrate utilisation, bacterial growth and mineral leach rates in order to relate them to one another.

The studying of the kinetics of bioleaching of chalcopyrite and other sulphide minerals in general has been hindered by a lack of a convenient theoretical and experimental approach for the measurements of bacterial growth, substrate utilisation, and mineral leach rates. The theoretical methadology being used to study the kinetics of chalcopyrite bioleaching, relates the rates of production of biomass and products with the rates of consumption of substrates. This theoretical approach has already been successfully applied to study the kinetics of bioleaching of pyrite (Boon, 1996) and arsenopyrite (Breed, 2000). This chapter outlines the application of the theoretical and experimental approach developed by Boon (1996) in studying the kinetics of bioleaching of chalcopyrite by mesophiles. A comprehensive application this theoretical methodology in studying the bioleaching of sulphide minerals has already been given by Boon (1996).

3.1 Definition of biomass specific rates

The approach which will be used is that of Roels (1983) where the basic rate equation is written in terms of the specific substrate utilisation rate. The energy derived from substrate utilisation is used for both biomass synthesis and cell maintenance. The specific rate of substrate utilisation is based on the growth component only and is therefore an indication of the amount of substrate consumed for cell growth. The specific rates of growth (Equation (3.1)), μ, and biomass substrate utilisation (equation (3.2)), q_s, are defined in units of hr^{-1} and $mole.molC^{-1}\ hr^{-1}$ respectively:

$$\mu = \frac{r_x}{C_x} \tag{3.1}$$

$$q_s = -\frac{r_s}{C_x} \tag{3.2}$$

During the bioleaching of chalcopyriyte, ferrous-ion and sulphur are the bacterial substrates. The specific biomass oxygen utilisation rate , q_{O_2}, or the specific biomass ferrous iron utilisation rate, $q_{Fe^{2+}}$ can be used as kinetic parameters in modelling the kinetics of the system. These specific parameters represent the bacterial activity during ferrous-ion oxidation and bioleaching. Table 3.1 indicates the definitions of these parameters where r_s denotes the rate of substrate utilisation in $mol.l^{-1}.hr^{-1}$ and C_x the bacterial concentration in $molC.l^{-1}$

Table 3.1: Definitions and units of specific biomass utilisation rates

Specific Utilisation Rate	Definition	Units
q_{O_2}	$-r_{O_2} / C_x$	$MoleO_2.molC^{-1}\ hr^{-1}$
$q_{Fe^{2+}}$	$-r_{Fe^{2+}} / C_x$	$MoleFe^{2+}.molC^{-1}\ hr^{-1}$

3.2 Microbial Growth Kinetics

Growth kinetics in a microbial system is expressed in terms of a rate equation for the specific growth rate ,μ , in terms of the growth limiting substrate. The Monod equation (Equation(3.3)) for enzyme kinetics expressing the specific growth rate dependence on the concentration of growth limited substrate (C_s) :

$$\mu = \frac{\mu_{max}}{1 + \frac{K_s}{C_s}} \tag{3.3}$$

In this equation, μ_{max} is the specific growth rate constant in hr^{-1} and K_s is the saturation constant in mol l^{-1}. The specific utilisation rate is a more fundamental expression since it includes the rate of substrate utilisation which provides the energy for metabolic growth. The Monod equation when written in terms of bacterial specific growth rate becomes Equation 3.4.

$$q_s = \frac{r_s}{C_x} = \frac{q_s^{max}}{1 + \frac{K_s}{C_s}} \tag{3.4}$$

In Equation (3.4) q_s is the biomass specific growth rate and q_{smax} is the maximum biomass specific growth rate. Equation (3.4) can be modified to Equation (3.5) by including a product inhibition term (Jones and Kelly, 1983). C_s and C_p signify the concentrations of substrate and products respectively in Equation (3.5)

$$q_s = \frac{r_s}{C_x} = \frac{q_s^{max}}{1 + \frac{K_s}{C_s} + \frac{K_s}{K_I}\frac{C_p}{C_S}} \tag{3.5}$$

In the logarithmic growth phase $K_s << C_s$ so the 2nd term is effectively discarded.

The specific oxygen utilisation rate (q_{O_2}) is a measure of the bacterial activity and is defined as the rate of oxygen substrate utilised for bacterial growth during bacterial ferrous-ion oxidation, bacterial sulphur oxidation and bioleaching as in Equation (3.6)

$$q_{O_2} = -\frac{r_{O_2}}{C_X} = \frac{q_{O_2}}{1 + \frac{K_s}{C_s}} \tag{3.6}$$

The bacterial growth yield, Y_{sx}, shown in equation (3.7) is a function of the bacterial growth and substrate utilisation :

$$Y_{sx} = \frac{r_x}{r_s} \tag{3.7}$$

Similar yields can then be defined for oxygen utilisation, Y_{OX}, bacterial ferrous utilisation, $Y_{Fe^{2+}X}$, and bacterial sulfur utilisation ,$Y_S{}^{\circ}{}_X$. Substrate utilisation provides energy for both growth and maintenance. This is expressed in terms of the Pirt equation (Pirt, 1975), where m_s is the maintenance coefficient (Equation's (3.8) and (3.9)).

$$-r_s = \frac{r_x}{Y_{SX}} = \frac{r_x}{Y_{SX}^{max}} + C_x m_s \qquad (3.8)$$

or

$$-\frac{r_s}{r_x} = \frac{1}{Y_{SX}} = \frac{1}{Y_{SX}^{max}} + \frac{m_s}{\mu} \qquad (3.9)$$

When written for oxygen as a substrate Equation (3.9) becomes Equation (3.10).

$$-\frac{r_{O_2}}{r_x} = \frac{1}{Y_{OX}} = \frac{1}{Y_{OX}^{max}} + \frac{m_o}{\mu} \qquad (3.10)$$

Equation (3.10) shows that the maximum yields and maintenance coefficients can be obtained from the inverse intercept and the slope of a plot of $(Y_{OX})^{-1}$ vs μ^{-1}, respectively.

3.3 The measurement of bacterial growth rates

Accurate measurements of the bacterial growth rates is necessary for the determination of specific kinetic parameters. Earlier workers enumerated free bacteria by using standard counting techniques (Konashi *et al.*, 1990). However, most of the mesophilic bacteria are found attached to the mineral surface during the bioleaching of chalcopyrite, and the remainder are planktonic (Murr, 1980; Rossi, 1990; Rawlings, 1997). This direct technique of cell growth estimation is therefore limited because it means that the dislodging of the attached bacteria is paramount to any accurate determination of cell numbers during bioleaching. Furthermore, it is thought that the average carbon content of *Acidithiobacillus ferrooxidans* decreases during batch growth and with an increase in dilution rate during continuous growth (Braddock *et al.*, 1984). This means that the size and carbon content of the micro-organism is a dependent on the conditions under which it is grown.. Therefore, direct carbon measurements is a more accurate measure of the bacterial growth rate rather than cell numbers.

During bioleaching, carbon dioxide is the only carbon source for bacterial assimilation. This means that the rate of carbon dioxide utilisation is directly related to the rate of bacterial growth as Equation (3.1).

$$-r_{CO_2} = r_x \qquad (3.11)$$

The bacterial concentration can therefore be measured during mineral bioleaching or bacterial ferrous-ion oxidation by integrating the measured carbon dioxide utilisation rates over time as in equation (3.12)

$$C_X(t) = C_X(0) + \int_0^t -r_{CO_2} dt \qquad (3.12)$$

The measurement of the carbon dioxide utilisation rate offers a convenient direct means of measuring the increase in the carbon content of the cells and therefore the bacterial growth rate. The bacterial concentration is then determined by integration of the measured rates of bacterial growth knowing the initial bacterial concentration in the system. Offgas analysis has been used to determine cell growth rates from carbon dioxide consumption rates (Pinches *et al.*, 1991; Nagpal *et al.*, 1993). This technique has recently already been successfully used to measure the rate of bacterial growth during pyrite bioleaching and bacterial ferrous-ion oxidation by *Acidithiobacillus ferrooxidans* and *Leptospirillum ferrooxidans* in batch (Boon, 1996) and continuous culture (Breed *et al.*, 1999(a)); Boon (1996). Boon (1996) has shown reasonably accurate parity between cell concentrations estimated from measured carbon dioxide utilisation rates and that obtained by periodic total organic carbon analysis (TOC) during the bioleaching of pyrite by mesophiles in batch cultures.

Other indirect methods of cell growth estimation involve the determination of protein and nitrogen (Jones and Kelly, 1993; Chang and Myerson, 1982).

A limitation in applying this technique of bacterial estimation is that the measured bacterial growth rate from the carbon dioxide utilisation rate represents the bacterial growth rates of all the bacterial species which are grown during bioleaching. In the case of chalcoyrite, both ferrous-ion and sulphur substrates result in two specific types of bacterial species, ie, iron and sulphur oxidisers respectively.

3.4 Degree of reduction balances

The bacterial oxidation of ferrous-ion and sulphur are important sub-processes in the bioleaching of chalcopyrite. A degree of reduction balance is performed by taking an elemental and charge balance over all the chemical the species involved in bacterial ferrous-

ion and sulphur oxidation, respectively. This enables the determination of the rate of either bacterial ferrous-ion or sulphur utilisation from the measured rates of oxygen and carbon dioxide utilization. The degree of reduction balances are shown for each respective bacterial sub-process in the subsequent sections.

3.4.1 Bacterial ferrous-ion oxidation

Boon (1996) derived a relationship between the rate of ferrous-ion consumption and the rates of oxygen and carbon dioxide utilisation. Bacterial ferrous-ion oxidation (Equation (3.13)),is coupled with an equation for bacterial growth (Equation(3.14)) (Roels, 1983) on ferrous-ion using carbon dioxide and Ammonium-ion as the sole carbon and nitrogen sources

$$4Fe^{2+} + O_2 + 4H^+ \mapsto 4Fe^{3+} + 2H_2O \tag{3.13}$$

$$CO_2, NH_4^+, H_2O \mapsto CH_{1.8}O_{0.5}N_{0.2} \tag{3.14}$$

Material balances on each element is shown in Equations (3.15)-(3.20).

$$C: r_x + r_{CO_2} = 0 \tag{3.15}$$

$$N: 0.2r_x + r_{NH_4^+} = 0 \tag{3.16}$$

$$H: 1.8r_x + 4r_{NH_4^+} + r_{H^+} + 2r_{H_2O} = 0 \tag{3.17}$$

$$O: 0.5r_x + 2r_{O_2} + 2r_{CO_2} + r_{H_2O} = 0 \tag{3.18}$$

$$Fe: r_{Fe^{2+}} + r_{Fe^{3+}} = 0 \tag{3.19}$$

$$z: r_{NH_4^+} + 2r_{Fe^{2+}} + 3r_{Fe^{3+}} + r_{H^+} = 0 \tag{3.20}$$

Six equations are solved for 8 unknowns to yield the rate of bacterial ferrous-ion utilisation, $-r_{Fe^{2+}}$, in terms of the oxygen,$-r_{O_2}$, and carbon dioxide, $-r_{CO_2}$, utilisation rates as shown in Equation (3.21).

$$-r_{Fe^{2+}} = -4r_{O_2} - 4.2r_{CO_2} \tag{3.21}$$

Similarly, the specific rates of ferrous-ion utilisation can be written in terms of the specific rates of oxygen and carbon dioxide utilisation as Equation (3.22).

$$q_{Fe^{2+}} = 4q_{O_2} + 4.2q_{CO_2} \tag{3.22}$$

The bacterial yield on ferrous-ion is defined as Equation (3.23),

$$Y_{Fe^{2+}X} = \frac{r_X}{-r_{Fe^{2+}}} \tag{3.23}$$

Boon (1996) combined Equations (3.13) and (3.14) to give a balanced equation for bacterial growth on ferrous-ion (Equation(3.24)) by using the definition shown in Equation (3.23).

$$CO_2 + 0.2NH_4^+ + [\frac{1-4.2Y_{Fe^{2+}X}}{4Y_{Fe^{2+}X}}]O_2 + [\frac{1}{Y_{Fe^{2+}X}}]Fe^{2+} + [\frac{1}{Y_{Fe^{2+}X}} - 0.2]H^+ \mapsto$$
$$CH_{1.8}O_{0.5}N_{0.2} + \frac{1}{Y_{Fe^{2+}X}}Fe^{3+} + [\frac{1}{2Y_{Fe^{2+}X}} - 0.6]H_2O \tag{3.24}$$

The yield on oxygen is related to the yield on ferrous-ion as Equation (3.25).

$$\frac{1}{Y_{OX}} = \frac{1-4.2Y_{Fe^{2+}X}}{4Y_{Fe^{2+}X}} \tag{3.25}$$

Similarly, the relationship between the maintenance coefficients on oxygen (m_0) and ferrous-ion ($m_{Fe^{2+}}$) was shown to be as that in Equation (3.26).

$$m_0 = \frac{1}{4}m_{Fe^{2+}} \tag{3.26}$$

3.5 Bacterial ferrous iron oxidation kinetics.

A number of models have been proposed to describe bacterial ferrous-ion oxidation (Nemati *et al.*,1998). Most of these models have been either empirical or Monod/Michaelis Menten based (Breed, 1999(a)). The specific bacterial ferrous-ion utilisation can be written in the form of inhibited Michaelis-Menten kinetics as Equation (3.38) (Boon, 1996).

$$q_{Fe^{2+}} = \frac{q^{max}_{Fe^{2+}}}{1 + \frac{K_s}{[Fe^{2+}][Fe^{2+}]_T} + \frac{K_s}{K_I}\frac{[Fe^{3+}]}{[Fe^{2+}][Fe^{2+}]_T}} \qquad (3.38)$$

where $q_{Fe^{2+}}$ is the specific ferrous-ion utilisation rate, $[Fe^{+2}]_T$ is the threshold ferrous concentration below which no bacterial growth occurs. Since $[Fe^{+2}]_T$ is small in comparison to $[Fe^{+2}]$, it is effectively discarded. Also the 2nd term is small since $K_s <<< [Fe^{+2}]$ as was shown in the case of *Leptospirillum ferroxidans* on pyrite (Boon , 1996). This model describing bacterial ferrous-ion oxidation can be simplified to express the kinetics as a function of the ferric/ferrous-ion ratio as Equation (3.38)

$$q_{Fe^{2+}} = \frac{q^{max}_{Fe^{2+}}}{1 + \frac{K_s}{K_I}\frac{[Fe^{3+}]}{[Fe^{2+}]}} \qquad (3.38)$$

By lumping together the kinetic constants ,K_s / K_I, as one constant ,$K_{Fe^{2+}}$, the model can be written as equation (3.39) (Boon, *et al.*, 1995).

$$q_{Fe^{2+}} = \frac{q^{max}_{Fe^{2+}}}{1 + K_{Fe^{2+}}\frac{[Fe^{3+}]}{[Fe^{2+}]}} \qquad (3.39)$$

Equation (3.39) can be written in terms of the specific oxygen utilisation rate, q_{O_2}, as shown in Equation (3.40) by relating the specific rate of ferrous-ion utilisation to the specific rates of oxygen and carbon dioxide utilisation. The rates of ferrous-ion utilisation can be related to the rates of oxygen and carbon dioxide utilisation by a degree of reduction balance on bacterial ferrous-ion oxidation.

$$q_{O_2} = \frac{q_{O_2}^{max}}{1 + K\frac{[Fe^{3+}]}{[Fe^{2+}]}} \quad (3.40)$$

3.6 Determination of the rate of oxygen utilisation for microbial sulphur oxidation in a chalcopyrite bioleach system

Previous studies have reported the ferric leaching of chalcopyrite in an acidic medium to follow the stochiometry shown in Equation (3.41) (Munoz *et al.*, 1979; Dutrizac, 1981; Dutrizac, 1989)

$$CuFeS_2 + 4Fe^{3+} \mapsto Cu^{2+} + 5Fe^{2+} + 2S^o \quad (3.41)$$

The bacterial growth rate is equal the rate of carbon dioxide utilisation since it is the only carbon source available for microbial synthesis. Both the bacterial specific oxygen utilisation rate and the microbial growth rate are measured online during bioleaching. For the case of pyrite, ferrous-ion is the only bacterial substrate and the measured oxygen and carbon dioxide utilisation rates are therefore only representative of bacterial ferrous-ion oxidation (Boon, 1996). However, according to the multiple sub-process mechanism, the measured rates in the case of chalcopyrite include the oxygen and carbon dioxide utilised for both ferrous-ion and sulphur oxidation sub-processes. The need therefore arises to determine the rates involved in each sub-process separately from a total oxygen and carbon dioxide utilisation measurement to establish the oxygen utilisation and growth rates of the iron oxidisers (or sulphur oxidisers), only, during chalcopyrite bioleaching.

In order to distinguish the contributions of ferrous-ion and sulphur oxidation to the measured oxygen utilisation rate, a stochiometric balance over the whole system is performed. The critical assumptions are the following:

1. The stochiometry of the ferric leaching of chalcopyrite is close to that presented in Reaction (3.41).
2. The microbial oxidation of ferrous-ion goes to completion
3. The microbial oxidation of sulphur goes to completion.
4. The microbial yield on oxygen for ferrous-ion and sulphur substrates are equal.
5. The system is not oxygen or carbon dioxide limited.

Taking a basis of 1 mole of $CuFeS_2$ completely oxidised to form 5 moles of ferrous-ion and 2 moles of sulphur via Reaction (3.41), the rate of oxygen utilisation for complete microbial oxidation of the formed ferrous iron and sulphur substrates can be stochiometrically determined from Reaction's (3.13) and (3.27). This means that 1.25 moles of oxygen are required for complete microbial ferrous-ion oxidation and 3 moles of oxygen required for complete sulphur oxidation per mole of $CuFeS_2$ completely oxidised. In this case the rate of oxygen utilisation for microbial sulphur oxidation, $-r_{O_2}^{S^o}$, is related to the rate of oxygen utilisation for microbial ferrous-ion oxidation, $-r_{O_2}^{Fe^{2+}}$, by the following ratio (equation (3.42):

$$\frac{-r_{O_2}^{Fe^{2+}}}{-r_{O_2}^{S^0}} = 2.4 \qquad (3.42)$$

The rates of oxygen and carbon dioxide utilisation measured from offgas includes the rate of oxygen and carbon dioxide utilisation of ferrous-ion and sulphur sub-processes shown in Equation's (3.43) and (3.44) respectively:

$$-r_{O_2}^{total} = -r_{O_2}^{Fe^{2+}} + (-r_{O_2}^{S^o}) \qquad (3.43)$$

$$-r_{CO_2}^{total} = -r_{CO_2}^{Fe^{2+}} + (-r_{CO_2}^{S^o}) \qquad (3.44)$$

Substitution of Equation (3.42) into Equation (3.43) suggests that the rate of oxygen utilisation for ferrous-ion and sulphur oxidation sub-processes can be determined from the total oxygen utilisation measurement via Equations (3.45) and (3.46) if the stochiometry in Equation (3.41) holds for chalcopyrite.

$$-r_{O_2}^{S^o} = -\frac{12}{17} r_{O_2}^{total} \qquad (3.45)$$

$$-r_{O_2}^{Fe^{2+}} = -\frac{5}{17} r_{O_2}^{total} \qquad (3.46)$$

The microbial yields on oxygen for ferrous-ion, $Y_{OX}^{Fe^{2+}}$, and sulphur oxidation, Y_{OX}^{S}, are expressed in the following relations (Equations (3.47) and (3.48)):

$$Y_{OX}{}^{S^o} = \frac{r_x{}^{S^o}}{r_{O_2}{}^{S^o}} \tag{3.47}$$

$$Y_{OX}{}^{Fe^{2+}} = \frac{r_x{}^{Fe^{2+}}}{r_{O_2}{}^{Fe^{2+}}} \tag{3.48}$$

The total microbial growth rate, $r_x{}^{total}$, is equal to the total rate of carbon dioxide utilization, $r_{CO_2}{}^{total}$, which is in-turn composed of the microbial growth rates on ferrous-ion, $r_x{}^{Fe^{2+}}$, and sulphur, $r_x{}^{S^o}$, substrates as in Equation (3.49).

$$-r_{CO_2}{}^{total} = r_x{}^{total} = r_x{}^{Fe^{2+}} + r_x{}^{S^o} \tag{3.49}$$

If the yields on oxygen for both ferrous-ion and sulphur oxidation are equal then substitution of Equation (3.45) into Equation (3.47) and (3.48) results in the rates of microbial growth for ferrous-ion oxidation and sulphur oxidation being similarly determined from the total rate of carbon dioxide utilisation as in Equation's (3.50) and (3.51) respectively:

$$-r_x{}^{S^o} = -\frac{12}{17} r_x{}^{total} \tag{3.50}$$

$$-r_x{}^{Fe^{2+}} = -\frac{5}{17} r_x{}^{total} \tag{3.51}$$

3.7 Determination of the Ferric/ferrous-ion ratio

The redox potential of the solution is dependent on the ferric/ferrous-ion pair. The ferric/ferrous-ion ratio is related to the redox potential of the solution via the Nernst equation (Equation(3.52)), which expresses the formal redox potential, $E^{'}_{h}$, as a function of the activity, γ_i, of the ferric/ferrous-ion pair:

$$E_h = E_0 + \frac{RT}{zF} \ln \frac{\gamma_{Fe^{3+}}}{\gamma_{Fe^{2+}}} \tag{3.52}$$

Equation (3.52) is also written in terms of molarities of the species and becomes equation (3.53):

$$E_h = E_0^{'} + \frac{RT}{zF} \ln \frac{[Fe^{3+}]}{[Fe^{2+}]} \tag{3.53}$$

whereby,

$$E_0^{'} = E_0 + \frac{RT}{zF} \ln \frac{\gamma_{Fe^{3+}}}{\gamma_{Fe^{2+}}} \tag{3.54}$$

If the reference electrode is not the standard hydrogen electrode (SHE) then equation (3.53) becomes equation (3.55).

$$E = E_0^{''} + \frac{RT}{zF} \ln \frac{[Fe^{3+}]}{[Fe^{2+}]} \tag{3.55}$$

The ferric/ferrous-ion ratio can then be determined from the measured redox potential and the calibration curve for the redox probe by applying Equation (3.55). The concentrations of ferric and ferrous-ion can be calculated from ferric/ferrous-ion ratio and the measured total iron by Equation (3.56) and (3.57), respectively.

$$[Fe^{2+}] = \frac{[Fe]_{tot}}{1 + \frac{[Fe^{3+}]}{[Fe^{2+}]}} \tag{3.56}$$

$$[Fe^{3+}] = \frac{[Fe]_{tot} \frac{[Fe^{3+}]}{[Fe^{2+}]}}{1 + \frac{[Fe^{3+}]}{[Fe^{2+}]}} \tag{3.57}$$

3.8 Experimental Methodology

The chemical leaching of chalcopyrite results in the formation of ferrous-ion and sulphur/sulphur compounds. Ferrous-ion can be directly measured by cerium sulphate

titration. It has already been shown that the concentration of dissolved copper does not affect the measured ferrous-ion concentrations when using this method. However, in the bioleaching systems, the ferrous-ion concentrations is usually very low in comparison to the primary oxidant, ferric-ion (Boon *et al.*, 1995). The total-iron concentration primarily is made up of ferric-ion. This makes it difficult to directly obtain accurate analyses for ferrous-ion and its therefore the rates of ferrous-ion utilization in solely ferrous-ion systems or bioleaching systems have to be measured indirectly via the oxygen and carbon dioxide utilization rates. A brief technical description of the off-gas system is shown in Chapter Four.

The usage of bioreactor offgas analysis enables the calculation of oxygen and carbon dioxide utilisation rates during the staged additions of mineral to a batch culture. The following calculations describe the methodology in estimating these rates from measured concentrations of oxygen and carbon dioxide in the bioreactor offgas.

The rates of oxygen and carbon dioxide consumption are calculated from the inlet and outlet concentrations, expressed as mass fractions, x, and the total inlet flowrates, by taking into account the change in flowrate due to oxygen and carbon dioxide consumption.

The total inlet, ϕ_{in}, and outlet ϕ_{out}, molar flowrates, is defined as the sum total of the nitrogen, ϕ_{N_2}, oxygen, ϕ_{O_2}, and carbon dioxide, ϕ_{CO_2}, inlet and outlet flowrates respectively, ie, Equation (3.58) and (3.59),

$$\phi_{in} = \phi_{N_2}^{in} + \phi_{O_2}^{in} + \phi_{CO_2}^{in} = \left(1 - x_{O_2}^{in} - x_{CO_2}^{in}\right) + x_{CO_2}^{in} + x_{O_2}^{in} \phi_{in} \tag{3.58}$$

$$\phi_{out} = \phi_{N_2}^{out} + \phi_{O_2}^{out} + \phi_{CO_2}^{out} = \left(1 - x_{O_2}^{in} - x_{CO_2}^{in}\right)\phi_{in} + \left(x_{O_2}^{out} - x_{CO_2}^{out}\right)\phi_{out} \tag{3.59}$$

since the flowrate of nitrogen into and out of the reactor is the same, viz, Equation (3.60),

$$\phi_{N_2} = \phi_{N_2}^{in} = \phi_{N_2}^{out} \tag{3.60}$$

Substituting Equation (3.58) into equation (3.59) yields Equation (3.61),

$$\phi_{out} = \frac{\left(1 - x_{O_2}^{in} - x_{CO_2}^{in}\right)}{\left(1 - x_{O_2}^{out} - x_{CO_2}^{out}\right)}\phi_{in} \tag{3.61}$$

A molar balance on oxygen and carbon dioxide yields the rate of oxygen,$-r_{O_2}$, and carbon dioxide, $-r_{CO_2}$, utilization as functions of the total inlet flowrate, ϕ_{in}, reactor volume, V, and mass fractions of these species in the inlet and outlet streams as shown in Equations (3.62) and (3.63).

$$-r_{O_2} = \frac{\phi_{in}}{V}\left[x_{O_2}^{in} - x_{O_2}^{out}\ \frac{\left(1 - x_{O_2}^{in} - x_{CO_2}^{in}\right)}{\left(1 - x_{O_2}^{out} - x_{CO_2}^{out}\right)}\right] \tag{3.62}$$

$$-r_{CO_2} = \frac{\phi_{in}}{V}\left[x_{CO_2}^{in} - x_{CO_2}^{out}\ \frac{\left(1 - x_{O_2}^{in} - x_{CO_2}^{in}\right)}{\left(1 - x_{O_2}^{out} - x_{CO_2}^{out}\right)}\right] \tag{3.63}$$

Chapter 4: Materials and Methods

4. Materials and Methods

4.1 Experimental equipment

Experiments were carried out in a sealed, baffled, 2 litre Z61104CT04 Applikon ADI Holland®, jacketed fermentor-type vessel made of borosilicate glass. The reactor had an h/d ratio of 1.3 and a working volume of 1 litre. The reactor internals consisted of three baffles, 10mm wide and 220mm long also constructed of 316 stainless steel arranged at 120 degrees to one another. The reactor vessel was closed on top by means of a rubber rimmed, 316 stainless steel headplate or cap which contained a number of ports to allow for the insertion of the shaft and blade of an agitator, the redox potential probe and an overhead condenser. Port outlets on the top and bottom of the glass jacket allowed connection to a waterbath via rubberized tubes (L/S 14™ Neoprene)

The reactor was maintained at the required temperature by circulating heated water from a Grant Y6 constant temperature water bath through the reactor jacket. No attempt was made to maintain a constant pH during the experiments. Experimentation commenced only after thermal equilibrium was achieved between the reactor solution and the circulating jacketed heating fluid. The temperature of the reactor solution itself was periodically checked and compared to the waterbath temperature reading via a thermometer to ensure thermal equilibrium between the reactor liquor and the circulating heated water.

Agitation for mixing and particle suspension was achieved by means of a 45° pitch bladed 316 stainless steel turbine impeller which was located at 20mm from the reactor base. The impeller was attached to a stainless steel shaft which was in-turn driven by an overhead Applikon ADI Holland® P100 automatic motorized stirrer. Speed control was achieved by means of a Applikon ADI Holland® 1012 stand alone speed controller connected to the motorized stirrer unit. This enabled a constant rotational speed of 400 $revmin^{-1}$.

The reactor set-up was also equipped with an Applikon ADI Holland® overhead reflux condenser to prevent any evaporative losses from the reactor solution. The cooling fluid circulated through the condenser was ethylene/glycol mixture (75% / 25%) and was kept refrigerated at temperatures below 0 °C in a Grant LTD6G Low temperature refrigerator bath.

The redox potential of the slurry in the reactor was measured by direct millivolt measurement using a Metrohm® ASI OR101431 Pt combination, double junction Ag/AgCL ORP glass

covered electrode connected via an optically isolated amplifier to an ADC digital converter on a single board microcomputer to a computer for data acquisition. This allowed the redox potential of the solution to be monitored continuously. The probe was inserted into the reactor solution through a porthole in the top reactor headplate.

4.2 Analyses and chemicals

Distilled water, along with analytical grade laboratory chemicals (Associated Chemical Enterprisers Pty Ltd) were used for all the experiments. The concentration of the ferrous-ion species were determined via the cerium-sulphate tritrametric method while the total copper and total iron were measured by Atomic Adsorption Spectroscopy (AAS). All samples drawn from the slurry during the experiment was filtered through a 8 μm Millipore filter and the residue recycled back to the leach liquor. The reactor solution was prepared in 1 litre distilled water, by adding the required amount of anhydrous ferric sulphate ($Fe_2(SO_4)_3$-xH_2O). pH was adjusted by adding the required amount of sulphuric acid (98%) whilst measuring with a pH probe attached to a Metrohm® pH meter. The redox probe calibrations were performed in the presence of Cupric-sulphate ($CuSO_4$). Titrations for determining the ferrous-ion concentration was performed with laboratory grade 0.5M cerium sulphate solution.

4.3 Off-gas Analysis System

The use of bioreactor offgas analysis enables the measurement of oxygen and carbon dioxide utilisation rates during the staged addition experiments. The bioreactor containing the culture and mineral is sealed aerated by a mass flow controller. The rates of oxygen and carbon dioxide utilization are established by measuring the difference between the oxygen and carbon dioxide concentrations in the feed and exit gas from the reactor as shown in the previous chapter. A diagram of this system is shown in Figure (4.1). The exit off gas passes through a condenser, where it is cooled to below 5°C. This allows for a minimization of evaporative water loss from the bioreactor. The dried off gas air is fed from the condenser into a manifold, which allows the measurement and sampling of the off-gas streams from several reactors. The manifold also measures the concentrations of the species in the feed air to the reactors.

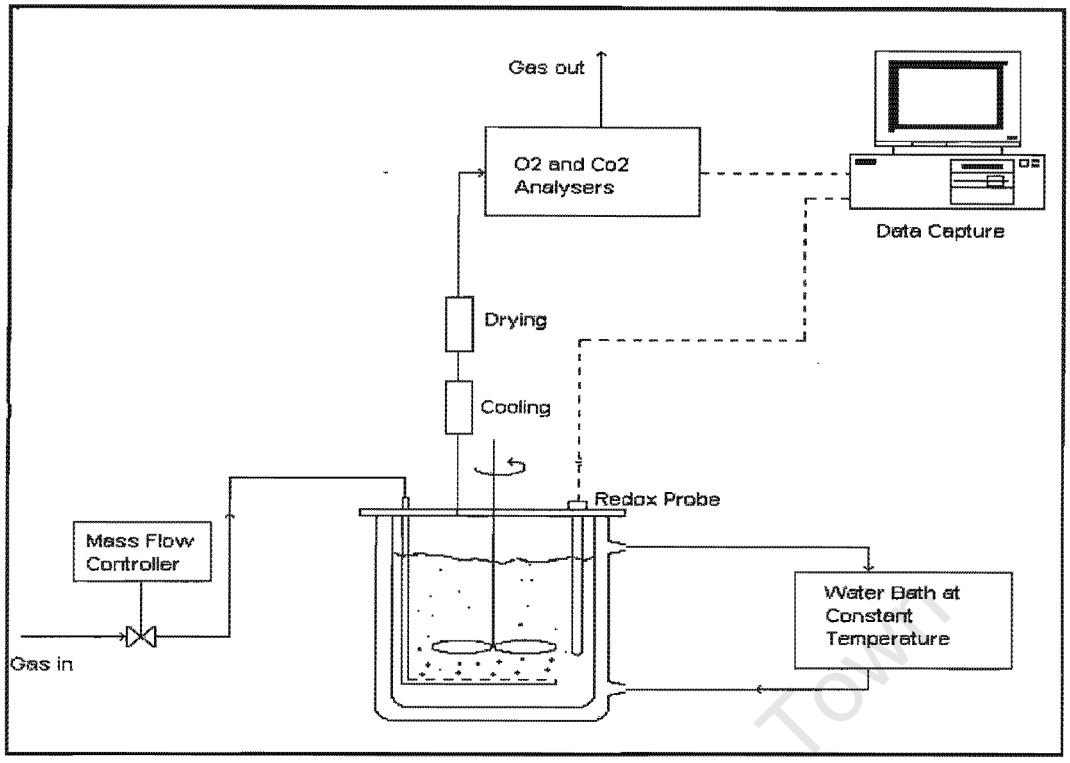

Figure 4.1: Diagramatic representation of a single bioreactor and the accompanying offgas measurement system

The off-gas stream sampling takes place successively, as a result of the opening and closing of solenoid valves (controlled by computer) which measure the off-gas and feed streams from each reactor in succession. Each reactor off-gas stream is sampled for 6 minutes, while the sampling cycle for all reactors is 30 minutes in total.

The off gas air from the reactor which is being sampled is then dried a second time by passing it through a water impermeable membrane, after-which it is fed into the oxygen paramagnetic analyzer and a carbon dioxide infra-red detector. For accurate measurement of the oxygen content of the stream, the oxygen analyser is set to ranges of 19-21%, while the carbon dioxide analyzer is set to measure between 0-500ppm. The measured oxygen and carbon dioxide concentrations from the off gas, together with the concentrations of these species in the feed stream are then logged and stored onto a microcomputer and used to calculate the rates of consumption.

4.4 Minerology of the concentrate

Two chalcopyrite concentrates were used in both the chemical ferric leach study and the bacterial staged addition experiments, viz,

1. An Otjihase Mine flotation concentrate from Namibia
2. A Mintek-supplied flotation concentrate

The elemental analysis for each concentrate is listed in Table 3-1. The sulphur content of the mineral sulphide was estimated by using the Leco SC32 sulfur analyser. The total iron and copper content of the concentrates was established by acid digestion of a known mass sample in nitric, hydroflouric and perchloric acid (Bailey, 1993). This enabled the amount of copper and iron to be measured via flame atomic adsorption spectroscopy (FAAS).

Table 4-1: Elemental Analysis of ground chalcopyrite concentrates

Element	Otjihase (%)	Mintek-supplied (%)
Copper	27.99	29.40
Iron	31.55	31.30
Sulphur	35.69	33.80
Zinc	0.85	
Silicon	1.21	3.68

Table 4-2: Minerological Analysis (XRD) of ground chalcopyrite concentrates

Mineral	Otjihase (%)	*Mintek-supplied (%)
Chalcopyrite	80.77	66
Pyrite	13.11	11
Pyrrhotite		<1
Sphalerite	1.26	3
Bornite	0.01	
Cub/Idiate	0.09	
Other sulphides	0.13	
Quartz	1.62	18
Fe-oxides	1.06	2
Feldspar	0.05	
Other silicates	1.73	
Other/Gangue	0.16	

*Minerological Analysis as obtained from suppliers

Table 4-1 indicates that the major constituents of the concentrates were Copper , Iron and sulphur. The minerological analysis of the concentrates using X-ray diffraction (XRD) is

shown in Table 4-2. The BET surface area analysis showed 1.2 m^2g^{-1} for the Otjihase concentrate and 0.8 m^2g^{-1} for the Mintek-supplied concentrate

Table 4-2 indicates that the major mineral constituents of the Otjihase and Mintek-supplied concentrates were chalcopyrite and pyrite.

4.5 Determination of the ferrous-ion and copper concentration

The ferrous-ion concentration was measured by titration with cerium sulphate solution. In order to establish the validity of this titrametric method for ferrous-ion determination, the effect of the cupric-ion concentration on the titrated ferrous-ion had to be established. For this purpose, ferrous-ion titrations were performed in the presence and absence of 0.01M cupric-ion (added as cupric sulphate) from known standards.

The total copper concentration was measured via Atomic Adsorption Spectroscopy (AAS).

4.6 Probe calibration

The proportions of ferric and ferrous-ions are affected by the total iron and other counterions present in solution. For this reason the redox probe needed to be calibrated at different total iron concentrations and different temperatures. The redox probe calibration was achieved by adding aliquots of ferrous-sulphate ($FeSO_4$-xH_2O) of known concentration to the reactor solution containing a known amount of ferric-sulphate, and measuring the response of the redox potential. The response of the redox potential data acquisition system was rapid and a stable reading was achieved within 5s of a 20 to 30 mV step in redox potential. Also, the effect of cupric-ion on the measured redox potential was considered at $[Fe]^{tot}$=0.2M, by performing the probe calibrations in the presence of 0.01 M and 0.1 M cupric-ion concentrations at both 35 and 55 °C. A similar probe calibration procedure was performed at 35 °C before the staged addition experiments.

The Nernst equation parameters RT/zF and E_o were determined from the slope and intercept of a plot of redox potential vs $\log([Fe^{3+}]/[Fe^{2+}])$

4.7 Bacterial Culture.

The bacteria used is a mixed mesophilic culture containing *Acidithiobacillus ferrooxidans, Acidithiobacillus thiooxidans* and *Leptospirillum ferrooxidans* originally supplied by Mintek. In addition to oxygen, carbon dioxide, ferrous-ion and/or sulphur substrate, bacteria require nitrogen, potassium and phosphorous as well as trace metals like magnesium and zinc for growth. The growth medium is a standard Zero K medium as used by Boon (1996) described in table (4.3). pH was adjusted to 1.5 by addition of 1M H_2SO_4. The required trace metals were sufficiently obtained from the mineral substrate itself, and therefore no additional trace metals were supplied either during culture maintenance or experimentation. The culture was initially grown batchwise at 3 % solids loading on Otjihase chalcopyrite for a period of 7 months. This was maintained as a stock culture which was is used as a source of innoculum in subsequent staged addition experiments.

A semi-continuous system was later implemented to maintain this stock culture. A known volume of bioreactor liquor is withdrawn and replaced with fresh feed and medium on a daily basis thus simulating a continuous set-up at a residence time of 6 days. This maintenance culture contained 3% solids, and was aerated at 200ml/min. The temperature was maintained at 35 °C. No attempt was made during culture maintenance or bacterial experimentation to ensure sterility.

Table 4-3: Constituents of Zero K growth medium

Constituent	Concentration in gl^{-1}
$(NH_4)_2SO_4$	1
K_2HPO_4	0.5
KCl	0.1
$MgSO_4\ 7H_2O$	0.2

4.8 Experimental Procedure of the chemical ferric leaches

The reactors were filled with the required solution and allowed to stand for 3 hrs in the heated jacket to allow the solution to reach the required temperature. The temperatures of the waterbaths were adjusted to 35 and 55 °C respectively for each separate batch run. Experimentation commenced with the addition of the required amount of ground mineral to ensure a homogeneous solids concentration of 1% in the slurry. The reactors were not aerated. The experiments were run batchwise over a 12 day period. The mineral oxidation

was followed by measuring the amount of copper and ferrous-ion solubalised during the batch leach along with the redox potential of the slurry. Samples were taken at regular intervals by extracting about 1% (10ml) of the liquor with a syringe. The liquor was compensated for the loss of volume by adding 10ml of fresh reactor solution.

The samples were filtered through a 8μm Millipore filter and the solids residue returned to the slurry mixture. Sampling was carried out every hour for the first 4 hrs and then once every day for a 12 day period. Table 4-4 shows the experimental conditions employed in the study.

Preliminary results from previous work showed an unusually high extraction of copper within the first 5 minutes of leaching for the Otjihase and Mintek-supplied concentrates. This phenomena was thought to be due to the reaction of surface fines. For this reason, the Otjihase and Mintek-supplied mineral samples used in the investigation were pretreated by ultrasound to remove any fines on the surface. This was done by placing 10 gm of mineral in 0.1 dm^3 of de-ionised water and immersing the sample into an ultrasound bath for 2 minutes. The fines rich supernatant was decanted leaving behind the surface-fines free mineral sample. The procedure was repeated to ensure that all the fines were removed. The cleaned mineral sample was then dried and weighed. It was established that this pretreatment procedure resulted in an approximate 0.7% loss in mineral mass.

Table 4-4: Experimental parameters used in the studying the ferric leaching of chalcopyrite

Experimental Parameter	Varied Value
Initial $[Fe]^{tot}$ ($moll^{-1}$)	0.1 and 0.2 at Temp = 35 °C
Temperature (°C)	35, 55 at initial $[Fe]^{tot}$ = 0.2 $moll^{-1}$ at pH=1.2
p H	1.4
Pulp Density (gl^{-1})	10
Particle size range (μm)	-38 for Otjihase and Mintek-supplied samples
Agitation speed (rpm)	400

4.9 SEM Analysis

The surfaces of the chemically unleached and leached mineral samples were studied via Scanning Electron Photomicrographs from the UCT Electron Microsscope Unit. The residue from the leach liquor was filtered via a 8μm millipore filter and sent for coating and

preparation for exposure under the Scanning Electron Microscope. SEM studies on the bacterial leached mineral residue from the staged addition experiments were not performed.

4.10 Estimation of the initial bacterial concentration during the staged additions

The bacterial concentration during the staged addition experiment is determined from the measured rates of carbon dioxide utilization by integrating the rates of carbon dioxide utilization over time. This calculation is outlined in the previous chapter. This method requires the initial cell concentration of the suspension to be known. The initial cell concentrations for the mineral bioleaching experiments was estimated by measuring the carbon dioxide utilization rate of the stock culture over a weeklong period. If it is assumed that 90% of the cells in the stock culture are attached while 10 % are unattached (Bailey, 1993), then the bacterial concentration of the innoculum to the staged addition experiments can be estimated by taking 10% off the final measured concentration value in the stock culture, and correcting for dilution.

4.11 Experimental procedure for the bacterial staged addition experiments

The changes in bacterial activity and the system redox potential which occur during a change in the availability of substrate is best shown by a staged addition experiment. This method of experimentation has successfully been used to track redox potential and oxygen utilisation rate changes for pyrite bioleaching using a predominantly *Leptospirillum-like* bacteria (Boon, 1996). Online carbon dioxide and oxygen utilisation rates are measured from the reactor offgas. The redox potential together with the calculated specific oxygen utilisation rate are used as a measure of the step changes in bacterial activity occurring during staged mineral additions to a batch culture.

In this experiment a known quantity of predominantly chalcopyrite concentrate was added successively to an active batch culture. Experimentation begins with a 1 litre suspension of a mixed mesophilic culture of known bacterial concentration, which was innoculated (50 % v/v) from the supernatant of a semi-continuously grown culture maintained on the same chalcopyrite concentrate at similar conditions prescribed in the experiment. The batch is allowed to run for 12 hrs or more with 2g/l of chalcopyrite before the first staged addition is made. This allows for the initial adaptation of the culture to the fresh mineral in order to reduce the period of lag phase associated with bacterial growth. Staged additions are then made every 3 hours bringing the mineral concentration up to 32 g/l.

Three sets of experiments resulting in six separate staged addition experiments were conducted, each varying in the initial concentration of total iron in the suspension and the source of chalcopyrite concentrate used. This was done to distinguish any effect of total-iron concentration on the obtained results. Each experiment was repeated with two separate chalcopyrite concentrates at the same conditions of temperature, pH, initial total-iron concentration and innoculum. The experimental conditions prescribed in each of these experiments is listed in Table 4.5.

Table 4-5: Conditions employed in staged addition experiments

Experimental Set	Temp (C)	pH	Initial $[Fe]^{tot}$ (gl^{-1})	Concentrate
1	35	1.5	1.2	Otjihase Chalcoyrite Mintek-supplied Chalcopyrite
2	35	1.5	12	Otjihase Chalcoyrite Mintek-supplied Chalcopyrite
3	35	1.5	12	Otjihase Chalcoyrite Otjihase pyrite

The total iron concentrations were measured in the innoculum taken from the stock culture which was diluted upon innoculation into the batch. During each experiment conducted at an initial total-iron concentration of $1.2g.l^{-1}$, mineral additions of 4, 6, 8 and 10 grams are made every two hours to the batch culture. For the experiment conducted at an initial total-iron concentration of $12g.l^{-1}$ an additional increase by 12gms of each respective mineral concentrate was made to bring the final mineral concentration up to $42g.l^{-1}$.

The bioreactor was completely sealed throughout the course of experimentation except at times of mineral additions. This prevented any contamination of foreign material entering the batch culture and allows for offgas measurement.

Chapter 5: Stochiometry of the Ferric Leaching of Chalcopyrite Concentrates

5 Stochiometry of Ferric sulphate Leaching of Chalcopyrite concentrates

Most workers agree that the dissolution of chalcopyrite in acidic ferric media produces elemental sulphur can be represented according to Equation (5.1) (Dutrizac, 1978; Munoz *et al.*, 1979; Dutrizac, 1981; Hirato *et al.*; 1987; Dutrizac, 1989)

$$CuFeS_2 + 4Fe^{3+} \mapsto Cu^{2+} + 5Fe^{2+} + 2S^0 \qquad (5.1)$$

However, recent work has shown that in addition to the products from Equation (5.1) minor amounts of sulphate is formed according to Equation (5.2) (Dutrizac, 1981; Dutrizac, 1989).

$$CuFeS_2 + 16Fe^{3+} + 8H_2O \mapsto Cu^{2+} + 17Fe^{2+} + 16H^+ + 2SO_4^{-2} \qquad (5.2)$$

The stochiometry of leaching of the chalcopyrite concentrate is also strongly affected by the presence of other sulphide minerals such as pyrite and sphalerite, even in small quantities. This means that the theoretical stochiometry and particularly the ratio of dissolved ferrous-ion to copper cannot be extended to describe the concentrates used in this study. The purpose of this section is to establish the stochiometry of leaching of the Otjihase and Mintek-supplied chalcopyrite concentrates in ferric sulphate solutions at the same conditions as those experienced in mesophilic bioleaching solutions, ie, at temperatures of 35-50 °C and pH's of 1-2.

The results of this are presented in Figures 5.1-5.9. Included in this section is the effect of copper on the measured redox potential, the effect of copper on the measured ferrous-ion concentrations along with a discussion of the observed trends in redox potential, and dissolved ferrous-ion and copper during the course of the experiment.

5.1 Effect of Copper on the measured Redox potential.

The ferric-ion leaching of chalcopyrite results in both ferrous-ion and cupric-ion being solubilised. In the absence of cupric-ion, the measured redox potential is directly proportional to the concentration of the ferric/ferrous-ion ratio. The presence of cupric-ion may affect the proportionality by significantly contributing to the measured redox potential by virtue of the Cuprous/Cupric couple. This would mean that the Nernst equation would contain an extra term to include the effect of the activity of the cuprous-ion on the redox potential. It was therefore necessary to establish the dependence or independence of the measured redox

potential on the dissolved copper concentration at conditions similar to those prescribed in the experiments.

The results of the investigation into the effect of the cupric-ion concentration on the measured redox potential is shown in figure 5.1. The variation in the measured redox potential is plotted as a function of the ferric/ferrous-ion ratio at $[Fe]^{tot}$ = 0.2M and $[Cu^{2+}]$ = 0.01M and 0.1M respectively. Figure 5.1 is also the result of the probe calibrations at 35 and 55 °C.

The results show a linear relationship between the measured redox potential and the logarithm of the concentration of the ferric/ferrous-ion ratio.

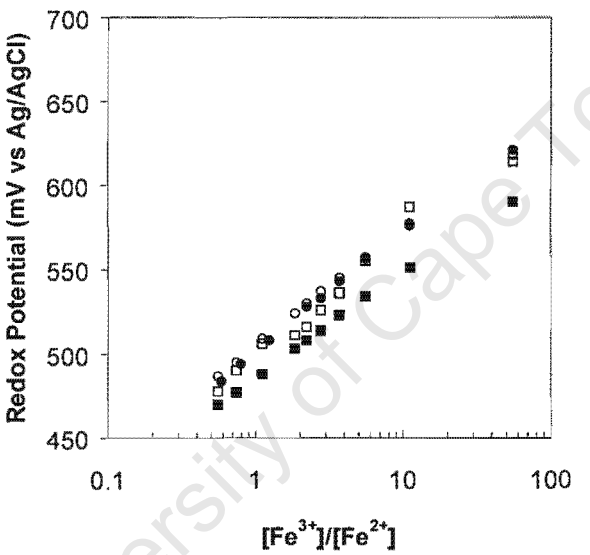

Figure 5.1: The relationship between the measured redox potential and the ferric/ferrous-ion ratio at [ ] $[Cu^{2+}]$ = 0.01M, Temperature = 35 °C; [■] $[Cu^{2+}]$ = 0.1M, Temperature = 35 °C; [o] $[Cu^{2+}]$ = 0.01M, Temperature = 55 °C; [•]$[Cu^{2+}]$ = 0.1M and Temperature = 55 °C. $[Fe]^{tot}$ = 0.2M in all cases.

Table 5-1 indicates the values of the slope (RT/zF) and intercept (E_0) of a linear regression analysis at the various cupric-ion concentrations and temperatures.

The slopes and intercepts of the Nernst equation plot at $[Cu^{2+}]$ = 0.1 M is only slightly higher than that at 0.01M at both temperatures. It is therefore apparent from Figure 5.1 and Table 5-1 that the concentration of cupric-ion, $[Cu^{2+}]$, does not have a significant effect on the value of the measured redox potential at concentrations up to $[Cu^{2+}]$ = 0.1M.

These results justify the neglect of the effect of cupric-ion activity in the Nernst equation for the range of copper concentrations obtained in the study. This is consistent with other workers who also established a linear proportionality between the measured redox potential and the ferric/ferrous-ion concentration in the presence of cupric-ion within the concentration range of $[Cu^{2+}]$ = 0.001-0.01at 40 °C (Hiroyoshi *et al.*, 2000).

There is no discernable difference between the slopes and intercepts at both cupric-ion concentrations. This is seen both at 35 and 55 °C. It is clear from Figure 5.1 and Table 5-1 that a larger temperature results in a higher slope and intercept. This result is consistent with the Nernst equation.

Table 5-1: Regression Analysis on the relationship between the measured redox potential and the ferric/ferrous-ion ratio at various cupric-ion concentrations. $[Fe]^{tot}$ = 0.2M in all cases.

Temp in °C	$[Cu^{2+}]$ in $moll^{-1}$	(RT/zF) in mV	$E^{"}_{o}$ in mV	R^2
35	0.01	26.78	493	0.94
35	0.1	25.40	487	0.99
55	0.01	27.43	507	0.99
55	0.1	29.46	503	0.99

This work demonstrates that the cupric-ion species has no significant effect on the measured redox potential. This means that the redox potential in primarily determined by the ferric/ferrous-ion couple during the chemical ferric leaching of chalcopyrite at cupric-ion concentrations as high as 0.1M. The effect of copper was not extended to higher cupric-ion concentrations since the copper solubalised during the mesophilic bioleaching or chemical leaching of chalcopyrite at temperatures lower than 55 °C, rarely exceeds this value at the solids concentrations and residence times employed in this study.

5.2 The effect of copper on the measured ferrous-ion concentration.

The validity of using the cerium sulphate titrametric method for the determination of ferrous-ion concentration was investigated by titrating for ferrous-ion in known standards prepared in the presence and absence of 0.01M cupric-ion. The initial ferric-ion and pH of the standards were held at similar conditions as those used in the mineral leaching experiments.

Figure 5.5 shows the concentrations of ferrous-ion measured via titration plotted against the known concentration of ferrous-ion, both in the presence and absence of 0.01M cupric-ion. The range of cupric-ion concentrations established from the ferric leaching of the chalcopyrite concentrates at all the conditions employed in the study fall below this cupric-ion concentration.

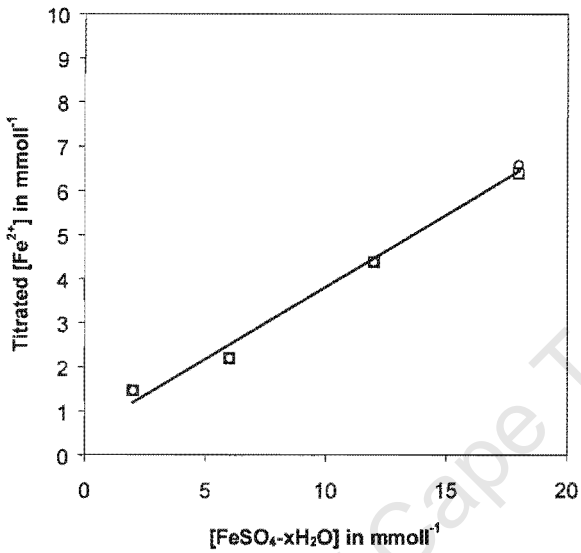

Figure 5.5: The variation of the $[Fe^{2+}]$ measured via titration with cerium sulphate against the known $[FeSO_4]$ in the [0] absence of cupric-ion and in the [ ] presence of 0.01 M $[CuSO_4]$. Initial $[Fe_2(SO_4)_3]$ = 0.2M in both cases. Linear regression fit predicts a constant of 0.328 and intercept of 0.536 for an R^2 of 0.98 both in the presence and absence of any copper.

The regression analysis of the data showed an accurate linear fit with a constant of 0.328 and intercept of 0.536 for an R^2 of 0.98 both in the presence and absence of any copper. Figure 5.2 and the regression data clearly show that there is no difference in the concentrations of measured ferrous-ion in the presence and absence of copper. This shows that the determined value of the ferrous-ion concentration via titration is independent of the copper present in solution. This result validates the use of cerium sulphate titrations to measure the concentration of ferrous-ion in solutions containing copper at dilute copper concentrations.

5.3 Redox Potential trend

The change in the redox potential of the slurry during the experiments is shown in Figure 5.3. Included in figure 5.3 is the redox potential measurements at initial total iron concentrations of 0.2 and 0.1M, as well as the redox potential trend observed at 35 and 55 °C for both concentrates. It is apparent from Figure 4.3 that the redox potential of the slurry decreases

during the course of the experiment. The decreasing trend is similar despite the differing initial total iron concentrations and concentrates.

The largest initial redox potential is seen at the largest initial total-iron concentration. This is consistent with the Nernst equation which expresses the redox potential as a function of the ferric/ferrous-ion ratio.

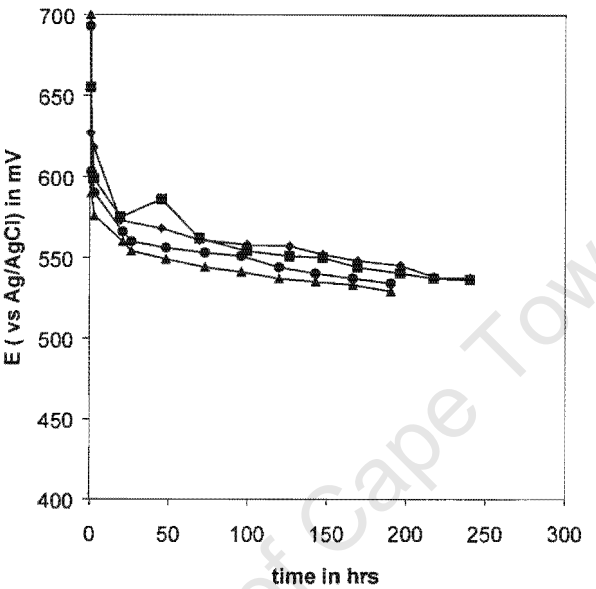

Figure 5.3: The variation in the redox potential with time for the Mintek supplied concentrate at [▲][Fe]^{tot} = 0.2M, Temp = 35 °C; and the Otjihase concentrate slurry at [◆] [Fe]^{tot} = 0.1M, Temp = 35 °C; [●][Fe]^{tot} = 0.2M, Temp = 35 °C; [■]Fe]^{tot} = 0.2M, Temp = 55 °C

Although the total iron concentration is the summation of both the concentrations of the ferric-ion and ferrous-ion species, the proportion of ferric-ion concentration at the start of the experiment is always much larger than the ferrous-ion concentration. This means that the initial total-iron concentration is essentially made up of the ferric-ion species. The larger initial ferric-ion concentration therefore results in a larger initial redox potential by virtue of the Nernst equation. It must be pointed out that the initial total iron concentration was estimated as ferric sulphate. The degree of hydration and the speciation of the ferric-ion complex will be examined in the subsequent section.

The decrease in the redox potential of the slurry with time is also consistent with the Nernst equation. This trend shows that the ferrous-ion concentration increases by virtue of the ferric-ions being consumed according to the half reaction shown in Equation (5.1) during the leaching of the concentrate.

$$Fe^{3+} + e^{-} \mapsto Fe^{2+} \quad (5.1)$$

The trend in the redox potential is similar at both the initial ferric-ion concentrations. It could be argued that the rate at which chalcopyrite is leached is a function of the redox potential or ferric/ferrous-ion ratio, instead of the absolute ferric-ion concentration. This is consistent with that observed for both pyrite (May *et al.*, 1997) and arsenopyrite (Breed *et al.*, 1997; Ruitenberg *et al.*, 1999).

5.4 Ferric-ion speciation

The degree of hydration of ferric sulphate in sulphuric acid determines the actual concentration of free ferric-ions in the slurry. It has already been mentioned that the speciation of ferric sulphate in sulphuric acid results in the formation of free ferric-ion, Fe^{3+} along with ferric sulphato, $FeSO_4^{+}$, and ferric bisulphato, $FeHSO_4^{2+}$ complexes according to Equation's (5.1) and (5.2) respectively.

Figure 5.4 shows the thermodynamically predicted distribution of these complexes as a function of the ferric sulphate concentration in sulphuric acid solutions, estimated from the published equilibrium constant data (Dry, 1984) and Equation's (2.8), (2.9) and (2.10) at 35 °C. The predictions were estimated using the using the procedure outlined in Chapter Two.

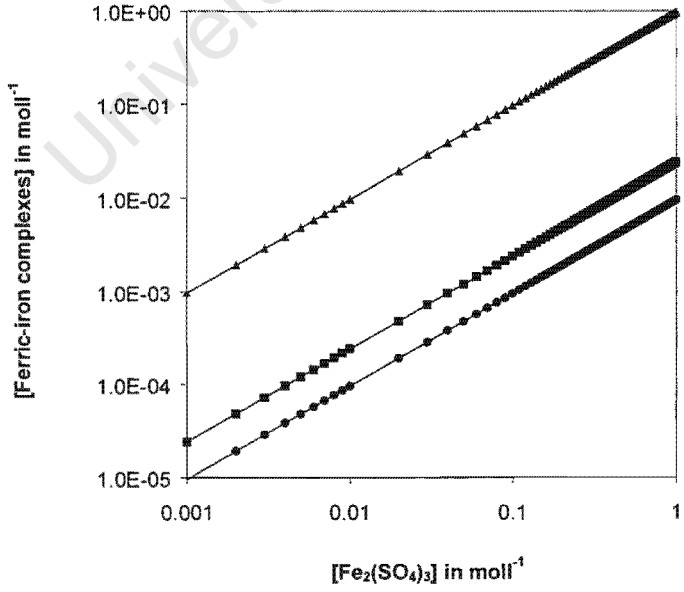

Figure 5.4: The distribution of the [•]free ferric-ion, Fe^{3+}; [▲]ferric sulphato, $FeSO_4^{+}$; and [■]ferric bisulphato, $FeHSO_4^{2+}$ complexes in $Fe_2(SO_4)_3$-H_2SO_4 solutions having different initial ferric sulphate concentrations at pH=1; Temperature = 35 °C.

It is clear from Figure 5.4 that the predicted distribution of ferric-ion species in not only confined to Fe^{3+}, but also significant quantities of $FeSO_4^+$ and $FeHSO_4^{2+}$. The dominant species appears to be $FeSO_4^+$ at all ferric sulphate concentrations. The exact role of each of the separate ferric complexes in the leaching of chalcopyrite still remains unclear. Past workers have assumed that the free ferric-ion or the ferric bisulphato complex are the primary leaching agents of chalcopyrite because they found the rate of leaching to be directly proportional to the free ferric-ion concentration. It was thought that the free ferric iron and ferric bisulphato complexes are much more easily reduced than the ferric sulphato complex, even though it is the dominant species at those ferric sulphate concentrations (Hirato *et al.*, 1987). This has been supported by other research which found that the rate of sphalerite dissolution was proportional to the sum of the free ferric-ion and ferric bisulphato complexes (Crundwell, 1988).

Based on the above, it was assumed in this study that the free ferric iron is the primary oxidant during the leaching of chalcopyrite, although it has been shown, at least from a theoretical analysis, that other ferric-ion complexes may well exist in significant quantities in the slurry.

5.5 Ferrous-ion and Copper dissolution

Figures 5.5(a) and 5.5(b) shows the variation in the ferrous-ion and cupric-iron concentration, respectively, with time at all the conditions investigated, *viz*, initial total iron concentrations of 0.1 and 0.2M, and at temperatures of 35 and 55 °C for the concentrates used in the study.

Figure's 5.5(a) and 5.5(b) indicate that the ferrous-ion and cupric-ion concentrations vary linearly with time initially, but then appears to slow down. This shows that the solubalisation of both ferrous-ion and cupric-ion within the first few hours is much more rapid in comparison to that observed afterward. It is also apparent form Figure's 5.5(a) and 5.5(b) that the shape of the dissolution curves are the same at all the initial total iron concentrations and at the different temperatures for both the concentrates used in the study. The curves show a rapid decline in the rate of oxidation. This is consistent with previous work carried out at 70 and 90 °C (Munoz *et al.*, 1979; Dutrizac, 1979; Dutrizac, 1981; Hirato *et al.*, 1987) who observed so-called parabolic kinetics for the ferric-sulphate leaching of chalcopyrite at similar leaching times at those employed in current study.

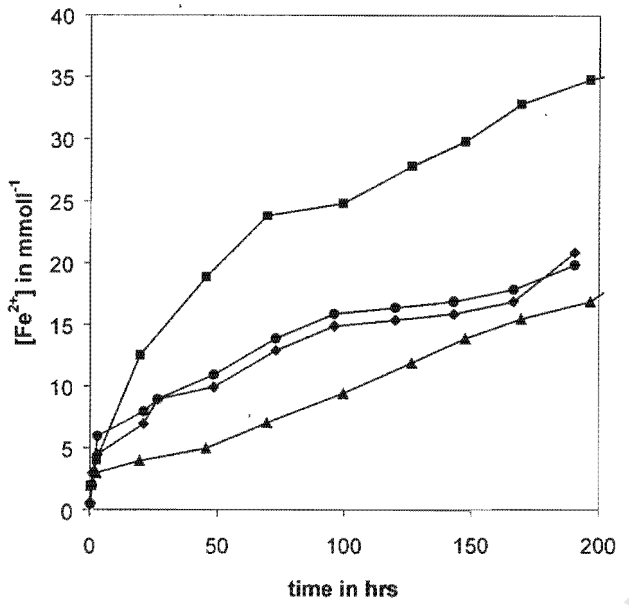

Figure 5.5(a): The variation in the ferrous-ion concentration with time at [●] $[Fe]^{tot}$=0.2M, Temp=35 °C; [▲][$Fe]^{tot}$=0.1M, Temp=35 °C; [■][$Fe]^{tot}$=0.2M, Temp=55 °C for the Otjihase chalcopyrite concentrate and [◆] $[Fe]^{tot}$=0.2M, Temp=35 °C for the Mintek-supplied chalcopyrite concentrate

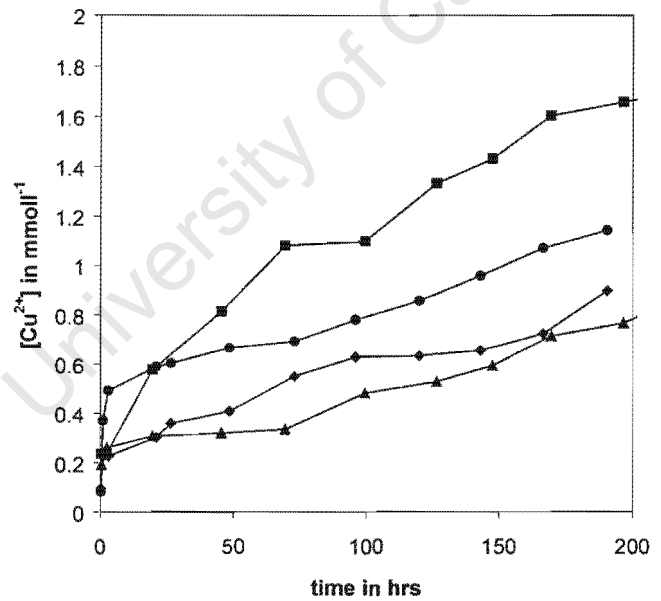

Figure 5.5(b): The variation in the cuprous-ion concentration with time at [●] $[Fe]^{tot}$=0.2M, Temp=35 °C; [▲][$Fe]^{tot}$=0.1M, Temp=35 °C; [■][$Fe]^{tot}$=0.2M, Temp=55 °C for the Otjihase chalcopyrite concentrate and [◆] $[Fe]^{tot}$=0.2M, Temp=35 °C for the Mintek-supplied chalcopyrite concentrate

The measurement of ferrous-ion during the initial rapid phase of leaching was hampered by a high concentration of ferric-ion. For this period only two or three accurate measurements were possible. Also, considerable difficulty was experienced in obtaining measurable

quantities of ferrous-ion via titration with cerium sulphate, especially at the high redox potentials seen in the initial linear phase of concentration vs time curves. Despite these limitations, a change in mechanism is evidently seen from the concentration vs time curves (Figure 5.5(a) and 5.5(b)) after the short initial phase.

The retarded rate of copper solubalisation from chalcopyrite with time as seen in Figure 5.5(b) suggest the rapid onset of passivation by either:

1. The build-up of reaction products layers such as sulphur on the mineral surface, or
2. The formation of an electronically insulating polysulphide layer on the surface, or
3. The co-precipitation of iron and copper compounds from the bulk onto the mineral surface

Since the slurry pH was initially 1.1 and did not vary by less that 0.2-0.3 units, so the second possibility seems unlikely. Furthermore, the slurry solution was visibly clear throughout the leach. It is thought that the low pH is tantamount to the prevention of iron hydrolysis and precipitation during the leaching reaction (Dutrizac, 1978). The detection of any polysulphide layers as well as the quantification of sulphur on the surface was beyond the scope of the study. However, Scanning Electron Photomicrographs (SEM) were taken of the mineral residue after 8 days of leaching in an attempt to visually establish any build-up of sulphur on the surface. (An analysis of these results is shown in the subsequent sections).

5.6 The effect of the initial ferric-ion concentration

It is apparent from Figure 5.5(a) and 5.5(b) that a significantly larger amount of ferrous-ion and copper is solubilised in the slurry containing a higher initial ferric-ion concentration. This suggests that the final conversion of chalcopyrite increases with an increase in the initial ferric-ion concentration. Table 5-2 lists the conversions calculated based on the measured amount of copper extracted after 8 days at the different initial ferric-ion concentrations.

Table 5-2: Chalcopyrite conversion calculated for the Otjihase concentrate based on the final copper concentration after 8 days

$[Fe^{3+}]_{initial}$ in $moll^{-1}$	X_{CuFeS2} in %
0.1	1.6
0.2	2.2

This appears to be consistent with previous workers who found that the rate of chalcopyrite leaching in ferric sulphate solution was dependent on the initial ferric-ion concentration up to 2 mol.l^{-1} (Dutrizac, 1981) and 0.1 mol.l^{-1} (Hirato *et al.*, 1987), but contradicts others workers who established no rate dependency on the initial ferric-ion concentration (Munoz et al; 1979).

Furthermore, the results shown in Figure's 5.5(a) and 5.5(b) suggest that generally the chemical ferric-ion leaching of chalcopyrite occurs as shown in Equation (5.2),

$$CuFeS_2 + (x-1)Fe^{3+} \mapsto Cu^{2+} + xFe^{2+} + Sulphur\text{-}species \qquad (5.2)$$

Equation (5.2) may include a term for the polysulphide layer as a reaction product and a hydronium-ion in the case of sulphate formation.

5.7 Ferrous-ion to Copper ratio

Figure 5.6 shows the variation in the measured ferrous-ion to copper ratio's obtained during the course of the experiment for all the conditions applied and for all the concentrates studied.

It is apparent from figure 5.6 that the ratio's of ferrous-ion to copper are not constant during the leaching of chalcopyrite. It can also be seen that the shape of the plot is similar for both initial total iron concentrations and temperatures employed during the study. It appears that the ratio's are generally smaller than 7 for the initial rapid phase and then increase to about 15 or higher at 50 hours, then finally settle at 20 for the Otjihase concentrate at 35 °C .

In the case of the Mintek-supplied concentrate the ratio's tend to be higher than 7 initially and increase to values of 23 after the initial phase for the similar conditions (initial $[Fe]^{tot}$= 0.2M , Temp=35 °C).

The effect of temperature is also shown in figure 5.6 by comparing the ratio's obtained at 35 °C and 55 °C at the same initial total iron concentration. At 55 °C, the ratio's reach the a final value of 22 much more rapidly than at 35 °C.

In an attempt to distinguish between the proposed reaction stochiometries for sulphur and/or sulphate formation and to establish the coefficient of x in Equation (5.2) the ferrous-ion

concentration was plotted against the copper concentration as shown in Figure 5.7. A linear regression of the results shown in Figure 5.7 is presented in Table 5-3.

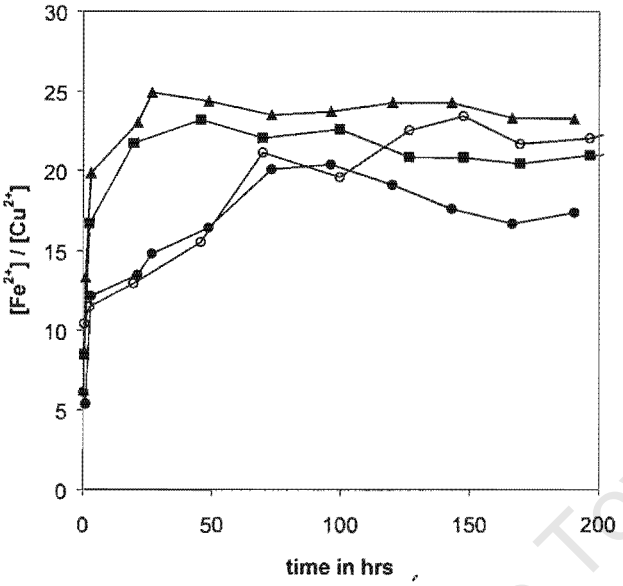

Figure 5.6: The variation in the ferrous-ion to cuprous-ion ratio with time at [●] $[Fe]^{tot}$=0.2M, Temp=35 °C; [○][Fe]^{tot}=0.1M, Temp=35 °C; [■][Fe]^{tot}=0.2M, Temp=55 °C for the Otjihase chalcopyrite concentrate and [▲] $[Fe]^{tot}$=0.2M, Temp=35 °C for the Mintek-supplied chalcopyrite concentrate

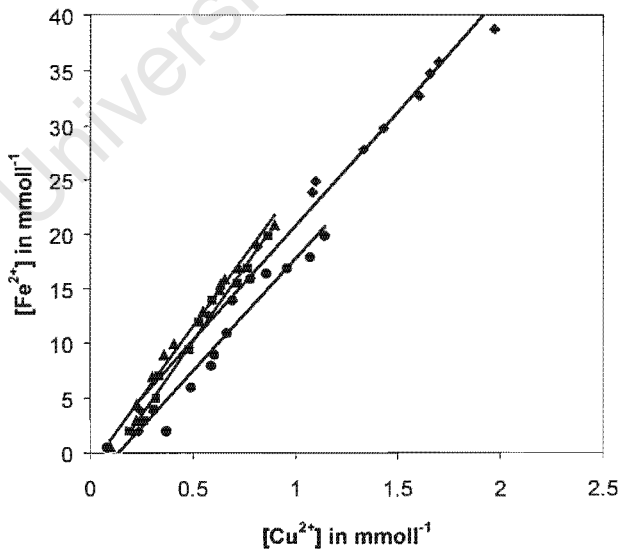

Figure 5.7: The variation in the ferrous-ion concentration as a function of the cuprous-ion concentration at [●] $[Fe]^{tot}$=0.2M, Temp=35 °C; [■][Fe]^{tot}=0.1M, Temp=35 °C; [◆][Fe]^{tot}=0.2M, Temp=55 °C for the Otjihase chalcopyrite concentrate and [▲] $[Fe]^{tot}$=0.2M, Temp=35 °C for the Mintek-supplied chalcopyrite concentrate

It is clear from Figure 5.7 and Table 5-3 that the coefficient, x, appears to support the stochiometry shown in Equation (5.2) for sulphate formation as opposed to Equation (5.1) for sulphur formation. This result was unexpected since most of the previous work on the ferric sulphate leaching of chalcopyrite found a larger proportion of sulphur formation than sulphate formation during the ferric-sulphate leaching of chalcopyrite (Braithworth *et al.*, 1976; Jones and Peters, 1976; Dutrizac, 1978; Munoz *et al.*, 1979; Dutrizac, 1981; Hirato *et al.*; 1987; Dutrizac, 1989). However, most previous workers carried out the studies at much higher temperatures (70-90 °C) than those used in this investigation.

The results obtained in Table 5-3 differ significantly from that which is theoretically predicted in Equation (5.1). The stochiometric coefficient obtained at an initial total iron concentration of 0.1 M, differed significantly from that obtained at the other conditions. Similarly the stochiometric coefficient established for the Mintek-supplied chalcopyrite concentrate was larger than those established for the Otjihase concentrate at the same experimental conditions.

Table 5-3: Results of the linear regression carried out on the data presented in figure 5.6, ie, the variation in the ferrous-ion concentration as a function of the cuprous-ion concentration for all the conditions and concentrates used in the study.

Initial $[Fe]^{tot}$ ($moll^{-1}$)	Chalcopyrite concentrate	Temperature (°C)	Coefficient (x)	R^2
0.1	Otjihase	35	26.391	0.983
0.2	Otjihase	35	19.052	0.927
0.2	Otjihase	55	19.296	0.980
0.2	Mintek-supplied	35	23.641	0.987

This variation in the stochiometric coefficients of ferrous-ion, in Table 5-3, suggest that the ferrous-ion to cupric-ion ratio is possibly affected by the ferric-ion leaching of the pyrite proportion as well as other sulphide mineral impurities present in both the Otjihase and the Mintek supplied concentrate.

However, the results presented in Figure 5.7 and Table 5-3 are dependent on the methodology employed in performing the linear regressions at each experimental condition. The regressions are carried out over the entire set of measured concentrations for each condition. It therefore does not take into account the sudden change in ferrous-ion to cupric-ion ratio's experienced after the first few hours of mineral leaching since all the data points are treated in a single regression at each condition. This means that the stochiometric coefficients

established in Figure 5.7 and Table 5-3 are more indicative of the second slower phase of mineral leaching than the first. This is because only two or three measurements were made within this rapid initial phase, as compared to 7 or 8 measurements in the subsequent slower phase. Despite this limitation, the results indicate that the stochiometry appears to be more consistent with sulphate formation than sulphur formation, at least for most of the reaction.

4.8 Conversion of chalcopyrite

In an attempt to confirm which of the above Reaction's ((5.1) or (5.2)) best describe the leaching of chalcopyrite under the conditions employed in this investigation, the conversion of chalcopyrite determined from the measured copper concentration was compared with that obtained based on the measured ferrous-ion concentration in solution (assuming that the chemical leaching results either in sulphur or sulphate formation). In doing this, the rate of chalcopyrite oxidation, r_{CuFeS2}, is related to the rate of ferrous-ion production, r_{Fe2+}, via the stochiometry of Equation (5.1) for assumed sulphur formation only, as Equation 5.3

$$-r_{CuFeS_2} = \frac{1}{5} r_{Fe^{2+}} \qquad (5.3)$$

Similarly, the rate of chalcopyrite oxidation is related to the rate of ferrous-ion production via the stochiometry of Equation (5.2) for assumed sulphate formation as Equation (5.4),

$$-r_{CuFeS_2} = \frac{1}{17} r_{Fe^{2+}} \qquad (5.4)$$

Furthermore, the actual measured rate of chalcopyrite oxidation was related to the rate of copper production as Equation (5.5)

$$-r_{CuFeS_2} = r_{Cu^{2+}} \qquad (5.5)$$

The conversion of chalcopyrite calculated using the above relations is shown in Figure 5.8 for all the conditions and concentrates used in the study.

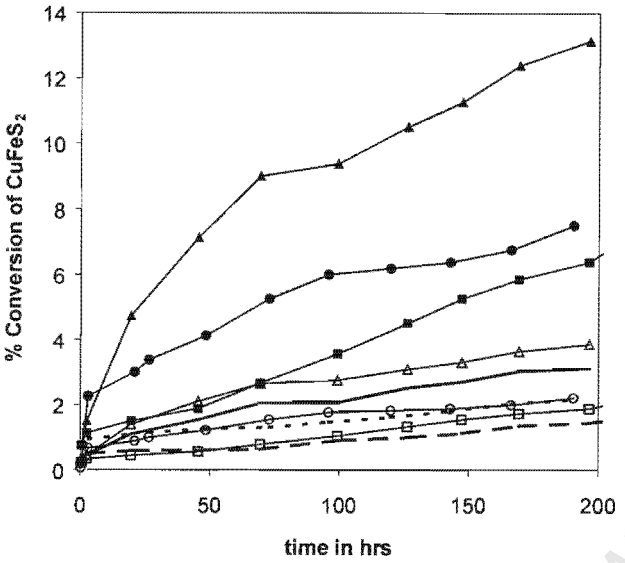

Figure 5.8: The variation of chalcopyrite conversion determined from the concentration of copper solubalised for the Otjihase concentrate at [--] initial $[Fe]^{tot} = 0.2M$, Temp = 35 °C; [— —] initial $[Fe]^{tot} = 0.2M$, Temp = 35 °C; [—]initial $[Fe]^{tot} = 0.2M$, Temp = 55 °C compared to the chalcopyrite conversion predicted using the measured concentration of ferrous-ion, based on equation (1) for sulphur formation at [•]initial $[Fe]^{tot} = 0.2M$, Temp = 35 °C; [■] initial $[Fe]^{tot} = 0.2M$, Temp = 35 °C; [▲]initial $[Fe]^{tot} = 0.2M$, Temp = 55 °C and equation (2) for sulphate formation at [o]initial $[Fe]^{tot} = 0.2M$, Temp = 35 °C; [□] initial $[Fe]^{tot} = 0.2M$, Temp = 35 °C; [Δ]initial $[Fe]^{tot} = 0.2M$, Temp = 55 °C.

Figure 5.8 shows a large discrepency between the conversions of chalcopyrite calculated using Equation (5.1) as the assumed stochiometry and the actual conversion obtained based on the copper measurements. It is also apparent from Figure 5.8 that the conversion of chalcopyrite calculated from Equation (5.4) is closest to that obtained based on the measured copper concentration. This result, together with those presented in Figures 5.5-5.8 and Table 5-3 suggests that the stochiometry of Equation (5.2) is the closest in describing the ferric sulphate leaching of the Otjihase and Mintek supplied chalcopyrite concentrates at least for the slower reaction phase which contributes the major portion of the reaction behavior over time. However this deduction is subject to limitations discussed in Section 5.10.

The results in Figure 5.8 also show that a very small proportion of the copper from the mineral is solubalised over the 8 day period (2 % at 35 °C) at the low temperatures used in this study. This result agrees with those of previous workers who established less than 5 % mineral solubilisation (measured as the amount of dissolved copper in solution) at 30 °C in 0.1M $Fe_2(SO_4)_3$-H_2SO_4 (Dutrizac, 1978)

5.9 Scanning Electron Photomicograph (SEM)Analysis.

The leached surfaces of the Otjihase and Mintek-supplied concentrates were examined by SEM photographs before and after 7 days of leaching in order to visually detect any layers of sulphur product. The results of this analysis is shown in Figures 5.9-5.12. Figures 5.9(a) and (c) illustrates the unleached photomicrograph of the Otjihase and Mintek-supplied concentrate respectively. Figures 5.9(b) and (d) indicate the images the surfaces of each respective concentrate after 7 days leaching at 35 °C in a 0.2 M initial $[Fe]^{tot}$ solution. Similarly, figure 5.9(e) illustrates an SEM image of the Otjihase concentrate after 7 days of leaching at 55 °C in a 0.2 M initial $[Fe]^{tot}$ solution.

The unleached surfaces shown in Figures 5.9(a) and (c) show a number of small particles on the surface. This is thought to be surface fines despite the treatment of the mineral samples by ultrasound. The Otjihase concentrate seems to exhibit a higher degree of surface roughness as compared to the Mintek-supplied concentrate. This could explain the slightly higher ferrous-ion and copper dissolution rates from the Otjihase concentrate experienced at the same conditions

The leached surfaces shown in Figure's 5.9(b)-5.9(d) are similar is visual appearance to the unleached surfaces shown in Figures 5.9(a) and (c). This is reasonable since less that 5 % conversion of chalcopyrite occurs at the employed conditions of temperature and leach time.

The surfaces of both the Otjihase and the Mintek-supplied concentrate seem to indicate tiny granules, although it remains unclear if these are infact sulphur deposits or not. It is evident from these figures that the surface of the leached particles of both concentrates are not covered with globules of granular sulphur as has been observed by previous workers for leaching after 3hrs at 95 °C (Dutrizac, 1989). There is also evidence of surface roughening although pitting is not seen in the case of leached particles. This is more clearly seen in figure 5.9(e) for leaching at 55 °C.

In summary, no quantifyable difference between the leached ad unleached surfaces can be seen from the SEM analysis.

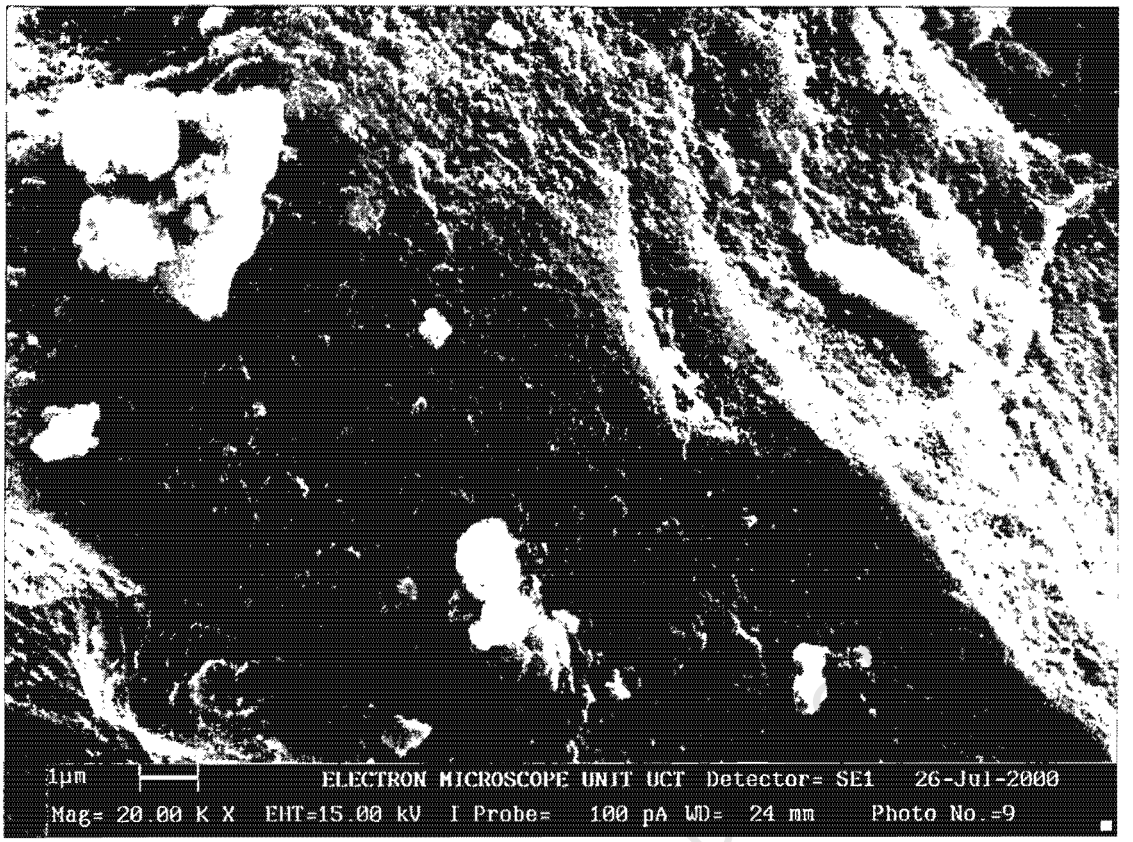

Figure 5.9(a): SEM of the surface of unleached Otjihase concentrate mineral particles for particle size range +25-38 µm

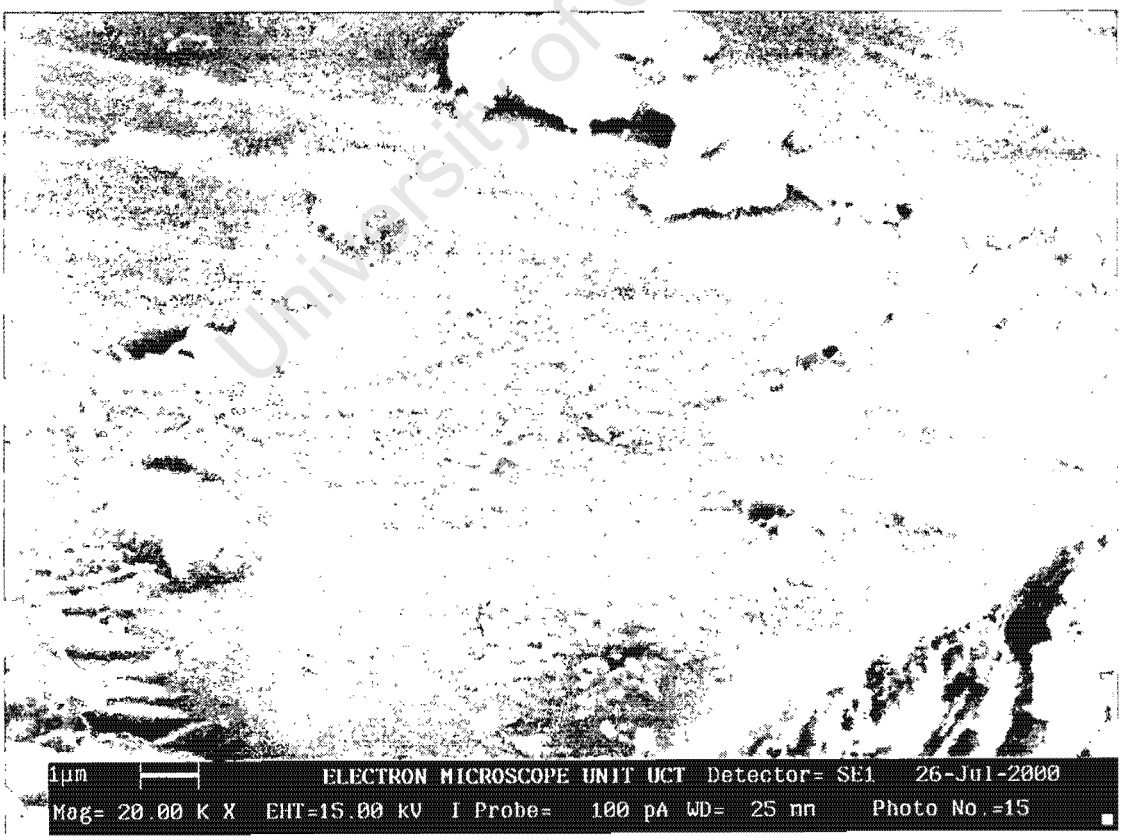

Figure 5.9(b): SEM of the surface of Otjihase concentrate particles after 7 days of leaching at initial $[Fe]^{tot}$ =0.2M, Temp = 35 °.

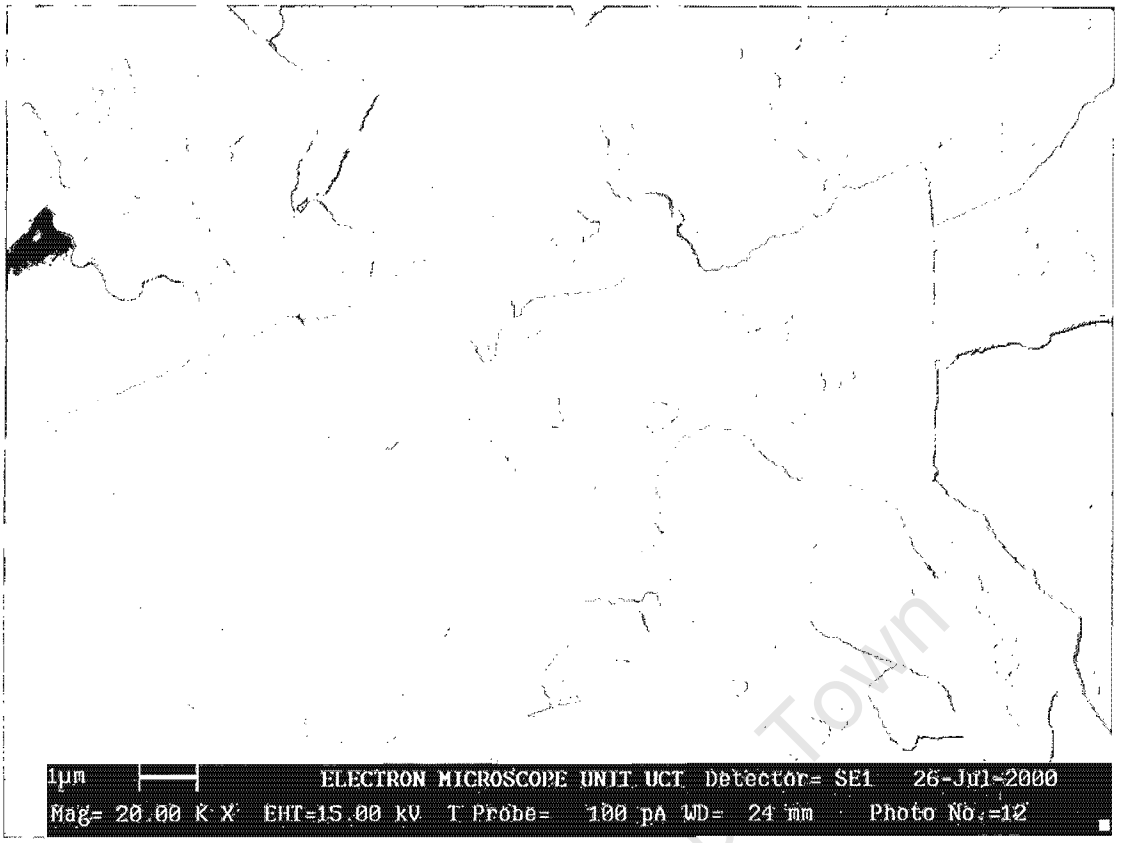

Figure 4.9(c): SEM of the surface of unleached Mintek-supplied concentrate mineral particles for particle size range +25-38 µm

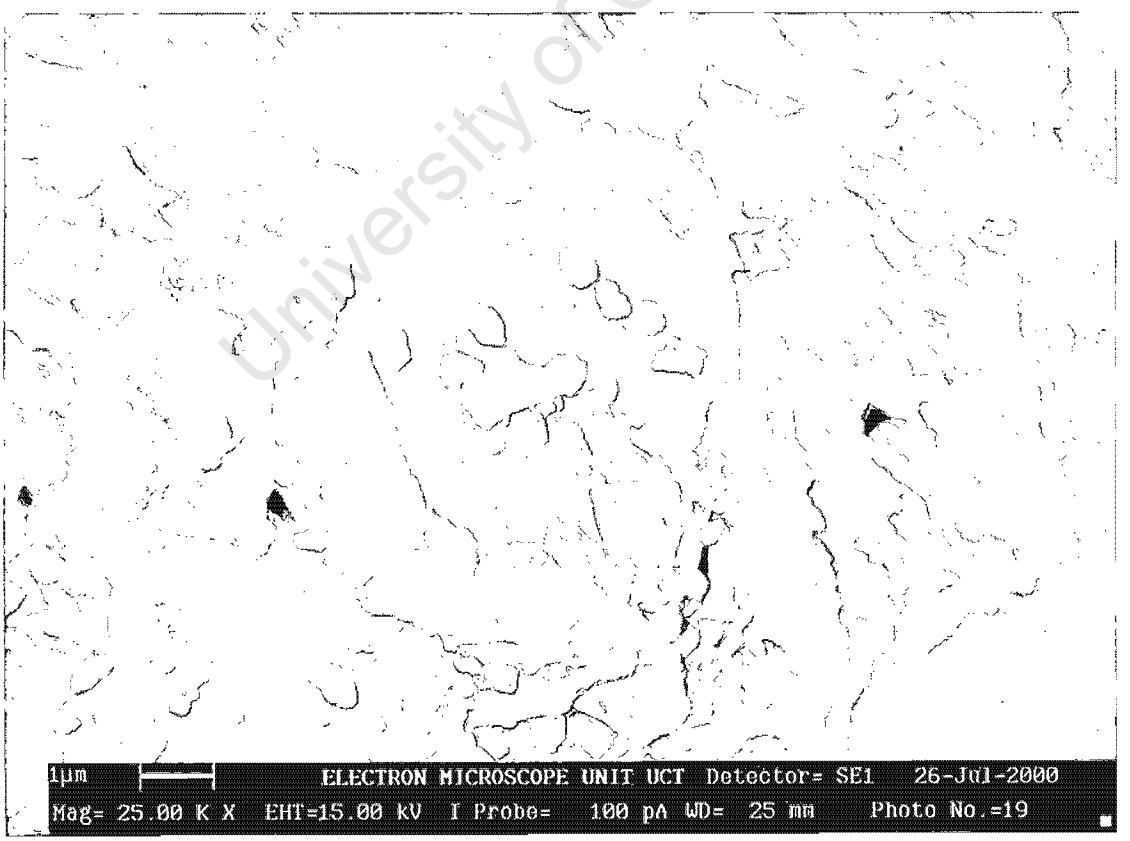

Figure 4.9(d): SEM of the surface of Mintek-supplied concentrate particles after 7 days of leaching at initial $[Fe]^{tot}$ =0.2M, Temp = 35 °.

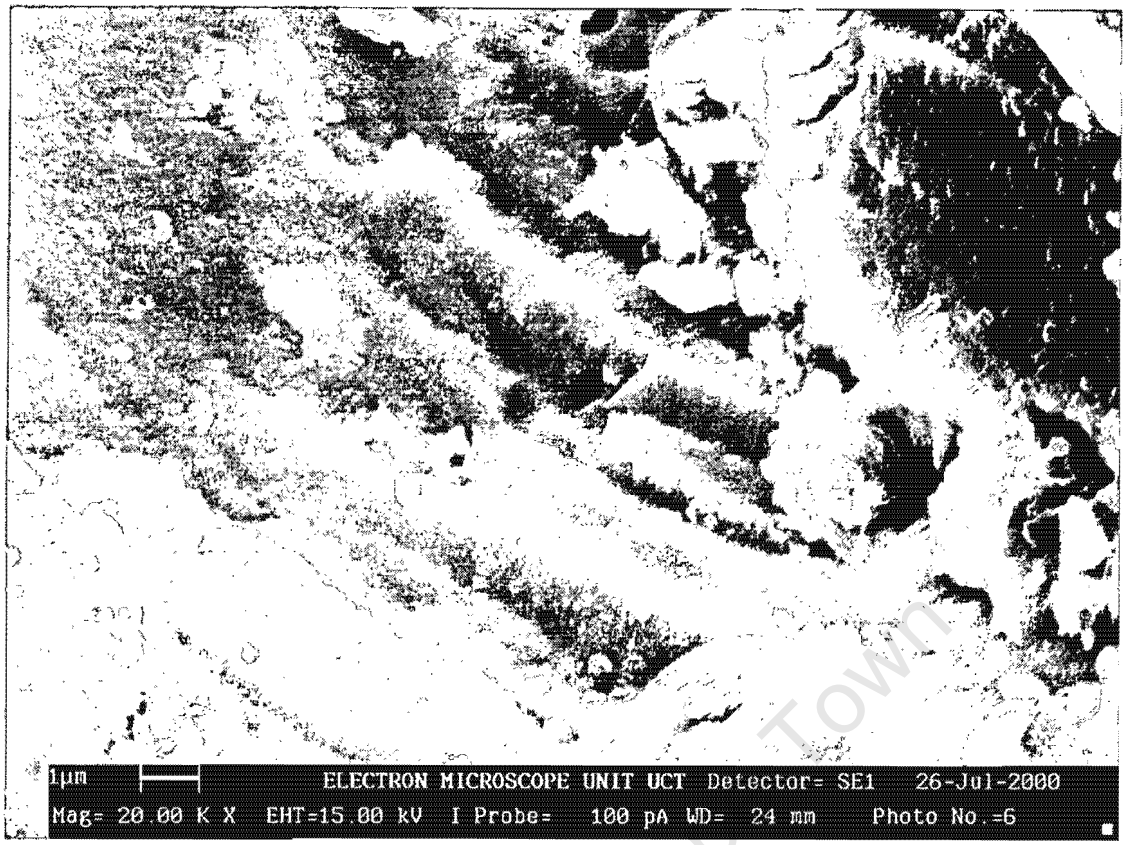

Figure 5.9(e): SEM of the surface of Otjihase concentrate particles after 7 days of leaching at initial $[Fe]^{tot}$ =0.2M, Temp = 55 °C

5.10 Limitations

The stochiometry of ferric sulphate leaching of the Otjihase and Mintek-supplied chalcopyrite concentrates are dependent on the amount of ferrous-ion and copper solubilised. It has already been shown that the ratio of these species are not constant during the reaction but vary over an 8 day period for both concentrates. The ratio of ferrous-ion to copper obtained for these concentrates appears to be closest to that which is theoretically predicted by Equation (5.2) for sulphate formation as opposed to sulphur formation for the chemical leaching of chalcopyrite. However, despite this observation, the interpretation of the results is both limited and hindered by the presence of other mineral sulphides in the concentrate.

5.10.1 The effect of pyrite and/or sphalerite leaching

The dissolved ferrous-ion to copper ratios would be dependent on the presence of rapidly leaching sulphide impurities which could reduce ferric-ion to ferrous-ion without releasing any copper. In this case the amount of ferrous-ion dissoluted from the two concentrates

would most likely be affected by the leaching of the pyrite which mainly yields sulphate and/or the sphalerite proportion of the concentrate which mainly yields sulphur.

The observed stochiometry of the Otjihase and Mintek-supplied concentrate leaching can therefore be broadly explained in terms of the five possibilities, *viz*,

i. Chalcopyrite leaching only to produce only ferrous-ion, copper and sulphur or sulphate as the primary sulphur species

ii. Chalcopyrite leaching accompanied by pyrite leaching to produce ferrous-ion, copper and both elemental sulphur and sulphate.

iii. Chalcopyrite leaching accompanied by both pyrite and sphalerite leaching to produce both elemental sulphur and sulphate.

iv. Chalcopyrite leaching accompanied by sphalerite leaching to produce both elemental sulphur and sulphate.

v. Initial chalcopyrite leaching to produce ferrous-ion, copper, sulphur or sulphate, followed by the rapid onset of passivation resulting in copper and ferrous-ion dissolution from polysulphide surface phases other than chalcopyrite.

It is impossible to physically separate the ferrous-ion contributed by the leaching of small quantities of interlocked pyrite or sphalerite within the mineral sulphide from that originating from the leaching of pure chalcopyrite itself.

The changing ferrous-ion to copper ratio seems to indicate that more than one reaction is involved in the ferric leaching of the chalcopyrite concentrate. This discounts the first possibility.

5.10.2 Galvanic interactions between chalcopyrite, pyrite and sphalerite.

Literature has cited evidence that the leaching behavior of sulphide minerals is strongly influenced by galvanic pairs between combinations of conducting and semiconducting mineral phases (Berry *et al.*, 1978; Natarajan, 1992). According to this theory, the rest potentials of base metal sulphides along with their actual proximity to one another play an

important role in the formation of galvanic couples and the preferential leaching of the one over mineral over the other. The rest potential of sphalerite (~-50mV vs SHE) is the smallest in comparison to chalcopyrite (~ -310mV vs SHE) and that of pyrite (~ -450 mV vs SHE) and this suggests that it is the most electrochemically active in comparison to chalcopyrite and pyrite. Furthermore, chalcopyrite is more electrochemical active than pyrite. However, when these minerals are in contact with one another (as is the case for the Otjihase and Mintek-supplied concentrates), galvanic interactions result in the sphalerite behaving anodically, while the chalcopyrite and pyrite is cathodically shielded. The selective leaching of sphalerite over chalcopyrite and inturn chalcopyrite over pyrite would be expected under these circumstances. This theory has been supported by an enhanced rate of copper dissolution from sulphide minerals containing chalcopyrite with interlocked pyrite as opposed to pure chalcopyrite (Berry *et al.*, 1978; Natarajan, 1992).

Galvanic interactions therefore result in the pyrite proportion of the concentrate being passivated to a large degree at the expense of chalcopyrite and sphalerite leaching. If this were the case then possibilities two and three could be discounted.

Earlier work (Dutrizac, 1982) presented Fe^{2+}/Cu^{2+} established during the ferric leaching of chalcopyrite for a variety of chalcopyrite concentrates containing various amounts of pyrite and sphalerite impurities. These results are not comparable with those obtained in the current investigation since they are presented for ferric chloride leaching as opposed to ferric sulphate leaching.

5.10.3 Surface Layer Passivation

The mechanism for chalcopyrite leaching would be further complicated by surface layer passivation. Since the SEM analysis of the surface's of leached minerals have not shown any significant sulphur formation on the surface, it could be argued that at low temperatures, the surface could be passivated by reaction products other than sulphur. This could possibly include a layer/s of iron deficient polysulphides such as Covellite (CuS) (Ammou Chokroum *et al*, 1979; Tiwari *et al.*, 1980; Parker *et al.*, 1981; McMillan *et al*, 1982; Warren *et al.*, 1982; Biegler and Horne, 1985; Holliday and Richmond, 1990; Hackl *et al.*, 1995; Gomez *et al.*, 1996) However, the reliability of the SEM's for the elucidation or visual observance of sulphur is questionable due to the SEM sample preparation techniques which possibly result in the removal of any sulphur present on the mineral surface. The implications of polysulphide passivation would mean that the both the dissolved copper and ferrous-ion

species dissolute from a surface layer other than chalcopyrite, which explains the apparent lack of correlation between the observed Fe^{2+}/Cu^{2+} and that predicted by equation 5.1. However the elucidation of any passivating layers on the surface is beyond the scope of this project and this further limits any absolute conclusions on the stochiometry of chalcopyrite leaching.

5.11 Postulated mechanism

The results presented in Figures 5.3-5.8, along with the regression analysis shown in Table 5-3 suggest that the ferric leaching of the chalcopyrite concentrates can be best described according to three primary reactions, each of which dominates at different stages in the leaching process. The initial rapid period could be characterized by the formation sulphur which predicts a ferrous-ion to cuprous-iron ration of 5, as shown in equation (5.1) (Dutrizac, 1978; Munoz *et al.*, 1979; Dutrizac, 1981; Hirato *et al.*; 1987; Dutrizac, 1989), *viz*,

$$CuFeS_2 + 4Fe^{3+} \mapsto Cu^{2+} + 5Fe^{2+} + 2S^0 \qquad (5.1)$$

The regression results suggest that equation (5.2) (Dutrizac, 1981, Dutrizac, 1989) describes the slower period experienced after the rapid initial phase, *viz*,.

$$CuFeS_2 + 16Fe^{3+} + 8H_2O \mapsto Cu^{2+} + 17Fe^{2+} + 16H^+ + 2SO_4^{-2} \qquad (5.2)$$

It is possible that the ferrous-ion/cupric-ion ratio is affected by the leaching of the both pyrite (May *et al.*, 1997) (equation (5.6)) and sphalerite (Driessens *et al.*, 1999)(equation (5.7)).

$$FeS_2 + 14Fe^{3+} + 8H_2O \mapsto 15Fe^{2+} + 16H^+ + 2SO_4^{-2} \qquad (5.6)$$

$$ZnS + 2Fe^{3+} \mapsto 2Fe^{2+} + Zn^{2+} + S^0 \qquad (5.7)$$

This is consistent with the postulate that the chemical oxidation of chalcopyrite to sulphate/sulphur and the chemical oxidation of other mineral sulphides such as pyrite and sphalerite (even in trace quantities) compete for the available ferric-ions.

5.12 Conclusions

1. The results show that the redox potential measured during the chemical leaching of chalcopyrite is only a function of the ferric/ferrous-ion ratio, and is independent of the copper concentration for $[Cu^{2+}] < 0.1$ $moll^{-1}$. The cerium sulphate titrametric method is suitable for measuring ferrous-ion in the presence of copper.

2. The ferric-sulphate leaching of chalcopyrite at temperatures of 35-55 °C shows changing kinetics throughout the course of the reaction. The initial reaction phase (1-2 hrs) is rapid and is characterised by a linear rate. The rate of reaction as seen from the amount of copper solubalised is rapidly retarded. The major portion of the reaction is characterised by a slow rate of dissolution. An increase in temperature improves the rate of reaction.

3. It appears that the rate of chalcopyrite chemical leaching is a dependent on the redox potential.

4. The ratio of ferrous-ion/cupric-ion measured from the solubalised species during the chemical ferric leaching of the Otjihase and Mintek-supplied chalcopyrite concentrates varies during the reaction. These ratio's varied from 5 to 20 for the Otjihase concentrate and 7 to 23 for the Mintek-supplied concentrate over an 8 day period at 35 °C.

5. The observed ferrous-ion/cupric-ion ratios is closer to that predicted for the chemical leaching of chalcopyrite to produce sulphate rather than sulphur. Regression analysis shows that a dissolved ferrous-ion/cupric-ion ratio of 19 and 23 describes the Otjihase and Mintek supplied concentrates respectively. The presence of pyrite and sphalerite as well as surface layer passivation complicates any absolute conclusion on the stochiometry for chalcopyrite chemical leaching in ferric-sulphate media.

Chapter 6: Results of the Staged Addition of Chalcopyrite Concentrates to a Batch Bioleach.

6.1 The staged addition of predominantly chalcopyrite-concentrates to a batch bioleach

This chapter presents the results and discussion of the staged addition of two predominantly chalcopyrite concentrates to a batch bioleach with mesophiles. This experimental methodology has been devised and successfully used by Boon, (1996) to study the kinetics of bioleaching of pyrite with *Leptospirillum ferroxidans* and to test the applicability of the two-step mechanism in describing the bioleaching of pyrite.

The experiments were performed on two separate chalcopyrite concentrates using a semi-continuously grown culture on the Otjihase chalcopyrite concentrate.

The results of six separate staged addition experiments are presented. Two experiments were conducted at two separate initial total-iron concentrations using two different chalcopyrite concentrates. Similarly a comparative experiment was conducted using a chalcopyrite and pyrite concentrate at a common initial total iron concentration with a culture drawn from the same source.

Successive, 2 hourly, additions of 2, 4, 6, 8 and 10 gms of each concentrate increased the mineral concentration in each reactor to 6, 12, 20 and 30 gl^{-1}, after an initial $2gl^{-1}$ adaptation period. The mineral concentration was increased to 42 gl^{-1} for the experimental set at initial total-iron concentration of 12 gl^{-1}. During the course of each experiment, the redox potential, oxygen and carbon dioxide utilisation rates were monitored continuously.

The results presented show the changes in each of the measured parameters over time during each experiment as well as the variation in the bacterial specific oxygen utilisation rate with ferric/ferrous-ion ratio. The bacterial specific oxygen utilisation rate is used as a measure of the bacterial activity. The ferric/ferrous-ion ratio was calculated by using the Nernst equation and parameters obtained by calibrating the redox potential probes at the same conditions of total-iron and temperature as that used in the experiments.

6.2 The effect of mineral additions on the redox potential.

Figure 6.1 and Figure 6.2 shows the measured redox potential during the course of the experiment. The effect of redox potential was investigated at $[Fe^{tot}]$ of 1.2 gl^{-1} (Figure 6.1) and at $[Fe^{tot}]$ of 10 gl^{-1} (Figure 6.2). The redox potential instantaneously decreased after every mineral addition in both experiments.

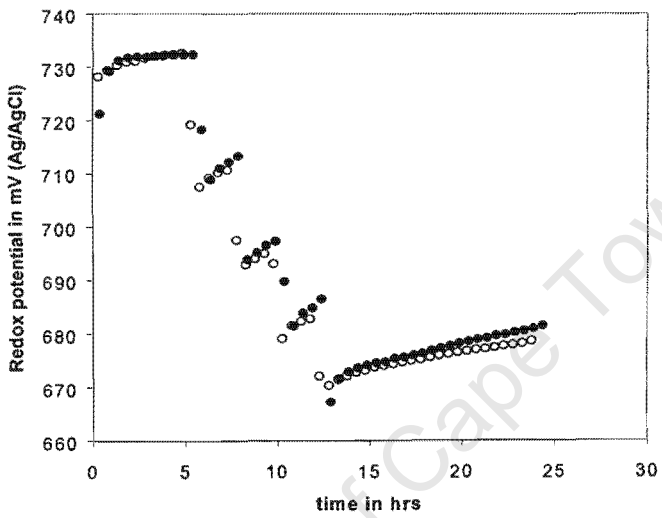

Figure 6.1: Comparison of the redox potential during staged addition of mineral to chalcopyrite batch culture for [•] Mintek-supplied concentrate and [o] Otjihase concentrate. $[Fe^{tot}]$ of 1.2gl^{-1}, Temp = 35 °C, pH = 1.5, particle size = +38-53 µm.

The decrease in redox potential with mineral addition was followed by a slight increase over the 2-3 hr period between additions.

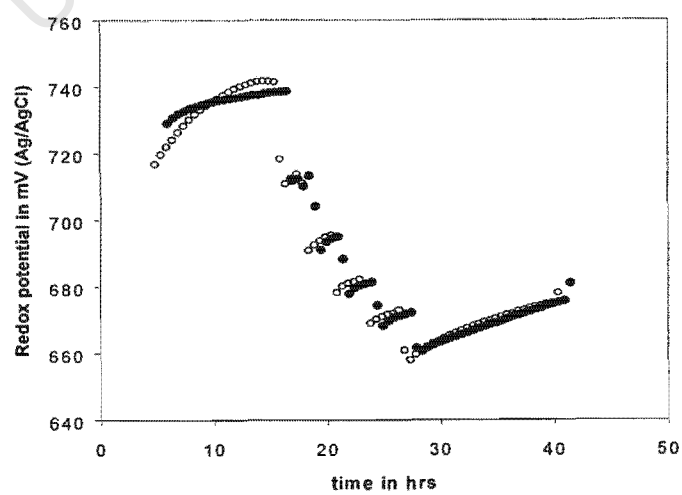

Figure 6.2 : Comparison of the redox potential during staged addition of mineral to chalcopyrite batch culture for [•] Mintek-supplied concentrate and [o] Otjihase concentrate. $[Fe^{tot}]$ of 12gl^{-1}, Temp = 35 °C, pH = 1.5, particle size = +38-53 µm.

6.3 The effect of the total iron concentration on the redox potential

The mineral concentration was increased up to a final concentration of 30 gl^{-1} in the experiment at $[Fe^{tot}]$ = 1.2 $g.l^{-1}$ and 40 $g.l^{-1}$ in the experiment at $[Fe^{tot}]$ = 10 gl^{-1}. The higher final mineral concentration in the latter experiment served to lower the redox potential as much as possible without incurring oxygen and carbon dioxide limitations. An increase in redox potential occurs after the last addition of mineral in both experiments. A steady state redox potential was achieved within minutes of mineral addition in both experiments. The redox potential trend in both experiments was close. This shows an agreement in the behavior of both chalcopyrite sources during the experiment. The is no observable effect of the total iron concentration on the redox potential trend.

6.4 The effect of pyrite and chalcopyrite additions on the redox potential

Figure 6.3 compares the redox potential for the staged addition of mineral during the batch bioleaching of pyrite and chalcopyrite using a diluted innoculum from a chalcopyrite batch culture. Both experiments were performed at $[Fe^{tot}]$ = 10 gl^{-1}. A similar trend in redox potential occurs for both pyrite and chalcopyrite experiments. The addition of mineral results in a greater decrease in redox potential in the pyrite experiment compared to the chalcopyrite experiment.

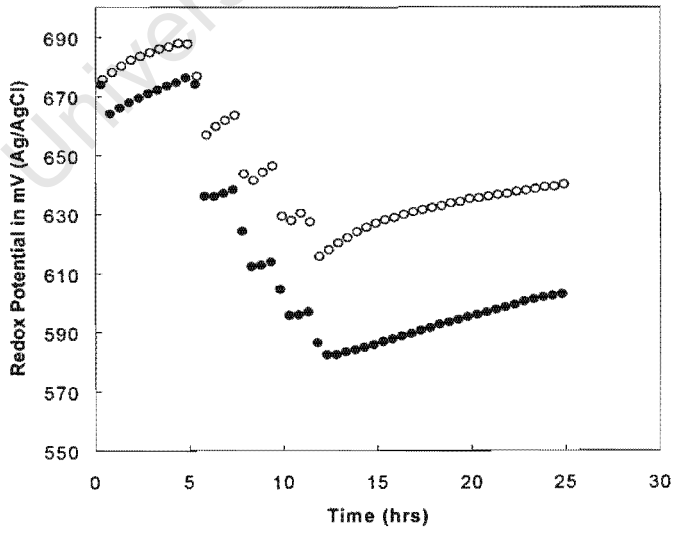

Figure 6.3: Comparison of the redox potential during staged addition of mineral to a [•] pyrite, and [o] chalcopyrite batch culture. $[Fe^{tot}]$ of 12gl^{-1}, Temp = 35 °C, pH = 1.5, particle size = +38-53 µm.

In Figure 6.3, the range of redox potentials is larger for the pyrite experiment (580 to 675 mV) as compared to the chalcopyrite experiment (615 to 690 mV). Table 6-1 compares the change in redox potential after every mineral addition in both experiments. It is shown that the addition of pyrite to a batch bioleach results in a greater decrease in the redox potential as compared to chalcopyrite.

The reasons for the greater decrease in redox potential in the case of pyrite compared to chalcopyrite is due to the difference in stochiometry and the rates of ferric-ion leaching during the bioleaching of pyrite and chalcopyrite. The relatively smaller decrease of redox potential during the chalcopyrite experiments is also due to the lower molar concentration of mineral substrate added compared to pyrite. According the stochiometry of ferric-ion oxidation (Equation 6.1), 15 moles of ferrous-ion are produced per mole of pyrite oxidised as compared to 5 moles for chalcopyrite oxidation (Equation 6.2). The ferric leaching of pyrite is presented as (Boon, 1996):

$$FeS_2 + 14Fe^{3+} + 8H_2O \mapsto 15Fe^{2+} + 2SO_4^{2-} + 16H^+ \qquad (6.1)$$

A faster rate of ferrous-ion production occurs during pyrite bioleaching as compared to chalcopyrite bioleaching. This causes the ferric/ferrous-ion ratio to drop by a larger amount after every mineral addition as compared to the chalcopyrite experiment.

Table 6-1 : The change in redox potential with mineral addition during staged additions of pyrite and chalcopyrite to a batch bioleach.

Mineral added (g)	ΔEh for Pyrite (mV)	ΔEh for Chalcopyrite (mV)
4	40	31
6	26	20
8	20	17
10	15	12

The rapid passivation of chalcopyrite during ferric-ion oxidation also plays a role in achieving a slower rate of ferrous-ion production during chalcopyrite bioleaching. The possibility of the build-up of diffusional barriers during the course of the experiment retards the rate of reaction during chalcopyrite and therefore affects the rate of ferrous-ion production. This factor contributes toward the smaller change in redox potential after every chalcopyrite addition in comparison the pyrite experiment.

The redox potential is determined by the ferric/ferrous-ion ratio. According to the multiple sub-process mechanism ferrous-ion and sulphur or sulphate is produced from the ferric leaching of the mineral sulphide as seen in Equation's (2.2.1) and (2.2.2). Ferric-ion and sulphuric acid are generated by bacterial ferrous-ion and bacterial sulphur oxidation respectively. The addition of chalcopyrite mineral to the batch culture results in the chemical ferric leaching rate, $r_{Fe^{2+}}^{chem}$, exceeding the rate of bacterial ferrous-ion oxidation, $r_{Fe^{2+}}^{bio}$. An increase in the production of ferrous-ion results in a decrease in the ferric/ferrous-ion ratio whilst providing additional substrate for the iron oxidisers.

The lowest redox potential value after the addition of mineral signifies the steady state which occurs when the chemical and bacterial rates are equal ie $r_{Fe^{2+}}^{chem} = r_{Fe^{2+}}^{bio}$.

The increase in the redox potential and subsequently the ferric/ferrous-ion ratio between additions is due to the bacterial consumption of ferrous-ions to produce ferric-ions. The decrease in redox potential in both the pyrite and chalcopyrite bioleaching experiments, with the increase in mineral concentration is consistent with the multiple sub-process mechanism since the rate of chemical production of ferrous-ion increases with every mineral addition.

This redox potential trend has been observed for the staged addition of pyrite to a batch bioleach (Boon, 1996)

By comparing the redox potential trends for pyrite and chalcopyrite-concentrates in Figure 6.3, along with the decreasing change in redox potential at the same mineral concentration shown in table 6-1, it is clear that the points of steady state after each mineral addition achieved for pyrite is much lower than those achieved for chalcopyrite. This is a direct result of the difference in $r_{Fe^{2+}}^{chem}$ for the pyrite and chalcopyrite cases. A faster $r_{Fe^{2+}}^{chem}$ during pyrite bioleaching results in a greater amount of ferrous-ions being produced in comparison to the chalcopyrite case. In the case of pyrite, the decreases in ferric/ferrous-ion ratio is then lower as compared to chalcopyrite..

The rate of bacterial ferrous-ion consumption, $r_{Fe^{2+}}^{bio}$, is directly related to the amount of ferrous-ion substrate available. The increase in redox potential between mineral additions is determined by $r_{Fe^{2+}}^{bio}$. A larger availability of ferrous-ion substrate in the case of pyrite results in a higher $r_{Fe^{2+}}^{bio}$ as compared to chalcopyrite. This is demonstrated by a slightly steeper and

more regular increase in the redox potential (Figure 6.3) between mineral additions as compared to chalcopyrite.

6.5 The effect of mineral additions on the oxygen and carbon dioxide utilisation rates.

Figure 6.4 shows the measured oxygen utilization rates ($-r_{O2}$) during the staged addition of Otjihase and Mintek-supplied chalcopyrite to a batch bioleach. Each experiment was conducted at $[Fe^{tot}] = 1.2\ gl^{-1}$ with innoculum drawn from the same source. Figure 6.5 shows the carbon dioxide utilization rate ($-r_{CO2}$) for the same set of experiments.

Both the $-r_{O2}$ and $-r_{CO2}$ for both concentrates are small during the initial 8 hrs of the experiment. This is because little substrate is available during that period. The increases in mineral concentration results in larger amounts of ferrous-ion and sulphur substrate. This is reflected by an increase in the $-r_{O2}$ and $-r_{CO2}$. A similar stepwise increase in the $-r_{O2}$ and $-r_{CO2}$ with every mineral addition is seen for both chalcopyrite concentrates.

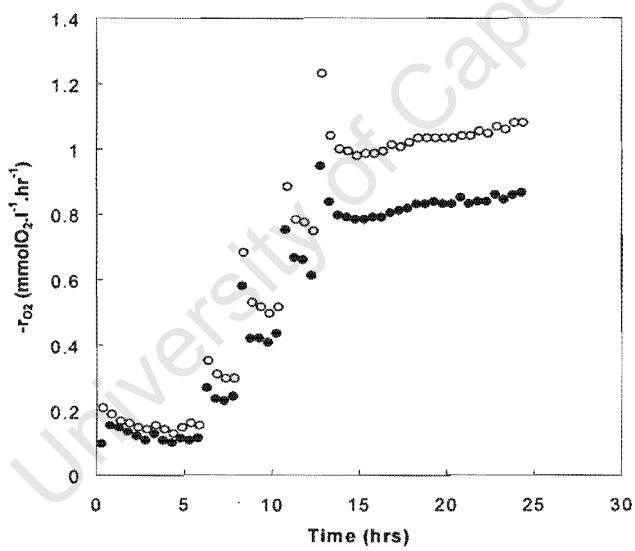

Figure 6.4 : Comparison of the measured oxygen ($-r_{O2}$) utilization rates during staged addition of [•] Otjihase chalcopyrite and [o] Mintek-supplied chalcopyrite to a batch culture. $[Fe^{tot}]$ of $1.2gl^{-1}$, Temp = 35 °C, pH = 1.5, particle size = +38-53 µm.

Figure 6.6 indicates the measured $-r_{O2}$ as a function of the mineral concentration for both concentrates. The measured $-r_{O2}$ for the Mintek-supplied concentrate is higher, particularly at $[CuFeS_2]$ of 20 $g.l^{-1}$ and 30 $g.l^{-1}$ even though the $-r_{CO2}$ is approximately equal.

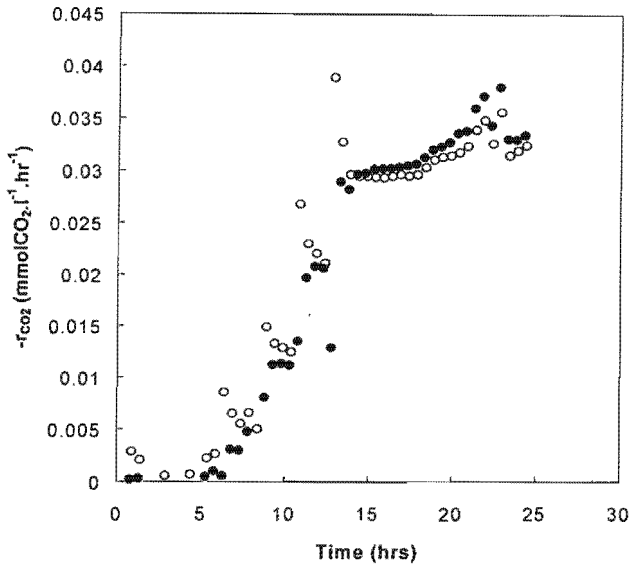

Figure 6.5 : Comparison of the measured carbon dioxide utilization rates ($-r_{CO2}$) during staged addition of [•] Otjihase chalcopyrite and [o] Mintek-supplied chalcopyrite to a batch culture. [Fe^{tot}] of 1.2gl^{-1}, Temp = 35 °C, pH = 1.5, particle size = +38-53 μm.

This difference in measured rates can possibly be attributed to the difference in composition of the two concentrates. The measured $-r_{O2}$ in both cases is characterized by an initial peak Immediately after the addition of mineral for both concentrates.

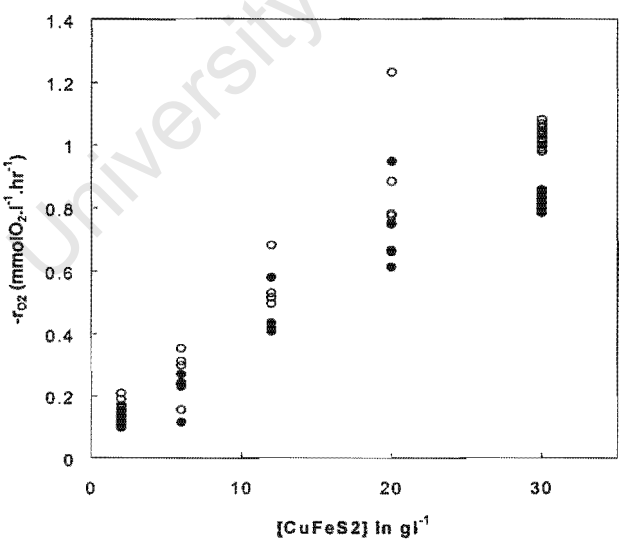

Figure 6.6 : Comparison of the measured oxygen ($-r_{O2}$) utilization rates during staged addition of [•] Otjihase chalcopyrite and [o] Mintek-supplied chalcopyrite to a batch culture indicated as a function of chalcopyrite concentration. [Fe^{tot}] of 1.2gl^{-1}, Temp = 35 °C, pH = 1.5, particle size = +38-53 μm.

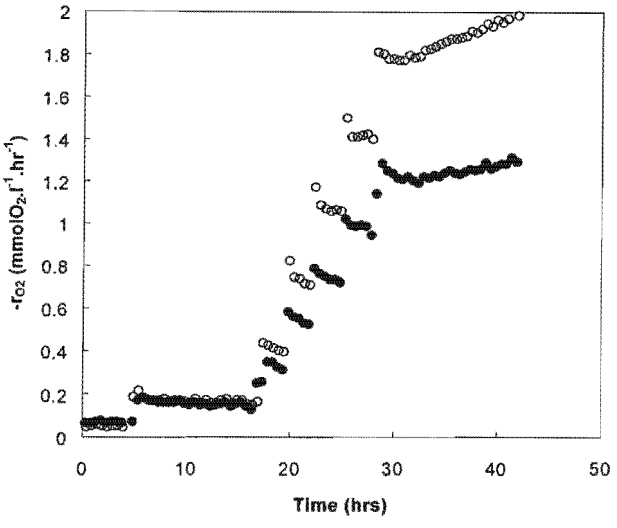

Figure 6. 7 : Comparison of the measured oxygen ($-r_{O2}$) utilization rates during staged addition of [•] Otjihase chalcopyrite and [o] Mintek-supplied chalcopyrite (with removed surface fines) to a batch culture. [Fe^{tot}] of 12gl^{-1}, Temp = 35 °C, pH = 1.5, particle size = +38-53 µm.

The variation in $-r_{O2}$ with mineral concentration can be seen in Figure's 6.4 and 6.5. This initial peak in measured rates is explained by the immediate reaction of fines attached to the surface of both concentrates. Figure's 6.7 and 6.8 show the measured $-r_{O2}$ and $-r_{CO2}$ for a staged addition experiment conducted at [Fe^{tot}] = 12 $g.l^{-1}$.

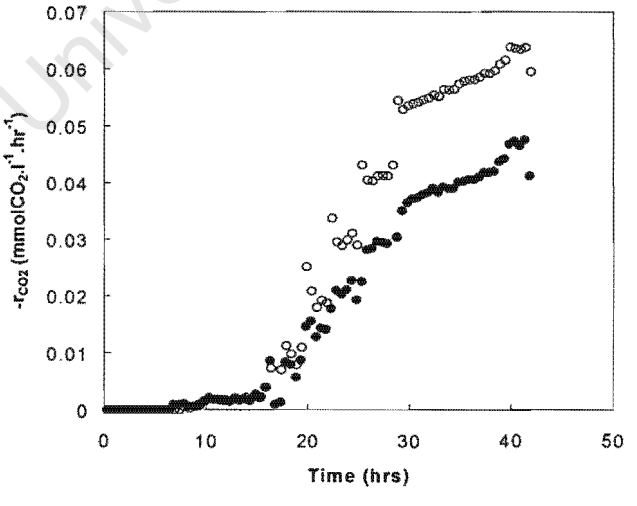

Figure 6.8 : Comparison of the measured carbon dioxide utilization rates ($-r_{CO2}$) during staged addition of [•] Otjihase chalcopyrite and [o] Mintek-supplied chalcopyrite (with removed surface fines)to a batch culture. [Fe^{tot}] of 1.2gl^{-1}, Temp = 35 °C, pH = 1.5, particle size = +38-53 µm.

The concentrates used in the experiments conducted at $[Fe^{tot}]$ = 1.2 $g.l^{-1}$were not treated in an ultra-sound bath. In the $[Fe^{tot}]$ = 12 $g.l^{-1}$ experiment the Mintek-supplied concentrate was treated in a ultrasonic bath prior to the experiment to remove any surface fines. A comparison of the measured $-r_{O2}$ and $-r_{CO2}$ for the two concentrates in Figures 6.7 and 6.8 indicate that the observed peaks immediately after addition of mineral is only seen for the untreated Otjihase chalcopyrite. The observed peaks in the prior experiments conducted at $[Fe^{tot}]$ = 1.2 $g.l^{-1}$ are therefore attributed to the reaction of surface fines.

6.6 The effect of total iron concentration on the measured $-r_{O2}$ and $-r_{CO2}$.

The effect of the total iron concentration can be seen by comparing Figures 6.4 and 6.5 with figures 6.7 and 6.8. The rates show similar trends at $[Fe^{tot}]$ = 12 gl^{-1} and $[Fe^{tot}]$ = 1.2 gl^{-1}. In both cases the measured $-r_{O2}$'s are larger for the Mintek-supplied concentrate than for the Otjihase concentrate. The measured rates are slightly larger at the higher total iron concentration than the lower total iron concentration. This is possibly due to the slightly larger bacterial concentration in the innoculum which was used in the $[Fe^{tot}]$ = 12 gl^{-1} experiment, although both innocula were drawn from the same supernatant of a chalcopyrite grown batch culture.

Figure 6.9 indicates the bacterial growth curves calculated from the measured $-r_{CO2}$ for the $[Fe^{tot}]$ = 1.2 gl^{-1} experiments and figure 6.10 shows the growth curves for the $[Fe^{tot}]$ = 12 gl^{-1} .

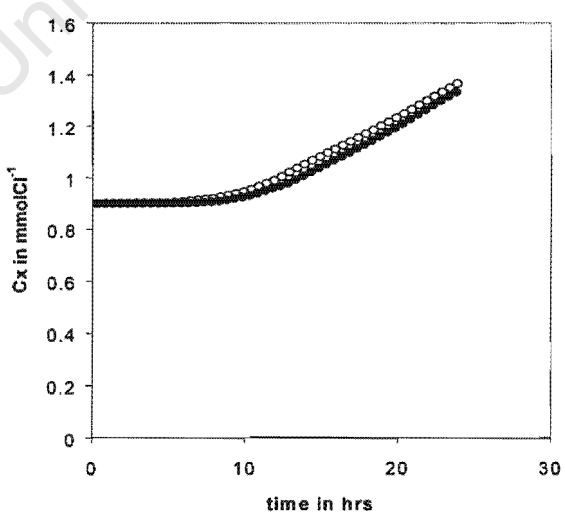

Figure 6.9 : Bacterial growth curve calculated from the measured carbon dioxide utilization rates ($-r_{CO2}$) during staged addition of [•] Otjihase chalcopyrite and [o] Mintek-supplied chalcopyrite to a batch culture. $[Fe^{tot}]$ of 1.2gl^{-1}, Temp = 35 °C, pH = 1.5, particle size = +38-53 µm.

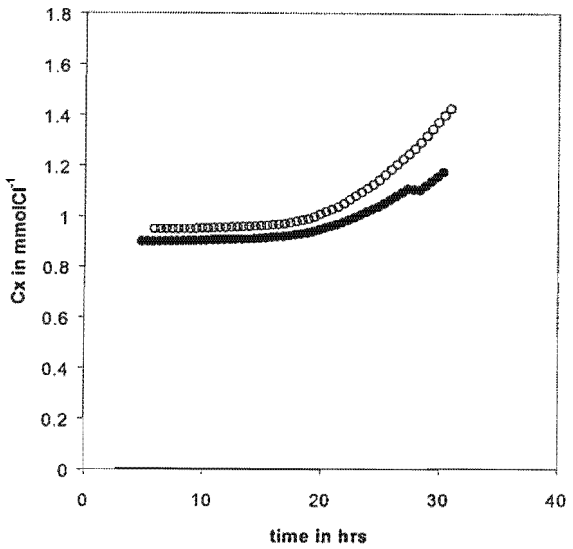

Figure 6.9 : Bacterial growth curve calculated from the measured carbon dioxide utilization rates ($-r_{CO2}$) during staged addition of [•] Otjihase chalcopyrite and [o] Mintek-supplied chalcopyrite (with removed surface fines) to a batch culture. [Fe^{tot}] of 12 gl^{-1}, Temp = 35 °C, pH = 1.5, particle size = +38-53 µm.

The growth curves are shown over a 24 hr period in each case. The Mintek-supplied concentrate showed a higher growth rate at the higher total iron concentration. The higher growth rate is coupled with a larger measured $-r_{O2}$ for this concentrate.

6.7 The effect of pyrite and chalcopyrite additions on $-r_{O2}$ and $-r_{CO2}$.

Figure 6.10 shows the measured $-r_{O2}$ during the staged addition of pyrite and chalcopyrite to a batch bioleach. Figure 6.11 indicates the measured $-r_{CO2}$. In both cases a stepwise increase in the rates are observed with every mineral addition. In the case of pyrite, the $-r_{O2}$ is at least twice as high . The higher $-r_{O2}$, together with the larger decrease in redox potential after every mineral addition, is coupled with a higher bacterial growth rate as shown in Figure 12. This is explained by a faster rate of ferrous-ion production by the ferric leaching of pyrite as compared to chalcopyrite. The reasons for this has been explained already. This results in a higher bacterial ferrous-ion utilization rate during pyrite bioleaching and therefore a larger $-r_{O2}$ in comparison to chalcopyrite. This increase in $-r_{O2}$ and $-r_{CO2}$, together with the decrease in redox potential after every mineral addition indicates the consistency in bioleaching behavior of both sulphide minerals.

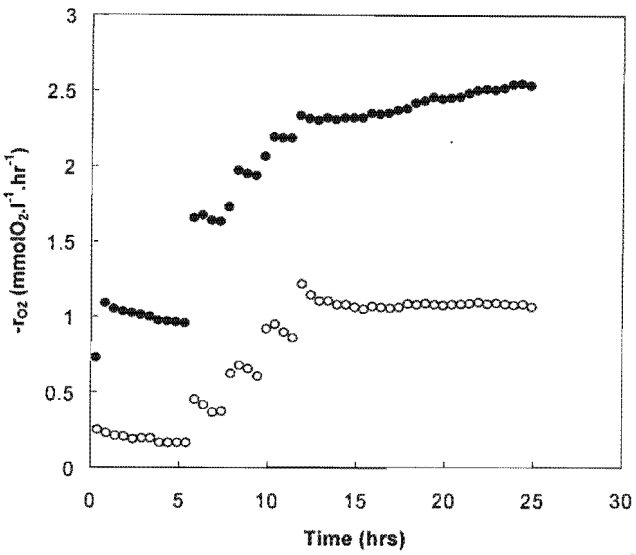

Figure 6.10 : Comparison of the measured oxygen ($-r_{O2}$) utilization rates during staged addition of [•] Otjihase pyrite and [o] Otjihase chalcopyrite to a batch culture. [Fe^{tot}] of 12gl^{-1}, Temp = 35 °C, pH = 1.5, particle size = +38-53 µm.

According to the multiple sub-process mechanism, the highest bacterial activity occurs when the largest amount of substrate is available. It is apparent from Figures 6.4, 6.5, 6.7, 6.8, 6.9 and 6.10 that the $-r_{O2}$ and $-r_{CO2}$ are maximum immediately after the addition of both chalcopyrite and pyrite mineral.

The stepwise increase in $-r_{O2}$ and $-r_{CO2}$ with mineral addition is explained in terms of the increased bacterial consumption of the available ferrous-ion and sulphur substrate at higher mineral concentrations. As explained previously, the addition of chalcopyrite to an active batch bioleach results in the generation of ferrous-ions by the chemical leaching of the mineral by ferric-ion. This means that $r_{Fe^{2+}}^{chem} > r_{Fe^{2+}}^{bio}$ immediately after addition.

The production of ferrous-ion and sulphur creates substrate for bacterial ferrous-ion and bacterial sulphur oxidation. The bacterial utilisation of these substrates results in a higher rate of oxygen utilisation after the addition of mineral.

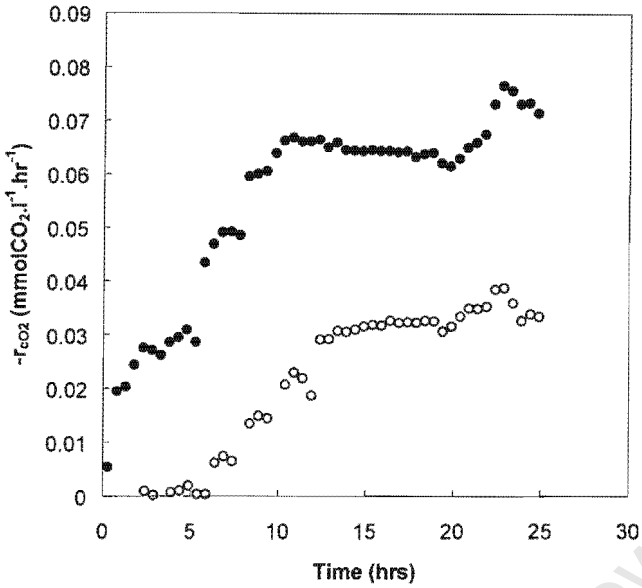

Figure 6.11 : Comparison of the measured carbon dioxide ($-r_{CO2}$) utilization rates during staged addition of [•] Otjihase pyrite and [o] Otjihase chalcopyrite to a batch culture. [Fe^{tot}] of 12gl^{-1}, Temp = 35 °C, pH = 1.5, particle size = +38-53 µm.

These trends are in agreement with that reported by Boon (1996) during the staged addition of Prieska pyrite to a predominantly *Leptospirillum ferrooxidans* batch culture.

The variation in $-r_{O2}$ in Figure 6.4 and 6.7 for both the Otjihase and Mintek-supplied chalcopyrite, together with the measured $-r_{O2}$ of Otjihase chalcopyrite shown in figure 6.10 display a maximum value immediately after the addition of mineral. There is also an observable decrease in $-r_{O2}$ for the time periods between mineral additions. In contrast, the variation in $-r_{O2}$ in Figure 6.10 for the Otjihase pyrite does not displays a fairly constant trend. For the case of pyrite the $-r_{O2}$ shows an increase with time after the final addition as opposed to chalcopyrite (Figure 6.10) where a decrease is observed. This is explained in terms of the rapid passivation of chalcopyrite during ferric leaching which results in a decreasing $r_{Fe^{2+}}^{chem}$ between mineral additions. The slowing of the $r_{Fe^{2+}}^{chem}$ in the case of chalcopyrite bioleaching causes a decreasing supply of ferrous-ion substrate. In contrast the $r_{Fe^{2+}}^{chem}$ of pyrite follows a constant stochiometry. Also, the $r_{Fe^{2+}}^{chem}$ for pyrite is constant at a particular redox potential (May *et. al*, 1997). Therefore, $r_{Fe^{2+}}^{bio}$ in this case does not decrease between mineral additions. In the case of chalcopyrite $r_{Fe^{2+}}^{chem}$ falls within range of a maximum and minimum value (Kamentani and Aoki, 1985) due to the build-up of diffusional barriers

and the subsequent passivation of the mineral. This is reflected by a decreasing $r_{Fe^{2+}}^{chem}$ and consequently a decrease in $r_{Fe^{2+}}^{bio}$ for the case of chalcopyrite between mineral additions. The maintenance of a steady state is only possible if $r_{Fe^{2+}}^{chem}$ depends on one reaction, as is the case of pyrite. This is not possible for chalcopyrite since $r_{Fe^{2+}}^{chem}$ depends on the rates of more than one reaction occurring in sequentially. A changing stochiometry during chemical ferric leaching of chalcopyrite results in a retarding $r_{Fe^{2+}}^{chem}$.

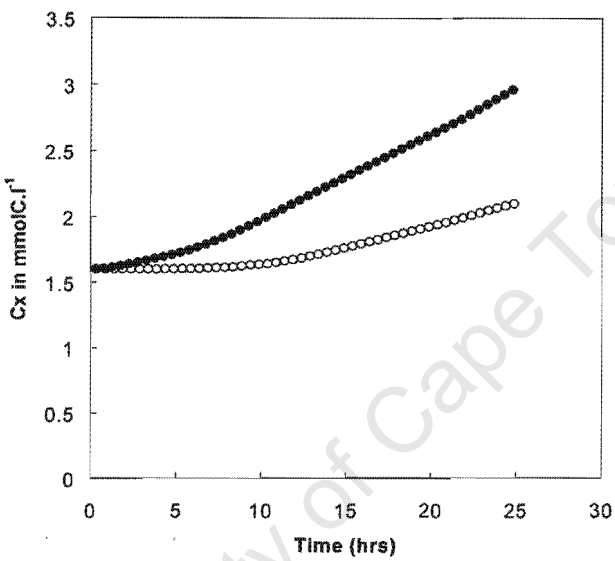

Figure 6.12 : Bacterial growth curve calculated from the measured carbon dioxide utilization rates ($-r_{CO2}$) during staged addition of [•] Otjihase Pyrite and [o] Otjihase Chalcopyrite to a batch culture. [Fe^{tot}] of 12 gl^{-1}, Temp = 35 °C, pH = 1.5, particle size = +38-53 µm.

The bacterial concentration in each experiment was calculated from the measured $-r_{CO2}$. This was achieved by integrating the bacterial growth rate over time. For this purpose the bacterial concentration of the innoculum had to be estimated. The innoculum in each case was drawn from the supernatant of an active semi-continuous chalcopyrite batch culture containing *Acidithiobacillus ferrooxidans*, *Leptospirillum ferrooxidans* and *Acidithiobacillus thiooxidans* from which the growth rate was measured for at least a weeklong period prior to the experiment. This enabled the estimation of the initial bacterial concentration.

6.8 The effect of mineral additions on the biomass specific oxygen utilization rate, (q_{O2}).

Figure 6.13 indicates the biomass specific oxygen utilization rate, q_{O2}, calculated from the measured $-r_{O2}$ and bacterial concentration after every mineral addition in the case of [Fe^{tot}] = 1.2 $g.l^{-1}$. Figure 6.14 shows q_{O2} at [Fe^{tot}] = 12 $g.l^{-1}$. Both the Otjihase chalcopyrite and the

Mintek-supplied chalcopyrite concentrate show similar trends in q_{O2}. The specific rates show a maximum immediately after the addition of mineral and then decrease until the next addition is made.

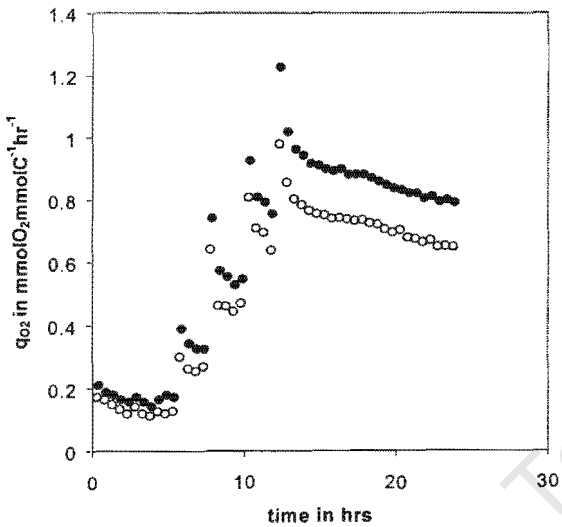

Figure 6.13 : Comparison of the calculated specific oxygen (q_{O2}) utilization rates during staged addition of [•] Mintek chalcopyrite and [o] Otjihase chalcopyrite to a batch culture. [Fe^{tot}] of 1.2gl^{-1}, Temp = 35 °C, pH = 1.5, particle size = +38-53 µm.

The q_{O2} is higher in for the Mintek-supplied chalcopyrite than for the Otjihase chalcopyrite especially at mineral concentrations above 6$g.l^{-1}$.

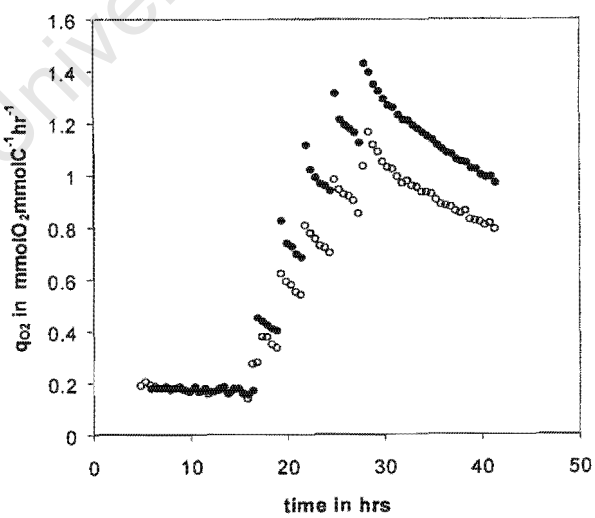

Figure 6.14 : Comparison of the calculated specific oxygen (q_{O2}) utilization rates during staged addition of [•] Mintek-supplied chalcopyrite and [o] Otjihase chalcopyrite to a batch culture. [Fe^{tot}] of 12gl^{-1}, Temp = 35 °C, pH = 1.5, particle size = +38-53 µm.

The higher q_{O2}'s observed in Figure 6.13 and 6.14 for the Mintek-supplied concentrate is due to the higher bacterial growth rates and consequently the larger biomass in the case of that mineral.. The highest q_{O2} is seen at the highest chalcopyrite concentration. The increase in chalcopyrite concentration results in more substrate being available per unit of bacteria in the form of dissolved ferrous-ion and sulphur. These increases in q_{O2} must be seen in conjunction with the increase in $-r_{O2}$ (Figure 6.8 and Figure 6.10) and the immediate decrease in redox potential or Ferric/Ferrous-ion ratio (Figure 6.1 and Figure 6.2).

Figure 6.15 shows the difference in the biomass specific rates for the case of pyrite and chalcopyrite. The innoculum used in these experiments were drawn from the same source. The q_{O2}'s were calculated from the measured $-r_{O2}$'s and the estimated bacterial concentrations. The difference between the calculated q_{O2}'s for pyrite and chalcopyrite are shown in Figure 6.16 as a function of mineral concentration. It is clear from both Figure 6.15 and 6.16 that the q_{O2}'s are between 2 and 5 times higher in the case of pyrite as compared to chalcopyrite, depending on the mineral concentration. The higher q_{O2}'s is as a result of a faster bacterial growth rate as well as higher $-r_{O2}$ in the case of pyrite. At each mineral concentration, a greater substrate availability in the case of pyrite results in the higher oxygen consumption per unit of biomass. This is due to the higher rate of ferrous iron production during the chemical leaching of pyrite as compared to chalcopyrite. The reasons for this difference in rates of ferrous-ion production during chemical leaching of pyrite and chalcopyrite has been discussed previously.

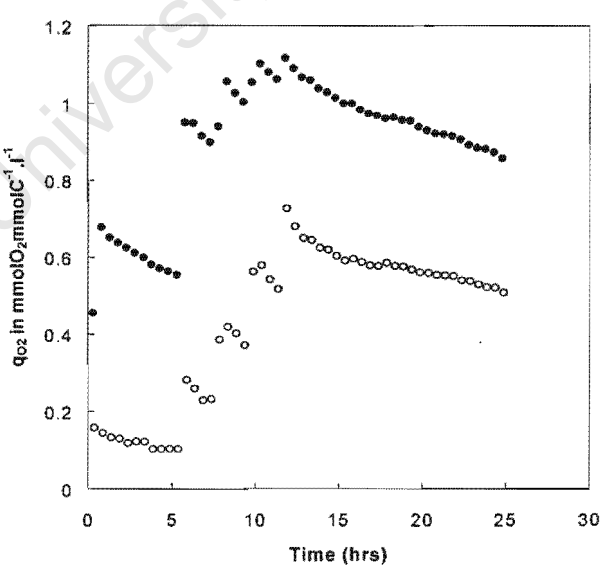

Figure 6.15 : Comparison of the calculated specific oxygen (q_{O2}) utilization rates during staged addition of [•] Otjhase pyrite and [o] Otjihase chalcopyrite to a batch culture. [Fe^{tot}] of 12gl^{-1}, Temp = 35 °C, pH = 1.5, particle size = +38-53 µm.

Pyrite bioleaching shows a higher oxygen consumption per unit of biomass despite the availability of only ferrous-ion substrate. The calculated q_{O2} include the oxygen utilized for both bacterial ferrous-ion and sulphur oxidation.

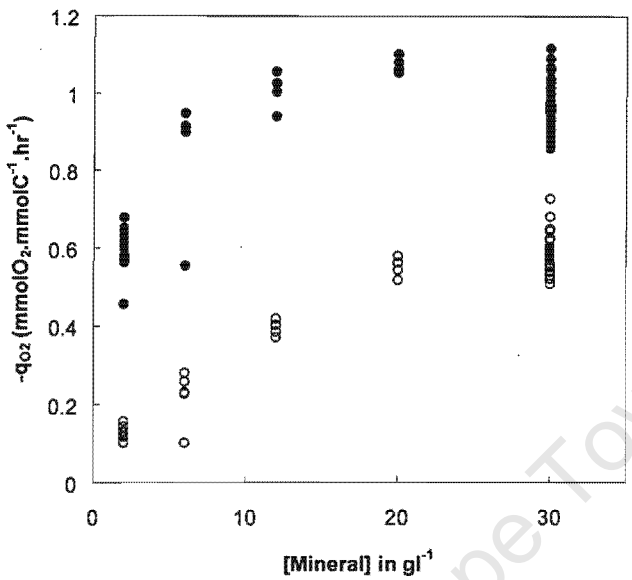

Figure 6.15 : Comparison of the calculated specific oxygen (q_{O2}) utilization rates during staged addition of [•] Otjhase pyrite and [o] Otjihase chalcopyrite to a batch culture expressed as a function of the mineral concentration. [Fe^{tot}] of 12gl^{-1}, Temp = 35 °C, pH = 1.5, particle size = +38-53 µm.

It was already shown that the rates of ferrous-ion production in the case of pyrite is larger than in the case of chalcopyrite. In comparing the calculated q_{O2} it is apparent that the bacterial growth rate on both ferrous-ion and sulphur substrates in the case of chalcopyrite, is smaller than the bacterial growth rate on ferrous-ion in the case of pyrite. It is still unclear as to what proportion of the biomass specific utilization rate is due to ferrous-ion oxidation and sulphur oxidation in the case of chalcopyrite.

6.9 Biomass Specific rates as a function of the ferric/ferrous-ion ratio.

Figure 6.17 indicates the calculated q_{O2} as a function of the Ferric/ferrous-ion ratio at [Fe^{tot}]=1.2 $g.l^{-1}$. Figure 6.18 indicates the trend at [Fe^{tot}]=12 $g.l^{-1}$. The redox potential is directly related to the Ferric/ferrous-ion ratio by the Nernst equation. Therefore Figure 6.17 and 6.18 indicates the behaviour of q_{O2} as a function of the redox potential. The observed trend is similar at both [Fe^{tot}]. Both the Mintek-supplied chalcopyrite and the Otjihase chalcopyrite show an increase in the q_{O2} with a decrease in the redox potential. This trend is similar to that observed by Boon (1996) during the bioleaching of Prieska Pyrite. The addition of mineral results in a greater ferrous-ion production which creates a greater amount

of substrate for the iron and sulphur oxidisers. It has also been shown that the addition of mineral instantaneously decreases the redox potential. The increase in q_{O2} with a decrease in Ferric/ferrous-ion ratio is therefore consistent with the multiple sub-process mechanism.

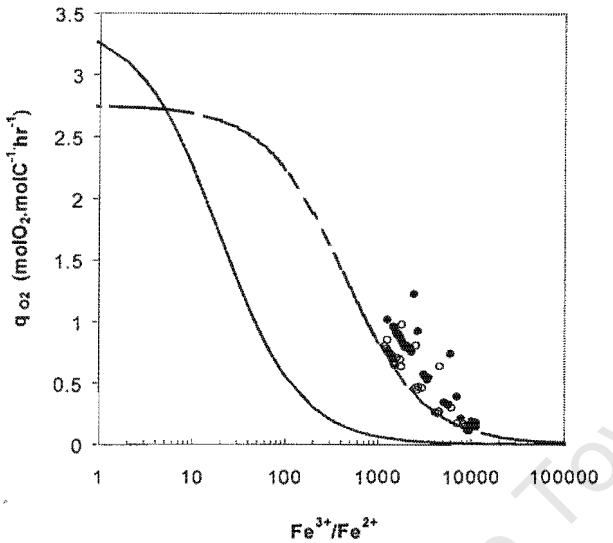

Figure 6.17 : Comparison of the calculated specific oxygen (q_{O2}) utilization rates during staged addition of [•] Mintek chalcopyrite and [o] Otjihase chalcopyrite to a batch culture as a function of the Ferric/ferrous-ion ratio. Superimposed is the Michaelis-Menten based ferrous-ion oxidation model for [—] *Acidithiobacillus ferrooxidans* and [– –] *Leptospirillum ferrooxidans* [Fe^{tot}] of 1.2gl^{-1}, Temp = 35 °C, pH = 1.5, particle size = +38-53 µm.

It is also clear from both Figure's 6.17 and 6.18, that the Mintek-supplied concentrate exhibits slightly higher q_{O2}'s than the Otjihase concentrate.

Superimposed on both figures are the Michaelis-Menten based models for bacterial ferrous-ion utilization for the case of *Acidithiobacillus ferro-oxidans* and *Leptospirillum ferro-oxidans*.

The parameters used for the model are shown in Table 6.3. The maximum specific oxygen utilization rate (q_{O2}^{max}) was extrapolated from that previously determined by Boon, (1996) at 30 °C. This was done by using the arrhenius equation dependency and an activation energy (E_a) of 68.4 KJ.mol^{-1} (Nemati *et al.*, 1998). The model parameter K was obtained for *Acidithiobacillus ferrooxidans* from the temperature dependency expression (Breed *et al*, 1999(a)). Also, both $q_{O_2}^{max}$ and K for *Leptospirillum ferrooxidans* was determined experimentally (Breed *et al*, 1999(a)).

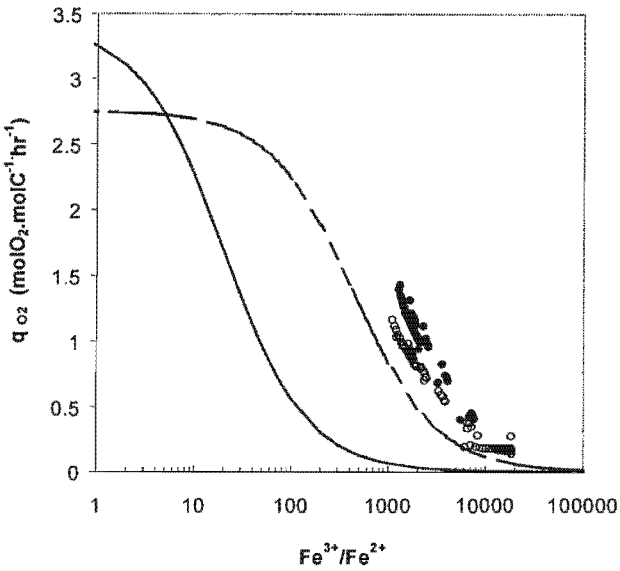

Figure 6.18 : Comparison of the calculated specific oxygen (q_{O2}) utilization rates during staged addition of [•] Mintek chalcopyrite and [o] Otjihase chalcopyrite to a batch culture as a function of the Ferric/ferrous-ion ratio. Superimposed is the Michaelis-Menten based ferrous-ion oxidation model for [—] *Acidithiobacillus ferrooxidans* and [– –] *Leptospirillum ferrooxidans* [Fe^{tot}] = 12 gl^{-1}, Temp = 35 °C, pH = 1.5, particle size = +38-53 μm.

The q_{O2}'s increased rapidly with the addition of mineral and then decreased with increasing ferric/ferrous-ion ratio. There is agreement between the measured specific oxygen utilization rate and that predicted by the model. The calculated q_{O2}'s for both chalcopyrite concentrates were obtained above ferric/ferrous-ion ratios of 1000 at both total iron concentrations. This is because of the small drop in redox potential with every mineral addition during the staged additions of chalcopyrite to a batch bioleach. The redox potential maintained itself above 650mV despite the addition of large amounts of chalcopyrite mineral.

Table 6-3: Parameters used in Bacterial ferrous-ion oxidation model modified for *Leptospirillum ferroxidans* (Breed *et al.*, 1999(a)) and *Acidithiobacillus ferroxidans* (Modified to account for temperature from Boon, (1996))

Bacterial strain	Temperature (°C)	q_{O2}^{max} ($mmolO_2mmolC^{-1}hr^{-1}$)	K
Leptospirillum ferrooxidans	35	0.0023	2.75
Thiobacilllus ferrooxidans	30	0.05	2.2
	35	0.051	3.4

The calculated specific rates are slightly higher than those predicted by the model for both *Acidithiobacillus ferrooxidans* and *Leptospirrilum ferrooxidans*. This could be due to the oxidation of sulphur and sulphur compounds.

The increasing trend in q_{O2} with mineral addition is consistent with the multiple sub-process mechanism. The addition of mineral decreases the redox potential (Figure's 6.1, 6.2 and 6.3) thereby decreasing the ferric/ferrous-ion ratio due to the $r^{chem}_{Fe^{2+}} > r^{bio}_{Fe^{2+}}$ immediately after addition. The production of ferrous-ion by chemical leaching lowers the ferric/ferrous-ion ratio. The production of ferrous-ion and sulphur substrate during the chemical ferric leaching of chalcopyrite results in an increase in the specific oxygen utilization rate due to a higher substrate consumption rate. This explains the observed increase in q_{O2} with a decrease in the ferric/ferrous-ion ratio (Figure 17 and 18).

6.10 The applicability of ferrous-ion oxidation kinetics.

Figures 6.17 and 6.18 also depicts the applicability of the Michaelis-Menten based bacterial ferrous-ion oxidation model in describing the kinetics during chalcopyrite bioleaching. The approach used in testing the applicability of the bacterial kinetic model involves comparing the biomass specific rates from measurements obtained during bioleaching of chalcopyrite (staged addition experiments) with those predicted by the models for bacterial ferrous-ion oxidation. This comparison is performed at equal process conditions of temperature, pH and total-iron concentration. The models for *Acidithiobacillus ferrooxidans* and *Leptospirillium ferrooxidans* describes the change in the biomass specific oxygen utilization rate, q_{O2}, with redox potential or ferric/ferrous-ion ratio. (The ferric/ferrous-ion ratio is determined by the redox potential and is related via the Nernst equation.) The model curves represent the bacterial activity of the mesophiles in the absence of chalcopyrite mineral, while the calculated specific rates in Figures 6.17 and 6.18 are indicative of the bacterial activity of the cell suspension in the presence of chalcopyrite mineral. A comparison of the measured values with those predicted by the model gives an indication of the extent to which the bacterial ferrous-ion oxidation models are applicable in describing the kinetics of the ferrous-ion oxidation step during mesophilic chalcopyrite bioleaching. This approach provides a quantifyable means of testing the applicability of these kinetic models in the presence of chalcopyrite.

The constants $\frac{K_s}{K_I}$ and the maximum specific oxygen utilization rate, $q_{O_2}^{max}$, are used in describing the kinetic model for bacterial ferrous-ion oxidation instead of the maximum specific ferrous-ion utilization rate, $q_{Fe^{2+}}^{max}$ as used by Boon (1996) and Breed *et al.* (1998). $q_{O_2}^{max}$ is an oxygen based parameter and describes the total amount of oxygen utilized per mole of biomass synthesized, while $q_{Fe^{2+}}^{max}$ represents the amount of ferrous-ion consumed per mole of biomass synthesized. The specific ferrous-ion utilization rate could not be used as a parameter in describing the measured oxidation kinetics in the presence of chalcopyrite for reasons outlined in the next section. The kinetic constants used are written in terms of oxygen, because of these limitations.

6.11 The effect of sulphur oxidation on the kinetics of bacterial ferrous-ion utilization.

During the staged addition experiments performed by Boon (1995), the specific ferrous-ion utilization rate was determined from the stochiometric relationship between oxygen and carbon dioxide utilization rates. This was possible because the oxygen utilized during the bioleaching of pyrite was due to ferrous-ion oxidation only, since the oxygen utilized for sulphate formation originates from water. The bioleaching of chalcopyrite involves the oxidation of sulphur and/or sulphur compounds together with the oxidation of ferrous-ion due to the formation of sulphur species during the chemical ferric leaching of the mineral. The measured oxygen utilization rate during the chalcopyrite staged addition experiment includes the oxygen utilized for both ferrous-ion and sulphur oxidation. The oxygen utilized for the ferrous-ion step will therefore depend on the respective species of iron and sulphur oxidisers and their relative numbers and growth rates.

The bacterial oxidation of sulphur compounds has not been studied during the course of this project. Also, the relative proportions of the sulphur to iron oxidisers and their respective growth rates is still unknown.

During the staged additions of pyrite to a batch bioleach (Boon, 1995) the bacterial growth rate was determined from the carbon dioxide utilization rate. In the case of chalcopyrite, as is the cse of the oxygen utilization rate, the measured carbon dioxide utilization rate includes the carbon assimilated by both ferrous-ion and sulphur oxidation. The growth rate calculated from the measured carbon dioxide utilization rate would therefore include the growth rates of both the iron and sulphur oxidising species (all the species present). In order to establish the

bacterial specific ferrous-ion and/or sulphur oxidation rates, it is necessary to develop methods for the determination of:

i. The ratio of ferrous-ion to sulphur oxidising micro-organisms
ii. their respective growth rates, and
iii. their yields on the respective ferrous-ion and sulphur substrates.

The estimation of the specific ferrous-ion utilization rate and the bacterial growth rate of the ferrous-ion oxidisers during bioleaching of sulphide minerals in which both ferrous-ion and sulphur oxidizing species are present, is one of the challenges facing the use of stage addition and batch experiments to study the mechanism and kinetics of bioleaching.

Despite the above mentioned limitations, the variation in the bacterial specific oxygen utilization rate, calculated form the total measured oxygen and carbon dioxide utilization rate during chalcopyrite bioleaching, displayed a similar trend to that seen for pyrite (Boon, 1996). When expressed as a function of ferric/ferrous-ion ratio, it showed good agreement with the *Leptospirillum ferrooxidans*, Michaelis-Menten based, bacterial ferrous-ion oxidation model.

In an attempt to distinguish between the contributions of ferrous-ion and sulphur oxidation to the measured oxygen utilization rate, a stochiometric balance, assuming complete bacterial ferrous-ion and sulphur oxidation during chalcopyrite bioleaching, was performed (shown in Chapter Thee). This suggests that $^{5}/_{17}$'s of the oxygen consumed during the bioleaching of chalcopyrite is due to bacterial ferrous-ion oxidation if the stochiometry of chemical leaching of chalcopyrite is that presented in Equation (2.2.1). This fraction is dependent on the relative amount of sulphur oxidising species present and the extent to which the sulphur formed on the surface by chemical ferric leaching is oxidised to sulphuric acid. This enables the estimation of the oxygen utilized for ferrous-ion oxidation from the total measured oxygen utilization rate.

However the result presented in chapter 5, show from the measured ferrous-ion to copper ratio, that the stochiometry of chemical leaching of the chalcopyrite concentrates used in this study is close to that of Equation (2.2.2). This was supported by the lack of any observable sulphur on the surface during chemical leaching experiments.

It is because of this discrepancy, that the ratio was not applied to the staged addition results.

6.12 Yields and maintenance

6.12.1 Measured yields on chalcopyrite

During the bioleaching of chalcopyrite, the oxidation of substrate (ferrous-ion and sulphur) generates energy for bacterial growth and maintenance. The relationship between the amount of oxygen consumed for biomass synthesis and maintenance is given by the Pirt equation, viz.,

$$\frac{r_{O_2}}{r_X} = \frac{1}{Y_{OX}} = \frac{1}{Y_{OX}^{max}} + \frac{m_0}{\mu} \qquad (6.2)$$

This includes the oxygen consumed for both ferrous-ion and sulphur oxidation. By means of a degree of reduction balance, the maximum yield of bacteria on ferrous-ion, $Y_{Fe^{2+}}^{max}$, is related to the maximum yield on oxygen, Y_{OX}^{max}, as :

$$Y_{OX}^{max} = \frac{4Y_{Fe^{2+}X}^{max}}{1 \quad 4.2Y_{Fe^{2+}X}^{max}} \qquad (6.3)$$

The maintenance coefficient of bacteria grown on ferrous-ion, m_{Fe2+}, is related to the maintenance based on oxygen, m_o, as :

$$m_o = \frac{m_{Fe^{2+}}}{4} \qquad (6.4)$$

The actual yield of biomass on ferrous-ion substrate, $Y_{Fe^{2+}X}$, and the actual yield on oxygen, Y_{OX} depends on the specific growth rate, μ. The Pirt equation shows that these yields increase at increasing growth rates. Thus a plot of the reciprocal of the actual yield on oxygen against the reciprocal growth rate, μ^{-1}, determines the slope, m_o, and intercept , $(Y_{OX}^{max})^{-1}$. In Figure 6.20 the ratio between the oxygen utilisation and bacterial growth rate for the staged addition of Otjihase and Mintek-supplied chalcopyrite to a batch culture at $[Fe^{tot}]=1.2g.l^{-1}$ is plotted against the reciprocal growth rate , $1/\mu$, by applying Equation 6.2

Similarly, Figure 6.21 indicates the Pirt equation plot for the staged addition of Otjihase and Mintek-supplied chalcopyrite to a batch culture at $[Fe^{tot}]=12g.l^{-1}$.

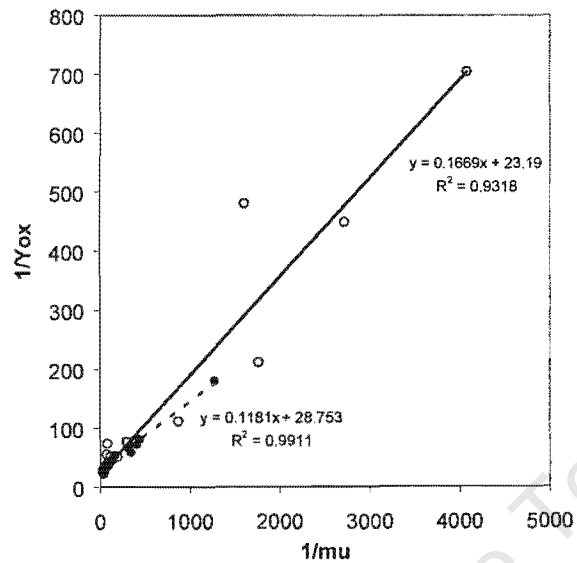

Figure 6.20 : Comparison of the Maximum Bacterial Yield on oxygen (Y_{Ox}) and maintenance coefficient (m_o) for the staged addition of [•] Mintek chalcopyrite and [o] Otjihase chalcopyrite to a batch culture. Superimposed is the linearized plots of the Pirt equation for [– –] Mintek and [—] Otjihase chalcopyrite $[Fe^{tot}] = 1.2\ gl^{-1}$, Temp = 35 °C, pH = 1.5, particle size = +38-53 µm.

The linearized plots, together with the regression analysis are shown in Figure's 6.20, 6.21 and 6.22.

The maximum bacterial yield's on oxygen, Y_{OX}^{max}, and their corresponding maintenance coefficients on oxygen, m_o, for the various concentrates at different $[Fe^{tot}]$ are summarized in Table 6-4.

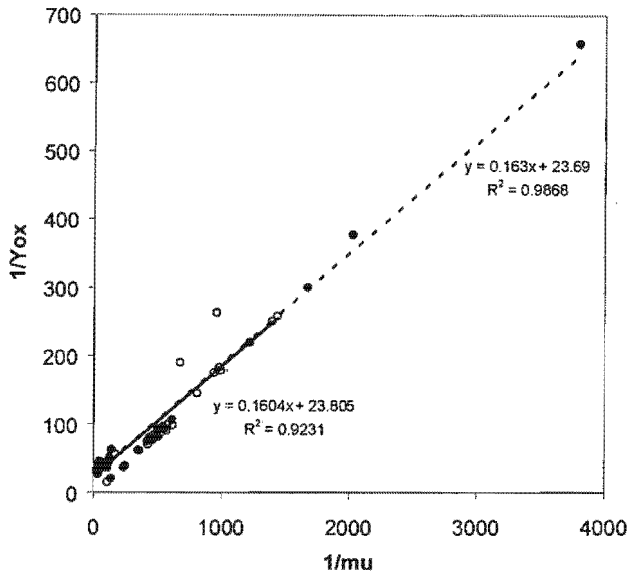

Figure 6.21 : Comparison of the Maximum Bacterial Yield on oxygen (Y_{Ox}) and maintenance coefficient (m_o) for the staged addition of [•] Mintek chalcopyrite and [o] Otjihase chalcopyrite to a batch culture. Superimposed is the linearized plots of the Pirt equation for [– –] Mintek and [—] Otjihase chalcopyrite [Fe^{tot}] = 12 gl^{-1}, Temp = 35 °C, pH = 1.5, particle size = +38-53 µm.

The maximum growth yield, Y_{OX}^{max}, is defined as the maximum amount of biomass (in mole of C) that can be produced per mole of oxygen consumed for either ferrous-ion and/or sulphur substrate utilization. Table 6-4 indicates that the Y_{OX}^{max} and m_o's are similar for both concentrates at both total iron concentrations. The maintenance coefficient, m_o, is defined as the amount of oxygen required per unit of time to maintain one C-mole of bacteria. The maximum yield and maintenance coefficients when expressed per mole of substrate are energetic parameters which can be considered constant for a certain bacteria and its substrate.

Table 6-4 also lists the Y_{OX}^{max} and m_o previously determined for *Acidithiobacillus ferrooxidans* (Boon, 1996) and *Leptospirillum ferrooxidans* (Van Scherpenzeel *et al.*, 1998) during bacterial ferrous-ion oxidation. The Y_{OX}^{max} and m_o in table 6-4 for *Acidithiobacillus ferrooxidans* and *Leptospirillum ferrooxidans* were derived by applying equation 6.2 and 6.3, respectively, to $Y_{Fe^{2+}}^{max}$ and m_{Fe2+} (Boon, 1996 and Van Scherpenzeel *et al.*, 1998). The Y_{OX}^{max} for the staged additions on chalcopyrite were obtained for 35 °C, whilst those for ferrous-ion oxidation by *Acidithiobacillus ferrooxidans* (Boon, 1996) and *Leptospirillum ferrooxidans*-like (Van Scherpenzeel *et al.*, 1998) bacteria were obtained at 30 °C. The

maximum yield on ferrous-ion and maintenance coefficient for *Leptospirillum ferrooxidans* (Breed *et al.*,1998) are the average values between 30 and 40 °C. It appears that there is a small variation in $Y_{Fe^{2+}}^{max}$ with temperature but no change in m_{Fe2+}, over the range 30 to 35 °C (Breed *et al.*,1999(a)).

From Table 6-4 it is clear that the values of Y_{OX}^{max} obtained for the stage addition experiments on a chalcopyrite batch culture are close to that determined for *Leptospirillum ferrooxidans* during growth on ferrous-ion, whilst the m_o is in the same order of magnitude. It is also apparent that the values of Y_{OX}^{max} agree more closely with the *Leptospirillum ferrooxidans*-like (Van Scherpenzeel *et al.*, 1998) bacteria than those determined for the batch (*Acidithiobacillus ferrooxidans*) and continuous growth (*L.ferroxidans*) on ferrous-ion by (Boon, 1996), or that determined for *Leptospirillum ferrooxidans* by (Breed *et al.*,1999(a)).

The measured maximum yields must be seen in conjunction with Figure's 6.17 and 6.18 showing the measured q_{O2} during the staged addition of chalcopyrite and the predicted variation in q_{O2} as functions of the ferric/ferrous-ion ratio for *Acidithiobacillus ferrooxidans* and *Leptospirillum ferrooxidans*. From these plots it appears that the measured q_{O2} is more indicative of *Leptospirillum ferrooxidans* than *Acidithiobacillus ferrooxidans*. The calculated Y_{OX}^{max} for the chalcopyrite staged additions agrees with that obtained for *Leptospirillum ferrooxidans*.

The innoculum used for the all the staged addition experiments was drawn from the supernatant of a previously grown chalcopyrite batch semi-continuous culture. Even though the bioleaching of chalcopyrite may result in the formation of amorphous sulphur due to the chemical ferric-ion leaching sub-process (Sand *et al.*, 1999) and incomplete bacterial sulphur oxidation, the sulphur would be found attached to the surface of the mineral particle(Munoz *et al.* 1979; Ammou-Chokroum *et al.*,1979; Dutrizac, 1981; Dutrizac, 1989; Hackl *et al.*, 1995 and Klauber *et al.*, 2000, Lu *et al.*, 2000).

This would mean that sulphur oxidation by *Acidithiobacillus ferrooxidans* and *Acidithiobacillus thiooxidans* would occur at the surface of the mineral particle instead of the in the supernatent of the batch culture, which suggests that the predominant species present in the supernatant are the iron oxidisers like *Leptospirillum ferrooxidans*.

Table 6-4: The Maximum Yield of Biomass on oxygen, Y_{OX}^{max}, and the maintenance coefficient, m_o, determined from the regression analysis in figure's 20 and 21 for the staged addition of Otjihase$^+$ and Mintek* supplied chalcopyrite to a batch culture compared with those determined by previous workers for continuous growth (unless otherwise indicated) on ferrous-ion only.

Bacterial culture	$[Fe^{tot}]$ mmol.l^{-1}	Y_{OX}^{max} molC.mol O_2^{-1}	m_o molO_2molC^{-1}hr^{-1}
Mixed (batch)	3	0.043$^+$	0.167$^+$
Mixed (batch)	3	0.035*	0.118*
Mixed (batch)	25	0.042$^+$	0.160$^+$
Mixed (batch)	25	0.042*	0.163*
Acidithiobacillus ferrooxidans (batch)[①]	210	0.053[①]	0.240[①]
Acidithiobacillus ferrooxidans [①]	210	0.051[①]	0.100[①]
Leptospirillum ferrooxidans-like[①]	210	0.053[①]	0.060[①]
Leptospirillum ferrooxidans-like[①]	340	0.053[①]	0.012[①]
Leptospirillum ferrooxidans		0.024[②]	0.199[②]
Leptospirillum ferrooxidans-like		0.046[③]	0.111[③]

[①] (Boon, 1996), [②] (Breed *et al.*, 1998), [③] (Van Scherpenzeel *et al.*, 1998)

The difference in maximum yields for *L.ferroxidans,* determined in the staged additions on chalcopyrite, and that determined during growth on ferrous-ion in continuous culture (Breed *et al*, 1999(a)) can possibly be attributed to the difference in subspecies. The continuous ferrous-ion growth culture (Breed *et al*, 1999(a)) originates from Fairview Mine while the culture grown on chalcopyrite was supplied by Mintek. This could account for a difference in the strain.

6.12.2 Yields on pyrite

Figure 6.22(a) and (b) compares the Pirt equation plot, together with the regression analysis of the staged addition of Otjihase chalcopyrite and Otjihase pyrite, respectively, to a batch culture at $[Fe^{tot}]=12g.l^{-1}$. A summary of the resulting maximum yields on oxygen and maintenance coefficient is shown in Table 6-6.

Table 6-6: The Maximum Yield of Biomass on oxygen, Y_{OX}^{max}, and the maintenance coefficient, m_o, determined from the regression analysis in figure's 6.22(a) and 6.22(b) for the staged addition of Otjihase pyrite* and chalcopyrite+ to a batch culture compared with those determined by previous workers for continuously growth on ferrous-ion only.

Mineral	Bacterial Culture	$[Fe^{tot}]$ gl^{-1}	Y_{OX}^{max} molC.mol O_2^{-1}	m_o $molO_2molC^{-1}hr^{-1}$
$CuFeS_2$	Mixed	10	0.040^+	0.112^+
FeS_2	Mixed	10	0.035^*	0.118^*

The Y_{OX}^{max} and m_o established for the chalcopyrite concentrate agrees with that calculated previously (Table 6-5). Also, the Y_{OX}^{max} established for the pyrite staged addition is in the same order of magnitude as those determined for chalcopyrite and is in agreement with the maximum yield on ferrous-ion established for *Leptospirillum ferrooxidans* by previous workers (Van Sherpenzeel *et al.*, 1998). This is a reasonable result since the innoculum used in both pyrite and chalcopyrite experiments were drawn from the same source.

In contrast to chalcopyrite , no elemental sulphur is formed during the bioleaching of pyrite. This oxygen utilized during the bioleaching of pyrite is only due to ferrous-ion oxidation (Boon, 1996). This means that during the bioleaching of pyrite the specific oxygen utilisation rates and growth rates are representative of the iron oxidisers only.

It has been previously reported that *Leptospirillum ferrooxidans* is the dominant iron oxidiser present during the bioleaching of pyrite(Boon, 1996) since the maximum yield of bacteria on pyrite per mole of oxygen consumed was the same as that for *Leptospirillum ferrooxidans* grown continuously on ferrous-ion.

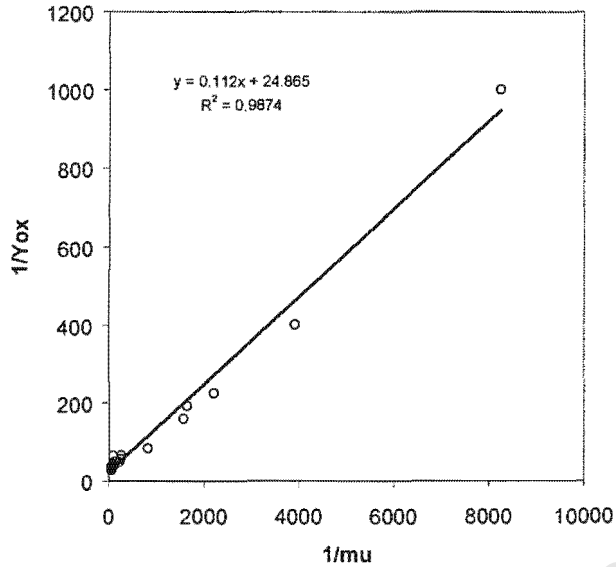

Figure 6.22(a) : The Maximum Bacterial Yield on oxygen (Y_{Ox}), 0.040 mol-C.molO_2^{-1}, and maintenance coefficient (m_o), 0.112 molO_2mol$C^{-1}hr^{-1}$, for the staged addition of [o] Otjihase chalcopyrite to a batch culture. Superimposed is the linearized plot of the Pirt equation for [—] Otjihase chalcopyrite. [Fe^{tot}] = 12 gl^{-1}, Temp = 35 °C, pH = 1.5, particle size = +38-53 µm.

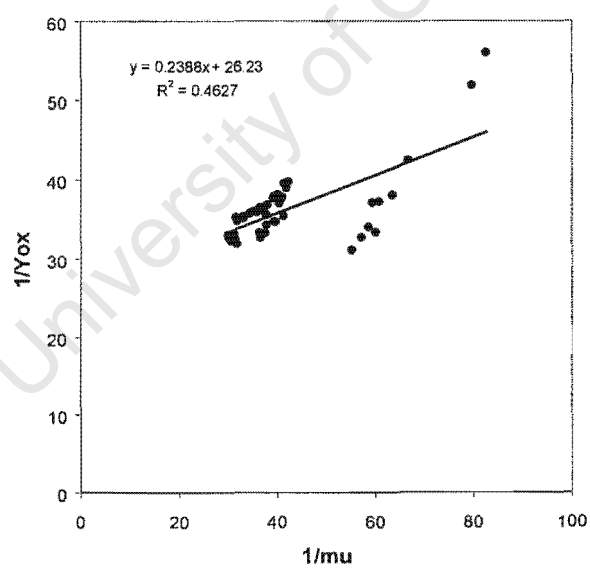

Figure 6.22(b) : The Maximum Bacterial Yield on oxygen (Y_{Ox}), 0.038 mol-C.molO_2^{-1}, and maintenance coefficient (m_o), 0.239 molO_2mol$C^{-1}hr^{-1}$, for the staged addition of [•] Otjihase pyrite to a batch culture. Superimposed is the linearized plot of the Pirt equation for [—] Otjihase pyrite. [Fe^{tot}] = 12 gl^{-1}, Temp = 35 °C, pH = 1.5, particle size = +38-53 µm.

6.13 Conclusions from the staged addition of chalcopyrite-concentrates to a batch bioleach

1. The results have shown the applicability of using staged mineral additions to a batch bioleach in order to test the applicability of the multiple sub-process mechanism in describing the bioleaching of chalcopyrite concentrates with mesophiles.

2. Consequently, the redox potential trend as well as the trends in the measured bacterial specific oxygen utilisation, obtained for these experiments illustrates the presence of separate chemical leaching and bacterial ferrous-ion oxidation steps only.

3. A comparison of the specific oxygen utilisation rates measured during the experiments and that predicted for bacterial ferrous-ion oxidation from existing models, suggest that *Leptospirillum ferrooxidans* would be the dominant iron oxidiser at the ferric/ferrous-ion ratios established in these experiments, since the model for *Acidithiobacillus ferrooxidans* shows negligible iron oxidation at ferric/ferrous-ratios above 100.

4. The question of sulphur oxidation during the bioleaching of chalcopyrite with mesophiles, and its contribution to the measured specific oxygen utilisation rate is still unresolved.

Chapter 7: Modeling Batch Bioleaching

7.1 Introduction

The bioleaching of chalcopyrite is thought to occur via a multiple sub-process mechanism involving chemical leaching of the mineral to produce ferrous-ion and sulphur compounds. The role of the iron-oxidisers is confined to regenerating ferric-ion by oxidising the ferrous-ion produced from the chemical leaching step. Similarly, the sulphur oxidisers play a role in generating sulphuric acid from the oxidation of sulphur/sulphur compounds (Sand *et al.*, 1999). The existence of a two step mechanism involving the chemical leaching and bacterial ferrous-ion consumption has already been shown for the case of pyrite (Boon, 1996).

The existence of the multiple step mechanism implies that there is a complex interaction between the chemical and bacterial sub-processes. However, it also suggests that the bioleaching process can be divided into three sequential sub-processes, *viz*,

1. the chemical leaching of chalcopyrite,
2. the bacterial oxidation of ferrous-ion, and
3. the bacterial oxidation of sulphur/sulphur compounds.

The kinetics of the chemical and bacterial steps can be independently studied and modeled at conditions similar to those experienced in a bioleaching system. The chemical and the bacterial iron-oxidation steps involve the production and consumption of ferrous-ion respectively. The ferrous-ion production/consumption rate forms the basis of any interaction between the kinetics of the first two sub-processes. Therefore, the rate of chemical production by mineral leaching together with the rate of bacterial consumption of ferrous-ion must be expressed as functions of the ferric/ferrous-ion ratio, which forms the common basis in linking the kinetics of the separate sub-processes.

Previous work has already applied this methodology, enabling the prediction of the steady-state performance of pyrite (Boon *et al.*, 1995, May *et al.*, 1997) and arsenopyrite bioleaching (Breed *et al.*, 1998; Ruitenberg *et al.*, 1998) systems. The purpose of this section is to illustrate the use of this thinking to predict the bioleaching behavior of a predominantly chalcopyrite concentrate during staged additions of the mineral to a batch culture. In the case of pyrite bioleaching, the overall process does not include any sulphur oxidation, since the chemical leaching of the mineral produces sulphate (May *et al.*, 1997). However, in the case of chalcopyrite, the contribution of the sulphur oxidation step provides a serious limitation in any rigorous application of this methodology.

To date most research has been focussed on the first two sub-processes with very little work being directed to understanding the third sub-process.

This chapter is organized into three major sections. The first deals with the kinetics of chemical ferric leaching of the chalcopyrite concentrate and briefly describes the work to date on establishing the rate of chemical leaching as a function of the redox potential or ferric/ferrous-ion ratio. The second section illustrates the kinetic models developed by previous workers for the bacterial ferrous-ion oxidation sub-process. The third brings together the kinetics of chemical leaching and the bacterial ferrous-ion oxidation step in order to describe the kinetic behavior of chalcopyrite bioleaching in a batch culture as an overall process.

7.2 The chemical leaching of chalcopyrite

As mentioned before, the chemical leaching of chalcopyrite is thought to proceed by Reactions (7.1) and (7.2) (Munoz *et al.*, 1979; Dutrizac, 1981; Hirato *et al.*, 1987; Dutrizac, 1989)

$$CuFeS_2 + 4Fe^{3+} \mapsto Cu^{2+} + 5Fe^{2+} + 2S^0 \qquad (7.1)$$

$$CuFeS_2 + 16Fe^{3+} + 8H_2O \mapsto Cu^{2+} + 17Fe^{2+} + 16H^+ + 2SO_4^{2-} \qquad (7.2)$$

The kinetics of chemical leaching of chalcopyrite during bioleaching must be expressed in terms of the ferric/ferrous-ion ratio in order to establish compatibility with the bacterial kinetics of ferrous-ion oxidation. Previous work has shown that the ferric leaching of pyrite and arsenopyrite is dependent on the redox potential or ferric/ferrous-ion ratio in a bioleaching system (Boon ,1996; May *et al.*, 1997; Breed *et al.*, 1997; Ruitenberg *et al.*, 1998). The reworking of previously published literature (Kametani and Aoki, 1985) and other recent findings (Hiroyoshi *et al.*, 2000; Furamera, 2000) found that the rate of chalcopyrite chemical leaching is also a function of the redox potential or ferric/ferrous-ion ratio. (The redox potential is related to the ferric/ferrous-ion ratio by the Nernst equation.)

Figure 7.1 (Furamera, 2000) shows the measured variation in the specific rate of ferrous-ion production (expressed per mole of available chalcopyrite concentrate) from the chemical leaching of a predominantly chalcopyrite concentrate at 35 °C with changing ferric/ferrous-

ion ratio. Also shown in figure 7.1 is the predicted rate of pyrite leaching established by previous workers at 30 °C (Boon *et al.*, 1995).

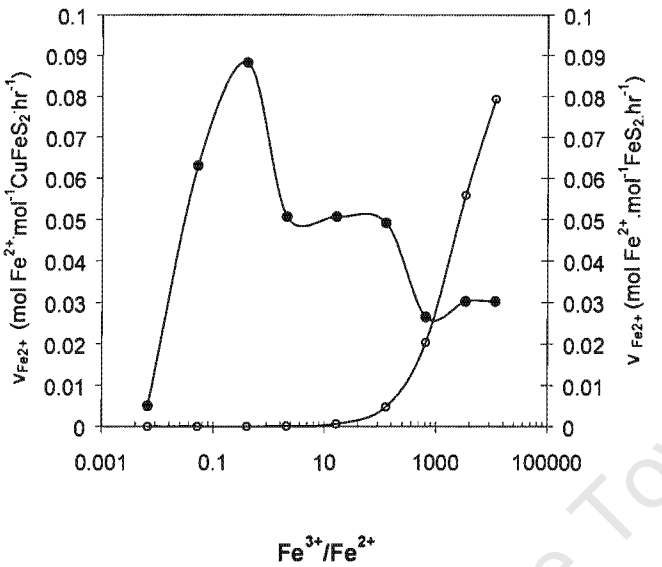

Figure 7.1: The variation in the measured specific ferrous-ion production rate with changing ferric/ferrous-ion during the ferric leaching of [●] Otjihase chalcopyrite at 35 °C (Furamera, 2000) and that predicted for [O] pyrite (Boon *et al.*, 1996) at 30 °C

Furamera (2000) conducted a study to establish the effect of redox potential on the rate of chemical ferric leaching of the Otjihase chalcopyrite concentrate in a sterile sulphuric acid suspension. In contrast to other studies on the ferric leaching of pyrite (May *et al.*, 1997) and arsenopyrite (Ruitenberg *et al.*, 1998), the technique employed was derived from Kametani and Aoki's (1985) work ,which involved measuring the rate of chemical leaching at constant redox potentials in the suspension. The application of this experimental methodology in establishing the rate of chemical leaching of chalcopyrite has already been discussed by Furamera (2000). What follows is a brief description of this technique.

The controlled addition of permanganate solution enabled the ferrous-ion produced during the chemical leaching of the mineral to be instantaneously re-oxidised to ferric-ion, thereby maintaining a constant redox potential or ferric/ferrous-ion ratio. The re-oxidation of ferrous-ion by permanganate to ferric-ion proceeds via the stochiometry shown in Reaction (3) (Kametani and Aoki, 1985).

$$KMnO_4 + 8H^+ + 5Fe^{2+} \mapsto K^+ + Mn^{2+} + 5Fe^{3+} + 4H_2O \qquad (7.3)$$

The amount of permanganate added to maintain a constant redox potential was related to the amount of ferrous-ion produced during the chemical leaching of the mineral via the stochiometry in Reaction (7.3). Reaction (7.3) enabled the rate of ferrous-ion production to be determined from the initial slope of a plot of dissolved ferrous-ion vs time at a particular redox potential. The rate of ferrous-ion can then be stochiometrically related to the rate of chalcopyrite consumption via Rquation (7.1) and (7.2).

It is apparent from Figure 7.1 that the leaching of the chalcopyrite concentrate passes through a maximum at low redox potentials or ferric/ferrous-ion ratios of 1, afterwhich a decline in the rate of leaching is seen for higher ferric/ferrous-ion ratios. The initial increasing trend in the mineral leach rate up to ferric/ferrous-ion ratio's of 1 compares well with that established by reworking previously published work at 90 °C (Kametani and Aoki, 1985). To date, no accepted empirical or fundamental mathematical model has been developed to describe rate of chalcopyrite leaching as a function of the ferric/ferrous-ion ratio.

The underlying mechanism responsible for the observed decrease in the rate of leaching after reaching the maximum is still not clearly understood. However, the results show that rate of chemical leaching of the chalcopyrite concentrate is much lower at high ferric/ferrous-ion ratio's as compared to low ferric/ferrous-ion ratios.

In contrast to the above trend for chalcopyrite, the specific rate of ferrous production established from the leaching of pyrite increases with increasing ferric/ferrous-ion ratio. The specific rate can be described by a Monod-type equation (Equation (7.4)), (Boon *et al.*, 1995) or the Butler-Volmer equation (Equation (7.5)) (May *et al.*, 1997). Both of these models predict an increase in the mineral leach rate with an increase in the ferric/ferrous-ion ratio.

$$\upsilon_{Fe^{2+}} = \frac{\upsilon_{Fe^{2+}}^{max}}{1 + B\dfrac{[Fe^{2+}]}{[Fe^{3+}]}} \qquad (7.4)$$

The Butler-Volmer equation is based on electrochemical corrosion theory and expresses the rate of pyrite leaching as an exponential function of the overpotential (E). It therefore appears to have a greater fundamental basis as compared to the Monod-type equation. May *et al.*, (1997) developed the Butler-Volmer model (Equation (7.5)) by using a dynamic redox potential measurements as opposed to the constant redox potential measurements used by Furamera(2000) for the chalcopyrite concentrate.

$$\upsilon_{Fe^{2+}} = \upsilon_0 \left(e^{\alpha\beta(E-E')} - e^{(1-\alpha)\beta(E-E')} \right) \quad (7.5)$$

The values for the parameters in the Equation (7.4) and (7.5) is listed in Table 7-1. The predicted variation in the specific rate of ferrous-ion production, as determined from Equation (7.4) from the parameters in Table 7-1, for the chemical leaching of pyrite is shown in Figure 7.1. The Monod-type model (Boon *et al.*, 1996) was chosen over the Butler-Volmer model (May *et al.*, 1997), despite the lack of any fundamental basis, because the parameters were established at 30 °C as opposed to the Butler-Volmer model which was defined at 25 °C by May *et al.* (1997). It therefore compares more accurately because of the similar temperature, as opposed to with the rate curve established for the chalcopyrite concentrate at 35 °C. Also, both models shown in Equations (7.4) and (7.5) predict similar shaped curves. However, the Butler-Volmer model does not appear to level off at high ferric/ferrous-ion ratio's.

Table 7-1: Parameters of equation (7.4) and (7.5) for models describing the ferric leaching of pyrite.

Workers	Temp	$\upsilon_{Fe^{2+}}^{max}$	B	υ_0	α	β	E`
Boon *et al.*, 1996	30 °C	0.244e-4	0.096				
May *et al.*, 1997	25 °C			4.8e-8	0.46	25.89	413

Figure 7.1 shows that the specific rate of leaching for the chalcopyrite concentrate is smaller than that of pyrite at ferric/ferrous-ion ratio's greater than 1000. This could mean that within that range of ferric/ferrous-ion ratio's the rate of pyrite leaching would exceed that of chalcopyrite in ores containing both minerals. However, previous studies have indicated that galvanic interactions between the minerals would result in the preferential leaching of chalcopyrite over pyrite (Berry *et al.*, 1978; Natarajan, 1992). Furthermore, it must be noted that the rates in Figure 7.1 are expressed per mole of mineral. The actual rate of ferrous-ion production can be calculated from the specific rate of ferrous-ion production by knowing the mineral molar concentration as in Equation (7.6),

$$-r_{Fe^{2+}}^{chem} = \upsilon_{Fe^{2+}}[CuFeS_2] \quad (7.6)$$

The actual rates of mineral leaching would depend on the relative quantities of each mineral species present in the ore.

7.3 Bacterial Ferrous-ion oxidation kinetics

7.3.1 Kinetic Model

Bacterial ferrous-ion oxidation occurs according to Reaction (7.7) (Boon *et al.*, 1996; Nemati *et al.*,1998)

$$4Fe^{2+} + O_2 + 4H^+ \mapsto 4Fe^{3+} + 2H_20 \qquad (7.7)$$

Earlier workers have modeled bacterial ferrous-ion oxidation in the form of Michaelis-Menten/Monod-based enzyme kinetics (Jones and Kelly, 1983; Braddock *et al.*, 1984). Later work ignored the threshhold ferrous-ion concentration in the Michaelis Menten model and expressed the kinetics in terms of bacterial specific parameters and only as a function of the ferric/ferrous-ion ratio as shown in Equation (7.8) (Boon *et al.*, 1995; Van Scherpenzeel *et al.*, 1998; Breed *et al.*, 1999(a)).

$$q_{Fe^{2+}} = \frac{-r^{bac}_{Fe^{2+}}}{C_x} = \frac{q^{max}_{Fe^{2+}}}{1 + K_{Fe^{2+}} \frac{[Fe^{3+}]}{[Fe^{2+}]}} \qquad (7.8)$$

where,

$q_{Fe^{2+}}$ is the bacterial specific ferrous-ion oxidation rate ($molFe^{2+}.molC^{-1}.h^{-1}$),

$q^{max}_{Fe^{2+}}$ is the maximum bacterial specific ferrous-ion oxidation rate ($molFe^{2+}.molC^{-1}.h^{-1}$),

C_x is the biomass concentration ($molC.l^{-1}$),

$-r^{bac}_{Fe^{2+}}$ is the bacterial ferrous-ion production rate ($molFe^{2+}.l^{-1}.h^{-1}$),

$K_{Fe^{2+}}$ is the kinetic constant for bacterial ferrous-ion oxidation (Dimensionless)

$[Fe^{2+}]$ is the ferrous-ion concentration (mol $Fe^{2+}.l^{-1}$)

$[Fe^{3+}]$ is the ferric-ion concentration (mol $Fe^{3+}.l^{-1}$)

This form of kinetics has been successfully applied to describe ferrous-ion oxidation by mesophiles like *Acidithiobacillus ferrooxidans* and *Leptospirillum ferrooxidans* in batch and continuous systems for the range of redox potentials prevalent in pyrite and arsenopyrite

bioleaching systems (Boon *et al.*, 1995; Hansford, 1997; Van Sherpenzeel *et al*, 1998; Breed *et al.*, 1999; Breed *et al.*, 1999(a), 1999(b)).

The specific bacterial ferrous-ion utilization rate is related to the bacterial specific oxygen utilization rate by a degree-of-reduction balance for ferrous-ion oxidation as Equation (7.9) (Boon, 1996),

$$q_{Fe^{2+}} = 4q_{O_2} + 4.2q_{CO_2} \qquad (7.9)$$

where,

$q_{O_2} = \frac{-r_{O_2}}{C_x}$ and is the bacterial specific oxygen utilization rate ($molO_2.molC^{-1}.h^{-1}$) and,

$q_{CO_2} = \frac{-r_{CO_2}}{C_x}$ is the bacterial specific carbon dioxide utilization rate ($molCO_2.molC^{-1}.h^{-1}$),

Similarly the bacterial ferrous-ion production rate, $-r^{bac}_{Fe^{2+}}$, is related to the oxygen, $-r_{O_2}$, and carbon dioxide utilization rates, $-r_{CO_2}$, as Equation (10) (Boon, 1996),

$$-r^{bac}_{Fe^{2+}} = -4r_{O_2} - 4.2r_{CO_2} \qquad (7.10)$$

Equation's (7.9) and (7.10) show that the bacterial ferrous-ion production rate and the specific bacterial ferrous-ion utilization rate can be directly obtained from measurements of the oxygen, $-r_{O_2}$, and carbon dioxide utilization rates, $-r_{CO_2}$, during bacterial ferrous-ion oxidation or bioleaching. This can be done because the carbon dioxide is the only source of carbon for assimilation and is therefore directly related to the rate of bacterial growth, ie, (Equation (7.11)),

$$r_x = -r_{CO_2} \qquad (7.11)$$

Figure 7.2 shows the predicted variation in the specific ferrous-ion utilization rate with changing ferric/ferrous-ion ratio for *Acidithiobacillus ferrooxidans* and *Leptospirillum ferrooxidans* at 35 °C by applying the Michaelis-Menten/Monod based model shown in Equation (8). The values for the maximum specific ferrous-ion utilization rate and the kinetic

constant, $K_{Fe^{2+}}$, is listed in Table 7-2. Both these kinetic parameters were experimentally determined for *Leptospirillum Ferrooxidans* (Breed *et al.*, 1999(a)).

Table 7-2: Values of the kinetic constant and the maximum bacterial specific ferrous-ion utilisation rate for equation (7.8) at 35 °C.

Bacterial strain	Temperature (°C)	$K_{Fe^{2+}}$	$q^{max}_{Fe^{2+}}$ ($molFe^{2+}molC^{-1}hr^{-1}$)
Leptospirillum Ferrooxidans	35	0.0023*	11.01*
Thiobacilllus Ferrooxidans	35	0.051+	13.6+

*Breed *et al.*, (1999(a)); +modified from Boon, (1996)

However, the maximum specific ferrous-ion utilization rate for *Acidithiobacillus ferrooxidans* was modified to account for temperature from that which was previously determined at 30 °C (Boon, 1996), using the arrhenius equation dependency and activation energy of 68.4KJmol^{-1}(Nemati and Webb, 1997).

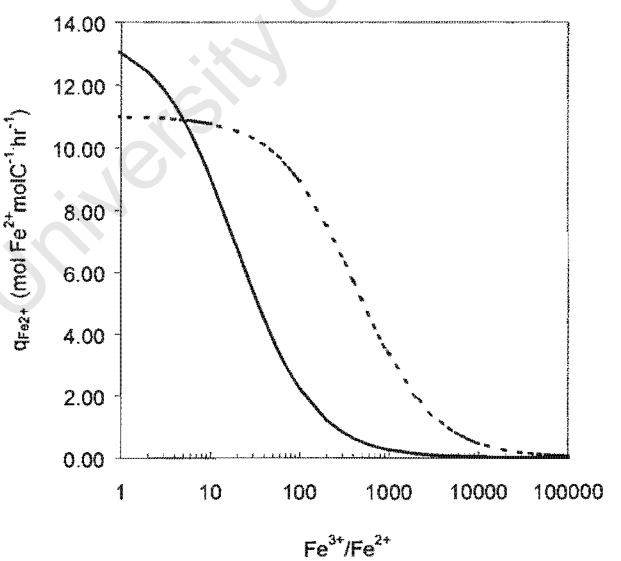

Figure 7.2: The predicted variation in the bacterial specific ferrous-ion utilization rate, $q_{Fe^{2+}}$, with changing ferric/ferrous-ion ratio from equation (no.)for [—]*Acidithiobacillus ferrooxidans* and [- -]*Leptospirillum ferrooxidans* at 35 °C.

The bacterial rate of ferrous-ion utilization can be calculated from the bacterial specific rate of ferrous-ion utilization at a known bacterial concentration by Equation (7.12),

$$-r^{bac}_{Fe^{2+}} = q_{Fe^{2+}} C_x \quad (7.12)$$

7.4 The kinetics of chalcopyrite batch bioleaching

7.4.1 Integrating the chemical leaching and bacterial oxidation kinetic models

Both Figure 7.1 and figure 7.2 are indicative of the chemical and one bacterial sub-process occurring during the bioleaching of the chalcopyrite concentrate. Till now, the kinetics of these two important sub-processes have been treated independently. However, the bioleaching of chalcopyrite involves these two sub-process occurring simultaneously. Therefore, any kinetic description of a system containing both chalcopyrite and bacteria would involve the integration of the kinetics of these two important sub-processes.

The bioleaching of chalcopyrite may involve an additional sulphur oxidation step. However the oxidation of sulphur formed during the chemical leaching results in the formation of sulphate and sulphuric acid (Sand *et al.*, 1999). It does not contribute towards the either the production or consumption of ferrous-ion. This means that the observed redox potential or ferric/ferrous-ion ratios are only dependent on the interaction between the chemical leaching and the bacterial ferrous-ion oxidation step. It can therefore be assumed that at steady state, the rate of chemical ferrous-ion production ($r^{chem}_{Fe^{2+}}$) from chemical ferric leaching is equal to the rate of bacterial ferrous-ion consumption ($-r^{bac}_{Fe^{2+}}$) as in Equation (7.13)

$$r^{chem}_{Fe^{2+}} = -r^{bac}_{Fe^{2+}} \quad (7.13)$$

During chalcopyrite bioleaching, the bacterial ferrous-ion and chemical sub-processes are linked by the rate at which the ferrous-ion is turned over. Both the kinetics of chemical leaching of chalcopyrite and bacterial ferrous-ion oxidation are expressed as functions of the ferric/ferrous-ion ratio. The integration of these two sub-processes is made possible by superimposing plots of the rate of ferrous-ion production and consumption from the chemical leaching and bacterial oxidation sub-processes, respectively, on the same set of axis. This is hypothetically illustrated in Figure 3. Figure 3 shows the chemical ferrous-ion production rate of pyrite and chalcopyrite at $30g.l^{-1}$, together with the rates of bacterial ferrous-ion consumption of *Acidithiobacillus ferrooxidans* and *Leptospirillum ferrooxidans* at $2mmolC.l^{-1}$, as functions of the ferric/ferrous-ion ratio calculated from Equation (7.8).

The kinetic constants for bacterial ferrous-ion oxidation were presented in Table 7-2. Similarly, the kinetic constants for the chemical leaching of pyrite was determined by Boon *et al.*, (1995) (shown in Table 7-1). The rate of ferrous-ion production from the chemical leaching of chalcopyrite was experimentally measured by other workers (Furamera, 2000).

The intersection of the chemical and bacterial curves in Figure 7.3 represent the rate at which ferrous-ion is turned over or a steady state between the chemical leaching and bacterial ferrous-ion oxidation sub-processes. It also represents the ferric/ferrous-ion ratio or redox potential at which the chemical ferrous-ion production and bacterial rates ferous-iron utilization are equal.

From Figure 7.3, it is clear that the chemical ferrous-ion production curve of the chalcopyrite concentrate, intersects the bacterial ferrous-ion oxidation curve of *Leptospirillum ferroxidans* at a lower rate of iron turnover but higher ferric/ferrous-ion ratio than *Acidithiobacillus ferrooxidans.*

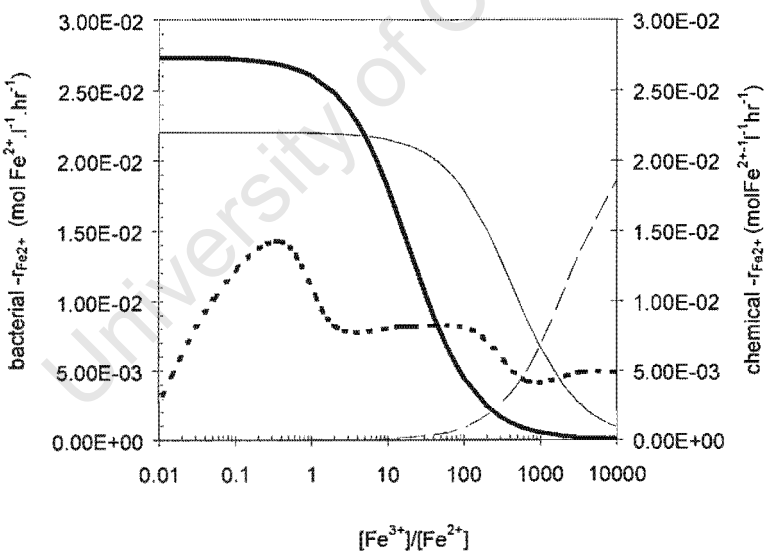

Figure 7.3: Variation in the predicted ferrous-ion consumption rate for bacterial ferrous-ion oxidation by [–]*Acidithiobacillus ferrooxidans* (modified from Boon, (1996)) and [—]*Leptospirillum ferrooxidans* (Breed *et al.*, 1998(a)) at 35 °C using eqn (8), together with the predicted ferrous-ion production rate for the chemical leaching of [— —]pyrite (Boon *et al.*, 1995) using eqn (4) and that measured for [---]chalcopyrite (Furamera, 2000), assuming $[C_x]$=2mmolCl^{-1}, $[CuFeS_2]$ and $[FeS_2]$=30 gl^{-1}

In contrast the chemical leaching curve of pyrite intersects the bacterial curve of *Leptospirillum ferroxidans* at a higher rate of ferrous-ion turnover than *Acidithiobacillus ferrooxidans.*

7.4.2 Describing the kinetics a predominantly chalcopyrite concentrate during batch bioleaching

During the staged addition experiment, successive mineral additions are made to a batch bioleach. This results in a changing mineral concentration as well as a changing bacterial concentration by virtue of bacterial growth.

Figure 7.4(a) shows the predicted rates of ferrous-ion production from the chemical leaching of the chalcopyrite-concentrate at initial mineral concentrations of 2, 6, 12, 20, 30 and 42 $g.l^{-1}$ respectively for a temperature of 35 °C, and initial total iron concentration of $12g.l^{-1}$. The curves in Figure 7.4(a) represent the rates of ferrous-ion production from chemical leaching of the chalcopyrite-concentrate, estimated from the specific rate ferrous-ion production shown in Figure 7.1 (Furamera, 2000) (by using Equation (6)), for the range of mineral concentrations and ferric/ferrous-ion ratios obtained in the experiment. Similarly, Figure 7.4(b) shows the predicted ferrous-ion production rates for the staged addition experiment conducted at a total iron concentration of $1.2gl^{-1}$ for chalcopyrite-concentrate concentrations of 2, 6, 12, 20 and 30 gl^{-1} respectively. The dashed arrows in Figure's 7.4(a) and (b) symbolize the direction of increase in the chemical leaching rate at constant ferric/ferrous-ion ratios curve with increasing mineral concentration.

Superimposed on Figure's 7.4(a) and (b) are the predicted rates of bacterial ferrous-ion consumption for *Leptospirillum ferrooxidans* at concentrations between 0.9 and 2 $mmolCl^{-1}$. The curves were obtained from specific bacterial ferrous-ion utilization rates by using Equation (7.8) and (7.12), with for model parameters shown in Table 7-2, estimated for the range of bacterial concentrations measured during the staged addition experiments.

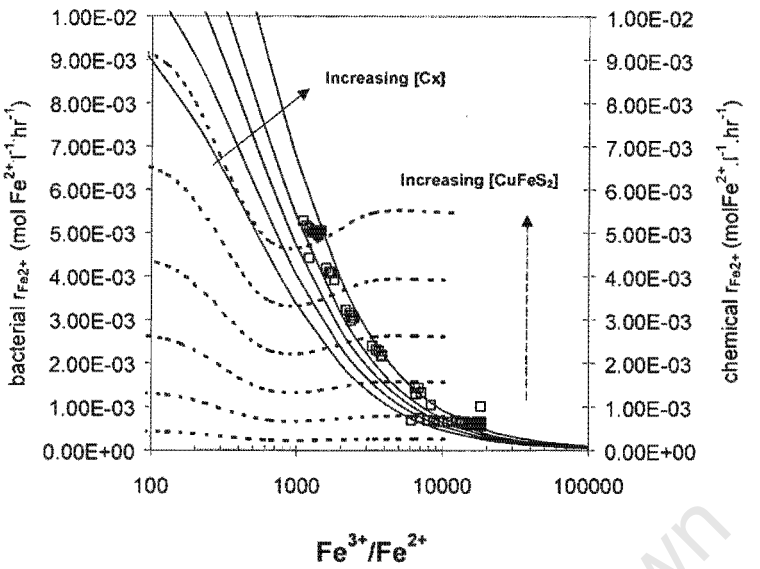

Figure 7.4(a): Variation in the measured rates of ferrous-ion production from chemical leaching (left axis) of the Otjihase chalcopyrite concentrate at (— — →)increasing concentrations for [- - -] 2; 6; 12; 20, 30 and 42 gl^{-1}, together with the predicted rate ferrous-ion consumption by *Leptospirillum ferrooxidans* from equation (8) (right axis) at (——→) increasing bacterial concentration for [—] 1, 1.2,1.4, 1.6 and 2 $mmolCl^{-1}$ at 35 °C as functions of the ferric/ferrous-ion ratio. [ ] shows the rates of ferrous-ion utilization calculated from the measured oxygen and carbon dioxide utilization rates during the staged addition of Otjihase chalcopyrite concentrate to a batch bioleach at 35 °C and initial $[Fe]^{tot} = 12gl^{-1}$

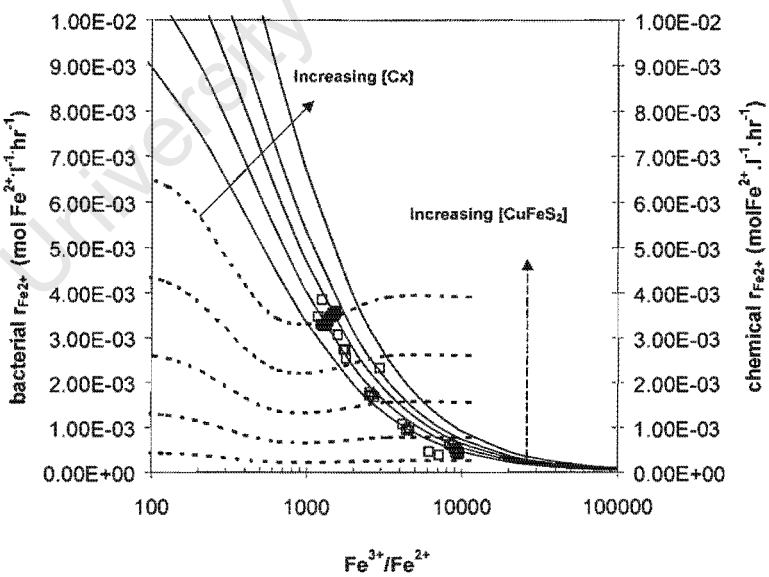

Figure 7.4(b): Variation in the predicted rates of ferrous-ion production from chemical leaching (left axis) of the Otjihase chalcopyrite concentrate at (— — →)increasing concentrations for [- - -] 2; 6; 12; 20 and 30 gl^{-1}, together with the measured rate ferrous-ion consumption by *Leptospirillum ferrooxidans* from equation (8) (right axis) at (——→) increasing bacterial concentration for [—] 1, 1.2,1.4, 1.6 and 2 $mmolCl^{-1}$ at 35 °C as functions of the ferric/ferrous-ion ratio. [ ] shows the rates of ferrous-ion utilization calculated from the measured oxygen and carbon dioxide utilization rates during the staged addition of Otjihase chalcopyrite concentrate to a batch bioleach at 35 °C and initial $[Fe]^{tot} = 1.2gl^{-1}$

The solid arrow in Figure's 7.4(a) and (b) symbolize the direction of increase of the bacterial ferrous-ion utilization curve with increasing bacterial concentration at constant ferric/ferrous-ion ratios.

Also shown on Figure's 7.4(a) and (b) are the experimental ferrous-ion utilization rates calculated from the measured oxygen and carbon dioxide consumption rates via Equation (7.10). (The rates were established on the assumption that all the oxygen utilized was due to bacterial ferrous-ion oxidation only.)

Figure's 7.4(a) and (b) show that the measured rates of ferrous-ion utilization fall within the predicted region of intersection between the chemical and bacterial curves . Figure's 7.4(a) and (b) show similar results at both initial total-iron concentrations.

7.4.3 Changing rate of iron turnover

The rate of ferrous-ion production from chemical leaching is faster than the rate of bacterial ferrous-ion consumption by the bacteria immediately after mineral addition. During this period, the rate controlling step is bacterial ferrous-ion consumption. This is accompanied by an immediate decrease in the redox potential after mineral addition. Simultaneously, the rate of bacterial growth on the ferrous-ion increases until enough cell mass is synthesized for the rates of chemical leaching and bacterial ferrous-ion consumption to equalize Similar results have been reported for the staged addition of pyrite to a batch culture consisting of *Leptospirillum ferrooxidans* (Boon, 1996). This initial equalization between the chemical ferrous-ion production and bacterial consumption rates is termed a steady state and is representative of the initial rate of iron turnover. This is the point which the model needs to predict.

The intersection between the chemical leaching and bacterial curves in figure 7.4(a) and (b) represent the iron turnover rate when the rate of ferrous-ion production from the chemical leaching of the chalcopyrite concentrate (at the particular mineral concentration) equals the rate of bacterial ferrous-ion consumption of the cell mass during the bioleaching of the chalcopyrite concentrate. However, dynamic changes in the chemical rate of mineral leaching and bacterial rate of ferrous-ion utilization affect the predicted intersection points shown in Figure 7.4(a) and (b). The chemical leach rate at a particular mineral concentration decreases with time due to surface area passivation (Munoz *et al.*, 1979; Dutrizac, 1981;

Dutrizac, 1989; Klauber *et al.*, 2000). According to the multiple sub-process mechanism, the rate of bacterial ferrous-ion consumption is dependent on the rate of ferrous-ion production because the chemical leaching of the mineral is the only source of iron-substrate needed for growth of the iron oxidisers. This means that in time, the chemical leaching curves at each mineral concentration shown in Figure's 7.4(a) and (b) decrease (vertically) at constant ferric ferrous-ion ratio's, while the bacterial curves increase (vertically) at the same ferric/ferrous-ion ratio.

It could therefore be argued that after the initial equalization between the chemical rate of ferrous-ion production and bacterial rates of ferrous-ion consumption rate a steady state condition occurs. However , once this condition is reached, the rates of ferrous-ion production and consumption remain equal but decrease in time. The decreasing iron turnover rate continues until the next mineral addition is made which results in a faster rate of chemical leaching and the cycle repeats itself at larger iron turnover values. This trend also explains observed increase in ferric/ferrous-ion ratio's (redox potential) after the initial steady state is reached, between mineral additions.

Figure 7.5 is a hypothetical diagramatic representation showing the trajectory of intersections between the chemical rates of ferrous-ion production and bacterial rates of ferrous-ion consumption between mineral additions.

In Figure 7.5 (1) indicates the rate of bacterial-ferrous-ion consumption at the first mineral addition. (2) indicates the rate of chemical ferrous-ion production at the first mineral addition. (1) – (3) shows the changing rate of bacterial ferrous-ion consumption with decreasing ferric/ferrous-ion ratio immediately after the first mineral addition. (2) – (3) shows the changing rate of chemical ferrous-ion production by mineral leaching as a function of the ferric/ferrous-ion ratio immediately after the first mineral addition. (3) indicates the point when the chemical and bacterial rates equalize after the first mineral addition establishing the initial rate of iron turnover. (3) – (4) shows the trajectory of the decreasing rates iron-turnover as a function of the ferric/ferrous-ion ratio before the next mineral addition.

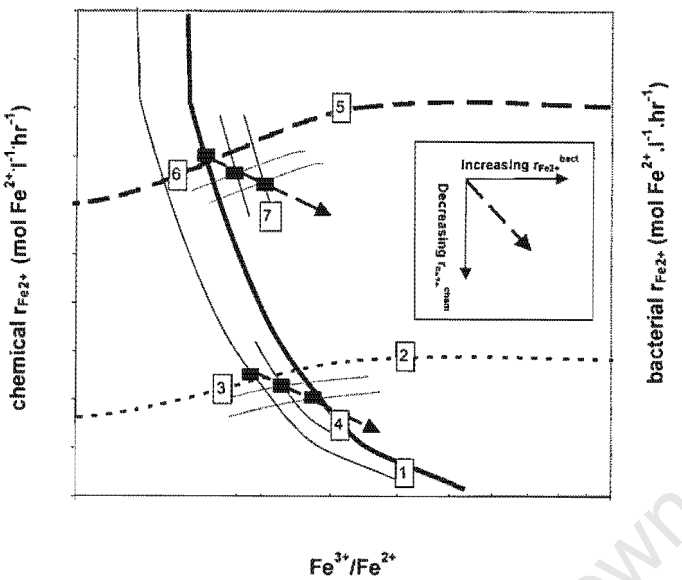

Figure 7.5: Diagramatic representation of the [■] rates of ferrous-ion turnover between mineral additions during the staged addition of chalcopyrite concentrate to a batch bioleach. [---] indicates chemical rates of ferrous-ion production by mineral leaching and [—] indicates the bacterial rates of ferrous-ion consumption both as functions of the ferric/ferrous-ion ratio. [— — →] shows the trajectory of decreasing rates of iron turnover as a function of increasing ferric/ferrous-ion ratio.

(4) shows the rate of iron turnover when the next mineral addition is made. (4) – (5) shows the instantaneous increase in the rate of chemical ferrous-ion production at the same ferric/ferrous-ion ratio when the second mineral addition is made. (5) – (6) shows the changing rate of chemical ferrous-ion production by mineral leaching as a function of the ferric/ferrous-ion ratio immediately after the next mineral addition. (4) – (6) shows the changing rate of bacterial ferrous-ion consumption with decreasing ferric/ferrous-ion ratio immediately after the second mineral addition. (6) indicates the point when the chemical and bacterial rates equalize to establish the initial rate of iron turnover after the second mineral addition. (6) – (7) shows the trajectory of the decreasing rates of iron turnover before the third mineral addition is made.

7.5 Conclusions and limitations

1. According to the multiple sub-process mechanism, it is possible to determine the kinetics of the chemical and bacterial sub-processes independently, and then use the kinetic constants and expressions to predict the dynamic performance of batch bioleach reactors.

2. The kinetics of both the chemical and bacterial sub-processes, are expressed as functions of the ferric/ferrous-ion ratio, which forms a common basis enabling the independently

determined kinetic parameters of each sub-process to be linked, in order to simulate the steady state behavior of a batch bioleach system.

3. The prediction of batch bioleaching behavior is achieved by superimposing the independently determined models for the initial rate of ferrous-ion production by chemical leaching of the chalcopyrite mineral concentrate and the rate of ferrous-ion utilization by the bacteria on the same set of axis, at a particular mineral and bacterial concentration . The intersection of the chemical and bacterial curves at a common ferric/ferrous-ion ratio represents the initial point of equalization between the chemical and bacterial rates of ferrous-ion production and utilization, respectively, and is the initial rate of iron turnover for a particular mineral concentration and bacterial concentration during the batch bioleach. However, the rate of ferrous-production from chemical leaching of the chalcopyrite concentrate (at a particular mineral concentration) changes both as a function of the ferric/ferrous-ion ratio and also decreases in time because of the depletion of leachable surface area. Similarly, the rate of bacterial ferrous-ion utilization for *Leptospirillum ferrooxidans* is shown not only to increase with decreasing ferric/ferrous-ion ratio, but also increases with increasing cell mass. This means that the chemical curves decrease in time while the bacterial curves increases in time resulting in a changing rate of iron turnover during the batch bioleaching of the concentrate.

4. The point of intersection of chemical and bacterial curves depends on the characteristics of the bacterial iron-oxidising species as well as the characteristics of the mineral concentrate used. The rate of ferrous-ion production from chemical leaching is specifically indicative of the leaching behavior of the Otjihase chalcopyrite concentrate. It therefore may include the contributions from the leaching of both pyrite and sphalerite impurities present in this mineral concentrate. This means that the predicted chemical leach kinetics within the range of ferric/ferrous-ion ratio's may not be representative of pure chalcopyrite.

5. It has been previously been shown the rate of chemical leaching of predominantly chalcopyrite concentrates is highest at low ferric/ferrous iron ratios typically between 1 and 10 (Kametani and Aoki, 1985; Hiroyoshi *et al.*, 2000; Furamera, 2000). The model has been applied to the range of ferric/ferrous-ion ratio's observed during the batch experimentation performed on the chalcopyrite concentrate, which is significantly higher than those required for optimal leaching rates. For this reason only *Leptospirillum ferrooxidans* was considered, since it has been shown that it is the dominant iron-oxidiser at the range of ferric/ferrous-ion ratio's obtained during the experiment. The predicted

rates of iron turnover may vary if *Acidithiobacillus ferrooxidans* was the predominant iron-oxidiser.

6. The bioleaching of chalcopyrite involves both the oxidation of ferrous-ion and sulphur compounds (Sand *et al.*, 1999). The contribution of sulphur oxidation to the measured oxygen and carbon dioxide utilization rates is still unknown. The bacterial rate of ferrous-ion utilization is estimated from the measured oxygen and carbon dioxide utilization rates during the batch bioleaching of the chalcopyrite concentrate (Boon *et al.*, 1995). This provides another limitation is measuring accurate bacterial ferrous-ion oxidation rates.

7. The model applied for *Leptospirillum ferrooxidans* has been shown to predict the region of iron turnover rates measured during the staged addition of a chalcopyrite to a batch bioleach, despite the above mentioned limitations.

Chapter 8: Conclusions and Recommendations

8 Conclusions and Recommendations

The broad objectives of this study was to test the applicability of the multiple sub-process mechanism in describing the bioleaching of chalcopyrite with mesophiles. In this mechanism the chalcopyrite mineral is chemically oxidised by ferric-ion to form ferrous-ion and sulphur/sulphur compounds, while the role of the bacteria is the bacterial oxidation of the ferrous-ion back to ferric form and the oxidation of sulphur/sulphur compounds via intermediates to sulphuric acid.

The specific objectives which were presented in Chapter 1 as, firstly, prescribing the state-of-the-art in the bioleaching of chalcopyrite with mesophiles by assessing the available literature, secondly, testing the applicability of the experimental and theoretical methodology developed by Boon (1996) in describing the kinetics of bioleaching of chalcopyrite with mesopiles and thirdly, testing the applicability of the Michaelis-Menten based bacterial ferrous-ion oxidation model for describing the bacterial ferrous-ion oxidation step during the bioleaching of chalcopyrite with mesophiles. The other objectives included establishing the kinetics of chemical ferric-ion leaching of chalcopyrite as a function of the redox potential or ferric/ferrous-ion ratio by reworking the available literature and attempting to predict the steady-state kinetic behaviour of the bioleaching of a predominantly chalcopyrite concentrate form separately determined chemical and bacterial kinetics.

This chapter describes the conclusions reached from the analysis of the review in Chapter Two, and the results in Chapters Six and Seven. It also presents recommendations for future work on the subject.

8.1 Establishing the state-of-the-art in the bioleaching and chemical leaching of chalcopyrite.

The rate chemical leaching of chalcopyrite is a function of the redox potential as was shown by reworking published literature (Kametani and Aoki, 1985). The rate passes through a maximum at low redox potentials (ferric/ferrous-ion ratio)and decreases with any further increase in redox potential (ferric/ferrous-ion ratio). The reasons for this decrease have not been established. This conclusion is consistent with that observed for other mineral sulphides like pyrite (May *et al.*, 1997) and arsenopyrite (Ruitenberg *et al.*, 1998), and with the reported faster rates of chalcopyrite chemical leaching at high ferrous-ion concentrations (Hiroyohi *et al.*, 2000). The build-up of product layers during the leaching of the chalcopyrite result in

diffusional barriers which passivate the rate of leaching. The exact nature of this layer is still unresolved.

The assessment of the literature on mesophilic chalcopyrite bioleaching has shown that the uncontrolled bacterial functioning of the iron oxidisers may be detrimental to the rate of leaching of chalcopyrite, because of their role in increasing and maintaining a high redox potential (ferric/ferrous-ion ratio) during mesophilic chalcopyrite bioleaching. They therefore have a tendency to poise the system at redox potentials which are higher than those required for optimal chemical leaching. This conclusion is also consistent with the multiple sub-process mechanism, since the mechanism assumes separate bacterial and chemical steps.

Further work should be focussed on trying to control the redox potential during bioleaching of chalcopyrite within the range which is optimal for chemical leaching of the mineral, ie, below 430 mV (SCE). (This value may depend on the characteristics of the chalcopyrite-concentrate). This could be done by varying the dissolved oxygen concentration within the system by controlling aeration.

8.2 The use of the theoretical and experimental methodology in testing the applicability of the multiple sub-process mechanism for chalcopyrite bioleaching.

The theoretical and experimental methodology developed by Boon (1996) in studying the kinetics of bioleaching of pyrite can be extended to studying the kinetics of bioleaching of chalcopyrite, since the bioleaching mechanism of both minerals are made up of a primary chemical leach to produce ferrous-ion, and bacterial ferrous-ion oxidation by iron oxidisers to regenerate ferric-ion. The presence of sulphur oxidisers in the case of the bioleaching of chalcopyrite complicates the measurement of bacterial specific kinetic parameters in that case. Despite this limitation, the trends of decreasing redox potentials and increasing specific oxygen utilisation rates with mineral additions during the stage additions of chalcopyrite concentrates to a batch bioleach is similar to that obtained for pyrite (Boon, 1996), and therefore provides convincing evidence of the existence of separate chemical leaching and bacterial ferrous-ion oxidation steps. This is consistent with the proposed multiple sub-process mechanism.

8.3 Applicability of bacterial ferrous-ion oxidation kinetic model

The kinetics of bacterial ferrous-ion oxidation, expressed in terms of the bacterial specific ferrous-ion utilisation rate, has been shown to increase with decreasing ferric/ferrous-ion ratio both during the bioleaching of pyrite and bacterial ferrous-ion oxidation. The kinetic expression is modelled according to a Michaelis-Menten/Monod based equation. During the staged additions of pyrite (Boon, 1996) the specific ferrous-ion utilisation rate was determined from the stochiometric relationship between the oxygen and carbon dioxide utilisation rates, while the bacterial growth rate was obtained from the carbon dioxide utilisation rate. This was possible because the oxygen and carbon dioxide consumed during the bioleaching of pyrite was due to bacterial ferrous-ion oxidation only. However, in the case of chalcopyrite, an additional sulphur oxidation step means that the measured oxygen and carbon dioxide utilisation rate encompasses the oxygen and carbon dioxide utilised for both sub-processes. This also means that the measured carbon dioxide utilisation rate during the bioleaching of chalcopyrite represents the growth rates of all the species present.

In order to establish the bacterial specific ferrous-ion or sulphur oxidation rates during the bioleaching of chalcopyrite, it is necessary to develop a method for determining the ratio of iron to sulphur oxidisers in the system, their respective growth rates and their yields on their respective substrates. This is one of the challenges facing the use of the bacterial specific ferrous-ion oxidation kinetics parameters in studying the kinetics of bioleaching in cultures containing both iron and sulphur oxidisers. In spite of this limitation, the variation in the measured specific oxygen utilisation rates with changes in the ferric/ferrous-ion ratio during the staged addition of chalcopyrite-concentrates to a batch bioleach, followed a similar trend to that predicted for the bacterial ferrous-ion oxidation by *Leptospirillum ferroxidans*. It can therefore be concluded that the Michaelis-Menten/Monod-based model describes the bacterial ferrous-ion oxidation step during the bioleaching of chalcopyrite with mesophiles.

Future work should attempt to selectively inhibit of either the ferrous-ion or sulphur oxidation sub-process during the bioleaching of chalcopyrite in an attempt to distinguish between the contributions of ferrous-ion and sulphur oxidation to the measured oxygen and carbon dioxide utilisation rate. A comparison of the rates measured whilst selectively inhibiting either one of the two sub-processes, with that measured without inhibition during the bioleaching of chalcopyrite, would establish the proportion of oxygen and carbon dioxide utilised for ferrous-ion oxidation and sulphur oxidation from the total measured rates.

8.4 Modeling the batch bioleaching of chalcopyrite

The existence of the multiple sub-process mechanism suggests that the overall bioleaching process can be reduced to three independent sub-processes, involving the chemical leaching of the mineral, bacterial ferrous-ion oxidation and bacterial sulphur oxidation. The kinetics of these sub-processes can be independently studied and then linked (if expressed as functions of a common basis) to predict the performance of batch bioleaching systems for a particular mineral and bacterial species as well as operating condition. This rationale has been illustrated by expressing both the independently determined chemical leach kinetics (written as the rate of ferrous-ion production) for a chalcopyrite concentrate, and the predicted bacterial ferrous-ion oxidation kinetics (written as the rate of bacterial ferrous-ion utilisation), as functions of the ferric/ferrous-ion ratio, for a particular mineral and bacterial concentration. The points if intersection of the chemical and bacterial curves represent the steady state between the chemical and bacterial rates of ferrous-ion production and consumption. The predicted intersection points and those calculated from the measured oxygen utilisation rates during the staged addition experiments are in close agreement.

The fate of the sulphur moiety was not considered. The presence of sulphide impurities in the mineral concentrate may have contributed to measured rates. Despite these limitations, this technique has already been shown to successfully predict the steady state performance of arsenopyrite concentrates during continuous bioleaching (Breed *et al.*, 1999) and does show the potential of being able to predict the performance of chalcopyrite batch bioleaching systems.

Future work should firstly, take into account the fate of sulphur oxidation, and secondly, attempt to predict the steady state at lower ferric/ferrous-ion ratios which are optimal for chemical leaching of chalcopyrite.

REFERENCES

1. Ammou-Chokroum, M., Sen, P.K., Fouques, F., 1981, " Electrooxidation of chalcopyrite in acid chloride medium , Kinetics , Stoichiometry and Reaction Mechanism " In: The Proceedings of the 13th International Mineral Processing Congress , Vol **13** , Laskowski, J., Elsevier BV© , New York, pp 759-809.

2. Almendras, E., Arriagada, F., Bustos, S., Herrera, L., Ruiz, P., Vargas, T., Wiertz, J., Badila-Ohlbaum R., 1987 "Surface transformation and electrochemical response of chalcopyrite in a bacterial leaching process," In: Biohydrometallurgical Processing: Proceedings of the International Symposium Warwick 1987, Ed. By P.R. Norris and D.P. Kelly, Science and Technology Letters, UK, pp. 259-271.

3. Ahonen, L., Hiltunen, P., Touvinen, O.H., 1986 "The role of pyrrhotite and pyrite in the bacterial leaching of chalcopyrite ores," In: Fundamental and Applied Biohydrometallurgy, Ed. By R.H. Lawrence, R.M.R. Branion, H.G. Ebner, Elsevier©, Amsterdam, pp. 13-22

4. Balaz, P., Kupka, D., Bastl, Z., Achimovicova, M., 1996 "Combined chemical and bacterial leaching of ultrafine ground chalcopyrite," Hydrometallurgy, 42, pp. 237-244.

5. Balaz., P., Spaldon, F., Luptakova, A., Paholic, G., Bastl, Z., Havlik, T., Briancin, J., 1991 "Feasibility of *Acidithiobacillus ferroxidans* bacterial leaching of chemically preleached chalcopyrite," International Journal of Mineral Processing, 32, pp. 133-146.

6. Bailey, A.D., 1993, "An Assessment of Oxygen Availability, Iron Build-up and the Relative Significance of Free and Attached Bacteria, as Factors Affecting Bio-oxidation of Refractory Gold-Bearing Sulphides at High Solids Concentrations" Ph.D. Thesis, University of Cape Town, Cape Town, South Africa

7. Bauer, J.P., Gibbs, H.L., Wadsworth, M.E., 1974, Patent No. RI-7823, United States Bureau of Mines.

8. Beckstead, L.W., Munoz, P.B., Sepulveda, J.L., Herbst, J.A., Miller, J.D., Olson, F.A., Wadsworth, M.E., 1976, "Acid ferric sulphate leaching of attritor-ground chalcopyrite concentrates," In: Extractive Metallurgy of Copper: Hydrometallurgy and Electrowining Vol II, Proceedings of the International Symposium on Copper Extraction and Refining, Vol. II, Ed by Yannopoulos, J.C., Agarwal, J.C., The Metallurgical Society of the AIME©, Nevada, USA.

9. Beckstead, L.W., Miller, J.D., 1977, "Ammonia oxidation leaching of chalcopyrite – reaction kinetics" Metallurgical Transactions B Vol **8B**, March, pp 19-29.

10. Berry, V.K., Murr, L.E., Hiskey, J.B., 1978, "Galvanic interaction between chalcopyrite and pyrite during bacterial leaching of low grade waste," Hydrometallurgy, 3, pp 309-326.

11. Bevilaqua-Mascarin, D., Garcia, O., Tuovinen, O.H., 1999 "Oxidative dissolution of chalcopyrite with *Acidithiobacillus ferroxidans*," In: Biohydrometallurgy and the Enviroment Toward the Mining of the 21st Century, Proceedings of the International

Biohydrometallurgy Symposium IBS-99, Ed. By R. Amils, A. Ballester, Elsevier© , Amsterdam, Part 9A, pp. 291-300

12. Bhattacharya, P., Sarkar, P., Mukherjea, R.N., 1990 "Reaction kinetics model for chalcopyrite bioleaching with *Acidithiobacillus ferrooxidans*," Enzyme Microb. Technol. Vol 12, pp873-876.

13. Blancarte-Zurita, M.A., Branion, R.M.R., Lawrence, R.W., 1987 "Microbiological leaching of chalcopyrite concentrates by *Thiobacillus ferrooxidans*. A comparative study of a conventional process and a catalysed process," In: Biohydrometallurgical Processing: Proceedings of the International Symposium Warwick 1987, Ed. By P.R. Norris and D.P. Kelly, Science and Technology Letters, UK, pp.273-285.

14. Blazy, P., Vestier, D., Cunin, P., Houot, R., 1976, "Copper Leaching from pyritic ores," In: Extractive Metallurgy of Copper: Hydrometallurgy and Electrowining Vol II, Proceedings of the International Symposium on Copper Extraction and Refining, Vol. II, Ed by Yannopoulos, J.C., Agarwal, J.C., The Metallurgical Society of the AIME©, Nevada, USA, Chapter 38

15. Blancarte-Zurita, M.A., Branion, R.M.R., 1986 "Particle size effects in microbial leaching of sulphide mineral concentrates by *Acidithiobacillus ferroxidans*," Biotechnology Bioengineering, 28, 75-755.

16. Blazquez, M.L., Alvarez, A., Ballester, A., Gonzalez, F., Munoz, J.A., 1999 "Bioleaching behaviour of chalcopyrite in the presence of silver at 35 and 68 °C," In: Biohydrometallurgy and the Enviroment Toward the Mining of the 21st Century, Proceedings of the International Biohydrometallurgy Symposium IBS-99, Ed. By R. Amils, A. Ballester, Elsevier© , Amsterdam, Part 9A, pp. 137-147.

17. Boon, M., Hansford, G.S., Heijnen, J.J., 1995, "The role of bacterial ferrous-ion oxidation in the bio-oxidation of pyrite," In: Biohydrometallurgical Processing: Proceedings of the International Biohydrometallurgy Symposium IBS-95, Ed. By T. Vargas, C.A. Jerez, J.V. Wiertz, H. Toledo, University of Chile, Santiago, Vol. **1**, pp. 153-163.

18. Boon, M., 1996, "Theoretical and Experimental Methods in the Modelling of Bio-oxidation of Sulphide Minerals" Ph.D. Thesis, Delft University of Technology, Delft, Netherlands

19. Braddock, J.F., Luong, H.V., Brown, E.J., 1984, "Growth kinetics of *Acidithiobacillus ferrooxidans* isolated from arsenic mine drainage," Applied Environmental Microbiology Vol. **48,** No. 1, pp.48-55.

20. Brierley, C.L., Brierley, J.A., 1978 "Microbian leaching of chalcopyrite at ambient and elevated temperatures," In: Metallurgical Applications of Bacterial Leaching and Related Microbiological Phenomena, Ed. By L.E. Murr, A.E. Torma, J.A. Breirley, Academic Press©, New York, pp. 447-490.

21. Brierley, C.L., Briggs, A.P.W., 1997 "Minerals Biooxidation/Bioleaching: Guide to Developing an Economically Viable Process," In: Proceedings of After the Discovery Short Course, Prospectors and Developers Association of Canada Workshop, Ontario, Canada, pp. 26-26

22. Brierley, C.L., Brierley, J.A., 1999 "Copper bioleaching: state-of-the-art," In Proceedings of Copper 99/Combre 99 Fourth International Conference Pheonix USA.

23. Brierley, C.L., Brierley, J.A., 1999 "Present and future commercial applications of biohydrometallurgy," In: Biohydrometallurgy and the Enviroment Toward the Mining of the 21st Century, Proceedings of the International Biohydrometallurgy Symposium IBS-99, Ed. By R. Amils, A. Ballester, Elsevier©, Amsterdam, Part 9A, pp. 81-89.

24. Biegler, T., Horne, M.D., 1985, "The electrochemistry of the surface oxidation of chalcopyrite," Journal of the Electrochemical Society: Electrochemical Science and Technology, June, pp 1363-1369.

25. Biwas, A.K., Davenport, W.G., 1994, "Hydrometallurgical Copper Extraction: Introduction and Leaching," In Extractive Metallurgy of Copper, 3rd Ed, Ed by Biswas, A.K., Davenport, W.G., Pergamon Press©, UK, Chapter 18.

26. Bosecker K., Toram, A.E., Brierley, A., 1979 "Microbiological leaching of a chalcopyrite concentrate and the influence of hydrostatic pressure on the activity of *Acidithiobacillus ferrooxidans*," European Journal of Applied Microbiology and Biotechnology, 7, pp. 85-90.

27. Buckley, A.N., Woods, R., 1984, "An X-Ray Photoelectron Spectroscopic study of the oxidation of chalcopyrite," Australian Journal of Chemistry, **37**, pp 2403-2413.

28. Braithwaite, J.W., Wadsworth M.E., 1976 "Oxidation of chalcopyrite under simulated conditions of deep solution mining," In: Extractive Metallurgy of Copper: Hydrometallurgy and Electrowining Vol II, Proceedings of the International Symposium on Copper Extraction and Refining, Vol. II, Ed by Yannopoulos, J.C., Agarwal, J.C., The Metallurgical Society of the AIME©, Nevada, USA, Chapter 39.

29. Breed, A.W., Harrison, S.T.L., Hansford, G.S., 1997, "A preliminary investigation of the ferric leaching of a pyrite/arsenopyrite flotation concentrate," Minerals Engineering Vol. 10, No. 9, pp 1023-1030.

30. Breed, A.W., Hansford, G.S., 1999, "Modeling Continuous bioleach reactors," Biotechnology and Bioengineering Vol. **64**, No. 6, pp. 671-677.

31. Breed, A.W., 2000, "Studies on the Mechanism and Kinetics of Bioleaching with Special Reference to the Bioleaching of Refractory Gold-bearing Arsenopyrite/pyrite Concentrates" Ph.D. Thesis, University of Cape Town, Cape Town, South Africa

32. Breed, A.W., Dempers, C.J.N., Searby, G.E., Gardner, M.N., Rawlings, D.E., Hansford, G.S., 1999(a), "The effect of temperature on the continuous ferrous-ion oxidation kinetics of a predominantly *Leptospirillum ferrooxidans* culture," Biotechnology and Bioengineering Vol. **65**, No. 1, pp. 44-53.

33. Breed, A.W., Hansford, G.S., 1999(b), "The effect of pH on the ferrous-ion oxidation kinetics of *Leptospirillum ferrooxidans* in continuous culture," The Biochemical Engineering Journal Vol. **3**, No. 1, pp 193-201.

34. Briceno, H., Rossi, M.C., 1988 "Bacterial leaching of copper concentrates: A preliminary feasibility study," In: Proceedings of Copper 87, Ed. By Cooper, W. Charles, E. Lago, E Gustavo, R. Ugarte, C. Guilermo, University of Chile, Santiago, Vol 3, pp.131-147.

35. Bruynesteyn, A., Duncan, D.W., 1974 "Effect of particle size on the microbiological leaching of a chalcopyrite bearing ore," In: Proceedings of the Solution Mining Symposium 1974, Chapter 22, pp324-337.

36. Corbett, C.M., Ingledew, W.J., 1987 "Is $Fe^{3+/2+}$ cycling an intermediate in sulphur oxidation by Fe^{2+} grown *Acidithiobacillus ferrooxidans*?," FEMS Microbiology Letters, 41, pp. 1-6.

37. Crundwell, F.K., 1987, "Kinetics and Mechanism of the oxidative dissolution of a zinc sulphide concentrate in ferric sulphate solutions," Hydrometallurgy, **19**, pp 227-242.

38. Crundwell, F.K., 1988, "The influence of electronic structure of solids on the anodic dissolution and leaching of semiconducting sulphide minerals," Hydrometallurgy, **21**, pp 155-190.

39. Chang, Y.C., Myerson, A.S., 1982 "Growth models of the continuous bacterial leaching of iron pyrite by Acidithiobacillus ferrooxidans," Biotechnology and Bioengineering Vol. 24, pp.889-902.

40. Das, A., Hanumantha Rao, K., Sharma, P., Natarjan, K.A., Forssberg, K.S.E., 1999 "Surface chemical and adsorption studies using *Acidithiobacillus ferroxidans* with reference to bacterial adhesion to sulphide minerals," In: Biohydrometallurgy and the Environment Toward the Mining of the 21st Century, Proceedings of the International Biohydrometallurgy Symposium IBS-99, Ed. By R. Amils, A. Ballester, Elsevier© , Amsterdam, Part 9A, pp.697-707.

41. Dogan, M.Z., Yuce, A.E., Girgin, S., 1999 "Leaching of Turkish copper ores with *Acidithiobacillus ferroxidans*, "In: Biohydrometallurgy and the Environment Toward the Mining of the 21st Century, Proceedings of the International Biohydrometallurgy Symposium IBS-99, Ed. By R. Amils, A. Ballester, Elsevier© , Amsterdam, Part 9A, pp.257-262.

42. Devasia, P., Natarajan, K.A., Rao, G.R., 1996 "Role of bacterial growth conditions and adhesion in the bioleaching of chalcopyrite by *Acidithiobacillus ferroxidans*," Miner, Metall. Process., 13, pp. 82-86.

43. Dew, D.W., Van Buuren, C., McEwan, K., Bowker, C., 1999 "Bioleaching of base metal sulphide concentrates: A comparison of mesophile and thermophile bacterial cultures," In: Biohydrometallurgy and the Enviroment Toward the Mining of the 21st Century, Proceedings of the International Biohydrometallurgy Symposium IBS-99, Ed. By R. Amils, A. Ballester, Elsevier© , Amsterdam, Part 9A, pp. 229-238.

44. Driessens, Y.P.M., Fowler, T.A., Crundwell, F.K., 1999, "A comparison of the bacterial and chemical leaching of sphalerite at the same solution conditions," In: Biohydrometallurgy and the Environment Toward the Mining of the 21st Century, Proceedings of the International Biohydrometallurgy Symposium IBS '99, R. Amils, A. Ballester, Elsevier©, Amsterdam, Part A, pp.201-208.

45. Dutrizac, J.E., MacDonald, R.J.C., 1974, "Ferric-ion as a leaching medium," Minerals Science Engineering, 6, pp 59-99.

46. Dutrizac, J.E., 1978, "The kinetics of dissolution of chalcopyrite in ferric ion media," Metallurgical Transactions B Vol **9B**, 1978, pp431-439.

47. Dutrizac, J.E., 1981, "The dissolution of chalcopyrite in ferric sulphate and ferric chloride media," Metallurgical Transactions B Vol **12B**, June, pp371-378.

48. Dutrizac, J.E., 1982, "Ferric ion leaching of chalcopyrite from different localities, " Metallurgical Transactions B Vol **13B**, September, pp303-309.

49. Dutrizac, J.E., 1989, "Elemental sulphur formation during the ferric sulphate leaching of chalcopyrite," Canadian Metallurgical Quarterly Vol **28**, pp 337-344.

50. Dutrizac, J.E., 1992, "The leaching of sulphide minerals in chloride media, " Hydrometallurgy, **29**, pp 1-45.

51. Dry, M.J., 1984 "The Kinetics of Low Grade Matte in Ferric Sulphate Solution," PhD Thesis, University of the Witwatersrand, Johannesburg, South Africa

52. Ehrlich, H.L., Fox, S.I., 1967 "Environmental effects on bacterial copper extraction from low-grade copper-sulphide ores," Biotechnology and Bioengineering Vol. IX, pp.471-485.

53. Eadington., P., 1977, "Study of oxidation layers on the surfaces of chalcopyrite by use of Auger electron spectroscopy," Transactions of the Institution of Mining and Metallurgy Sec C: Mineral Processing and Extractive Metallurgy, **86**, Dec., pp C186 – C189.

54. Espejo, P.T., Ruiz P., 1987 "Growth of free and attached *Acidithiobacillus ferrooxidans* in ore suspension," Biotechnology and Bioengineering Vol. XXX, pp. 586-592.

55. Furamera, T.A., 2000, "A study of the ferric leaching of chalcopyrite under controlled solution potential," M.Sc. Thesis, Department of Chemical Engineering, University of Cape Town, Cape Town, South Africa.

56. Gomez, C., Figueroa, M., Munoz, J., Blazquez, M.L., Balester, A., 1996, " Electrochemistry of chalcopyrite," Hydrometallurgy, **43**, pp 331-344.

57. Hackl, R.P., Dreisinger, D.B., Peters, King, J.A., 1995, "Passivation of chalcopyrite during oxidative leaching in sulphate media," Hydrometallurgy, **39**, pp 25-48.

58. Hansford, G.S., 1997, "Recent developments in modelling the kinetics of bioleaching," In: Biomining: Theory, Microbes and Industrial Processes, Ed by D.E. Rawlings, ©Springer-Verlag and Landes Bioscience, Berlin, Ch. 8, pp. 153-175.

59. Hansford, G.H., Furamera, T.A., Jaffer, M.A., Searby, G.E., "Preliminary results of an investigation on the mechanism of bioleaching of chalcopyrite," In: ALTA COPPER 1999 Copper Sulphides Symposium and Copper Hydrometallurgy Forum, Technical Proceedings of the 5th Annual Forum on Copper Sulphides and Copper Hydrometallurgy, ALTA Metallurgical Services, Melbourne, Australia.

60. Hirato, T., Kinoshita, M., Awakura., Y., Majima, H., 1987, "The leaching of chalcopyrite with ferric sulphate, " Metallurgical Transactions B Vol **18B**, September, pp 489-496.

61. Hirato, T., Kinoshita, M., Awakura., Y., Majima, H., 1986, "The leaching of chalcopyrite with ferric chloride, " Metallurgical Transactions B Vol **17B**, March, pp 19-28.

62. Hiroyoshi, N., Hirato, M., Hirajima, T., Tsunekawa, M., 1997, "A case of ferrous-sulphate addition enhancing chalcopyrite leaching," Hydrometallurgy, 47, pp. 37-45

63. Hiroyoshi, N., Hirato, M., Hirajima, T., Tsunekawa, M., 1998, "Ferrous-promoted chalcopyrite leaching-Ferric formation and its effects on the leaching," Journal of the Mining and Materials Processing Institute of Japan Vol. 114, No. 11, pp. 795-800.

64. Hiroyoshi, N., Hirato, M., Hirajima, T., Tsunekawa, M., 1999, "Inhibitory effect of iron-oxidising bacteria on ferrous-promoted chalcopyrite leaching," Biotechnology and Bioengineering Vol. 64, No. 4, August pp. 478-483.

65. Hiroyoshi, N., Hirato, M., Hirajima, T., Tsunekawa, M., 2000, "A model for ferrous-promoted chalcopyrite leaching," Hydrometallurgy, 57, pp. 31-38.

66. Hiskey, J.B., 1993, "Chalcopyrite semiconductor electrochemistry and dissolution," In: Extractive Metallurgy of Copper, Nickel and Cobalt Vol I: Fundamental Aspects, Proceedings of the Paul E Queneau International Symposium, Ed by Reddy, R.G., Weizenbach, R.N., The Minerals , Metals and Materials Society©, Denver, USA

67. Holliday, R.I., Richmond, W.R., 1990, "An electrochemical study of the oxidation of chalcopyrite in acidic solution," Journal of Electroanalytical Chemistry, **288**, pp 83-98

68. Inledew, W.J., 1982 "*Acidithiobacillus ferroxidans:* The bioengergetics of an acidophilic chemolithotroph" Biochimica et Biophysica Acta, 683, pp. 89-177.

69. Jones, C.A., and Kelly, D.P., 1983, "Growth of *Thiobaciullus ferrooxidans* on ferrous-ion in chemostat culture: influence of product and substrate inhibition," Journal of Chemical Technology and Biotechnology Vol. **33B**, No. 4, pp.241-261.

70. Jordan, M.A., Barr, D.W., Phillips, C.V., 1993 "Iron and sulphur speciation and cell surface hydrophobicity during bacterial oxidation of a complex copper concentrate," Minerals Engineering Vol. 6, No. 8-10, pp. 1001-1011.

71. Jyothi, N., Sudha, K.N., Nataragan K.A., 1989 "Electrochemical aspects of selective bioleaching of sphalerite and chalcopyrite from mixed sulphides," International Journal of Mineral Processing, 27, pp. 189-203.

72. Jaffer, M.A., 1999, "The Effect of Redox Potential on the Rate of Chalcopyrite Oxidation: Literature Predictions," Research report prepared for the Council of Mineral Technology of South Africa, Ed by Hansford, G.S., Gold Fields Mineral Bioprocessing Laboratory, Department of Chemical Engineering, University of Cape Town.

73. Jones, D.L., and Peters E., 1976, "The leaching of chalcopyrite with ferric sulphate and ferric chloride," In: Extractive Metallurgy of Copper: Hydrometallurgy and Electrowining Vol II, Proceedings of the International Symposium on Copper Extraction and Refining, Vol. II, Ed by Yannopoulos, J.C., Agarwal, J.C., The Metallurgical Society of the AIME©, Nevada, USA, Chapter 32

74. Johansson, C., Shrader, V., Suissa, K., Adutwum, K., Kohr, W., 1999 "Use of GEOCOAT™ Process for the reovery of copper from chalcopyrite," In: Biohydrometallurgy and the Enviroment Toward the Mining of the 21st Century, Proceedings of the International Biohydrometallurgy Symposium IBS-99, Ed. By R. Amils, A. Ballester, Elsevier©, Amsterdam, Part 9A, pp.

75. Le Roux, N.W., Wakerley, D.S., 1987 "Leaching of chalcopyrite ($CuFeS_2$) at 70 °C using *Sulfolobus*," In: Biohydrometallurgical Processing: Proceedings of the International Symposium Warwick 1987, Ed. By P.R. Norris and D.P. Kelly, Science and Technology Letters, UK, pp. 305-317.

76. Lawson, E.N., Nicholas, C.N., Pellat, H, 1995, "The toxic effects of chloride ions on *Acidithiobacillus ferrooxidans*," In: Biohydrometalurgical Processing I, Proceedings of the International Biohydrometallurgy Symposium IBS '95, T. Vargas, C.A. Jerez, J.V. Wiertz, H., Toledo, Universidad de Chile, Santiago, Vol I, pp.201-208

77. Kingma, J.G., Silva, M, 1980 "Growth of iron-oxidising *Thiobacilli* in the presence of chalcopyrite and galena," Applied and Environmental Microbiology Vol. 39, No. 2, pp 635-641.

78. Kawakami K., Sato J., Kusunoke KA, Kusakabe K and S Morooka, 1988 "Kinetic study of oxidation of pyrite slurry by ferric chloride," Int. J. of Min. Proc., 27, pp189-203

79. Kametani, H., and Aoki, A., 1985, "Effect of suspension potential on the oxidation rate of copper concentrate in sulphuric acid solution," Metallurgical Transactions B Vol. 16B, Dec., pp 695-705

80. Klauber, C., Parker A., van Bronswijk, W., Watling, H., 2000, "Sulphur speciation of leached chalcopyrite surfaces determined by X-ray photoelectron spectroscopy," Submitted to International Journal of Mineral Processing, January

81. Khinvasara, N.J., Agate A.D., 1987 "Bioreactor leaching of chalcopyrite concentrate from Mosaboni, India,"," In: Biohydrometallurgical Processing: Proceedings of the International Symposium Warwick 1987, Ed. By P.R. Norris and D.P. Kelly, Science and Technology Letters, UK, pp. 297-303.

82. Konashi, Y., Asai, S., Katoh, H., 1990, "Bacterial dissolution of pyrite by *Acidithiobacillus ferrooxidans*," Bioprocess Engineering **5**, pp.231-237.

83. Lawson, E.N., Nicholas, C.N., Pellat, H, 1995, "The toxic effects of chloride ions on *Acidithiobacillus ferrooxidans*," In: Biohydrometalurgical Processing I, Proceedings of the International Biohydrometallurgy Symposium IBS '95, T. Vargas, C.A. Jerez, J.V. Wiertz, H., Toledo, Universidad de Chile, Santiago, Vol I, pp.201-208

84. Linge, H.G., 1976, "A study of chalcopyrite dissolution in acidic ferric nitrate by potentometric titration," Hydrometallurgy, 2, pp 51-64.

85. Lu, Z.Y., Jeffrey, M.I., Lawson, F., 2000, "An electrochemical study of the effect of chloride ions on the dissolution of chalcopyrite in acidic solutions," Hydrometallurgy, 56, pp. 145-155.

86. Lu, Z.Y., Jeffrey, M.I., Lawson, F., 2000, "The effect of chloride ions on the dissolution of chalcopyrite in acidic solutions," Hydrometallurgy, 56, pp. 189-202.

87. Mehta, A.P., Murr, L.E., 1982 "Kinetic study of sulphide leaching by galvanic interaction between chalcopyrite, sphalerite and pyrite in the presence of *T.Ferrooxidans* (30 °C) and a thermophilic micro-organism," Biotechnology and Bioengineering, 24, pp. 919-940

88. Mehta, A.P., Murr, L.E., 1983 "Fundamental studies of the contribution of galvanic interaction to acid bacterial leaching of mixed sulphide minerals," Hydrometallurgy, 9, pp.235-256.

89. May, N., Ralph, D.E., Hansford, G.S., 1997, "Dynamic redox potential measurement for determining the ferric leaching kinetics of pyrite," Minerals Engineering Vol. 10, No. 11, pp 1279-1290

90. Murr, L.E., 1980 "Theory and practice of copper sulphide leaching in dumps an in-situ," Mineral Science Engineering Vol 12, No. 3, pp121-189.

91. Murr, L.E., Berry, V.K., 1976 "An electron microscope study of bacterial attachment to chalcopyrite: microstructural aspects of leaching," In: Extractive Metallurgy of Copper: Hydrometallurgy and Electrowining Vol II, Proceedings of the International Symposium on Copper Extraction and Refining, Vol. II, Ed by Yannopoulos, J.C., Agarwal, J.C., The Metallurgical Society of the AIME©, Nevada, USA, Chapter 34, pp. 671-689.

92. McMillan, R.S., MacKinnon, D.J., Dutrizac, J.E., 1982, "Anodic dissolution of n-type and p-type $CuFeS_2$," Journal of Applied Electrochemistry, **12**, pp 743-757.

93. Morrison, S.R., 1980, "Electrochemistry at Semiconductor and Oxidised Metal Electrodes," Plenum Press©, New York

94. Munoz, P.B., Miller, J.D., Wadsworth, M.E., 1979, "Reaction mechanism for the acid ferric sulphate leaching of chalcopyrite," Metallurgical Transactions B Vol **10B**, June, pp 149-158.

95. Murr, L.E., Hiskey, J.B., 1981, "Kinetic effects of particle size and crystal dislocation density on dichromate leaching of chalcopyrite," Metallurgical Transactions B Vol **12B**, pp 255-267.

96. Miller, P.C., Rhodes, M.K., Winby, R., Pinches, A., Van Staden, P.J. 1999 "Commercialization of bioleaching for base-metal extraction," Minerals and Metallurgical Processing Vol. 16, No. 4, pp.42-50.

97. Natarajan, K.A., 1992, "Electroleaching of base metal sulphides," Metallurgical Transactions B, **23B**, pp 5-11.

98. Nagpal, S., Dahlstrom, D., Oolman, T., 1993 "Effect of carbon dioxide concentration on the bioleaching of a pyrite-arsenopyrite ore concentrate," Biotechnology and Bioengineering Vol. 41, pp.459-464.

99. Nemati, M., Harrison, S.T.L., Webb, C., Hansford G.S., 1998, "Biological oxidation of ferrous-sulphate by *Acidithiobacillus ferrooxidans*: A Review on the Kinetic Aspects," Biochemical Engineering Journal Vol. **1**, pp.171-190.

100. Nemati, M., Webb, C., 1997, "A kinetic model for biological oxidation of ferrous-ion by *Acidithiobacillus ferrooxidans*," Biotechnology and Bioengineering Vol. **53**, No. 5., pp. 478-486.

101. Palencia, I., Garcia, M.J., Alba, J., Carranza, F., 1987 "Effects of pH and high density cultures on the silver catalyzed leaching of chalcopyrite," In: Biohydrometallurgical Processing: Proceedings of the International Symposium Warwick 1987, Ed. By P.R. Norris and D.P. Kelly, Science and Technology Letters, UK, pp. 287-296..

102. Parker, A.J., Paul, R.L., Power, G.P., 1981, "Electrochemical aspects of leaching copper from chalcopyrite in ferric and cupric salt solutions," Australian Journal of Chemistry, **34**, pp 13-34.

103. Parker, A.J., Paul, R.L., G.P., Power, 1981, "Electrooxidation of the oxidative leaching of copper from chalcopyrite," Journal of Electroanalytical Chemistry, **118**, pp 305-316.

104. Pizarro, J., Jedlicki, E., Orellana, O., Romero, J., Espejo, R.T., 1996 "Bacterial populations in samples of bioleached copper ore as revealed by analysis of DNA obtained before and after cultivation," Applied and Environmental Microbiology Vol. 62, No. 4, pp.1323-1328.

105. Pinches, A., Chapman, J.T., Te Riele, W.A..M., Van Staden, M, 1988 "The performance of bacterial leach reactors for the pre-oxidation of refractory gold-bearing sulphide concentrates," In: Biohydrometallurgical Processing: Proceedings of the International Symposium Warwick 1987, Ed. By P.R. Norris and D.P. Kelly, Science and Technology Letters, UK, pp. 329-344.

106. Pirt, S.J., (ed.) 1975, "Principles of microbe and cell cultivation," John Wiley and Sons Inc.©, New york

107. Pronk, J.T., De Bruyn, J.C., Kuenen, J.G., 1992 Anaerobic growth of Acidithiobacillus ferroxidans," Applied and Environmental Microbiology Vol. 58, No. 7, pp 2227-2230

108. Rawlings, D.E., (ed.) 1997, "Biomining: theory, microbes and industrial process," Springer-Verlag and Landes Bioscience©, Berlin

109. Rawlings, D.E., Coram, N.J., Gardner, M.N., Deane, S.M., 1999(a), "*Acidithiobacillus caldus* and *Leptospirillum ferrooxidans* are widely distributed in continuous flow biooxidation tanks used to treat a variety of metal containing ores and concentrates," In: Biohydrometallurgy and the Enviroment Toward the Mining of the 21st Century, Proceedings of the International Biohydrometallurgy Symposium IBS-99, Ed. By R. Amils, A. Ballester, Elsevier© , Amsterdam, Part A, pp. 777-786.

110. Rhodes, M.K., Deeplaul, V., Van Staden, P.J, "Bacterial oxidation of Mt Lylle concentrates," In: ALTA COPPER 1999 Copper Sulphides Symposium and Copper Hydrometallurgy Forum, Technical Proceedings of the 5th Annual Forum on Copper Sulphides and Copper Hydrometallurgy, ALTA Metallurgical Services, Melbourne, Australia.

111. Roels, J.A., 1983 "Energetics and Kinetics in Biotechnology," Elsevier Biomedical Press©, Amsterdam

112. Rossi, G., (ed.) 1990, "Biohydrometallurgy," McGraw-Hill Book Company GmbH©, Hamburg

113. Ruitenberg, R., Hansford, G.S., Reuter, M.A., Breed, A.W., 1999, "The ferric leaching kinetics of arsenopyrite," Hydrometallurgy, **52**, pp. 37-53.

114. Sato, H., Nakazawa, H., Kudo, Y., 2000 "Effect of silver chloride on the bioleaching of chalcopyrite concentrate," International Journal of Mineral Processing, 59, pp. 17-24.

115. Sakaguchi, H., Silver, M., 1976 "Microbiological leaching of a chalcopyrite concentrate by *Acidithiobacillus ferrooxidans*," Biotechnology and Bioengineering Vol. XVIII, pp. 1091-1101.

116. Sapieszko, R.S., Patel, R.C., Matijevic, E., 1977, Journal of Physical Chemistry Vol **81**, pp 1061

117. Saxena, N.N., Mandre, N.R., 1992, "Mixed control kinetics of copper dissolution for copper ore using ferric chloride," Hydrometallurgy, **28**, pg 111-117

118. Schnell, H.A., 1997 "Bioleaching of Copper," In: Biomining: Theory, Microbes and Industrial processes, Ed. By Rawlings, D.E., Springer-Verlag and Landes Bioscience©, Berlin, pp.21-42.

119. Suzuki, I., Takesue, T.L., Yuthasastrakosal, T.D., Oh, J.K., "Ferrous-ion and sulphur oxidation and ferric-ion reduction activities of *Acidithiobacillus ferrooxidans* are affected by growth on ferrous-ion, sulphur, or a sulphide ore, "Applied and environmental Microbiology, 56, pp1620-1626.

120. Schippers, A., Sand, W., 1999, "Bacterial leaching of metal sulphides proceeds by two indirect mechanisms via thiosulphate or via polysulphides and sulphur," Applied Environmental Microbiology, **65**, pp 319-321.

121. Shrihari, Kumar, R., Gandhi, K.S., Natarajan, K.A., 1991 "Role of cell attachment in leaching of chalcoyrite mineral by *Acidithiobacillus ferroxidans*," Appl. Microbiol. Biotechnol., 36, pp. 278-282.

122. Schlitt, W.J., 1999, "Hydrometallurgical treatment of copper ore," The Journal of the South African Institute of Mining and Metallurgy, March/April, pp 75-92.

123. Sullivan, J.D., 1933, Transactions of the AIME Vol. **511**, pp 106.

124. Third, K.A., Cord-Ruwish R., Watling H.R., 2000 "The role of iron-oxidising bacteria in the stimulation or inhibition of chalcopyrite bioleaching," Hydrometallurgy, 57, pp.225-233.

125. Tiwari, B.L., Kolbe, J., Hayden, J.W., 1980, "Leaching of high solids, attritor ground chalcopyrite concentrate by in situ generated ferric sulphate solution," Metallurgical Transactions B Vol **11B**, March, pp 89- 93.

126. Tkacova, K., Balaz, P., 1988, "Stuctural and temperature sensitivity of leaching of chalcopyrite with iron(III) sulphate," Hydrometallurgy, **12** , pp 103-112.

127. Toro, L., Di Cesara, S., Paponette B., Lepidi, A., 1989 "Biochemical and chemical events in copper solubalization from a chalcopyrite concentrate by *Acidithiobacillus*

ferrooxidans in batch culture," International Journal of Mineral Processing, 26, pp. 153-162.

128. Touvinen, O.H., Kelley, B.C., Groudev, S.N., 1991 "Mixed cultures in biological processes and mineral biotechnology," In: Mixed Cultures in Biotechnology, Ed. By J.G. Zeikus, E.A. Johnson, McGraw Hill Inc., New York, Chapter 13, pp.373-427.

129. Warren, G.W., Wadsworth, M.E., El-Raghy, S.M., 1982, "Passive and transpassive anodic behaviour of chalcopyrite in acidic solutions," Metallurgical Transactions B Vol **13B**, Dec., pp 571-579.

130. Warren, G.W., Wadsworth, M.E., 1984, "The electrochemical oxidation of chalcopyrite in ammoniacal solutions," Metallurgical Transactions B Vol **15B** , June, pp 288-297.

131. Vazquez, M., Espejo, R.T., 1997, "Chemolithotrophic bacteria in copper ores leached at high sulphuric acid concentration," Applied and Environmental Microbiology Vol. 63, No. 1, pp. 332-334.

132. Van Scherpenzeel, D.A., Boon, M., Ras, C., Hansford, G.S., Heijnen, J.J., 1998, "The kinetics of ferrous-ion oxidation by *Leptospirillum*-like bacteria in continuous cultures, " Biotechnol. Prog. Vol. **14**, pp. 425-433.

133. Van Staden, P.J., 1998 "The Mintek/Bactech Copper Bioleach Process," In: ALTA COPPER 1999 Copper Sulphides Symposium and Copper Hydrometallurgy Forum, Technical Proceedings of the 5th Annual Forum on Copper Sulphides and Copper Hydrometallurgy, ALTA Metallurgical Services, Melbourne, Australia

134. Van Aswegen, P.C., 1993, "Commissioning and operation of biooxidation plants for the treatment of refractory gold ores," In: Hydrometallurgy Fundamentals, Technology and Innovations: Proceedings of Milton E Wadsworth (IV) International Symposium Hydrometallurgy, AIME, Utah, USA

NOMENCLATURE

Symbol	Description	Units
$[Fe^{2+}]$	Ferrous-ion concentration	$Moll^{-1}$
$[Fe^{3+}]$	Ferric-ion concentration	$Moll^{-1}$
$[Fe]^{tot}$	Total-iron concentration	$Moll^{-1}$
$[Fe^{2+}]_T$	Threshold Ferrous-ion concentration	$Moll^{-1}$
$[Fe^{3+}]_T$	Threshold Ferric-ion concentration	$Moll^{-1}$
C_s	Substrate concentration	$Moll^{-1}$
C_p	Product concentration	$Moll^{-1}$
$\gamma_{Fe^{2+}}$	Activity of ferrous-ion	
$\gamma_{Fe^{3+}}$	Activity of ferric-ion	
E_h	Solution redox potential measured against SHE	V
E_o`	Standard Redox potential	V
E	Solution redox potential	V
μ	Specific growth rate of bacteria	h^{-1}
q_s	Bacterial specific substrate utilisation rate	$Mol.molC^{-1}.h^{-1}$
$q_{Fe^{2+}}$	Bacterial specific ferrous-ion utilization rate	$MolFe^{2+}.molC^{-1}.h^{-1}$
$q_{Fe^{2+}}^{max}$	Maximum bacterial specific ferrous-ion utilization rate	$MolFe^{2+}.molC^{-1}.h^{-1}$
$q_{O_2}^{max}$	Maximum bacterial specific oxygen utilization rate	$MolO_2.molC^{-1}.h^{-1}$
q_{O_2}	Bacterial specific oxygen utilization rate	$MolO_2.molC^{-1}.h^{-1}$
q_{CO_2}	Bacterial specific carbon dioxide utilization rate	$MolCO_2.molC^{-1}.h^{-1}$
$-r_s$	Rate of substrate utilisation	$Mol.l^{-1}.h^{-1}$
$r_{Fe^{2+}}^{chem}$	Chemical rate of ferrous-ion production	$Mol.l^{-1}.h^{-1}$
$r_{Fe^{2+}}^{bac}$	Bacterial rate of ferrous-ion consumption	$Mol.l^{-1}.h^{-1}$
$r_{Fe^{2+}}$	Rate of ferrous-ion production	$Mol.l^{-1}.h^{-1}$
$r_{Fe^{3+}}$	Rate of ferric-ion production	$Mol.l^{-1}.h^{-1}$
r_{H^+}	Rate of proton production	$Mol.l^{-1}.h^{-1}$

r_{H_2O}	Rate of water production	$Mol.l^{-1}.h^{-1}$
$r_{NH_4^+}$	Rate of ammonium production	$Mol.l^{-1}.h^{-1}$
$r_{SO_4^{2-}}$	Rate of sulphate production	$Mol.l^{-1}.h^{-1}$
r_{S^0}	Rate of sulphur production	$Mol.l^{-1}.h^{-1}$
$r^{bac}_{Fe^{2+}}$	Rate of bacterial ferrous-ion consumption	$MolFe^{2+}.l^{-1}.h^{-1}$
$-r_{O_2}$	Oxygen utilization rate	$MolO_2.l^{-1}.h^{-1}$
$-r_{CO_2}$	Carbon Dioxide utilization rate	$MolCO_2.l^{-1}.h^{-1}$
r_x	Bacterial growth rate	$MolC.l^{-1}.h^{-1}$
$-r^{Fe^{2+}}_{O_2}$	Oxygen utilization rate for bacterial ferrous-ion oxidation	$Mol.l^{-1}.h^{-1}$
$-r^{S^0}_{O_2}$	Oxygen utilization rate for bacterial sulphur oxidation	$Mol.l^{-1}.h^{-1}$
$-r^{Fe^{2+}}_{CO_2}$	Carbon dioxide utilization rate for bacterial ferrous-ion oxidation	$Mol.l^{-1}.h^{-1}$
$-r^{S^0}_{CO_2}$	Carbon dioxide utilization rate for bacterial sulphur oxidation	$Mol.l^{-1}.h^{-1}$
$-r^{Total}_{O_2}$	Total measured oxygen utilization rate	$Mol.l^{-1}.h^{-1}$
$-r^{Total}_{CO_2}$	Total measured carbon dioxide utilization rate	$Mol.l^{-1}.h^{-1}$
$-r^{Total}_{x}$	Total measured bacterial growth rate	$Mol.l^{-1}.h^{-1}$
C_x	Bacterial concentration	$MolC.l^{-1}$
$C_x(t)$	Bacterial concentration at time t	$MolC.l^{-1}$
$C_x(0)$	Initial bacterial concentration	$MolC.l^{-1}$
$K_{Fe^{2+}}$	Kinetic constant in bacterial ferrous-ion oxidation model	$MolFe^{2+}.l^{-1}$
K	Kinetic constant in bacterial ferrous-ion oxidation model written for specific oxygen utilisation	$MolO_2.l^{-1}$
K_s	Ferrous-ion substrate saturation constant in Monod equation	$MolFe^{2+}.l^{-1}$
K_I	Michaelis-Menten Ferric-ion product inhibition constant	$MolFe^{3+}.l^{-1}$
R	Gas Constant	$KJmol^{-1}K^{-1}$

F	Faraday Constant	
T	Temperature	Kelvin
z	No. of electrons	
ϕ_{in}	Inlet air flowrate	$Mole.h^{-1}$
ϕ_{out}	Outlet air flowrate	$Mole.h^{-1}$
$\phi_{N_2}^{in}$	Flowrate of nitrogen in	$Mole.h^{-1}$
$\phi_{N_2}^{out}$	Flowrate of nitrogen out	$Mole.h^{-1}$
$\phi_{O_2}^{in}$	Flowrate of oxygen in	$Mole.h^{-1}$
$\phi_{O_2}^{out}$	Flowrate of oxygen out	$Mole.h^{-1}$
$\phi_{CO_2}^{in}$	Flowrate of carbon dioxide in	$Mole.h^{-1}$
$\phi_{CO_2}^{out}$	Flowrate of carbon dioxide out	$Mole.h^{-1}$
$x_{O_2}^{in}$	Mole fraction of oxygen in inlet air	$Mole.Mole^{-1}$
$x_{O_2}^{out}$	Mole fraction of oxygen in outlet air	$Mole.Mole^{-1}$
$x_{CO_2}^{in}$	Mole fraction of carbon dioxide in inlet air	$Mole.Mole^{-1}$
$x_{CO_2}^{out}$	Mole fraction of carbon dioxide in outlet air	$Mole.Mole^{-1}$
V	Reactor volume	l
Y_{SX}	Bacterial yield on substrate	$MoleC.Mole^{-1}$
Y_{OX}	Bacterial yield on oxygen	$MoleC.MoleO_2^{-1}$
Y_{SX}^{max}	Maximum bacterial yield on substrate	$MoleC.Mole^{-1}$
Y_{OX}^{max}	Maximum bacterial yield on oxygen	$MoleC.Mole\ O_2^{-1}$
$Y_{Fe^{2+}X}$	Bacterial yield on ferrous-ion	$MoleC.Mole(Fe^{2+})^{-1}$
Y_{S^0X}	Bacterial yield on sulphur	$MoleC.MoleS^{-1}$
$Y_{OX}^{Fe^{2+}}$	Bacterial yield on oxygen for ferrous-ion oxidation	$MoleC.Mole\ O_2^{-1}$
Y_{OX}^{S}	Bacterial yield on oxygen for sulphur oxidation	$MoleC.MoleO_2^{-1}$
m_o	Maintenance coefficient on oxygen	$MolO_2.molC^{-1}.h^{-1}$

m_{Fe}^{2+}	Maintenance coefficient on ferrous-ion	$MolFe^{2+}molC^{-1}.h^{-1}$
$[Fe]^{tot}$	Total-iron concentration	$Mol.l^{-1}$
Initial $[Fe]^{tot}$	Initial Total-iron concentration	$Mol.l^{-1}$
$[Cu^{2+}]$	Cupric-ion concentration	$mol.l^{-1}$
$[FeHSO_4^{2+}]$	Ferric bisulphato concentration	$mol.l^{-1}$
$[FeSO_4^{+}]$	Ferric sulphato concentration	$mol.l^{-1}$
$K_{FeSO_4^+}$	Equilibrium constant	dimensionless
$K_{FeHSO_4^{2+}}$	Equilibrium constant	dimensionless
K_{HSO_4}	Equilibrium constant	dimensionless
$r_{Cu^{2+}}$	Rate of copper production	$mol\ l^{-1}hr^{-1}$
$-r_{CuFeS_2}$	Rate of chalcopyrite consumption	$mol\ l^{-1}hr^{-1}$
X_{CuFeS_2}	Chalcopyrite conversion	%
x	Stochiometric coefficient	dimensionless
E	Redox potential	mV
E^o	Standard redox potential	mV
R	Gas constant	$KJmol^{-1}K^{-1}$
T	Temperature	°C or K
z	Charge transfer coefficient	
F	Faraday Constant	

APPENDIX I: Reworking of Published Literature (Kametani and Aoki, 1985)

APPENDIX I a: Effect of redox potential

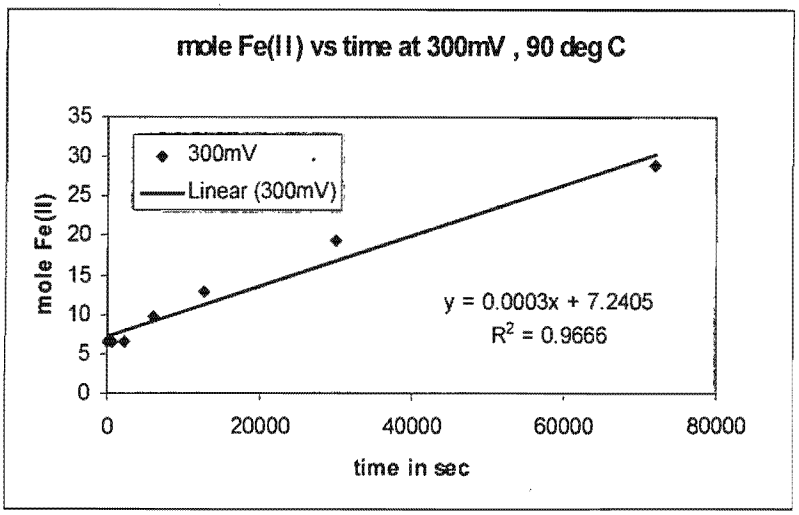

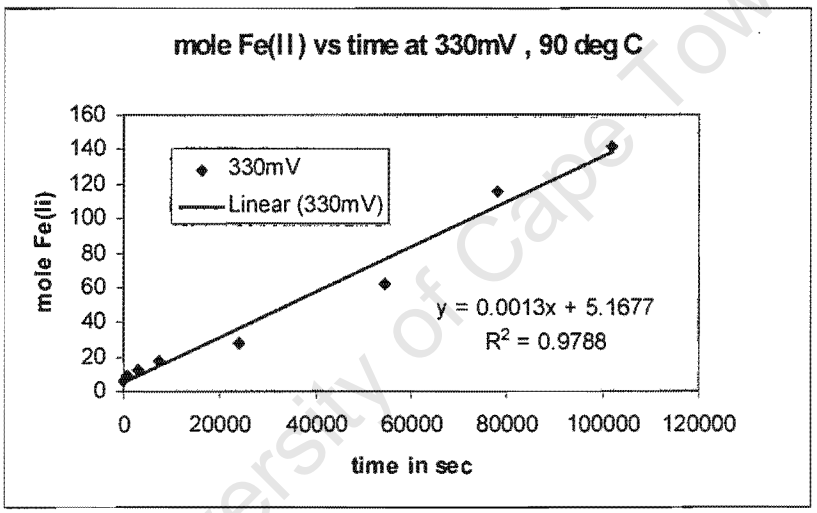

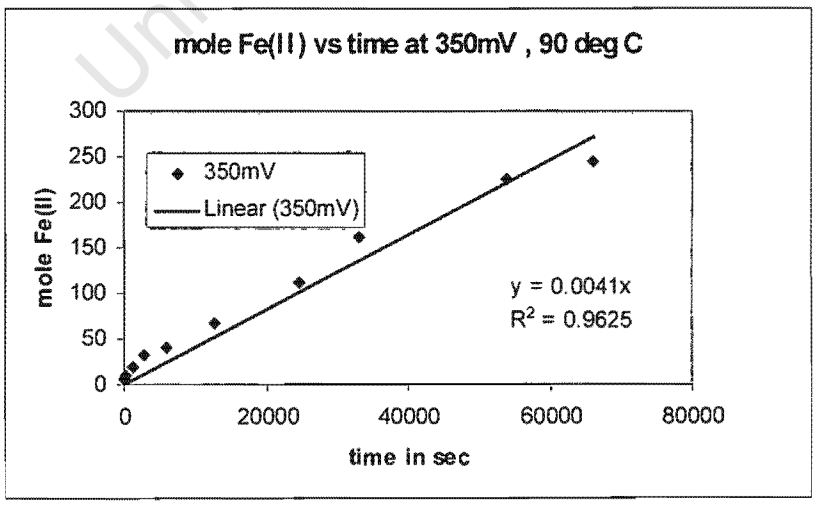

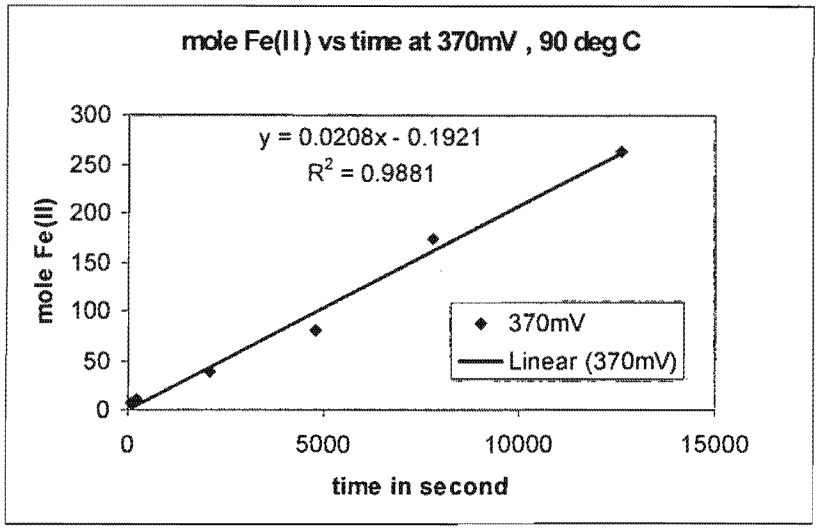

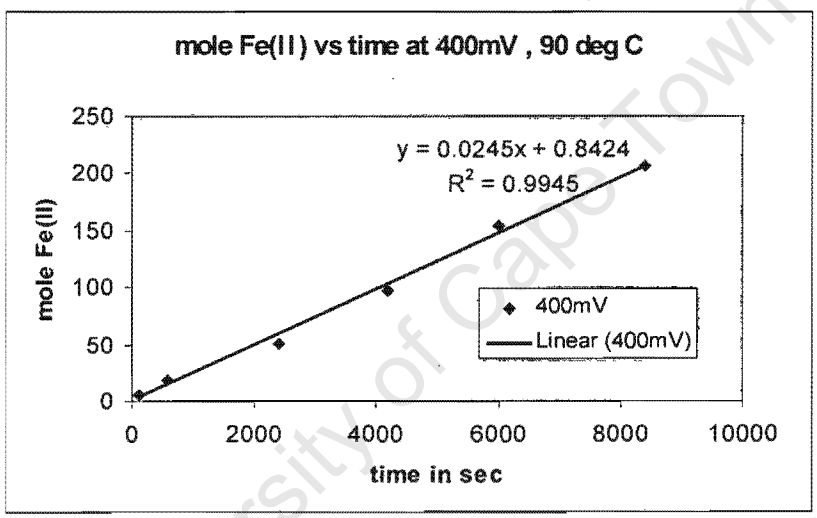

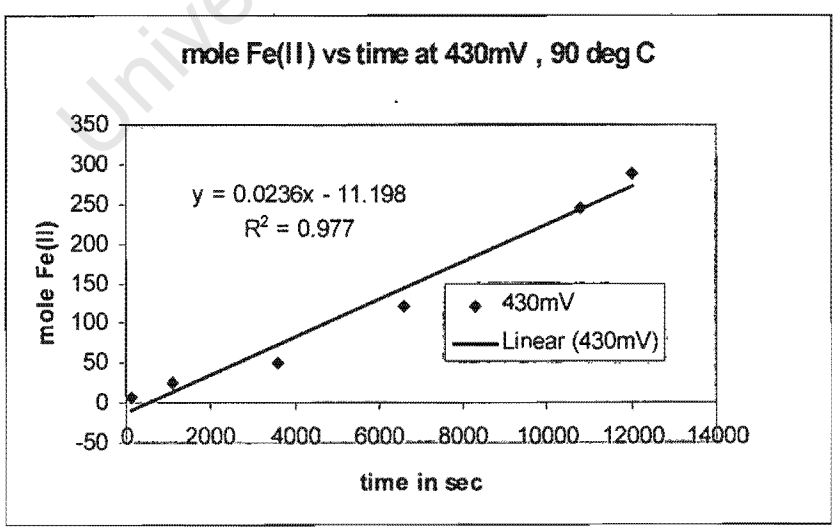

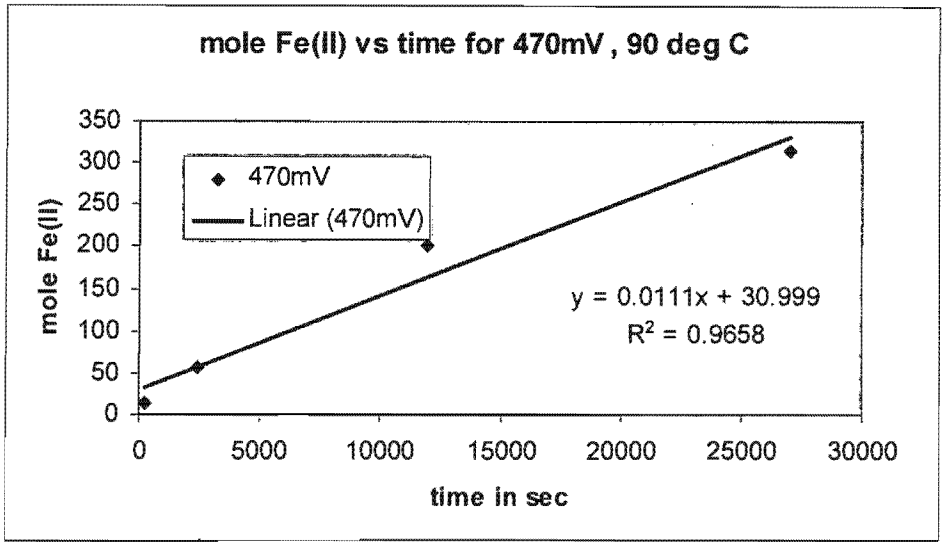

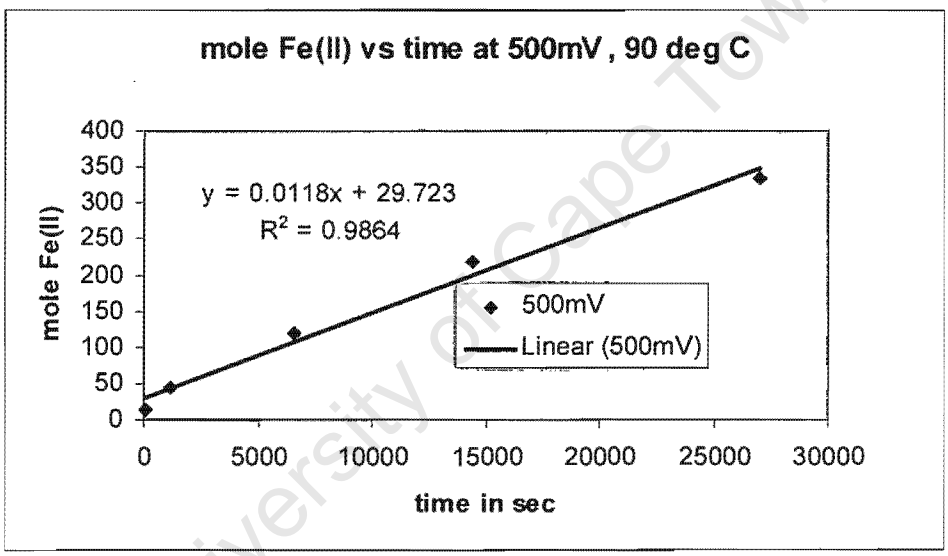

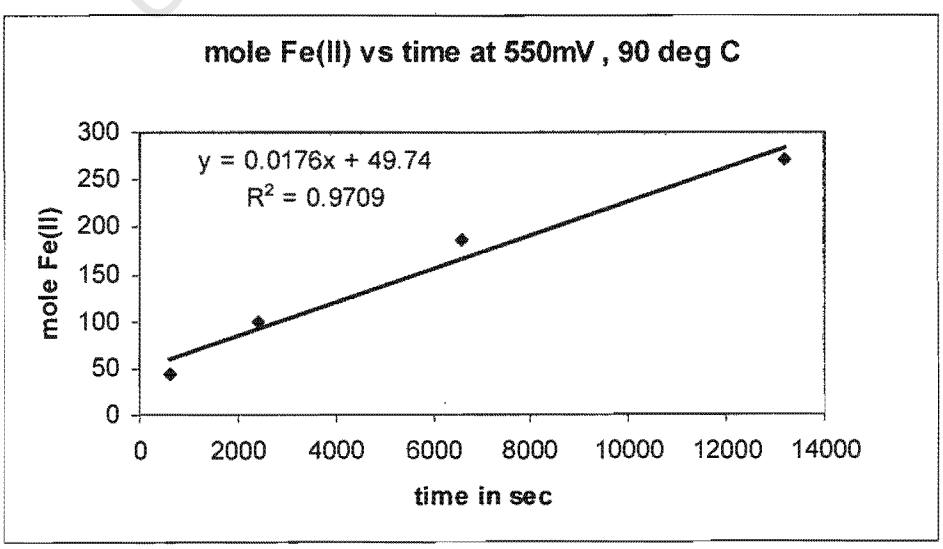

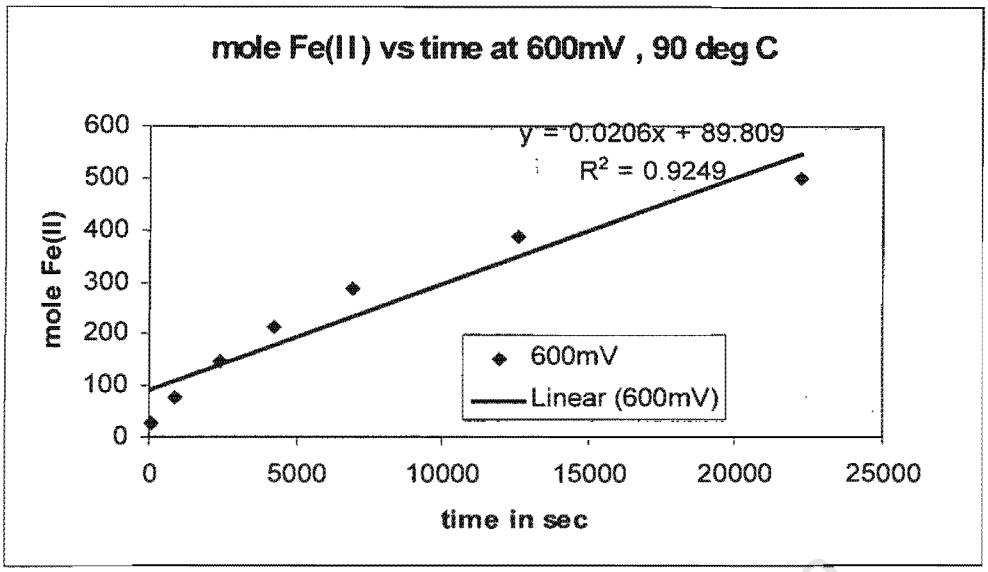

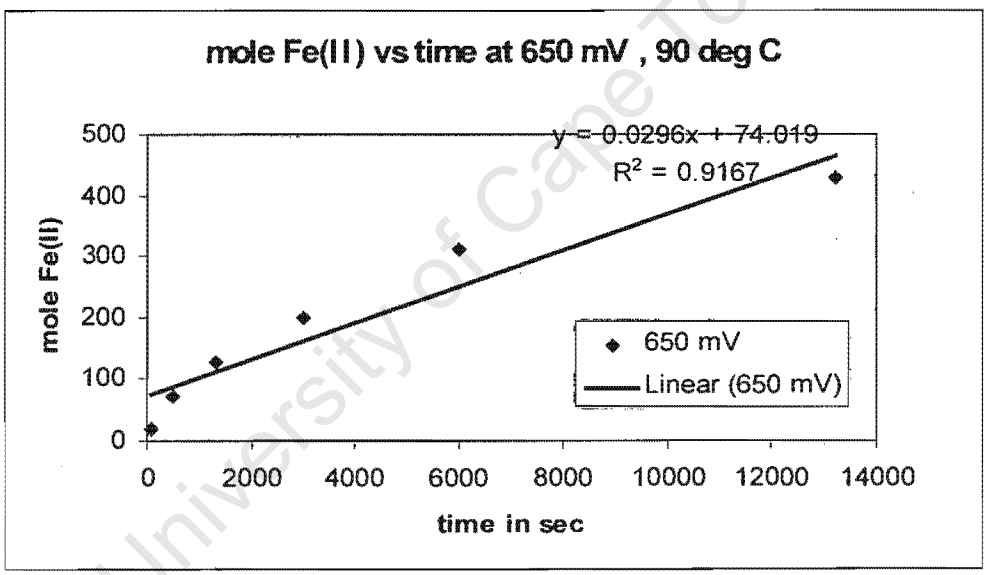

APPENDIX I b: Effect of temperature

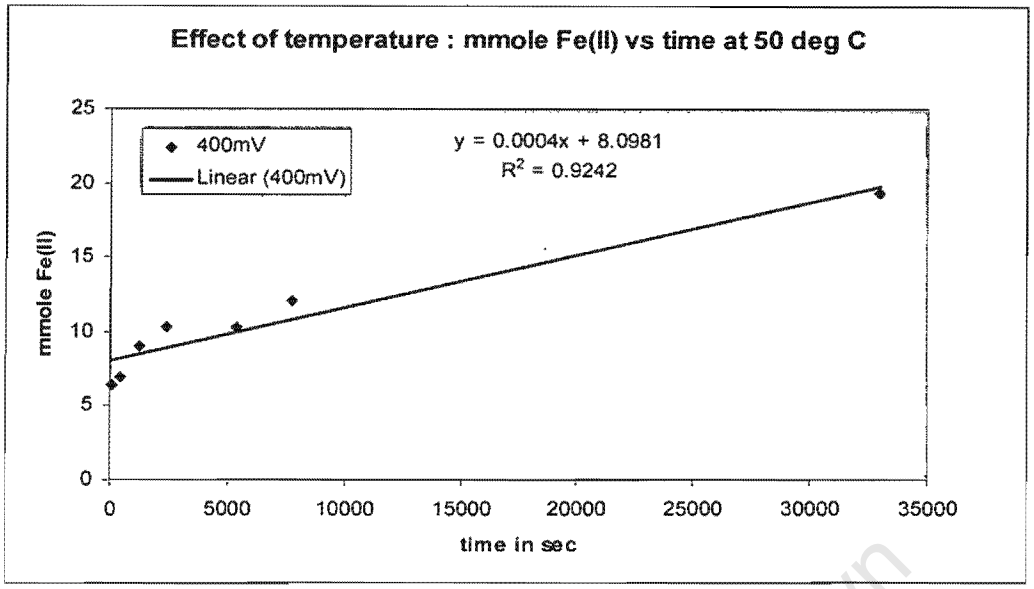

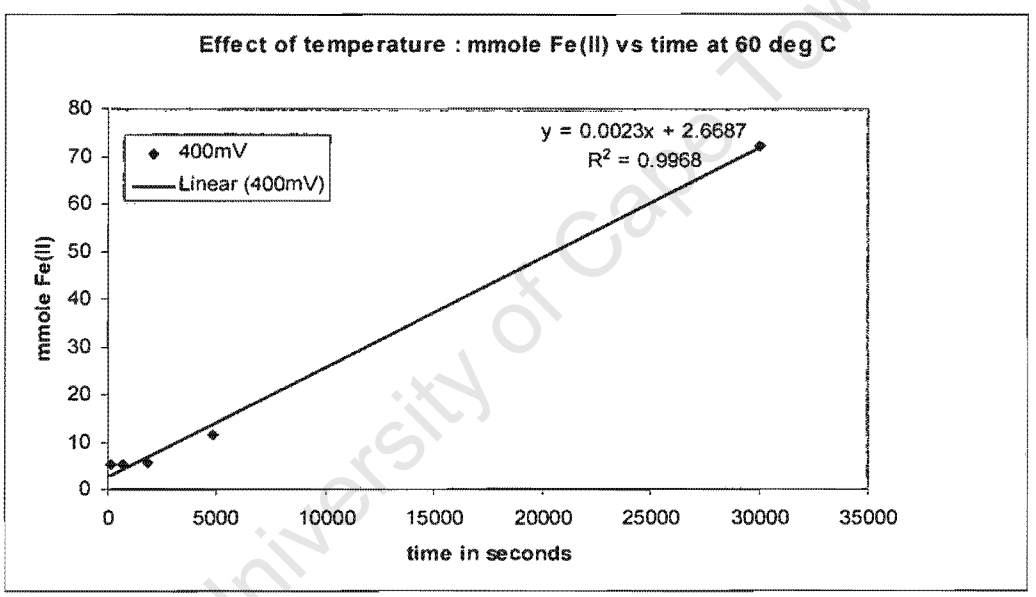

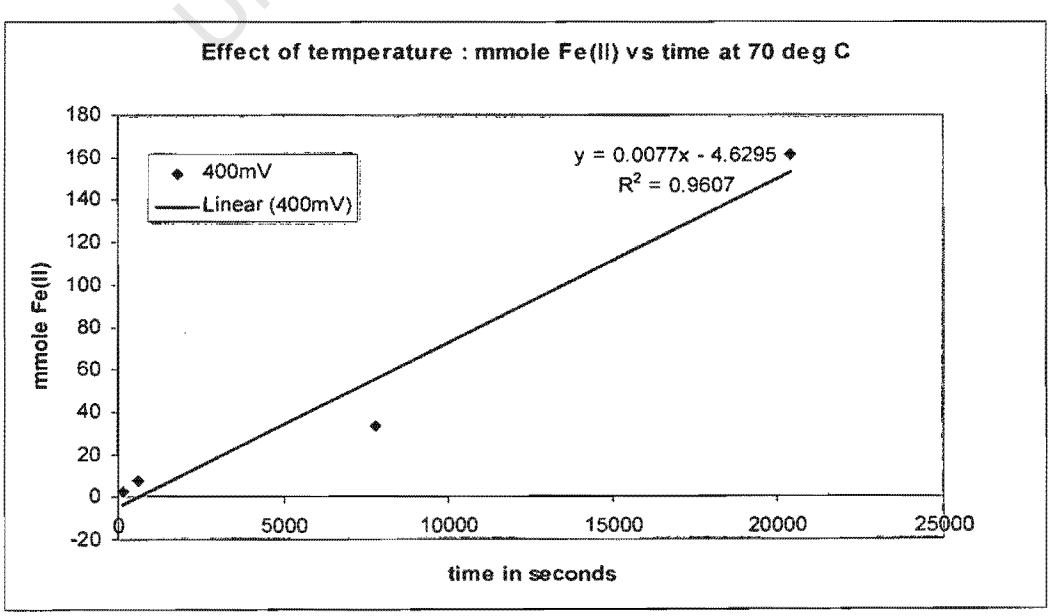

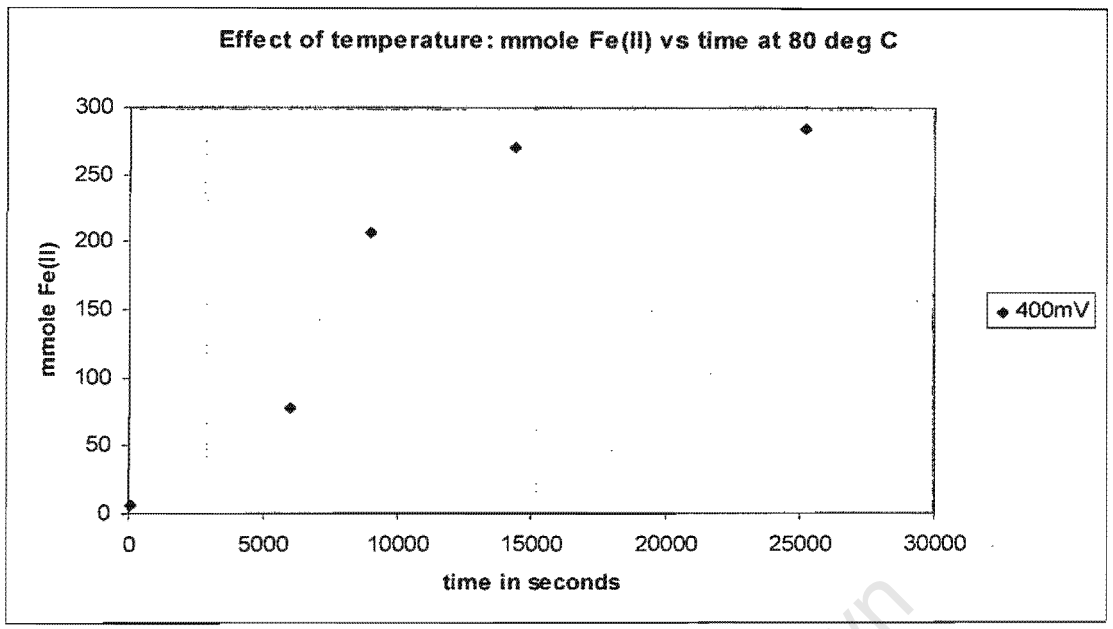

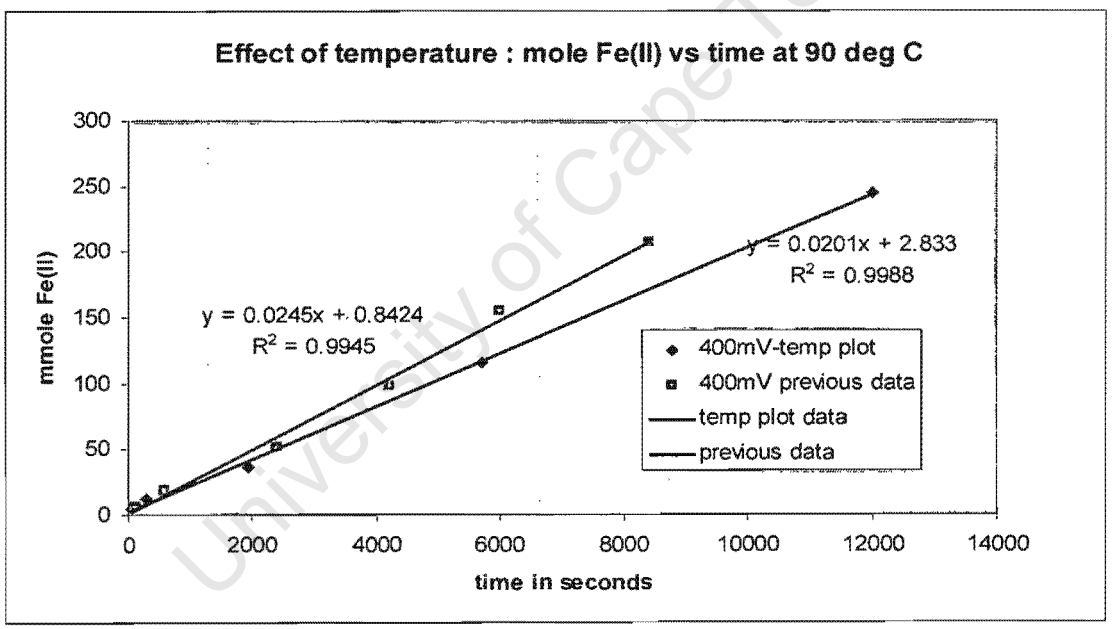

APPENDIX II : Calculation of the kinetics of chemical ferric leaching of chalcopyrite from literature.

Table AII-1: Data calculated from Furamera (2000) for the rate of ferrous-iron production from chemical leaching of Otjihase Chalcopyrite Concentrate at 35 °C

Redox Potential mV	Fe(III)/Fe(II)	Fe(II)/Fe(III)	Si KMnO4 mol/m^2/hr	Si Fe(II) mol/m^2/hr	Conversion factor m^2/molCuFeS2	mu Fe(II) mol/mol/hr	rFe(II) 2g/l mol/l/hr	rFe(II) 6g/l mol/l/hr	rFe(II) 12g/l mol/l/hr	rFe(II) 20g/l mol/l/hr	rFe(II) 30g/l mol/l/hr	rFe(II) 42g/l mol/l/hr
350	0.0066829	149.636674	2.00E-04	1.00E-03	5.043636364	5.04E-03	4.34E-05	0.00013	0.00026	0.000434	0.000651	0.000911109
400	0.052044	19.2144966	2.50E-03	1.25E-02	5.043636364	6.30E-02	5.42E-04	0.001627	0.003254	0.005423	0.008135	0.011388856
450	0.4053032	2.46728873	3.50E-03	1.75E-02	5.043636364	8.83E-02	7.59E-04	0.002278	0.004556	0.007593	0.011389	0.015944399
490	2.0936653	0.47763127	2.01E-03	1.01E-02	5.043636364	5.07E-02	4.36E-04	0.001308	0.002616	0.00436	0.00654	0.00915664
540	16.30483	0.06133152	2.01E-03	1.01E-02	5.043636364	5.07E-02	4.36E-04	0.001308	0.002616	0.00436	0.00654	0.00915664
590	126.97708	0.00787544	1.95E-03	9.75E-03	5.043636364	4.92E-02	4.23E-04	0.001269	0.002538	0.00423	0.006345	0.008883308
630	655.92253	0.00152457	1.05E-03	5.25E-03	5.043636364	2.65E-02	2.28E-04	0.000683	0.001367	0.002278	0.003417	0.00478332
670	3388.2838	0.00029513	1.20E-03	6.00E-03	5.043636364	3.03E-02	2.60E-04	0.000781	0.001562	0.002603	0.003905	0.005466651
700	11609.812	8.6134E-05	1.20E-03	6.00E-03	5.043636364	3.03E-02	2.60E-04	0.000781	0.001562	0.002603	0.003905	0.005466651

where units of specific rates are shown as,

Si $KMNO_4$ is in mol $KMnO_4$ m^{-2} $CuFeS_2$ hr^{-1}
Si Fe(II) is in mol Fe^{2+} m^{-2} $CuFeS_2$ hr^{-1}
Mu Fe(II) is in mol Fe^{2+} mol^{-1} $CuFeS_2$ hr^{-1}
rFe(II) is in mol Fe^{2+} l^{-1} hr^{-1}

Molar Mass of $CuFeS_2$ = 189 $g.gmol^{-1}$
Surface area per mole of $CuFeS_2$ for +38-53 μm size particles = 5.043 $m^2molCuFeS_2^{-1}$

Redox Probe Calibration parameters:

RT/zF= 24.36 mV
E_o = 472 mV

Table AII-2: Rates of ferrous-iron production calculated from (Dutrizac, 1981)

Fe(III)/Fe(II) initial	k mg/hr	rCu mmol/l/hr	rCuFeS2 mol/l/hr	rFe(II) mol/l/hr	mu Fe(II) mol/mol/hr	Si Fe(II) molFe(II)/cm^CuFeS2.hr
0.06	1.8	0.028571	2.86E-05	0.000142857	33.75	0.000194665
0.1	1.8	0.028571	2.86E-05	0.000142857	33.75	0.000194665
0.2	2	0.031746	3.17E-05	0.00015873	37.5	0.000216294
0.3	3	0.047619	4.76E-05	0.000238095	56.25	0.000324441
1	7.8	0.12381	0.000124	0.000619048	146.25	0.000843547

Table AII-3: Rates of ferrous-iron production calculated from (Hirato *et al.*, 1987)

Fe(III)/Fe(II) initial	r CuFeS2 mol/cm^2/hr	Si Fe(II) mol/cm^2/hr
0.1	4.00E-08	0.0000002
0.2	9.00E-08	0.00000045
1	1.20E-07	0.0000006

Where units of specific rates are shown as,

Si Fe(II) is in mol Fe^{2+} m^{-2} $CuFeS_2$ hr^{-1}
Mu Fe(II) is in mol Fe^{2+} mol^{-1} $CuFeS_2$ hr^{-1}
rFe(II) is in mol Fe^{2+} l^{-1} hr^{-1}

rFe(II) = 5[rCuFeS2] assuming the stochiometry shown in equation (2.2.1) for the ferric leaching of $CuFeS_2$

Molar Mass of $CuFeS_2$ = 189 $g.gmol^{-1}$
Molar Mass of Copper = 63 g $gmol^{-1}$

Surface area per mole of $CuFeS_2$ for 16 μm size particles = 1.73e-5 $cm^2 molCuFeS_2^{-1}$

APPENDIX III: Calculation of the parameters of bacterial ferrous-ion oxidation kinetics.

Table AIII-1: Values of the specific oxygen utilisation rate (q_{O_2})and the rate of ferrous-ion utilisation (rFe(II))predicted by the Michaelis-Menten Model for bacterial ferrous-ion oxidation by *Acidithiobacillus ferroxidans* at 35 °C (Modified from Boon, 1996)

Fe(III)/Fe(II)	Eh	q Fe2+	q O2	rFe(II)	rO2	rFe(II)	rO2	rFe(II)	rFe(II)
		Tf	tf	Cx=2mmolC/l	Cx=1.5mmolC/l	Cx=1.5mmolC/l	Cx=1.5mmolC/l	Cx=1.4mmolC/l	Cx=1.2mmolC/l
	mV	molFe(II)/(hr.molC)	molFe(II)/(hr.molC)	molFe(II)/l.hr	molO2/l.hr	molFe(II)/l.hr	molO2/l.hr	molFe(II)/l.hr	molFe(II)/l.hr
100000	877.653054	0.002980748	0.000670187	5.3615E-05	1.0723E-05	4.2892E-06	9.38262E-07	3.75305E-06	3.21696E-06
90000	874.756786	0.002976544	0.000744636	5.95709E-05	1.19142E-05	4.76567E-06	1.04249E-06	4.16996E-06	3.57425E-06
80000	871.630824	0.003350771	0.000837693	6.70154E-05	1.34031E-05	5.36123E-06	1.17277E-06	4.69106E-06	4.02093E-06
70000	868.0869	0.003829319	0.000957133	7.65864E-05	1.53173E-05	6.12691E-06	1.34026E-06	5.36105E-06	4.59518E-06
60000	863.995741	0.00446733	0.001116833	8.93466E-05	1.78693E-05	7.14773E-06	1.56357E-06	6.25429E-06	5.3608E-06
50000	859.156927	0.005360446	0.001340111	1.07209E-04	2.14418E-05	8.57671E-06	1.87616E-06	7.50462E-06	6.43254E-06
40000	853.234687	0.006669901	0.001674975	1.33998E-04	2.67996E-05	1.07198E-05	2.34497E-06	9.37988E-06	8.03988E-06
30000	845.599614	0.008931742	0.002232936	1.78635E-04	3.57276E-05	1.42909E-05	3.12611E-06	1.25044E-05	1.07181E-05
20000	834.83857	0.013393238	0.003348631	2.67865E-04	5.3573E-05	2.14292E-05	4.68763E-06	1.87505E-05	1.60719E-05
10000	816.442443	0.026760262	0.006690067	5.35205E-04	1.07041E-04	4.28164E-05	9.36609E-06	3.74644E-05	3.21123E-05
9000	813.646175	0.029727168	0.007431792	5.94543E-04	1.18909E-04	4.75635E-05	1.04045E-05	4.1618E-05	3.56726E-05
8000	810.520213	0.033433979	0.008358495	6.6858E-04	1.33716E-04	5.34944E-05	1.17019E-05	4.68076E-05	4.01208E-05
7000	806.97629	0.03819692	0.00954923	7.63938E-04	1.52788E-04	6.11151E-05	1.33889E-05	5.34757E-05	4.58365E-05
6000	802.86513	0.044542337	0.011135584	8.90847E-04	1.78169E-04	7.12677E-05	1.55898E-05	6.23593E-05	5.34508E-05
5000	798.048316	0.053416005	0.013354001	0.001068332	2.13664E-04	8.54656E-05	1.86956E-05	7.47824E-05	6.40992E-05
4000	792.124086	0.066704865	0.016676216	0.00133441	2.66819E-04	0.000106728	2.33467E-05	9.33868E-05	8.00458E-05
3000	784.489004	0.088795438	0.022198859	0.001777591	3.55182E-04	0.000142073	3.10784E-05	0.000124314	0.000106555
2000	773.727959	0.133192111	0.033298528	0.002665524	5.31048E-04	0.000212416	4.64567E-05	0.000185867	0.000159313
1000	755.331832	0.262971104	0.065742776	0.005259942	0.001051888	0.000420754	9.20399E-05	0.000368816	0.000315565
900	752.535564	0.291567103	0.072891777	0.005832134	0.001166427	0.000466507	0.000102049	0.000408194	0.000349681
800	749.403602	0.327141086	0.081785272	0.006542482	0.001308856	0.000523426	0.000114499	0.000457998	0.000392569
700	745.855679	0.372802103	0.093150527	0.007456204	0.001491041	0.000596163	0.000130411	0.000521643	0.000447123
600	741.77452	0.43237726	0.108184315	0.008654753	0.001730851	0.000692336	0.000151458	0.000605832	0.000519284
500	736.933705	0.51601877	0.129004682	0.010321038	0.002064208	0.000825683	0.000180607	0.000722426	0.000619223
400	731.013475	0.639995208	0.15974881	0.012777569	0.002555008	0.001022382	0.000223648	0.000894593	0.000766784
300	723.378383	0.836926221	0.20873155	0.016877852	0.003355571	0.001342282	0.000293024	0.001174497	0.001006711
200	712.617348	1.220937268	0.305234317	0.024418575	0.004885375	0.00195535	0.000427329	0.001709312	0.001465125
100	694.221322	2.241720665	0.560430221	0.044833442	0.008966888	0.003586753	0.000784603	0.003139409	0.002690663
90	691.424953	2.445242827	0.611560707	0.048924485	0.009784897	0.003913959	0.000855185	0.00342474	0.002935491
80	688.298991	2.691430197	0.672857549	0.05383366	0.010767332	0.004306824	0.000941241	0.003768552	0.003230188
70	684.755068	2.992231379	0.748057845	0.059844653	0.011968893	0.00478757	0.001047261	0.004189124	0.003590678
60	680.663909	3.366102609	0.842025702	0.067362056	0.013472411	0.005388964	0.001178839	0.004715344	0.004041723
50	675.829095	3.851971099	0.962992775	0.077039422	0.015407885	0.006163154	0.001348119	0.005392758	0.004622365
40	669.902865	4.498189935	1.124547484	0.089963588	0.017992776	0.007197104	0.001574366	0.006297466	0.005397628
30	662.287782	5.404939885	1.351234921	0.108098879	0.021619776	0.008647903	0.001891729	0.007565918	0.006485928
20	651.506738	6.78959317	1.697398292	0.135938366	0.027187821	0.010831265	0.002369344	0.009472714	0.008123464
10	633.110611	9.055958545	2.263989636	0.181111917	0.036223383	0.014489534	0.003169585	0.012678342	0.010866715
9	630.314343	9.372513642	2.34312841	0.187452027	0.037490055	0.014996022	0.00328038	0.013121519	0.011247016
8	627.168381	9.712000996	2.428000249	0.194240082	0.0388848	0.015539202	0.0033992	0.013596801	0.011654401
7	623.644457	10.07709619	2.519251548	0.201540812	0.040308082	0.016123231	0.003526952	0.014107809	0.012092407
6	619.553288	10.47051869	2.617629671	0.209410837	0.041882207	0.01675283	0.003664682	0.014658726	0.012564622
5	614.714484	10.89601387	2.724003467	0.217920268	0.043584406	0.017433622	0.003813805	0.015254419	0.013075217
4	608.792264	11.35755598	2.839388996	0.227115112	0.045423022	0.01817209	0.003975145	0.015900578	0.013628997
3	601.157171	11.85982836	2.964957091	0.237198567	0.047439711	0.018976565	0.004150975	0.0166039	0.014231914
2	590.396127	12.40879982	3.102199955	0.0248178	0.04968352	0.01985408	0.00434306	0.01737232	0.01489056
1	572	13.01063949	3.252734872	0.026021879	0.005204375	0.02081750	0.00455382	0.018215315	0.015613127
0.9	569.203752	13.07438321	3.268595803	0.026148766	0.005229753	0.020919013	0.004578034	0.018304136	0.01568926
0.8	566.07777	13.1384487	3.284612174	0.026276897	0.005255379	0.021021518	0.004598457	0.018393826	0.015766138
0.7	562.533647	13.20214512	3.300786281	0.02640529	0.005281258	0.021125032	0.00462101	0.018484403	0.015843774
0.6	556.442687	13.26848186	3.317120465	0.026536964	0.005307393	0.021229571	0.004643969	0.018575875	0.015922178
0.5	553.603873	13.33445846	3.333617114	0.026668937	0.005333787	0.02133515	0.004667064	0.018668256	0.016001362
0.4	547.661643	13.40111468	3.350278666	0.026802229	0.005360446	0.021441783	0.00469039	0.018761561	0.016081338
0.3	540.046561	13.46843042	3.367107604	0.026936861	0.005387373	0.021549489	0.004713951	0.018855803	0.016162117
0.2	529.285516	13.53642566	3.384106465	0.027072852	0.00541457	0.021658281	0.004737749	0.018950996	0.016243711
0.1	510.889389	13.60511134	3.401277834	0.027210223	0.005442045	0.021768178	0.004761789	0.019047156	0.016326134
0.09	508.093121	13.63201824	3.40300456	0.027224036	0.005444807	0.021779229	0.004764206	0.019056826	0.016334427
0.08	504.967159	13.61893216	3.40473304	0.027237884	0.005447573	0.021790291	0.004766626	0.019066505	0.016342719
0.07	501.423236	13.62585311	3.406963277	0.027251706	0.005450341	0.021801365	0.004769049	0.019076194	0.016351024
0.06	497.332077	13.63278109	3.408196273	0.027265562	0.005453112	0.02181245	0.004771473	0.019085894	0.016359337
0.05	492.493262	13.63971613	3.409829032	0.027279432	0.005455886	0.021823546	0.00477390	0.019095603	0.016367659
0.04	486.571032	13.64665822	3.411864555	0.027293316	0.005458663	0.021834653	0.00477833	0.019105322	0.01637599
0.03	478.93595	13.65360738	3.413401849	0.027307215	0.005461443	0.021845772	0.004778763	0.01911505	0.016384329
0.02	468.174905	13.66056363	3.415140907	0.027321127	0.005464225	0.021856902	0.004781197	0.019124789	0.016392678
0.01	449.778778	13.66752696	3.416881741	0.027335054	0.005467011	0.021866043	0.004783634	0.019134538	0.016401032
0.009	448.98251	13.66822369	3.417055922	0.027336447	0.005467289	0.021869158	0.004783878	0.019135513	0.016401888
0.008	448.056548	13.66892048	3.417230121	0.027337841	0.005467568	0.021870273	0.004784122	0.019136489	0.016402705
0.007	447.012825	13.66981735	3.417494337	0.027339235	0.005467847	0.021871388	0.004784368	0.019137464	0.016403541

Table AIII-1: Values of the specific oxygen utilisation rate and the rate of ferrous-ion utilisation predicted by the Michaelis-Menten Model for bacterial ferrous-ion oxidation by *Leptospirillum ferroxidans* at 35 °C (Breed *et al.*, 1999(a))

Fe(III)/Fe(II)	Eh mV	q Fe2+ LT mol Fe(II)/(hr.mol C)	q O2 LT mol O2/(hr.mol C)	rO2 Cx=2 mmolC/l mol O2/l.hr	rFe2+ Cx=2mmolC/l mol Fe2+/l.hr	rO2 Cx=1.8 mmolC/l mol O2/l.hr	rFe2+ Cx=1.8 mmolC/l mol Fe2+/l.hr	rO2 Cx=1.4mmolC/l mol O2/l.hr	rFe2+ Cx=1.4mmolC/l mol Fe2+/l.hr	rFe2+ Cx=1.3mmolC/l mol Fe2+/l.hr	rFe2+ Cx=1mmolC/l mol Fe2+/l.hr
100000	677.55305	0.047662336	0.011915584	2.38312E-05	9.53247E-05	1.90649E-05	7.62597E-05	1.66818E-05	6.67273E-05	5.71948E-05	4.76623E-05
90000	674.75679	0.052932692	0.013233173	2.64663E-05	0.000105865	2.11731E-05	8.46923E-05	1.85264E-05	7.41058E-05	6.35192E-05	5.29327E-05
80000	671.63062	0.059513312	0.014878328	2.97567E-05	0.000119027	2.38054E-05	9.52216E-05	2.08297E-05	8.33189E-05	7.14162E-05	5.95135E-05
70000	668.0959	0.067962963	0.016990741	3.39815E-05	0.000135926	2.71852E-05	0.000108741	2.3787E-05	9.51481E-05	8.15556E-05	6.7963E-05
60000	663.99574	0.079208633	0.019802158	3.96043E-05	0.000158417	3.16835E-05	0.000126734	2.7723E-05	0.000110892	9.50504E-05	7.92086E-05
50000	659.15693	0.094913793	0.023728448	4.74569E-05	0.000189828	3.79655E-05	0.000151862	3.32198E-05	0.000132879	0.000113897	9.49138E-05
40000	653.2347	0.118387097	0.029596774	5.91935E-05	0.000236774	4.73548E-05	0.000189419	4.14355E-05	0.000165742	0.000142065	0.000118387
30000	645.60001	0.157285714	0.039321429	7.86429E-05	0.000314571	6.29143E-05	0.000251657	0.00005505	0.0002202	0.000188743	0.000157286
20000	634.83857	0.234255319	0.05856383	0.000117128	0.000468511	9.37021E-05	0.000374809	8.19894E-05	0.000327957	0.000281106	0.000234255
10000	616.44244	0.45875	0.1146875	0.000229375	0.0009175	0.0001835	0.000734	0.000160563	0.00064225	0.0005505	0.00045875
9000	613.64817	0.507373272	0.126843318	0.000253687	0.001014747	0.000202949	0.000811797	0.000177581	0.000710323	0.000608848	0.000507373
8000	610.52021	0.567525773	0.141881443	0.000283763	0.001135052	0.00022701	0.000908041	0.000198634	0.000794536	0.000681031	0.000567526
7000	606.97629	0.643859649	0.160964912	0.00032193	0.001287719	0.000257544	0.001030175	0.000225351	0.000901404	0.000772632	0.00064386
6000	602.88513	0.743918919	0.18597973	0.000371959	0.001487838	0.000297568	0.00119027	0.000260372	0.001041486	0.000892703	0.000743919
5000	598.04632	0.8808	0.2202	0.0004404	0.0017616	0.00035232	0.00140928	0.00030828	0.00123312	0.00105696	0.0008808
4000	592.124	1.079411765	0.269852941	0.000539706	0.002158824	0.000431765	0.001727059	0.000377794	0.001511176	0.001295294	0.001079412
3000	584.489	1.393670886	0.348417722	0.000696835	0.002787342	0.000557468	0.002229873	0.000487785	0.001951139	0.001672405	0.001393671
2000	573.7279	1.966071429	0.491517857	0.000983036	0.003932143	0.000786429	0.003145714	0.000688125	0.0027525	0.002359286	0.001966071
1000	555.33163	3.336363636	0.834090909	0.001668182	0.006672727	0.001334545	0.005338182	0.001167727	0.004670909	0.004003636	0.003336364
900	552.53358	3.586319218	0.896579805	0.00179316	0.007172638	0.001434528	0.005738111	0.001255212	0.005020847	0.004303583	0.003586319
800	549.4096	3.876760563	0.969190141	0.00193838	0.007753521	0.001550704	0.006202817	0.001356866	0.005427465	0.004652113	0.003876761
700	545.8658	4.218390805	1.054597701	0.002109195	0.008436782	0.001687356	0.006749425	0.001476437	0.005905747	0.005062069	0.004218391
600	541.77452	4.62605042	1.156512605	0.002313025	0.009252101	0.00185042	0.007401681	0.001619118	0.006476471	0.005551261	0.004626051
500	536.93571	5.120930233	1.280232558	0.002560465	0.01024186	0.002048372	0.008193488	0.001792326	0.007169302	0.006145116	0.00512093
400	531.01348	5.734375	1.43359375	0.002867188	0.01146875	0.00229375	0.009175	0.002007031	0.008028125	0.00688125	0.005734375
300	523.37839	6.514792899	1.628698225	0.003257396	0.013029586	0.002605917	0.010423669	0.002280178	0.00912071	0.007817751	0.006514793
200	512.61735	7.54109589	1.885273973	0.003770548	0.015082192	0.003016438	0.012065753	0.002639384	0.010557534	0.009049315	0.007541096
100	494.22122	8.951219512	2.237804878	0.00447561	0.017902439	0.003580488	0.014321951	0.003132927	0.012531707	0.010741463	0.00895122
90	491.42495	9.121789581	2.280447395	0.004560895	0.018243579	0.003648716	0.014594863	0.003192626	0.012770505	0.010946147	0.00912179
80	488.29899	9.298986089	2.324746522	0.004649493	0.018597973	0.003719594	0.014878378	0.003254645	0.013018581	0.011158784	0.009298986
70	484.75307	9.483204134	2.370801034	0.004741602	0.018966408	0.003793282	0.015173127	0.003319121	0.013276486	0.011379845	0.009483204
60	480.66391	9.674868189	2.418717047	0.004837434	0.019349736	0.003869947	0.015479789	0.003386204	0.013544815	0.011609842	0.009674868
50	475.82509	9.874439462	2.468609865	0.00493722	0.019748879	0.003949776	0.015799103	0.003456054	0.013824215	0.011849327	0.009874439
40	469.90269	10.08241758	2.520604396	0.005041209	0.020164835	0.004032967	0.016131868	0.003528846	0.014115385	0.012098901	0.010082418
30	462.26776	10.29934518	2.574836295	0.005149673	0.02059869	0.004119738	0.016478952	0.003604771	0.014419083	0.012359214	0.010299345
20	451.50674	10.52581282	2.631453205	0.005262906	0.021051626	0.004210325	0.0168413	0.003684034	0.014736138	0.012630975	0.010525813
10	433.11051	10.76248334	2.690620835	0.005381242	0.021524967	0.004304993	0.017219974	0.003766869	0.015067477	0.01291498	0.010762483
9	430.31434	10.7867115	2.696677875	0.005393356	0.021573423	0.004314685	0.017258738	0.003775349	0.015101396	0.012944054	0.010786712
8	427.18836	10.81107692	2.70276923	0.005405538	0.021622154	0.00432443	0.017297723	0.003783877	0.015135508	0.012973292	0.010811077
7	423.64446	10.83554788	2.70888697	0.005417774	0.021671096	0.004334219	0.017336877	0.003792442	0.015169767	0.013002658	0.010835548
6	419.5533	10.86013032	2.71503258	0.005430065	0.021720261	0.004344052	0.017376208	0.003801046	0.015204182	0.013032156	0.01086013
5	414.7144	10.88482452	2.72120613	0.005442412	0.021769649	0.00435393	0.017415719	0.003809688	0.015238754	0.013061789	0.010884825
4	408.79225	10.90963139	2.727407848	0.005454816	0.021819263	0.004363853	0.01745541	0.003818371	0.015273484	0.013091558	0.010909631
3	401.15717	10.93455152	2.73363788	0.005467276	0.021869103	0.004373821	0.017495282	0.003827093	0.015308372	0.013121462	0.010934552
2	390.39613	10.9595859	2.739896476	0.005479793	0.021919172	0.004383834	0.017535337	0.003835855	0.01534342	0.013151503	0.010959586
1	372	10.98473411	2.746183527	0.005492367	0.021969468	0.004393894	0.017575575	0.003844657	0.015378628	0.013181681	0.010984734
0.9	369.20373	10.98725638	2.746814095	0.005493628	0.021974513	0.004394903	0.01757961	0.00384554	0.015382159	0.013184708	0.010987256
0.8	366.07777	10.98977881	2.747444702	0.005494889	0.021979558	0.004395912	0.017583646	0.003846423	0.015385689	0.013187735	0.010989779
0.7	362.53365	10.99230239	2.748075596	0.005496151	0.021984605	0.004396921	0.017587684	0.003847306	0.015389223	0.013190763	0.010992302
0.6	358.44269	10.99482714	2.748706785	0.005497414	0.021989654	0.004397931	0.017591723	0.00384819	0.015392758	0.013193793	0.010994827
0.5	353.60307	10.99735304	2.749338261	0.005498677	0.021994706	0.004398941	0.017595765	0.003849074	0.015396294	0.013196824	0.010997353
0.4	347.68184	10.99988011	2.749970028	0.00549994	0.02199976	0.004399952	0.017599808	0.003849958	0.015399832	0.013199856	0.01099988
0.3	340.04656	11.00240834	2.750602085	0.005501204	0.022004817	0.004400963	0.017603853	0.003850843	0.015403372	0.01320289	0.011002408
0.2	329.26552	11.00493773	2.751234432	0.005502469	0.022009875	0.004401975	0.0176079	0.003851728	0.015406913	0.013205925	0.011004938
0.1	310.88939	11.00746828	2.751867071	0.005503734	0.022014937	0.004402987	0.017611949	0.003852614	0.015410456	0.013208962	0.011007468
0.09	308.09312	11.0077214	2.75193035	0.005503861	0.022015443	0.004403089	0.017612354	0.003852703	0.01541081	0.013209266	0.011007721
0.08	304.96716	11.00797453	2.751993633	0.005503987	0.022015949	0.00440319	0.017612759	0.003852791	0.015411164	0.013209569	0.011007974
0.07	301.42324	11.00822768	2.752056919	0.005504114	0.022016455	0.004403291	0.017613164	0.00385288	0.015411518	0.013209873	0.011008228
0.06	297.33209	11.00848083	2.752120207	0.00550424	0.022016962	0.004403392	0.017613569	0.003852968	0.015411873	0.013210177	0.011008481
0.05	292.49326	11.008734	2.7521835	0.005504367	0.022017468	0.004403494	0.017613974	0.003853057	0.015412228	0.013210481	0.011008734
0.04	286.57103	11.00898717	2.752246793	0.005504494	0.022017974	0.004403595	0.017614379	0.003853146	0.015412582	0.013210785	0.011008987
0.03	278.93595	11.00924038	2.752310094	0.00550462	0.022018481	0.004403696	0.017614785	0.003853234	0.015412937	0.013211089	0.01100924
0.02	268.17491	11.00949358	2.752373395	0.005504747	0.022018987	0.004403797	0.01761519	0.003853323	0.015413291	0.013211392	0.011009494
0.01	249.77575	11.00974678	2.752436694	0.005504873	0.022019494	0.004403898	0.017615595	0.003853411	0.015413645	0.013211696	0.011009747
0.009	246.98251	11.0097721	2.752443024	0.005504886	0.022019544	0.004403908	0.017615635	0.00385342	0.015413681	0.013211727	0.011009772
0.008	243.85556	11.00979742	2.752449355	0.005504899	0.022019595	0.004403919	0.017615676	0.003853429	0.015413716	0.013211757	0.011009797
0.007	240.31263	11.00982274	2.752455685	0.005504911	0.022019645	0.004403929	0.017615716	0.003853438	0.015413752	0.013211787	0.011009823
0.006	236.22147	11.00984806	2.752462015	0.005504924	0.022019696	0.004403939	0.017615757	0.003853447	0.015413787	0.013211818	0.011009848
0.005	231.38265	11.00987339	2.752468347	0.005504937	0.022019747	0.004403949	0.017615797	0.003853456	0.015413823	0.013211848	0.011009873
0.004	225.46042	11.00989871	2.752474677	0.005504949	0.022019797	0.004403959	0.017615838	0.003853465	0.015413858	0.013211878	0.011009899
0.003	217.82534	11.00992403	2.752481008	0.005504962	0.022019848	0.00440397	0.017615878	0.003853473	0.015413894	0.013211909	0.011009924
0.002	207.06429	11.00994935	2.752487338	0.005504975	0.022019899	0.00440398	0.017615919	0.003853482	0.015413929	0.013211939	0.011009949
0.001	188.66617	11.00997468	2.752493669	0.005504987	0.022019949	0.00440399	0.017615959	0.003853491	0.015413965	0.01321197	0.011009975
0.0009	185.8719	11.00997721	2.752494302	0.005504989	0.022019954	0.004403991	0.017615964	0.003853492	0.015413968	0.013211973	0.011009977
0.0008	182.74584	11.00997974	2.752494935	0.00550499	0.022019959	0.004403992	0.017615968	0.003853493	0.015413972	0.013211976	0.01100998
0.0007	179.20201	11.00998227	2.752495568	0.005504991	0.022019965	0.004403993	0.017615972	0.003853494	0.015413975	0.013211979	0.011009982
0.0006	175.11006	11.00998481	2.752496202	0.005504992	0.02201997	0.004403994	0.017615976	0.003853495	0.015413979	0.013211982	0.011009985
0.0005	170.27204	11.00998734	2.752496835	0.005504994	0.022019975	0.004403995	0.01761598	0.003853496	0.015413982	0.013211985	0.011009987
0.0004	164.34961	11.00998987	2.752497468	0.005504995	0.02201998	0.004403996	0.017615984	0.003853496	0.015413986	0.013211988	0.01100999
0.0003	156.71473	11.0099924	2.752498101	0.005504996	0.022019985	0.004403997	0.017615988	0.003853497	0.015413989	0.013211991	0.011009992
0.0002	145.95386	11.00999494	2.752498734	0.005504997	0.02201999	0.004403998	0.017615992	0.003853498	0.015413993	0.013211994	0.011009995
0.0001	127.55756	11.00999747	2.752499367	0.005504999	0.022019995	0.004403999	0.017615996	0.003853499	0.015413996	0.013211997	0.011009997
0.00009	124.76129	11.00999772	2.75249943	0.005504999	0.022019995	0.004403999	0.017615996	0.003853499	0.015413997	0.013211997	0.011009998
0.00008	121.63533	11.00999797	2.752499494	0.005504999	0.022019996	0.004403999	0.017615997	0.003853499	0.015413997	0.013211998	0.011009998
0.00007	118.0914	11.00999823	2.752499557	0.005504999	0.022019996	0.004403999	0.017615997	0.0038535	0.015413998	0.013211998	0.011009998
0.00006	114.00024	11.00999848	2.75249962	0.005504999	0.022019997	0.004403999	0.017615998	0.0038535	0.015413998	0.013211998	0.011009998
0.00005	109.16143	11.00999873	2.752499683	0.005504999	0.022019997	0.004403999	0.017615998	0.0038535	0.015413998	0.013211998	0.011009999
0.00004	103.2392	11.00999899	2.752499747	0.005504999	0.022019998	0.004404	0.017615998	0.0038535	0.015413999	0.013211999	0.011009999
0.00003	95.60412	11.00999924	2.75249981	0.005505	0.022019998	0.004404	0.017615999	0.0038535	0.015413999	0.013211999	0.011009999
0.00002	84.84307	11.00999949	2.752499873	0.005505	0.022019999	0.004404	0.017615999	0.0038535	0.015413999	0.013211999	0.011009999
0.00001	66.44585	11.00999975	2.752499937	0.005505	0.022019999	0.004404	0.017616	0.0038535	0.015414	0.013212	0.01101

Calculation of the maximum specific oxygen utilisation rate, $q_{O_2}^{max}$, and kinetic constant, K, of the Michaelis Menten Model for the bacterial ferrous-ion oxidation kinetics of *Acidithiobacillus ferroxidans* at 35 °C.

The model for bacterial ferrous-ion oxidation of *Acidithiobacillus ferrooxidans* and *Leptospirillum ferrooxidans* is shown as Equation (AIII.1) (Breed et al., 1990(a)) with kinetic parameters in Table AIII-3.

$$q_{Fe^{2+}} = \frac{q_{Fe^{2+}}^{max}}{1 + K\frac{[Fe^{3+}]}{[Fe^{2+}]}} \qquad \text{(AIII.1)}$$

The maximum specific oxygen utilisation rate, $q_{O_2}^{max}$, is calculated from the maximum specific ferrous-ion utilisation rate, $q_{Fe^{2+}}^{max}$, by a degree of reduction balance for bacterial ferrous-ion oxidation as shown in equation (AIII.2), and neglecting the $q_{CO_2}^{max}$ term since its contribution has been shown to be less than 5% to maximum specific ferrous-ion utilisation rate (Boon, 1996)

$$q_{Fe^{2+}}^{max} = 4q_{O_2}^{max} + 4.2q_{CO_2}^{max} \qquad \text{(AIII.2)}$$

Table AIII-3: Values of the maximum bacterial specific ferrous-ion utilisation rates, $q_{Fe^{2+}}^{max}$, and there respective kinetic constants in bacterial ferrous-ion oxidation (Breed *et al.*, 1999(a))

Bacteria Species	Temp (°C)	$q_{Fe^{2+}}^{max}$ molFe^{2+}molC^{-1}hr^{-1}	K
L.Ferrooxidans	**30**	**8.65**	**1.8e-3**
	35	**11.01**	**2.3e-3**
	40	**13.58**	**3.3e-3**
Leptospirillum-Like	**30**	**6.8**	**5e-4**
T.Ferrooxidans*	**30**	**8.8**	**5e-2**

*Reported from Boon, 1996

The effect of temperature on the kinetics of ferrous-ion oxidation by *Acidithiobacillus Ferrooxidans* has been described using the Arrhenius equation (AIII.3) (Nemati *et al.*, 1998, Breed *et al.*, 1999(a)).

$$q_{Fe^{2+}}^{max} = k_o e^{\frac{-Ea}{RT}} \qquad \text{(AIII.3)}$$

Nemati *et al.*, (1998) has reported an activation energy, E_a,of 68.4Kjmol^{-1} for the bacterial ferrous-ion oxidation of *Acidithiobacillus Ferrooxidans*. k_o is not a function of temperature and is established by substituting the $q_{Fe^{2+}}^{max}$ value shown for *Acidithiobacillus Ferrooxidans* in table AIII-3 at 30 °C , along with the reported activation energy into (AIII.3). This established k_o value is then resubstituted into equation (AIII.3), along with the reported activation energy to calculate $q_{Fe^{2+}}^{max}$ at 35 °C. The results of this calculation are shown in Table AIII-4.

Calculation of K:

The linear dependency of the bacterial ferrous-ion oxidation kinetic constant, K, with temperature is shown to in figure AIII.1 and equation AIII.4 for *Leptospirillum ferroxidans* (Breed *et al.*, 1999(a)).

$$K = 0.0002T - 0.0435 \qquad \text{(AIII.4)}$$

It is assumed that the same linear temperature dependency applies to *Acidithiobacillus ferroxidans*.

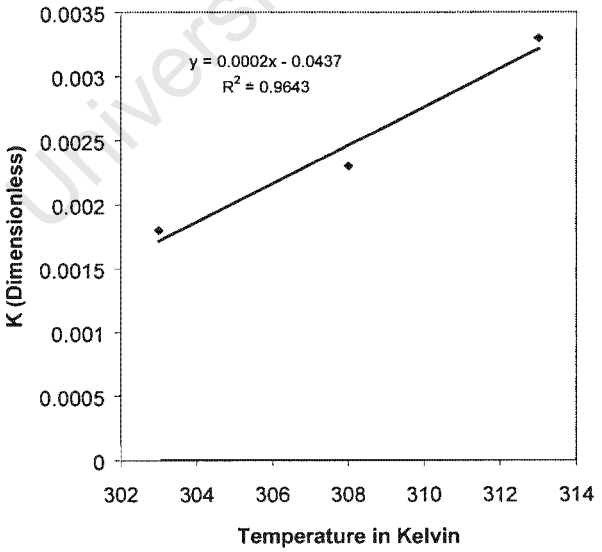

Figure AIII.1: Variation of the Michaelis-Menten bacterial ferrous-ion oxidation kinetic constant (K) with temperature for *Leptospirillum ferroxidans* between 30 and 40 °C (Breed *et al.*, 1999(a)) Regression analysis results in a slope of 2e-4 (K^{-1}) and intercept of 0.0437 for an R^2 of 0.96

The slope of the K vs Temp curve in figure AIII.1 is used to extrapolate the value for K at 35 °C, from the reported value of K for *Acidithiobacillus ferroxidans* shown in Table AIII-3 (Boon, 1996).

Table AIII-4: The maximum specific ferrous-ion and oxygen utilisation rates, along with the kinetic constant K for *Acidithiobacillus ferroxidans* reported by previous workers (Boon, 1996; Breed *et al.*, 1999(a)) and those modified to account for temperature.

Kinetic parameter	Temp = 30 °C	Temp = 35 °C
Activation energy ($Kjmol^{-1}$)	68.4	68.4
k_o	5.45e12	5.45e12
$q^{max}_{Fe^{2+}}$ ($molFe^{2+}molC^{-1}h^{-1}$)	8.80	13.67
$q^{max}_{O_2}$ ($molO_2molC^{-1}h^{-1}$)	2.20	3.42
K (Dimensionless)	0.05	0.051

The results of using the kinetic parameters for *Leptospirillum ferrooxidans* (Table AIII-1) and *Acidithiobacillus ferrooxidans* (Table AIII-4) at 35 °C in Equation AIII.1 written for the specific oxygen utilisation rate is shown in Tables AIII-1 and AIII-2 respectively.

Calculation of the rate of ferrous-ion utilisation , $r_{Fe^{2+}}$

The rate of ferrous-ion utilisation at 35 °C for *Acidithiobacillus ferrooxidans* and *Leptospirillum ferrooxidans* shown in Tables AIII-1 and AIII-2, respectively, is related to the rates of oxygen and carbon dioxide consumption via a degree of reduction balance (Equation AIII.5) andnegelecting the contribution from the carbon dioxide utilisation rate.

$$-r_{Fe^{2+}} = -4r_{O_2} - 4.2r_{CO_2} \qquad \text{(AIII.5)}$$

The oxygen utilisation rate is calculated from the specific oxygen utilisation rate via Equation (AIII.6)

$$-r_{O_2} = q_{O_2}C_x \qquad \text{(AIII.6)}$$

The specific oxygen utilisation rate is predicted from the Michaelis Menten model with kinetic parameters shown in Table AIII-3 and AIII-4 for bacterial ferrous-ion oxidation of *Leptospirillum ferrooxidans* and *Acidithiobacillus ferrooxidans* at various ferric/ferrous-ion ratios